ROLES OF DRUG BASICITY, MELANIN BINDING, AND CELLULAR TRANSPORT IN DRUG INCORPORATION INTO HAIR

by

Chad Randolph Borges

A dissertation submitted to the faculty of
The University of Utah
in partial fulfillment of the requirements for the degree of

Doctor of Philosophy

Department of Pharmacology and Toxicology

University of Utah

December 2001

THE UNIVERSITY OF UTAH GRADUATE SCHOOL

SUPERVISORY COMMITTEE APPROVAL

of a dissertation submitted by

Chad R. Borges

This dissertation has been read by each member of the following supervisory committtee and by majority vote has been found to be satisfactory.

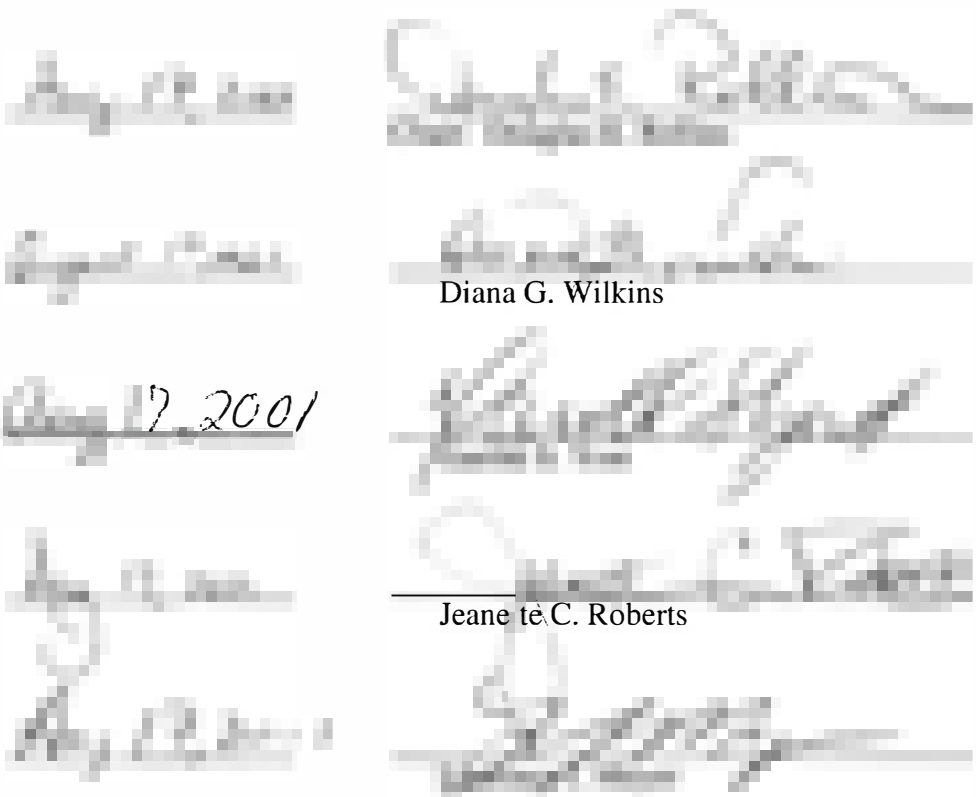

Diana G. Wilkins

Jeane te C. Roberts

THE UNIVERSITY OF UTAH GRADUATE SCHOOL

FINAL READING APPROVAL

To the Graduate Council of the University of Utah:

I have read the dissertation of Chad R. [redacted] in its final form and have found that (1) its format, citations, and bibliographic style are consistent and acceptable: (2) its illustrative materials including figures, tables, and charts are in place; and (3) the final manuscript is satisfactory to the supervisory committee and is [redacted] for submission to The [redacted]

[redacted] 29, 2001
Date

[redacted] E. Rollins
Chair, Supervisory Committee

Approved for the Major Department

[redacted]
Chair/Dean

Approved for the Graduate Council

[redacted]
David S. Chapman
Dean of the Graduate School

ABSTRACT

Hair has become a widely accepted alternative matrix for forensic drug testing. This project examined the roles of drug basicity, drug-melanin binding, and cellular transport of drugs in the phenomenon of preferential incorporation of drugs into darker versus lighter colored hair.

Validated assays were developed then used to profile the melanin content in human hair of various colors. Melanin content was then correlated with codeine incorporation into the analyzed hair.

Black hair from rats dosed with the basic drug amphetamine was found to contain three times the concentration of amphetamine than white hair from the same rats. In contrast, no difference in N-acetylamphetamine (N-AcAp) content was found between black hair and white hair from rats dosed with N-AcAp, a nonbasic amphetamine analog.

Cocaine and amphetamine, two drugs that show a hair color bias, bound to eumelanins and mixed eu-/pheomelanins to varying degrees, but not to pure pheomelanin. Benzoylecgonine (BE) and N-AcAp, drugs that do not show a hair color bias, did not to bind to any subtype of melanin.

Pigmented melanocytes (PM) took up large amounts of the basic drugs amphetamine and cocaine (levels of uptake dependent on melanin content), while keratinocytes and non-pigmented melanocytes (NPM) took up only small amounts of amphetamine. None of the studied cells took up N-AcAp above background levels.

While keratinocytes and NPM quickly effluxed most of an influxed basic drug, PM were slow to efflux and only partially effluxed the drug, if efflux media was not refreshed. BE was quickly effluxed from both PM and NPM.

Cultured cells influxed amphetamine and cocaine to far greater extents than N-AcAp and BE. This is in accord with the fact that the *non-plasma-protein-bound* AUCs of BE and N-AcAp are much greater than cocaine and amphetamine, yet cocaine and amphetamine incorporate into hair to far greater extents than do N-AcAp and BE, regardless of hair color.

In conclusion, the data presented in this dissertation demonstrate that amphetamine and cocaine exhibit preferential hair color incorporation (unlike their net neutral analogs N-AcAp and BE) and do so through nondiffusion mediated cellular uptake and subsequent retention via eumelanin binding.

TABLE OF CONTENTS

ACKNOWLEDGMENTS

I would like to extend much thanks and appreciation to my advisors, Dr. Douglas E. Rollins and Dr. Diana G. Wilkins, for their guidance and counsel in my graduate research and study. Their instruction has been of great value in teaching me the ways of the analytical laboratory.

I would also like to thank the other members of my dissertation committee: Dr. Garold S. Yost, Dr. Jeanette C. Roberts, and Dr. Laurence J. Meyer. I have had the pleasure of working in each of their laboratories for a significant period of time during my graduate training. They have each brought a unique and valuable perspective to this project.

The rest of the staff at the Center for Human Toxicology has been a great group of people to work with. In particular, I am grateful to Dr. Matthew H. Slawson and Dr. Deanna Hubbard who have provided me with hands-on training for some of the various aspects of this project.

In addition, I would like to thank all the additional professors and students here at the University of Utah and at my undergraduate alma matter, Walla Walla College, who have taught me many things and helped shape my scientific philosophy.

The concluding research on this project would not even have been possible without the valuable cell culture donations of Dr. Dorothy Bennett and Mr. Simon Hill of

St. George's Hospital Medical School, London, UK and Dr. Gerald Krueger and Ms. Cynthia Jorgensen of the University of Utah. To them I am greatly indebted.

I also express my thanks to the National Institutes of Health and the University of Utah Graduate School, which have provided the financial support for my graduate education.

Finally, I would like to express my heartfelt thanks to my family—to my wife, Laurie, who has been my number one fan and supporter, to my parents, James and Joanne Borges, for their unending encouragement and love, and to my extended family, for their constant support and enthusiasm.

This acknowledgments section would not be complete without an expression of gratitude to my Creator, the Alpha the Omega, "Trust in the Lord with all thine heart; and lean not unto thine own understanding. In all thy ways acknowledge Him, and He shall direct thy paths." Proverbs 3:5, 6.

CHAPTER 1

OVERVIEW

Introduction

Hair analysis for xenobiotics began in 1858 with efforts to determine arsenic levels in the hair of a corpse (1). Modern hair testing took another century to begin development. The knowledge about and technology for hair testing has expanded dramatically since the mid 1950s. Today, however, there are still many poorly understood aspects of hair testing, particularly in regard to the fundamental chemistry and biology of how different drugs with their unique and distinctive chemical features incorporate into hair. Ideally, hair testing would be a convenient, non-invasive technique with a long window of detection for monitoring all drugs of abuse. While many drugs are currently tested for in hair, our fundamental knowledge regarding the characteristics and mechanisms for the incorporation of certain drugs into certain hair types is incomplete. What roles, for example, do external exposure, hair treatments, and even hair color play in the incorporation of each tested drug in hair? Fair and accurate hair testing relies upon our knowledge and understanding of these factors. As such, the research presented herein seeks to more fully investigate the roles of hair color (pigmentation), and hair cell drug transport in drug incorporation into hair.

History of Hair Testing

The history of hair analysis for xenobiotics began in 1858 with the publication of Casper's 'Praktisches Handbuch der Gerichtlichen Medizin' (1) , which translated means, 'Practical Guide to Legal Medicine'. The account describes the determination of arsenic in the hair of a body exhumed 11 years after burial. The modern saga of hair analysis begins in 1954, with the publication of research conducted by Goldblum *et al.* describing the detection of barbiturates in guinea pig hair via ultraviolet spectrophotometry (after sample extraction) (2). Twenty years later Harrison *et al.* (3) described the incorporation of ^{14}C radiolabeled D-amphetamine into guinea pig hair. In a 1979 review of the potential of hair as a diagnostic tool, Maugh (4) described efforts to use hair as both a forensic tool and matrix for medical diagnoses. Original efforts to employ hair as a forensic tool sought to use trace element profiles from hair to link suspect(s) to the scene of a crime. Such efforts were soon shown to be futile due to the fact that trace element profiles vary with time and location of head hair. Evidence of severe exposure to trace elements such as lead, arsenic, cadmium, and mercury (4) was, however, obtainable. Ideas to develop elemental analysis of hair as a diagnostic tool were fairly widespread at the time. Efforts in this arena attempted to diagnose disorders such as cystic fibrosis, celiac disease, phenylketonuria, protein-calorie malnutrition (Kwashiorkor), zinc deficiency (ironically, severe zinc deficiency causes hair loss), iron deficiency, juvenile onset diabetes, and learning deficiencies. These efforts, however, did not make a significant contribution to modern medicine. Perhaps due to the excitement surrounding mineral analysis in hair, laboratories began to spring up that would offer nutritional consulting through hair analysis. Surprisingly, this practice is still under debate (5-9).

Early hair analysis for trace elements was accomplished through the use of techniques such as neutron activation analysis, photon activation analysis, atomic absorption spectroscopy, and particle-induced x-ray emission. Detection of foreign nonmetallic (i.e., organic or drug) substances in hair was, at the time, essentially precluded due to the lack of techniques sensitive enough to quantitate the low levels of drugs present in hair samples from donors who had not been given repeated, near lethal doses of the drug in question. Research into hair analysis for drugs continued, and in 1979 a seminal paper by Baumgartner *et al.* (10) demonstrated the detection of opiates in hair through the use of radioimmunoassay (RIA). In addition to their novel techniques, Baumgartner and co-workers succeeded in demonstrating the presence of opiates in hair three months after drug administration as well as time dependent drug deposition along the hair shaft. Soon the field began to grow with regular publications beginning in the early 1980s (11-15). Initial applications of hair testing focused primarily on opiates, phencyclidine, phenobarbital, and cocaine. This was probably due to the availability of antibodies against these drugs. The next major advancement involved the development of electron impact ionization mass spectrometric (EI-MS) methods for the identification of methamphetamine in hair (16). The use of this technology was soon extended to the analysis of tricyclic antidepressants (17), nicotine (17), chloroquine (18) and monodesethylchloroquine (18). Interestingly, although it was not a goal of their investigation, the study by Ishiyama *et al.* (17) provided the first evidence of a potential hair color bias in drug incorporation into hair. Their results indicate an approximate four fold greater concentration of methamphetamine in the hair of C57 black mice versus the hair of ddY white mice. The only comment made by the authors in regard to this

occurrence stated that Harrison's (3) data (which suggested that amphetamine might be incorporating into or binding to melanin in hair) was not supported by their data because they observed methamphetamine in white hair as well as black hair. Thus they suggested that drugs probably bind to protein rather than melanin. An additional improvement to the previous EI-MS methods was provided by Suzuki *et al.* (19) in applying chemical ionization techniques for mass spectrometric analysis of amphetamines in hair. This resulted in significantly better sensitivity and paved the way to modern techniques for drug detection in hair.

Anatomy and Physiology of Hair

In humans, hair formation first begins primarily on the head when an embryo is approximately 60 days old with the formation of a rudimentary dermal papilla (20). The dermal papilla is a group of specialized undifferentiated fibroblast cells, derived from the mesoderm, that initially form as a clump of cells in the dermis just below the epidermis. The entire hair follicle including associated modified structures such as sebaceous glands, are ultimately derived from the dermal papilla. After the initial cellular organization of the dermal papilla, a peg of cells begins growing into the dermis, pushing the dermal papilla deeper into the dermis and eventually forming an involution. At this stage, the forming hair shaft begins to differentiate, initiating anagen, the first phase of the hair growth cycle, discussed below. During this phase, undifferentiated keratogenic epidermal matrix cells from the dermal papilla begin to move upward. Their anatomical fate as part of the hair structure is determined by their initial position relative to the dermal papilla, which remains at the base of the hair follicle (21-24). As cells migrate upward, the hair shaft begins to form from the middle matrix cells. These cells produce

large amounts of keratin proteins and eventually harden in a process known as keratinization, which, chemically, is the result of crosslinking of sulfhydryl groups of keratin proteins to form disulfide bonds. Anatomy of the fully formed hair bulb and hair follicle with surrounding structures can be seen in Figures 1.1 (adapted from Robbins (25)) and 1.2, respectively. The ultimate chemical composition of hair varies with location on the body and between individuals, however, it may be of interest in relationship to proceeding sections, that hair consists of protein (65-95%), water (15-35%), lipids (1-9%), melanin (0.2-1.5%) (see Chapter 2), and trace amounts of minerals (0.25-0.95%) (26).

Hair follicles do not continue to grow forever. Rather, after a certain period of growth (anagen), hair follicles undergo a transitional phase, known as catagen, during which cell division halts, the base of the hair shaft keratinizes, and the bulb begins to degenerate. At this point, the hair follicle enters a resting phase, known as telogen, where no cellular proliferation occurs and the now fully keratinized hair shaft can easily be removed from the follicular canal. An increase in metabolic and proliferative activity of the matrix cells reinitiates anagen. This increase in activity is now thought to be due to the division and migration of stem cells from the bulge of the outer root sheath located near the connection point of the arrector pili muscle (27). Figure 1.3 (adapted from Paus and Cotsarelis (28)) demonstrates the relative amount of time spent in each phase of the hair growth cycle.

Routes of Drug Incorporation into Hair

Drugs can be deposited into and onto hair via a number of routes including through systemic circulation, perspiration, sebum, skin, and the external environment

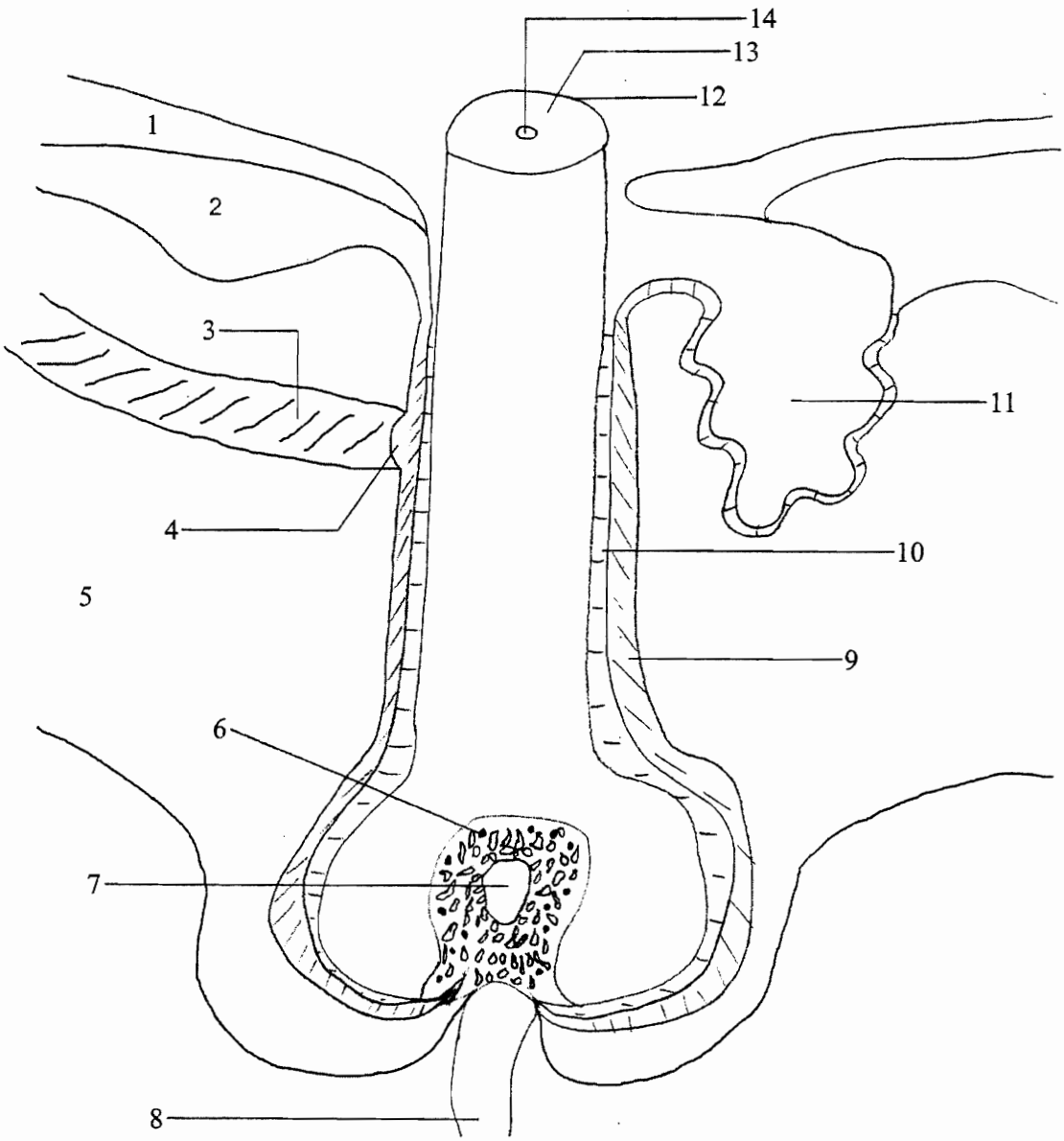

Figure 1.1 *Hair follicle anatomy.* Adapted from Robbins (25) 1) Stratum corneum 2) Epidermis 3) Arrector pili muscle 4) Bulge 5) Dermis 6) Melanocyte 7) Dermal papilla 8) Arteriole 9) Outer root sheath 10) Inner root sheath 11) Sebaceous gland 12) Cuticle 13) Cortex 14) Medulla

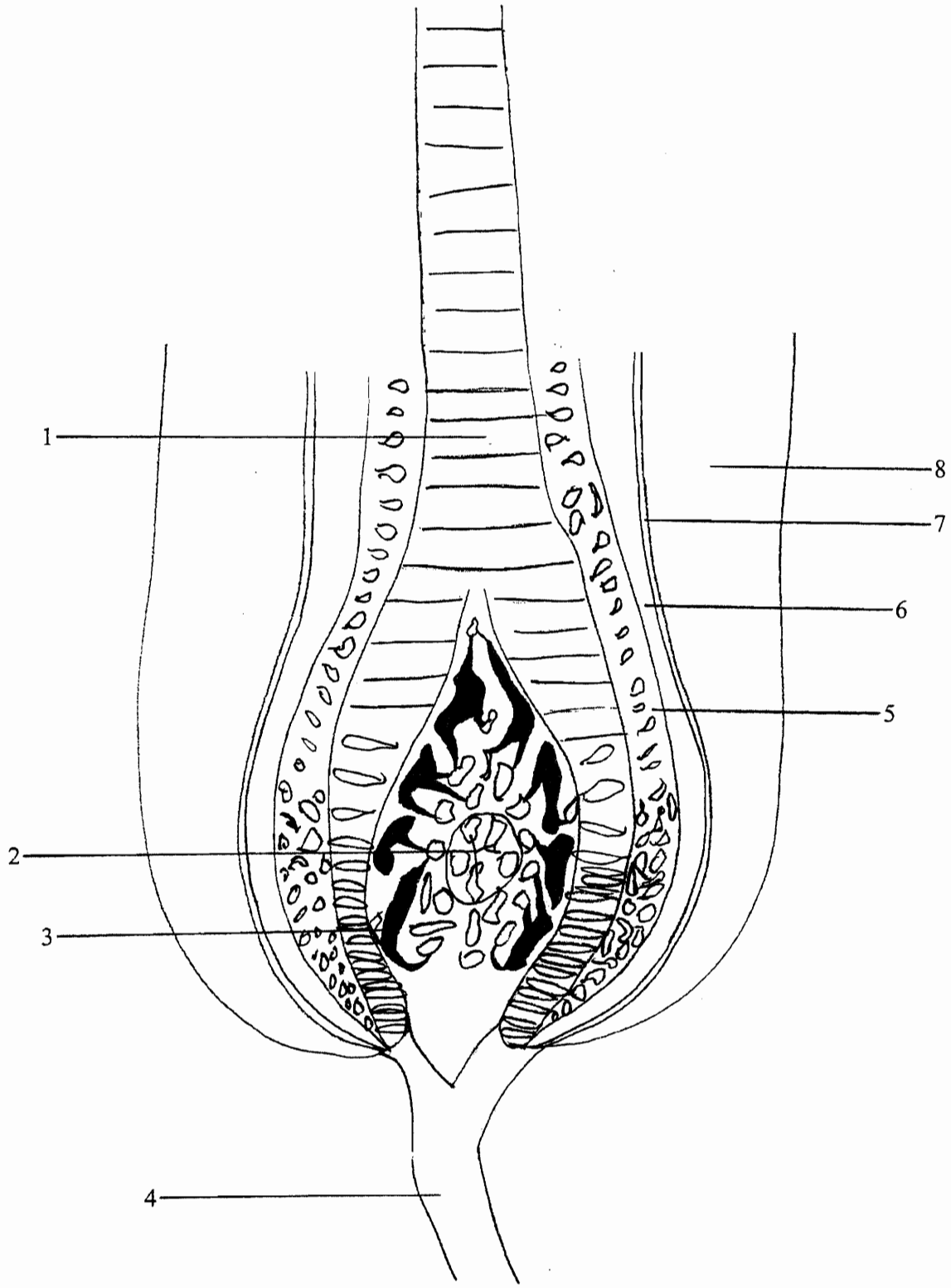

Figure 1.2 *Hair bulb anatomy.* 1) Hair shaft 2) Dermal papilla 3) Melanocyte 4) Arteriole 5) Inner root sheath cuticle 6) Inner root sheath (Huxley's layer) 7) Inner root sheath (Henle's layer) 8) Outer root sheath

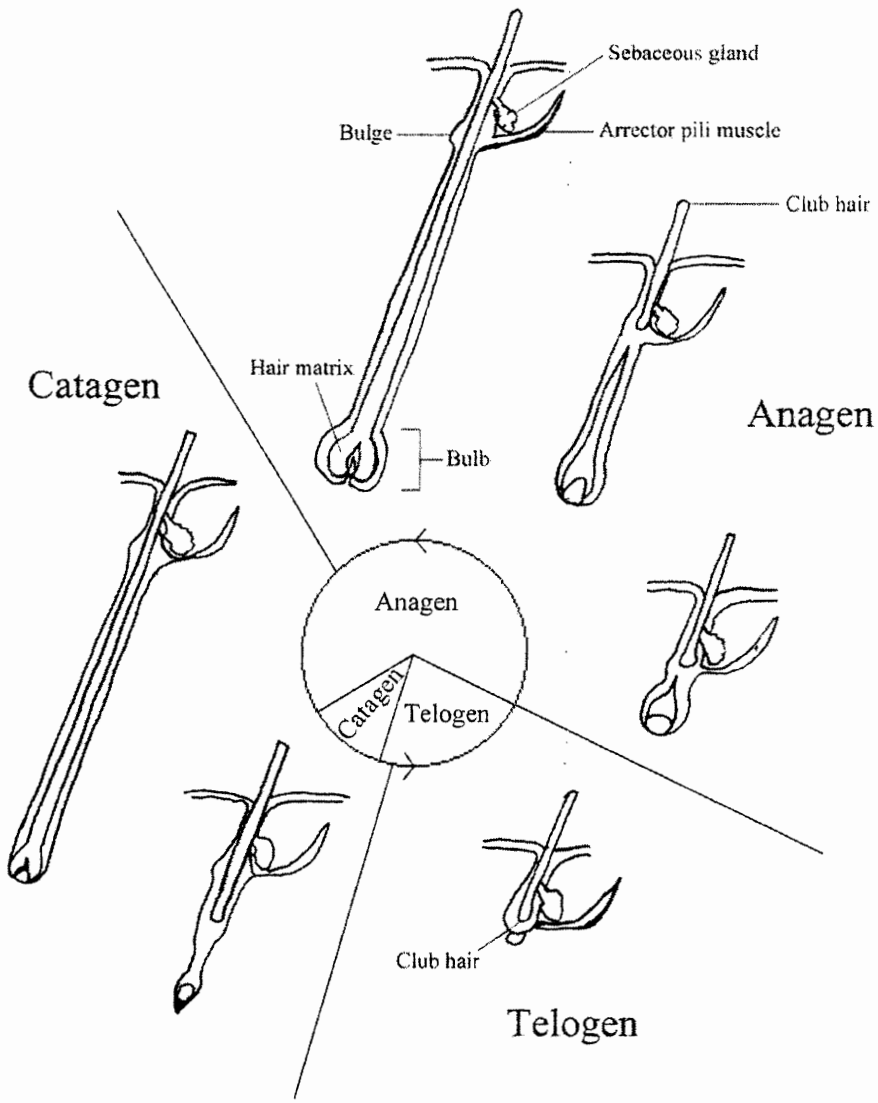

Figure 1.3 *Stages of the hair growth cycle.* Adapted from Paus and Cotsarelis (28). Hair growth begins with anagen (far right) and ends in telogen (lower right).

(29, 30). Perspiration, sebum, and the external environment can only deposit drug on the outside of the hair follicle. For most hair testing purposes this is an undesirable situation, since drug on the external surface of hair is not indicative of ingestion. In an ideal situation, hair testing would only analyze drug incorporated into hair through systemic circulation. This would allow for the least number of interferences and inconsistencies, e.g., drug from smoke or other residue in the environment, and inconsistencies due to inter-individual differences in perspiration and sebum secretion. This would also eliminate the need for hair washing procedures prior to analysis. The real situation is not ideal, however, as each of the above routes may substantially contribute to drug incorporation into hair.

Nevertheless, hair analysis relies on the fact that drugs can be incorporated from systemic circulation into hair follicles. This route for drug incorporation into hair is arguably the most important because it provides the basis for consistent, reliable measurements of drug ingestion, and, at least in rat models, is the route by which the majority of drug is incorporated into hair. (Environmental exposure is easily controlled in animal studies, and, except for the soles of their feet, rats lack sweat glands.) The simplest model for drug incorporation into hair from the bloodstream involves passive diffusion of drug from arterial capillaries to extracellular fluid to the inside of hair forming cells. Once inside the cells, the drug must be retained long enough for the cell to move up and out of the zone of differentiation and biological synthesis. While in certain drug-animal models, drugs may incorporate into hair from the bloodstream in a linear, dose-dependent manner suggestive of passive diffusion down a concentration gradient from blood into hair (31), accumulating evidence argues that this model is probably not

accurate (29). A number of drugs incorporate into hair to a greater extent than their metabolites or related compounds despite the fact that the area under the plasma concentration versus time curve (AUC) is much greater for the compounds that are barely detected in hair. For example, in various animal and human models, Δ^9-tetrahydrocannabinol (THC) (32-35), cocaine (29, 36-39), nicotine (40), amphetamine (41, 42) and 6-acetylmorphine (43), all are found in greater concentrations in hair than 11-nor-9-carboxy-Δ^9-tetrahydrocannabinol (THC-COOH), BE and ecgonine methyl ester, cotinine, N-AcAp, and morphine, respectively, while the AUCs or plasma concentrations of the metabolites (or related compounds) are much greater than the plasma concentrations of the parent compound. These data suggest that factors other than passive diffusion down a concentration gradient or even simple selective diffusion through a semipermeable membrane may be important. Factors such as selective transport of certain drug molecules into hair forming cells and binding of drugs by hair components (i.e., protein, melanin, and possibly lipids) may play major roles in determining the amount of a given drug incorporated into hair. Although little, if any, research has been conducted to determine whether hair cells may take up drugs by mechanisms other than passive diffusion through the cell membrane, a fair amount of research has been done to characterize the binding of drugs to hair components (i.e., protein (44-49), melanin (50-62), and lipids (63)). A major controversy still exists in this area, especially in relation to the ability of drugs to bind to melanin, and whether or not this can produce a hair color bias (40, 63-74).

Nakahara (75) (and others) have carried out a large amount of research to determine what physicochemical factors are most important for a drug to be incorporated

into hair. Findings indicate that the greater the melanin affinity (40, 43, 63-71), lipophilicity (41, 75), and basicity (41, 42, 75) of a drug, the more it incorporates into hair.

Melanin affinity is important because it represents a mechanism whereby significant amounts of drug can bind inside hair cells and be retained as the cells keratinize and move up into the hair shaft. A large number of drugs have been shown to bind to melanin, including amphetamine (55, 56, 76), chloroquine (51, 53, 57), chlorpromazine (47, 48, 51, 54), cocaine (55, 56, 76), phencyclidine, methylenedioxymethamphetamine (43), tricyclic antidepressants (56), 1-methyl-4-phenylpyridinium (MPP^+) (77, 78), clenbuterol, nortestosterone, diethylstilbesterol (54), paraquat (50, 51), and streptomycin (79) to name a few. Even some cationic metals such as iron, manganese, copper, lead, nickel, magnesium, zinc, cadmium, aluminum, scandium, lanthanum, and indium (51, 80-83) are documented to bind to melanin. The exact chemical nature of drug-melanin binding is not well understood, but it is thought to involve various types of binding interactions between drugs and melanin orthoquinones, phenolic groups, carboxylic acids, indole-amines, and/or van der Waals interactions between stacked indole units (50, 51, 53, 83). Because of their affinity for certain types of drugs (e.g., basic drugs), melanins appear to play a major role in the incorporation of such drugs into pigmented hair (40, 63-71). Interestingly, drugs can also bind to melanins in locations throughout the body other than hair. In fact, many of these cases have implicated toxicological effects (58). For example, drug binding to the uveal tract of the eye (84, 85), ear (cochlear) (86, 87), and neuromelanin (77, 78, 88, 89) has been implicated in the negative toxic effects of the drugs to surrounding tissues. Lipophilicity

is important because it is thought to allow permeation through biomembranes such as in capillary beds and hair cell membranes. Interestingly, Nakahara (43) showed that for 19 drugs, when melanin affinity (K_a) is multiplied by lipophilicity (log P, see Kaliszan *et al.* (90)) and correlated to the hair incorporation ratio ((ICR) = [Drug in Hair]/Plasma AUC), an R^2 value of 0.979 is obtained. Basicity is probably related to melanin affinity, i.e. positively charged, basic drugs bind best to negatively charged, acidic melanin. The isoelectric point of hair is approximately 3.7 (91) and is probably mostly derived from the acidity of melanin, however, acidic sites on hair keratin cannot be ruled out as drug binding sites (45). Data from Dehn *et al.* (92) suggest that drugs such as nicotine and cotinine may be covalently incorporated into the melanin polymer. While this phenomenon is of interest from a biochemical standpoint, it cannot contribute to drug detection in hair because the drug molecules would have to be cleaved during the extraction process at the exact carbon-carbon juncture where they were initially joined to the melanin polymer. Covalently bound compounds would not be detectable with currently available techniques.

Chemistry, Anatomy, and Physiology of Melanins

The two critical ingredients for cellular biosynthesis of melanin are the amino acid tyrosine and the rate limiting enzyme tyrosinase. In the Golgi apparatus-derived (93) melanosome, tyrosine undergoes a series of oxidations to produce both the black colored eumelanin and the reddish-brown colored pheomelanin polymers (Figure 1.4). The structures of eumelanin and pheomelanin are not shown because they are varied and not well characterized. Eumelanin is a polymeric combination of carbon-carbon linked indolequinones and carboxylated pyrroles derived primarily from 5,6-dihydroxyindole

Figure 1.4 *Biosynthetic pathways of (A) eumelanin and (B) pheomelanin.*

A

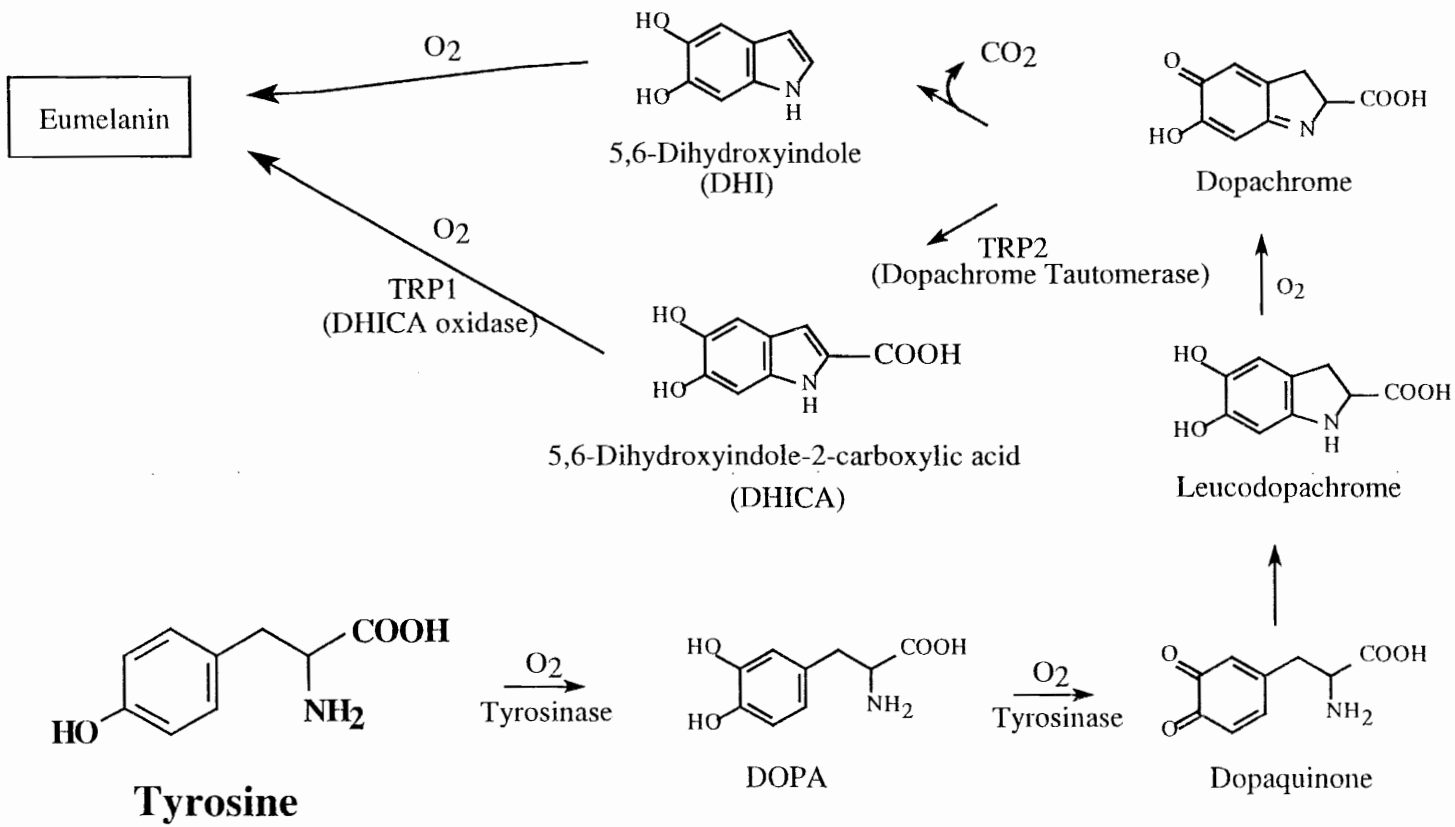
Eumelanin
O2
5,6-Dihydroxyindole
(DHI)
CO2
Dopachrome
COOH
O2
TRP1
(DHICA oxidase)
TRP2
(Dopachrome Tautomerase)
O2
5,6-Dihydroxyindole-2-carboxylic acid
(DHICA)
Leucodopachrome
Tyrosine
O2
Tyrosinase
DOPA
O2
Tyrosinase
Dopaquinone

B

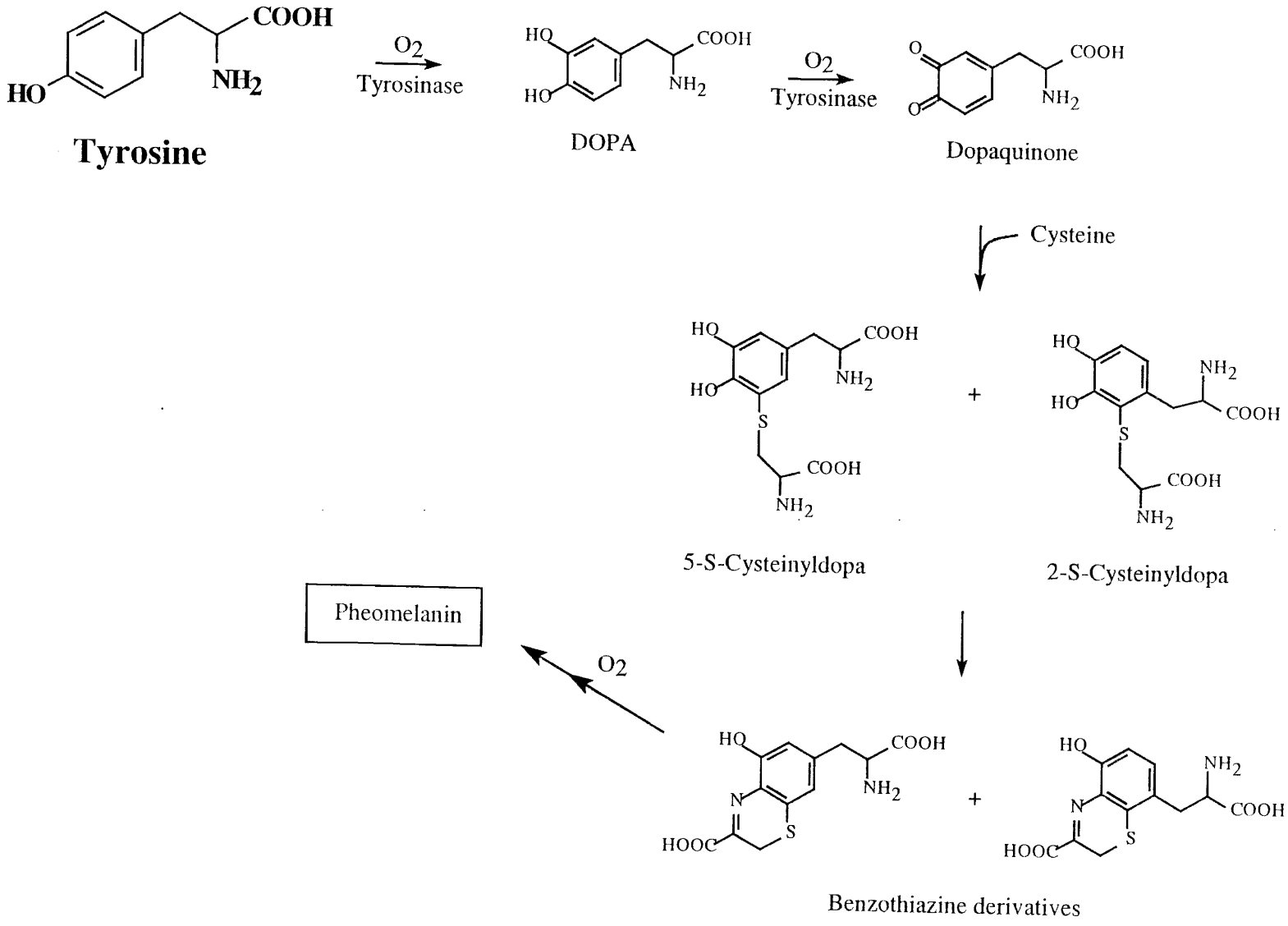
HO
COOH
NH2
O2
Tyrosinase
Tyrosine
DOPA
Dopaquinone
Cysteine
5-S-Cysteinyldopa
2-S-Cysteinyldopa
Pheomelanin
Benzothiazine derivatives
HOOC
S
N

(DHI) and 5,6-dihydroxyindole-2-carboxylic acid (DHICA), while pheomelanin also includes related benzothiazine units derived primarily from 2-cysteinyl-S-Dopa (2-CysDOPA) and 5-cysteinyl-S-Dopa (5-CysDOPA) (94, 95).

Melanocytes derived from the neural crest associate with the matrix cells in a relationship whereby melanin granules, known as melanosomes, are transferred to the keratogenic matrix cells (96-98). This process, which gives hair its color, is thought to occur through both exocytosis of melanosomes and uptake by keratinocytes and/or keratinocyte phagocytosis of invading melanocyte dendrites (93, 98-102). As with most other biological processes, melanin biosynthesis is under the control of hormones, receptors, and enzymes. Pro-opiomelanocortin is produced in the pituitary gland and (as relates to melanogenesis) is cleaved to produce adrenocorticotropin and modified to produce α-melanocyte stimulating hormone (103). These peptide hormones activate G-protein coupled melanocortin receptors (104) which activate adenylyl cyclase and lead to an increase in intracellular cyclic adenosine monophosphate (cAMP) (103, 105). cAMP activates protein kinase C beta which, in turn, activates tyrosinase through phosphorylation of serine residues in the cytoplasmic domain of the melanosomal-membrane bound protein (105, 106).

Melanogenesis is also regulated by light during the tanning process. Light produces two tanning phases—immediate tanning and delayed tanning (107). Melanin formed during immediate tanning appears to be structurally different from constitutive melanin. Although exact structures are not known, it is derived from photo-oxidation polymerization products of melanogenic precursors such as DHI and DHICA. Its formation is oxygen dependent (107). Delayed tanning is not oxygen dependent and

produces a longer lasting tan due to increased melanin synthesis, melanin transfer to, and distribution in epidermal cells (107). Although the biochemical pathway for delayed tanning is not well understood, studies by Schallreuter and co-workers (104) suggest that UVB can release TNF-α, which induces GTP-cyclohydrolase I, which, in turn, synthesizes L-erythro-5,6,7,8-tetrahydrobiopterin (6BH4), a cofactor for phenylalanine hydroxylase which converts phenylalanine to tyrosine—the amino acid required for melanin synthesis. 6BH4 is known to inhibit tyrosinase by a noncompetitive allosteric mechanism (108), but UVB light can photo-oxidize 6BH4 to 7,8-dihydroxanthopterin, reactivating tyrosinase and overall enhancing pigmentation (104, 109). Evidence presented by Palumbo *et al.* (110), suggests that in addition to its well known copper cofactor, tyrosinase may also require Fe^{2+} to act as a redox exchanger with the cupric ions at the active site of the enzyme. The summary of scientific literature available on tyrosinase research suggests that it is indeed a complexly regulated enzyme. Other, perhaps independent, pathways may also be involved in delayed tanning. Additional data suggest that DNA damage induced by UV light can induce melanin production (111). Interestingly a primary mediator of this response appears to be the thymine dinucleotides produced during DNA excision repair after UV irradiation. Presented to cells alone in the absence of UV light, such dinucleotide dimers can induce melanin production that closely mimics that induced by UV irradiation itself. The biochemical pathways underlying this process, as well as UV light-induced tanning in general, however, remain to be confirmed and fully elucidated.

Modern Hair Testing

Applications for Hair Testing

Even though all the time course, metabolic, and potential hair color bias effects have not been completely worked out for hair testing, hair testing is now the most widely accepted alternative to urinalysis for drug testing in the United States (112). Among hair testing's applications include preemployment screening, drug recidivism screening for patients in antiabuse programs, athlete testing, school drug testing, and home hair testing kits (for parents to screen their children). Hair testing has been applied to virtually every drug-testing situation. An interesting proposal for the use of hair testing would be in compliance monitoring programs (113-119). The purposes of such analyses would include monitoring patient compliance of prescribed medications (i.e., neuroleptics, antiepileptics, buprenorphine, and methadone) and even potentially using an "inert" drug such as ofloxacin that moves up in the hair shaft with time to track another drug's ingestion during a specified monitoring period. In theory, drugs stay with the hair cells they incorporate into and move along with the hair shaft as it grows. This phenomenon has been documented for ofloxacin (120), rhodamine, and fluorescein (49).

Advantages of Hair Testing

There are two primary advantages that hair testing provides over traditional urinalysis and plasma testing methods. First, hair testing is less invasive; collecting a few hairs from the scalp takes less effort for both laboratory personnel and the patient than does acquiring a urine or plasma specimen. Integrity of the sample can also be ensured because laboratory personnel (or potential employers) can collect the sample directly from the subject without the difficulties of having to trust the subject or having to observe

urination. Second, hair testing provides a larger window of detection than does plasma or urinalysis. A commonly sited time frame for detection of common drugs of abuse is 90 days (112), although this has not been rigorously tested for every drug tested for in hair.

Disadvantages of Hair Testing

There are a few difficulties specific to hair testing that are not encountered with traditional plasma and urine testing. First, drugs from the environment (i.e., smoke) can adhere to the outside of hair and produce a positive test result even if no drug has been ingested systemically. This can be a problem with all drugs that are smoked (which, unfortunately, includes all the major drugs of abuse). In theory it may be possible to circumvent this difficulty by applying a proper wash procedure to the hair prior to analysis. The wash procedure must be documented to wash off only external drug contamination (without removing systemically incorporated drug, presumably inside the hair shaft) and to remove all external contamination. Paulsen *et al.* (121) have demonstrated that several currently employed laboratory hair wash procedures (including methanol, 0.1 M phosphate, pH 6.0 and pH 8.0, and isopropanol and phosphate buffer, pH 5.5) can significantly alter the reported levels of cocaine in hair from systemic incorporation. Unpublished data from the Center for Human Toxicology at the University of Utah indicate that both rat and human hair exposed to cocaine freebase smoke, even after washing with phosphate buffer, pH 5.5 and methanol, contains enough cocaine to potentially be reported positive for drug abuse—if benzoylecgonine (BE) is not taken into account. If not handled carefully and appropriately, the former phenomenon can lead to false negative results and the latter to false positive results. Therefore special care to properly interpret hair testing results, e.g., employing a BE to

cocaine minimum ratio (that is, a metabolite to parent drug minimum ratio) for a positive test and performing thorough validation studies, must be taken to produce accurate hair testing reports.

In addition to smoke, drugs can also be deposited on the hair from perspiration and sebum. It would not present a problem if this route of incorporation produced a positive test, but interindividual differences in the concentration of drug in perspiration and sebum and the amount of perspiration and sebum secreted are just starting to be investigated (122, 123) and may play significant roles in determining hair test outcomes if wash procedures are routinely employed.

A second major difficulty involving hair testing is the effect of hair treatments such as bleaching and dyeing on hair test outcomes. Included in this category is head shaving, which, if head hair is the only validated hair type for drug testing, could easily provide a means of evading hair testing. The effects of hair treatments such as bleaching and dyeing on hair drug test outcomes are not well investigated. However, studies by Kidwell and DeLauder (124, 125) suggest that cosmetic hair treatments may alter the physical properties of hair, thereby altering its drug binding capacity and increasing its accessibility to external contamination; thus potentially altering a hair test outcome.

A third problem plaguing hair testing and a major focus of this dissertation is the potential for hair color bias; that is, the phenomenon where more drug is incorporated into dark hair than light colored hair—all else held equal. Hair color bias arises for a drug because of its binding affinity for the hair melanin itself. As mentioned above, because of their affinity for certain types of drugs (e.g., basic drugs) (50-62), melanins appear to play a major role in the incorporation of such drugs into pigmented hair (40,

63-71). The existence of a hair color bias means that for hair testing to be fair to all members of society, hair testing for drugs that demonstrate a hair color bias must include normalization to the amount of melanin in hair—especially, and perhaps specifically, the amount of eumelanin in hair. Studies at the Center for Human Toxicology at the University of Utah (126) have shown that incorporation of codeine into human hair is highly correlated with the amount of eumelanin in hair while the amount of pheomelanin does not seem to matter much. This is in agreement with studies to be presented later in this dissertation showing that pure eumelanins bind basic drugs but that pure pheomelanins do not bind basic drugs.

In summary, hair testing provides advantages over traditional drug testing techniques that make it a very attractive alternative matrix for drug detection. As hair testing technology becomes more popular, however, we must make sure not to extend hair testing beyond our fundamental knowledge of the chemical and biological processes involved in drug incorporation into hair. Only in this manner can society be assured of fair and accurate drug testing outcomes from this innovative technique.

Research Objectives

The overall objectives of this research were to assess the ability of basic and non-basic related drugs to incorporate into black and white hair, bind to melanin, and move into and out of hair cells. The following hypotheses and specific aims were designed to accomplish these goals:

1. Hypothesis: The amount of melanin in hair is directly proportional to the amount of systemically administered codeine that is incorporated into hair.

Specific Aim 1a: Establish subtype specific melanin assays for quantitating the amounts of DHI, DHICA, 2-CysDOPA, and 5-CysDOPA-derived melanin in biological melanin-containing samples.

Specific Aim 1b: Correlate the amount of each melanin subtype in hair to the amount of codeine incorporated into the hair through linear regression analysis.

2. Hypothesis: Amphetamine will show a hair color bias while its non-basic analog N-AcAp will not.

Specific Aim 2: Determine the concentrations of amphetamine and N-AcAp in black and white rat hair (from the same animal) after systemic administration of the drugs.

3. Hypothesis: Drugs that demonstrate a hair color bias will bind to DHICA-melanin with the same affinity, but greater capacity than to DHI-melanin, and with lower affinities and capacities for 2-CysDOPA-melanin and 5-CysDOPA-melanin. Analogs of these drugs that do not demonstrate a hair color bias will not bind to any type of melanin.

Specific Aim 3: Determine the *in vitro* binding affinities and capacities of cocaine, BE, amphetamine, and N-AcAp for DHICA-melanin, DHI-melanin, mixed DHI/2-CysDOPA-melanin, mixed DHI/5-CysDOPA-melanin, and pure 5-CysDOPA-melanin.

4. Hypothesis: Drugs that incorporate into hair to greater extents than their net-neutral congeners will be taken up faster, be effluxed slower, and have higher equilibrium uptake concentrations than their congeners—in keratinocytes, PM, and NPM. In addition, basic drugs will be transported at the same rate into PM and NPM, but will have higher equilibrium concentrations in PM than their nonbasic analogs. Finally, plasma protein binding will not completely account for the drug to metabolite or congener ratio differences seen in plasma and hair. That is, hair cell selectivity (as opposed to free drug

concentration in plasma) is suspected as the major factor in determining how much of a drug gets into hair cells.

Specific Aim 4a: Profile the influx and efflux time courses of cocaine, BE, amphetamine and N-AcAp in cultured keratinocytes, PM, and NPM, and relate this data to *in vivo* data for drug incorporation into hair.

Specific Aim 4b: Determine the extent of plasma protein binding of cocaine, BE, amphetamine, and N-AcAp to assess the relative amounts of free cocaine vs. free BE in plasma (after cocaine administration), and free amphetamine vs. free N-AcAp (after equi-dosing of either drug).

CHAPTER 2

RELATIONSHIP OF MELANIN DEGRADATION PRODUCTS TO ACTUAL MELANIN CONTENT: APPLICATION TO HUMAN HAIR[a]

Numerous studies have confirmed that melanin pigments play an important role in the incorporation of drugs into hair (3, 40, 63-65, 69-71, 127, 128). This may lead to a hair color bias in the interpretation of hair testing results. The purpose of this investigation was to determine the yield of melanin subtype-specific chemical markers produced from chemical degradations of pure melanin subtypes, then apply this information to profile the melanin content and character of a range of human hair types.

Melanins are highly heterogeneous pigment polymers that give hair and skin their color. These pigments are typically divided into two categories: the black eumelanins and the reddish-brown pheomelanins. Eumelanin is composed of the tyrosine-derived indole units DHI and DHICA (129, 130) (Figure 2.1). Pheomelanin is composed of tyrosine and cysteine-derived units, generally thought to be constructed into benzothiazine monomers that make up the pheomelanin polymer (96). 5-CysDOPA and 2-CysDOPA are thought to be the major pheomelanin building blocks (132) (Figure 2.1). It must be kept in mind, however, that *in vivo*, melanins are generally not homopolymers

---

[a] Relationship of Melanin Degradation Products to Actual Melanin Content: Application to Human Hair" by Chad R. Borges *et al.*, from Analytical Biochemistry, Volume 290, 116-125, copyright © 2001 by Academic Press, reprinted, with modification, by permission of the publisher.

Figure 2.1 *Biological synthesis and chemical degradation pathways of: A) eumelanin and B) pheomelanin.* (Adapted from Ozeki *et al.* (131) and Kolb *et al.* (132))

A

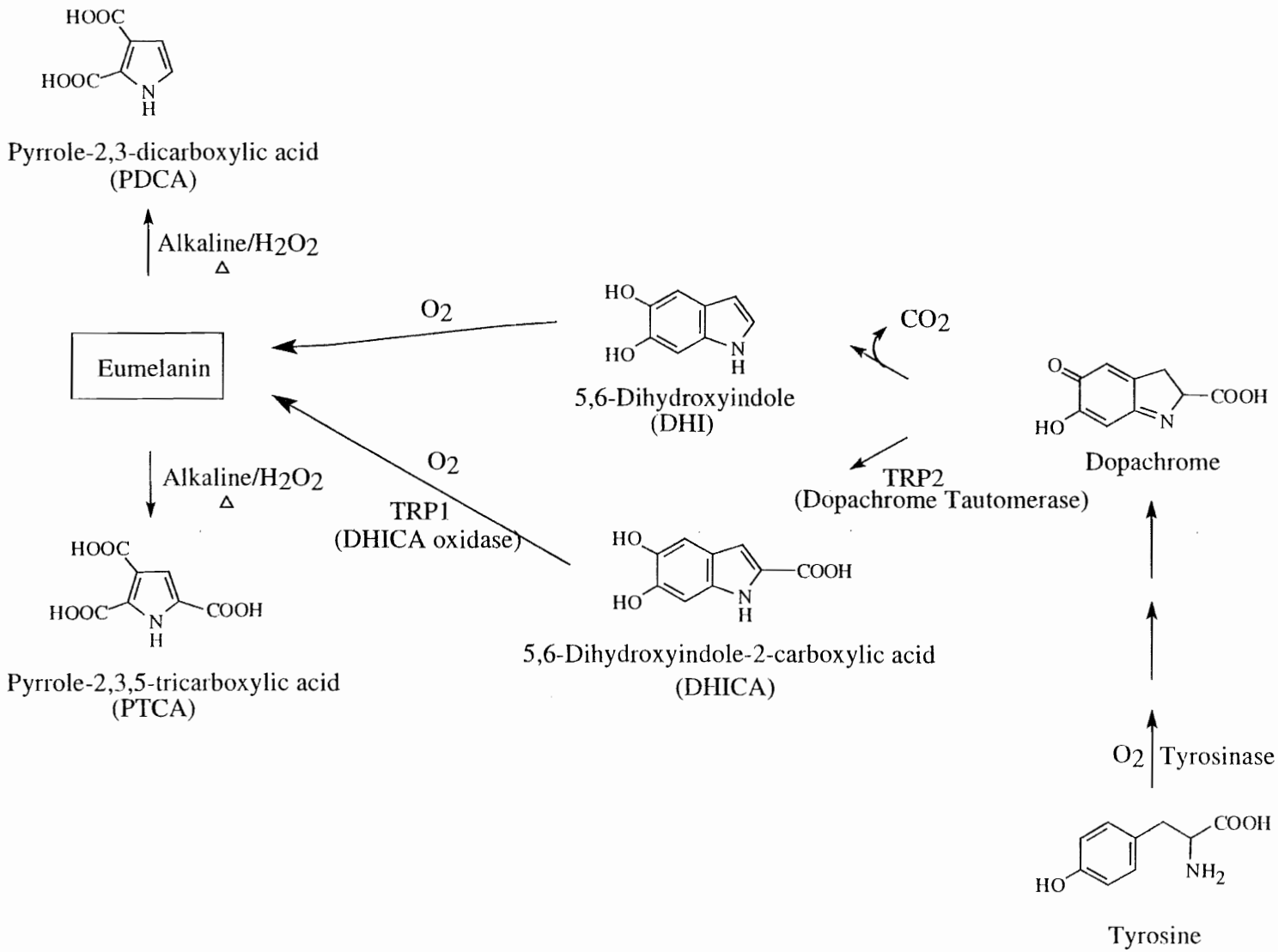
HOOC
HOOC
N
H
Pyrrole-2,3-dicarboxylic acid
(PDCA)
Alkaline/H2O2
Δ
O2
Eumelanin
HO
HO
N
H
5,6-Dihydroxyindole
(DHI)
CO2
O
HO
COOH
N
Dopachrome
TRP2
(Dopachrome Tautomerase)
Alkaline/H2O2
Δ
O2
TRP1
(DHICA oxidase)
HOOC
HOOC
COOH
N
H
Pyrrole-2,3,5-tricarboxylic acid
(PTCA)
HO
HO
COOH
N
H
5,6-Dihydroxyindole-2-carboxylic acid
(DHICA)
O2
Tyrosinase
COOH
HO
NH2
Tyrosine

B

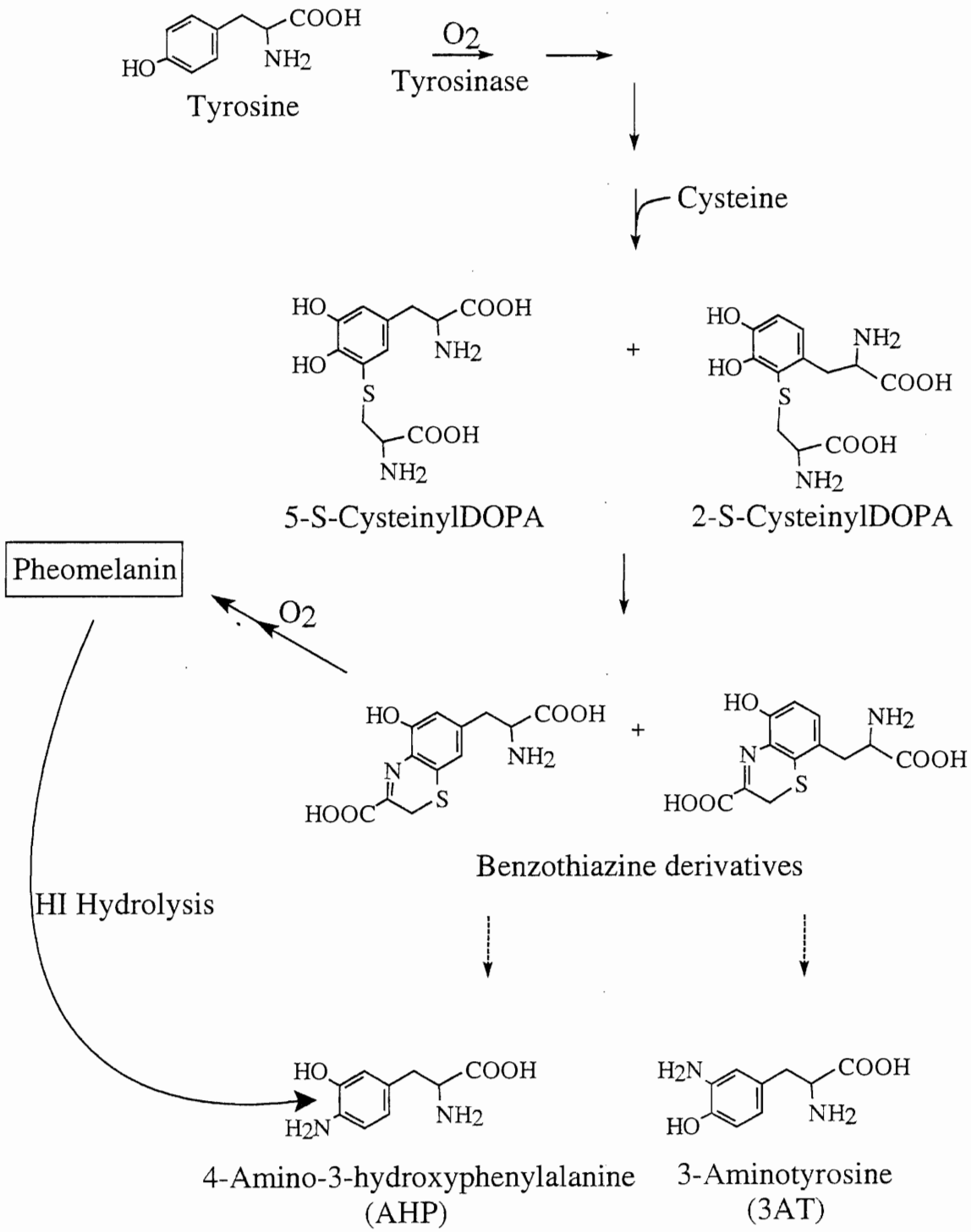
Tyrosine
O2
Tyrosinase
Cysteine
5-S-CysteinylDOPA
2-S-CysteinylDOPA
Pheomelanin
O2
Benzothiazine derivatives
HI Hydrolysis
4-Amino-3-hydroxyphenylalanine
(AHP)
3-Aminotyrosine
(3AT)

of a single building block or even made solely from eumelanin or pheomelanin monomers—rather they are mostly ill-defined heteropolymers made up of both eumelanin and pheomelanin building blocks (96).

Melanins are biologically synthesized through what is thought to be a free radical-mediated process (133-135) in the melanosomes of melanocytes with the aid of the enzyme tyrosinase. In the cell, melanins are covalently linked to proteins to produce structures referred to as melanoproteins. Once melanoproteins are made they are transferred to keratinocytes (96, 136) where they are effectively displayed on the body's surface. While the biological role of melanin is not completely understood, it is known that eumelanin in dark skinned individuals serves in a photo-protective manner against damaging ultraviolet light. On the other hand, large amounts of pheomelanin in light skinned/freckled individuals appears to make them more susceptible to skin cancer (137-139). The natural role of melanin in hair, however, remains unknown.

It is not a "natural" role, but recent studies have shown that melanin plays a crucial role in binding many drugs that are incorporated into hair. Interestingly, a number of drugs with a basic nitrogen moiety such as cocaine (63), methadone, (140), codeine (127), phencyclidine (69), haloperidol (70), ofloxacin (71), and nicotine (40) have all been shown to incorporate in greater amounts into hair of darker vs. lighter pigmentation. At the same time the nonbasic, but nitrogen-containing drug phenobarbital has been shown to have no preferential incorporation into hair of darker pigmentation over hair of lighter pigmentation (65). The theme for preferential incorporation into hair of darker pigmentation appears to be a basic nitrogen moiety. This is not surprising when one considers both the relatively high content of negatively charged carboxyl groups on

melanin (96, 129) and the fact that substances with cationic properties such as amines and metals are bound to melanin through ionic interactions (58, 83).

If the role of melanins in drug uptake into hair is to be fully understood, the chemical nature and quantity of the melanins in hair must be elucidated. Sensitive HPLC methods for characterizing specific melanin subtypes, that is, DHI and DHICA in eumelanin, and 5-CysDOPA and 2-CysDOPA in pheomelanin, have been developed (130, 132). These methods involve chemically degrading eumelanins and pheomelanins with hydrogen peroxide and hydriodic acid, respectively, to produce PDCA, PTCA, AHP, and 3AT (Figure 2.1)—chemical markers for DHI, DHICA, 5-CysDOPA, and 2-CysDOPA, respectively.

This chapter reports the yields of PDCA, PTCA, AHP, and 3AT that are produced upon alkaline hydrogen peroxide or hydriodic acid degradation of melanins made solely from monomers of DHI, DHICA, 5-CysDOPA, or 2-CysDOPA, using modified versions of the original degradation methods (130, 132, 141). The eumelanin assay was modified to include sodium hydroxide as the alkaline agent. This permits complete degradation of hair samples during the incubation time. Thus the yields for PDCA and PTCA that were previously reported (130) for this assay needed to be re-determined. The previously reported yield for combined 3AT and AHP from 5-CysDOPA melanin was 20% (141). Individual yields from 3AT and AHP from 2-CysDOPA melanin and 5-CysDOPA melanin, respectively, are now reported. To ensure accuracy when analyzing biological samples, cross-reactivity studies were conducted to account for production of chemical degradation markers from unexpected sources. The modified methods and newly determined yields were used to determine the melanin subtype composition of a variety

of human hair samples. Finally, the melanin content was correlated to codeine incorporation to assess any possible relationship between the two variables.

Materials and Methods

Materials

Tyrosinase, 3AT, hydriodic acid, and hydrogen peroxide were purchased from Sigma Chemical Co. (St. Louis, MO). Hypophosphorous acid (H_3PO_2) was purchased from Aldrich Chemical Co. (Milwaukee, WI). DHI and DHICA were made according to the method of Wakamatsu and Ito (142). 5-CysDOPA and 2-CysDOPA were made according to the method of Ito *et al.* (143). PDCA and PTCA were made according to the method of Ito and Wakamatsu (130). AHP was isolated from hydriodic acid hydrolyzed 5-CysDOPA melanin by the solid phase extraction method described below for extraction of AHP and 3AT from hydriodic acid hydrolysates, but using 2 M HCl instead of 0.3 M KCl to elute AHP from the columns. Eumelanins were made according to the method of Ito *et al.* (144) and pheomelanins were made according to the method of Ito and Fujita (141). The structure and purity of all synthetic compounds (except melanins) were confirmed by NMR and/or mass spectrometry (see Appendix). ^{1}H NMR spectra were obtained on a Bruker AF-200 MHz spectrometer. Mass spectra for synthetic compounds were obtained with a HP 1100 series LC/MSD mass spectrometer in FIA mode equipped with an electrospray ion source. All other chemicals used were of the highest purity available.

Melanin Analysis

Melanins were prepared for analysis by homogenization in water at a concentration of 2 mg/ml using a glass homogenizer operated by a drill press. Hair was cut into small (< 2 mm) pieces prior to being weighed out. Typically 0.2 mg melanin and 5 mg hair were used for analysis.

Eumelanin analysis. Samples were chemically degraded then analyzed for PDCA and PTCA via the method of Ito and Wakamatsu (130) with modifications: To a given sample (~5 mg) in 100 µl water in a screw-capped tube was added 820 µl 0.5 M NaOH, 80 µl 3% H_2O_2, and 40 nmol phthalic acid as an internal standard. Samples were then heated in a boiling water bath for 20 min. After cooling, 20 µl 10% Na_2SO_3 and 250 µl 6 M HCl were added. Samples were then extracted twice with 7 ml ethyl acetate. The ethyl acetate was dried under a stream of air at 45 °C and the residue redissolved in 1 ml starting HPLC mobile phase. HPLC analysis was carried out with a Waters 600E multisolvent delivery system equipped with a Waters 600 controller and Waters 717plus autosampler. One hundred microliter samples were injected onto a Phenomenex (Torrance, CA) Luna 5 µm C18 250 x 4.6 mm column at a temperature of 55 °C. Analytes were detected with a Varian 9050 variable wavelength UV detector set at 280 nm. HPLC mobile phase consisted of 0.01 M potassium phosphate buffer, pH 2.1, and methanol at a flow rate of 0.8 ml/min under the following gradient: 98%/2% Aqueous/organic ramped evenly from time 0 to 14 min to 40%/60% aqueous/organic, held at 40%/60% aqueous/organic for 6 min followed by ramping back to 98%/2% aqueous/organic over 5 min. Amounts of PDCA and PTCA were quantitated using PDCA:phthalic acid and PTCA:phthalic acid peak height ratios compared to a standard

curve made from pure PDCA and PTCA standards subjected to alkaline hydrogen peroxide degradation.

Pheomelanin analysis. Samples were analyzed for pheomelanin content according to the method of Kolb *et al.* (132) with modifications. To a 100 µl suspension of melanin (0.2 mg) or hair (5 mg) in water placed in a screw-capped tube was added 500 µl 57% HI, 20 µl 50% H_3PO_2, and 20 nmol L-α-methylDOPA (L-α-MD) as an internal standard. Samples were capped tightly and hydrolyzed at 130 °C in an oil bath for 16 hrs. After cooling, samples were evaporated under reduced pressure in a Savant (Holbrook, NY) Speed-Vac SPD121P concentrator at 55 °C. Users of this device should note that HI can corrode the top of the lower magnet assembly and thus eventually compromise the vacuum established in the concentrator. Dried residue was redissolved in 1 ml 0.05 M lithium phosphate buffer, pH 4.0, but not adjusted to pH 4.0. AHP and 3AT were extracted with aromatic sulfonic acid (SCX) solid phase extraction (SPE) columns (International Sorbent Technology, Mid Glamorgan, U.K.) containing 100 mg sorbent and a 1 ml reservoir volume. SPE columns were washed with 1 ml methanol (2x), and then 1 ml lithium phosphate buffer (3x) prior to sample application. Columns were washed with 1 ml water (2x) then eluted with 2 ml 0.3 M KCl, pH 8.5. Twenty microliters of eluant were injected into the same HPLC system used for eumelanin analysis, but equipped with a Waters 464 pulsed electrochemical detector equipped with a glassy carbon electrode set at +400 mV relative to a Ag/AgCl reference electrode. Mobile phase consisted of 99% 0.01 M potassium phosphate buffer, pH 5.7 containing 1 mM sodium octanesulfonate, and 0.1 mM disodium EDTA / 1% methanol at a flow rate of 0.9 ml/min. Amounts of AHP and 3AT were quantitated using AHP:L-α-MD and

3AT:L-α-MD peak height ratios compared to a standard curve made from pure AHP and 3AT standards subjected to hydriodic acid hydrolysis.

Statistical Analysis

Comparisons between groups were made with a two-tailed Student's t-test assuming homogeneity of variances. Results significant at $p \leq 0.05$ are reported.

Results

Degradation product yields

Representative chromatograms from melanin samples obtained from alkaline hydrogen peroxide degradation and hydriodic acid hydrolysis are shown in Figures 2.2A and B. The small PDCA peak height is explained by the relatively low yield of PDCA. Degradation product yields from their respective pure melanins as well as overall assay precision can be seen in Table 2.1. Degradation product yields are based on a mass / mass ratio of the amount of degradation product detected / amount melanin degraded. As seen from these data, yields of melanin degradation products are quite consistent. To demonstrate assay linearity with different sample sizes, varied amounts of both hair and melanin were subjected to both eumelanin and pheomelanin analysis. As shown in Figure 2.3 and Table 2.2, increasing amounts of melanin or hair produce linearly increasing amounts of melanin degradation markers. Figure 2.3 demonstrates that as increasing amounts of eumelanin are oxidized, linearly increasing amounts of PDCA and PTCA are produced. Table 2.2 shows that in general, linear relationships are found for plots of the amount of degradation marker produced vs. the amount of pure melanin subtype degraded, and for plots of the amount of melanin subtype found in a hair sample

Figure 2.2 *Sample chromatograms from melanin chemical degradation:* A) Alkaline hydrogen peroxide degradation of 0.2 mg melanin made from 75% DHI / 25% DHICA (w/w). B) Hydriodic acid hydrolysis of 25 μg melanin made from 50% 5-CysDOPA / 50% 2-CysDOPA (w/w) (100 nA full scale).

A

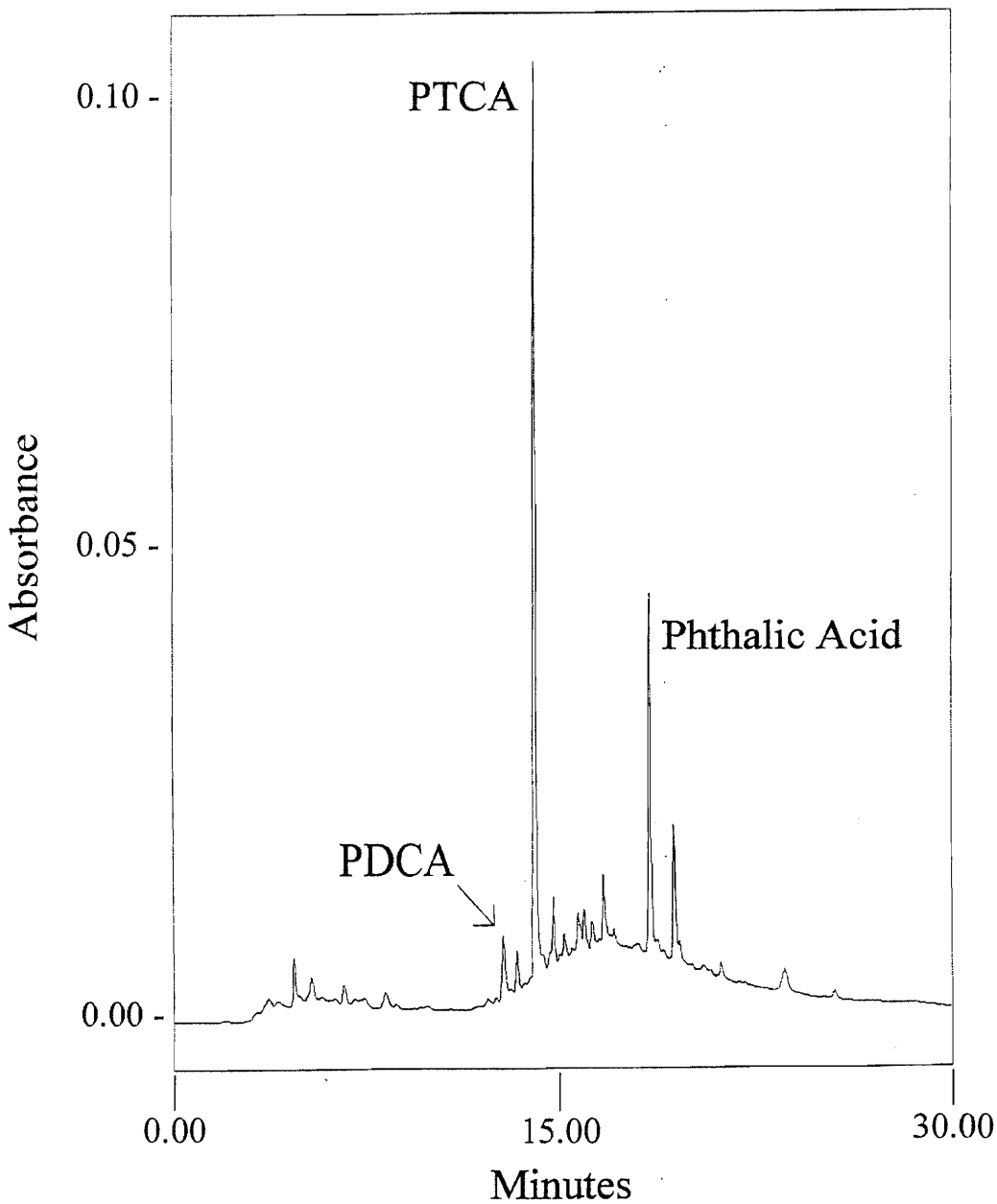
0.10 -
0.05 -
0.00 -
Absorbance
PTCA
Phthalic Acid
PDCA
0.00
15.00
30.00
Minutes

B

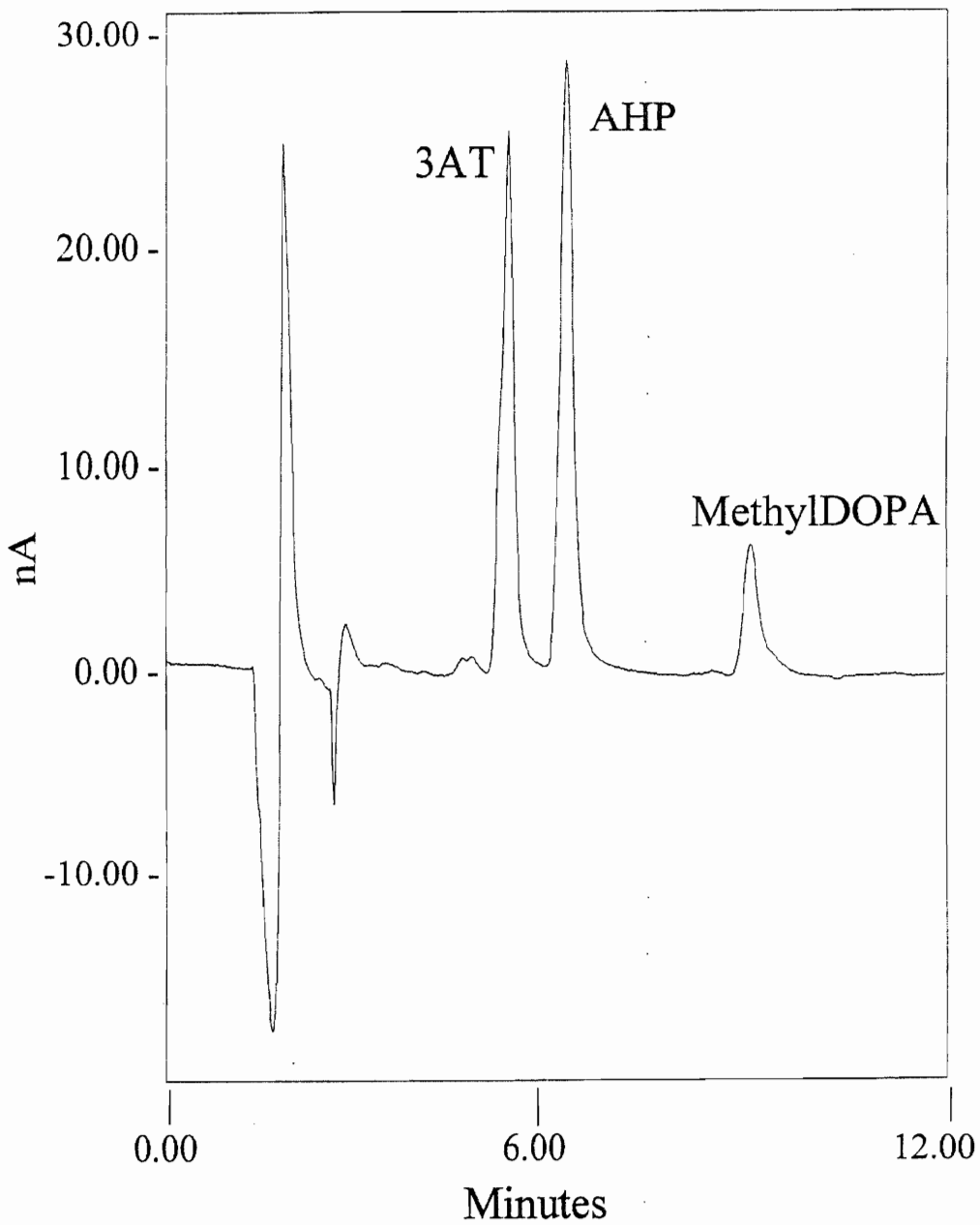
30.00
20.00
10.00
0.00
-10.00
nA
3AT
AHP
MethylDOPA
0.00
6.00
12.00
Minutes

Table 2.1

Percent yield of degradation markers from pure melanins and assay precision with human hair samples.

	PDCA Yield	PTCA Yield	AHP Yield	3AT Yield
Melanins[b]				
Intra assay[c]	0.37% ± 0.007%	4.5% ± 0.21%	23% ± 2.0%	16% ± 0.52%
Inter assay[d]	0.37% ± 0.025%	4.8% ± 0.22%	23% ± 1.2%	16% ± 0.87%
	DHI Melanin	DHICA Melanin	5-CysDOPA Melanin	2-CysDOPA Melanin
Hair[e]				
Intra assay[c]	13000 ± 420	6400 ± 710	400 ± 38	1200 ± 37
Inter assay[d, f]	14000 ± 1700	6200 ± 90	680 ± 58	1000 ± 45

[b]Expressed as the amount of degradation product detected / amount melanin degraded (w/w percent yield ± standard deviation).

[c]n=4

[d]n=3

[e]Expressed as ng melanin per mg hair (± standard deviation). Black hair was used for PDCA and PTCA determination and red hair was used for AHP and 3AT determination.

[f]For pheomelanin data, interassay precision was assessed with hair from a different individual than that used to assess intra-assay precision.

Figure 2.3 *Plot of the amount of eumelanin degradation marker produced vs. the amount of eumelanin analyzed.* This plot demonstrates the melanin assay linearity found when increasing amounts of melanin or human hair are subjected to analysis. See Table 2.2 for complete data set and statistical analysis.

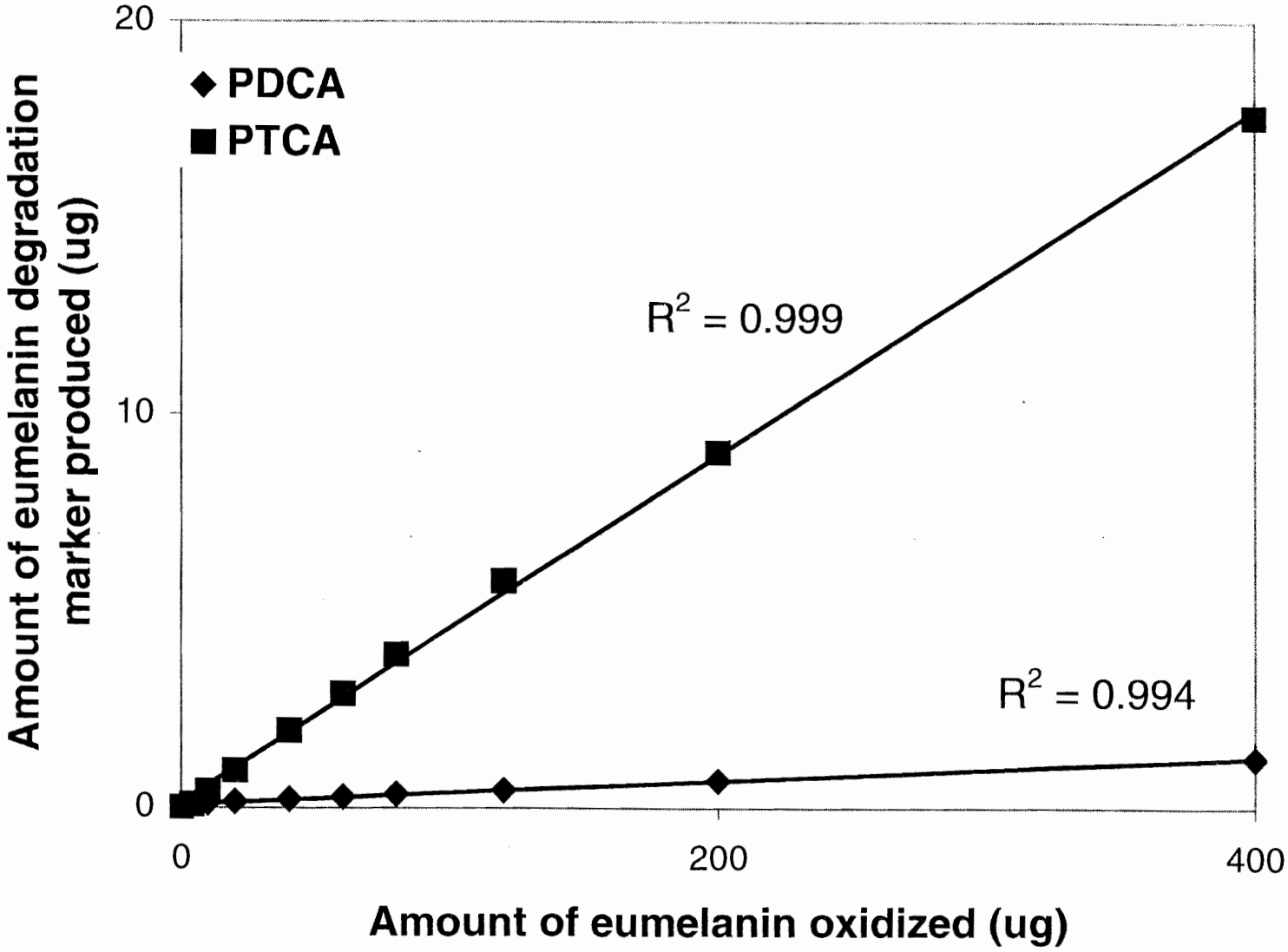
20
10
0
PDCA
PTCA
R^2 = 0.999
R^2 = 0.994
0
200
400
Amount of eumelanin degradation marker produced (ug)
Amount of eumelanin oxidized (ug)

Table 2.2

Regression analysis on melanin assay linearity, shown as increasing amounts of pure melanin subtype or human hair is subjected to analysis. For degradation markers (PDCA, PTCA, 3AT, and AHP), the data corresponds to a plot of the amount of degradation marker produced (in μg) vs. the amount of pure melanin subtype degraded (in μg). For a melanin subtype (the remaining entries), the data correspond to a plot of the amount of melanin subtype found in a hair sample (in μg) vs. the amount of hair subjected to analysis (in mg). Errors are expressed in terms of standard deviation as demonstrated by Anderson (145).

	R^2	Slope	Slope error	y-intercept	y-intercept error
PDCA	0.994	0.00297	6.96×10^{-5}	0.0752	0.011
PTCA	0.999	0.0441	0.000421	0.126	0.0633
DHI-melanin	0.999	13.0	0.205	0.157	0.889
DHICA-melanin	0.998	6.17	0.201	1.11	0.871
3AT	0.990	0.143	0.00627	0.0690	0.0961
AHP	0.988	0.208	0.00804	0.212	0.123
2-CysDOPA-melanin	0.995	1.21	0.0553	0.096	0.182
5-CysDOPA-melanin	0.987	0.203	0.00965	0.00684	0.0318

vs. the amount of hair subjected to analysis. The limits of quantitation and (limits of detection) were as follows: DHI-melanin 10 μg (10 μg); DHICA-melanin 1 μg (0.50 μg); 2-CysDOPA-melanin 240 ng (120 ng); and 5-CysDOPA-melanin 170 ng (85 ng). (Occasionally, larger injection volumes were used to increase signal to noise up past limits of quantitation.)

Degradation Product Cross-reactivity

To assess melanin degradation product cross-reactivity, that is, production of degradation markers from melanins other than the primary producer of a specific degradation marker, eumelanins were subjected to pheomelanin analysis and vice versa. Results (shown in Table 2.3) demonstrate that PTCA is produced from DHI melanin and that PDCA and PTCA are produced from 5-CysDOPA and 2-CysDOPA pheomelanins. However, based on their precision (Table 2.3), cross-reactivity results are consistent and thus can be accounted for when calculating melanin composition.

Analysis of Heteropolymeric Melanins

To test the reliability of the chemical degradation assays in analyzing heteropolymeric melanins, a series of mixed composition eumelanins, mixed composition pheomelanins, and mixed eu-/pheomelanins were made and subjected to analysis. As an outside verification that the mixed eumelanins were of expected monomer composition, samples of each mixed eumelanin polymer were subjected to elemental analysis by combustion (after being dehydrated overnight at room temperature under a vacuum), Galbraith Laboratories, Inc., Knoxville, TN. As the number of DHI monomer units in the melanin is increased, one expects the percent carbon and percent nitrogen content of

Table 2.3

Crossreactivity table—production of melanin markers from unexpected melanin sources. Values expressed as the ratio of nmol degradation product observed per nmol of expected degradation product ± standard deviation. n=4 for each determination.

	PDCA	PTCA	AHP	3AT
DHI-melanin	-	1.1 ± 0.083	Not detected	Not detected
DHICA-melanin	Not detected	-	Not detected	Not detected
5-CysDOPA-melanin	2.6 ± 0.052	5.8 ± 0.11	-	Not detected
2-CysDOPA-melanin	2.2 ± 0.11	7.6 ± 0.17	Not detected	-

that melanin to increase. Shifts in elemental analysis results agree with the monomer composition results (as determined by chemical degradation analysis) as eumelanin monomer composition is shifted from DHI to DHICA: 75% DHICA / 25% DHI melanin was 53.43% C and 7.72% N; 50% DHICA / 50% DHI melanin was 54.10% C and 7.74% N; 25% DHICA / 75% DHI melanin was 56.09% C and 7.83% N. Because the pheomelanin monomers are structural isomers of each other, one cannot tell via changes in elemental composition what the changes in pheomelanin polymer composition are. However, because the monomers are structural isomers, their relative incorporation into the polymer is expected to be approximately equal. Thus, due to lack of an available second verification procedure, an outside verification of pheomelanin subtype composition was not carried out. More eumelanin and less pheomelanin were found in the mixed eu-/pheomelanin polymer than was expected from the starting monomer composition. This was verified by elemental analysis results, which confirm that the sulfur content of the mixed eu-/pheomelanin heteropolymer mixture is less than 3.9%. The theoretical dehydrated value is 5.4%. The presence of more eumelanin and less pheomelanin in this polymer mixture than was expected from starting monomer composition is thought to be due to the fact that pheomelanin is slightly soluble in the conditions under which the polymer was isolated once it had been formed. Overall, the fact that chemical degradation results agree with the actual synthetic melanin compositions (as verified by elemental analysis) (see Figure 2.4 for chemical degradation assay results) indicates that the assays can reliably assess the composition of heteropolymeric melanins. Figure 2.4A demonstrates that when eumelanins are synthesized from different monomer compositions, the alkaline hydrogen peroxide

Figure 2.4 *Analysis of: A) Mixed eumelanin series, B) Mixed pheomelanin series, and C) Melanin made from 25% (w/w) of all four melanin subtypes.* Results agree with elemental analyses and are expressed as calculated percent composition based on the mass of degradation product found, divided by the mass/mass % yield of that degradation product (expressed as a fraction) from a melanin made solely from the monomer that produces that degradation product, divided by the total mass of melanin degraded, and multiplying by 100 to obtain a percent value. n=4 for each mixed melanin. Error bars indicate standard deviation.

A

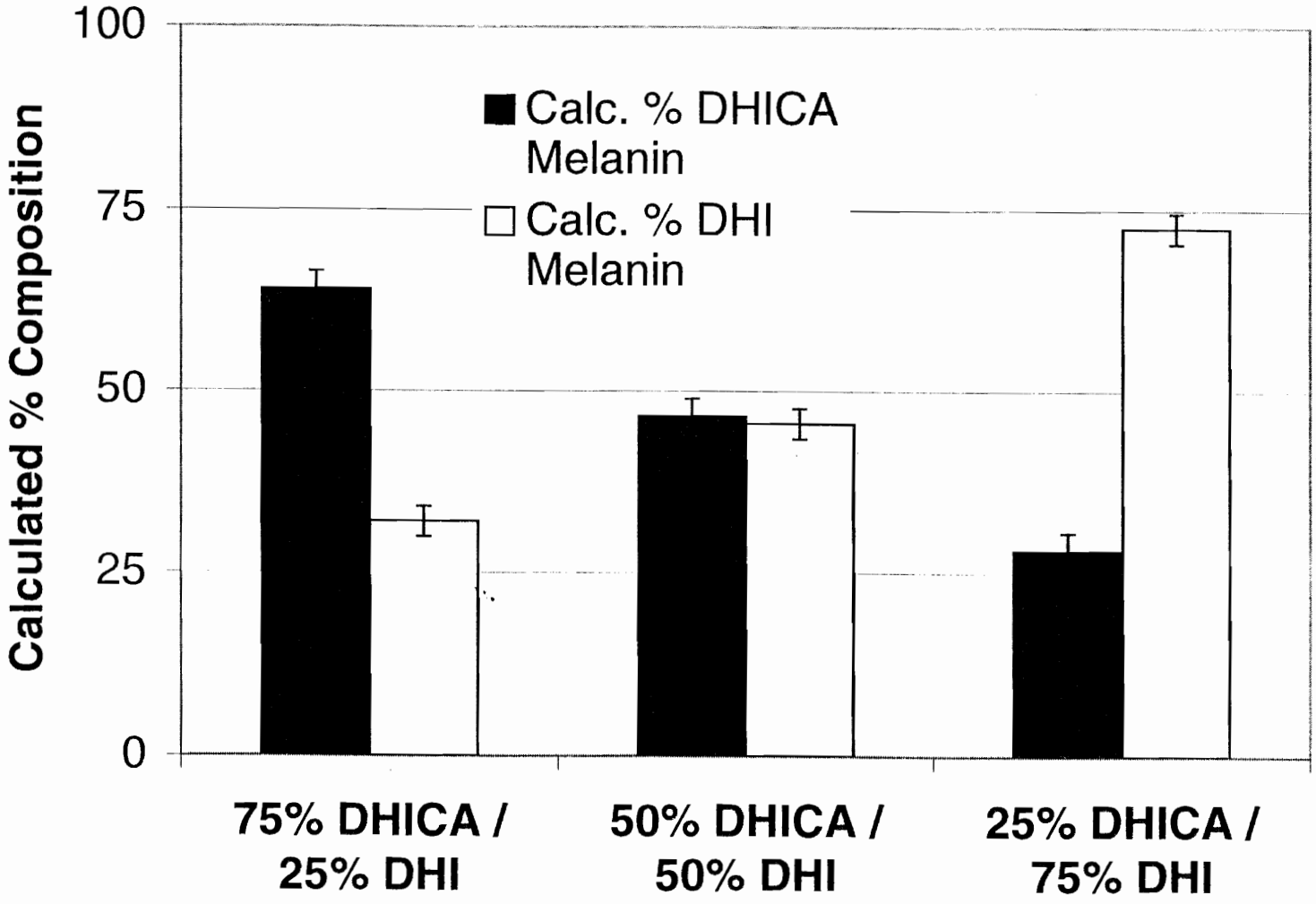
100
75
50
25
0
Calculated % Composition
Calc. % DHICA Melanin
Calc. % DHI Melanin
75% DHICA / 25% DHI
50% DHICA / 50% DHI
25% DHICA / 75% DHI

B

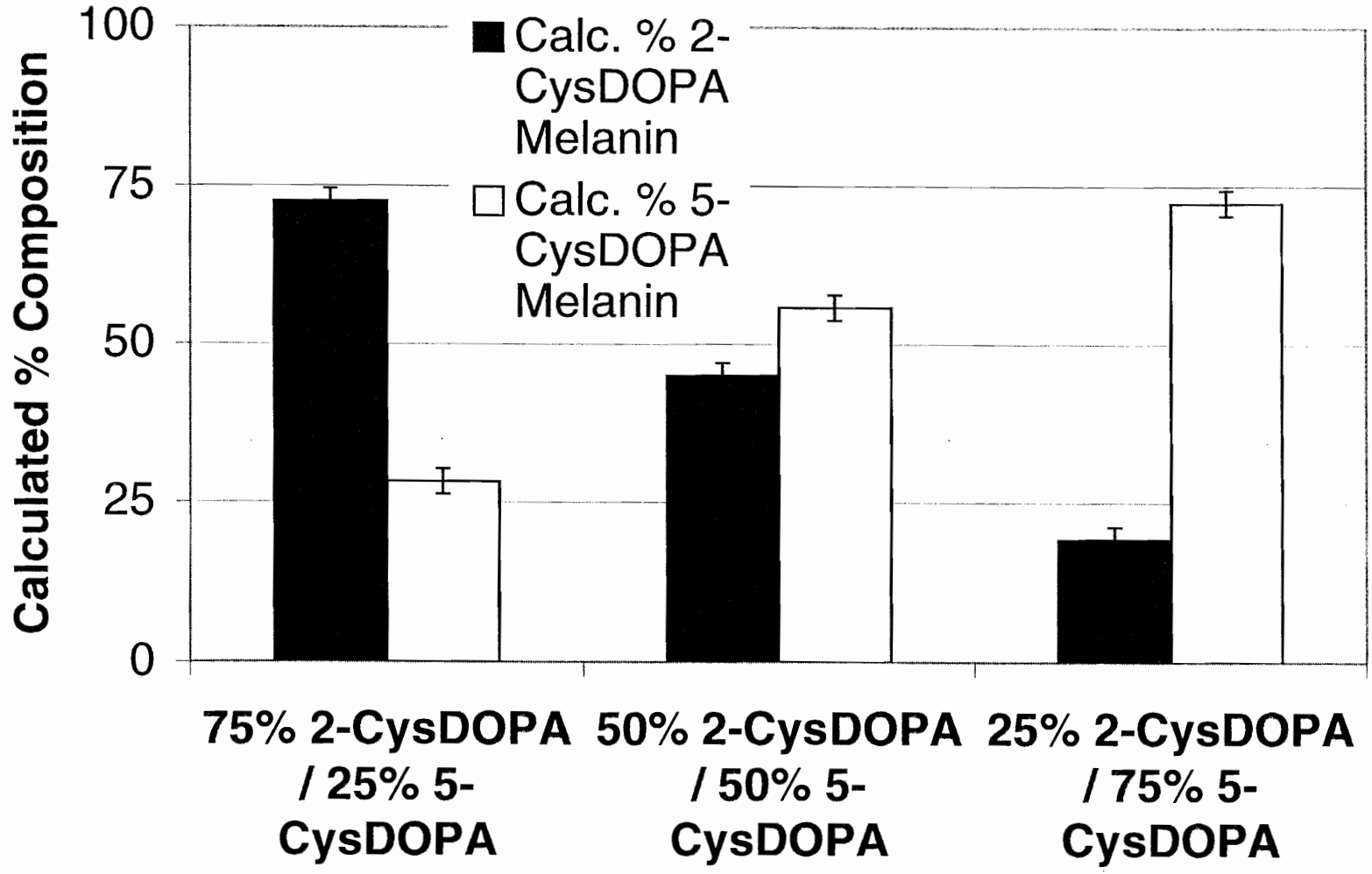
Calculated % Composition
100
75
50
25
0
Calc. % 2-CysDOPA Melanin
Calc. % 5-CysDOPA Melanin
75% 2-CysDOPA / 25% 5-CysDOPA
50% 2-CysDOPA / 50% 5-CysDOPA
25% 2-CysDOPA / 75% 5-CysDOPA

C

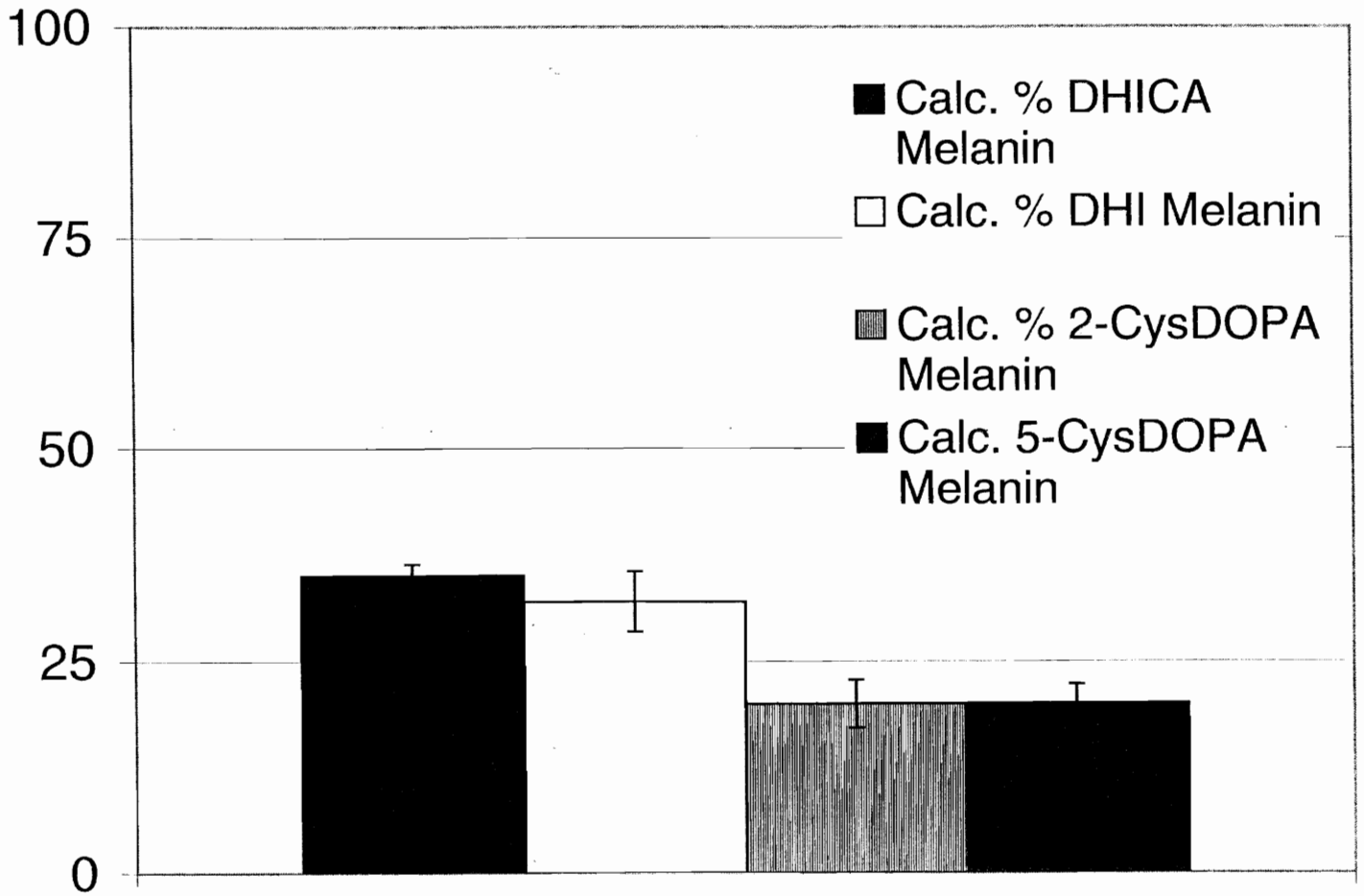
100
75
50
25
0
Calc. % DHICA Melanin
Calc. % DHI Melanin
Calc. % 2-CysDOPA Melanin
Calc. 5-CysDOPA Melanin

oxidation assay will provide accurate information regarding the composition of the heteropolymeric eumelanins. Likewise, Figure 2.4B shows that when pheomelanins are synthesized from different monomer compositions, the reductive HI hydrolysis assay will provide accurate information regarding the composition of the heteropolymeric pheomelanins. And finally, Figure 2.4C shows that even when mixed eu-/pheomelanin copolymers are made, the eumelanin and pheomelanin assays can determine the relative composition of each melanin subtype.

Melanin Composition of Human Hair Types

The melanin composition of different colored hair from 44 donors was assessed (3 African-Americans with black hair, 1 American-Indian with black hair, 6 Asians with black hair, 6 Anglo-Americans with black hair, 2 Hispanics with black hair, 12 Anglo-Americans with brown hair, 8 Anglo-Americans with blond hair, and 6 Anglo-Americans with red hair) (Figure 2.5). Hair color determinations were made by visual inspection prior to melanin analysis. Results show that black-haired individuals (regardless of race) have the most DHI and DHICA melanin while red-haired Anglo-Americans have the most 5-CysDOPA and 2-CysDOPA melanin. Caucasians with black hair have less total melanin in their hair than other races with black hair examined in the study.

To correlate hair melanin content to codeine (a basic drug, pKa 8.2, Figure 2.6) incorporation after a single oral dose, a scatter plot of total eumelanin vs. hair codeine content divided by plasma AUC was made (Figure 2.7). (Experimental design and codeine content of these human hair samples was previously determined by Rollins *et al.* (126)). A linear regression analysis (Microsoft Excel 2000) on these data produces an r^2 coefficient of 0.73, meaning that 73% of the variation in the data can be accounted for by

Figure 2.5 *Analysis of human hair for melanin subtypes:* A) Eumelanin. *Significantly different from all black hair ($p < 0.0001$). †Significantly different from African-American black hair ($p < 0.01$). ‡Significantly different from Asian black hair (total and DHI melanin only) ($p < 0.05$). #Significantly different from brown hair ($p < 0.05$). B) Pheomelanin. $^{\Phi}$Significantly different from red hair (total pheomelanin and both subtypes) ($p < 0.01$). See results section for the number of samples from each group. Error bars indicate standard deviation.

A

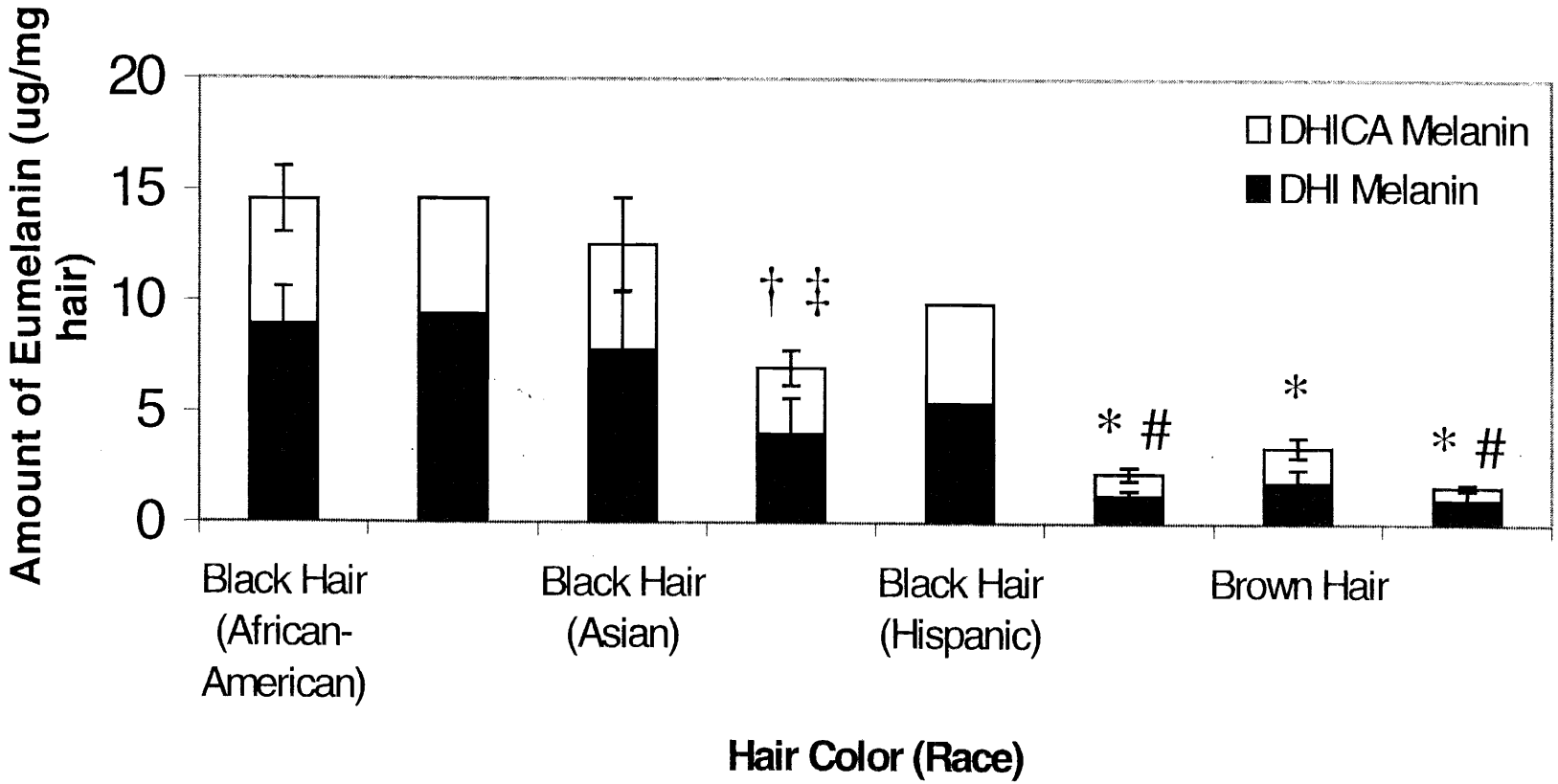
Amount of Eumelanin (ug/mg hair)
20
15
10
5
0
DHICA Melanin
DHI Melanin
† ‡
* #
*
* #
Black Hair (African-American)
Black Hair (Asian)
Black Hair (Hispanic)
Brown Hair
Hair Color (Race)

B

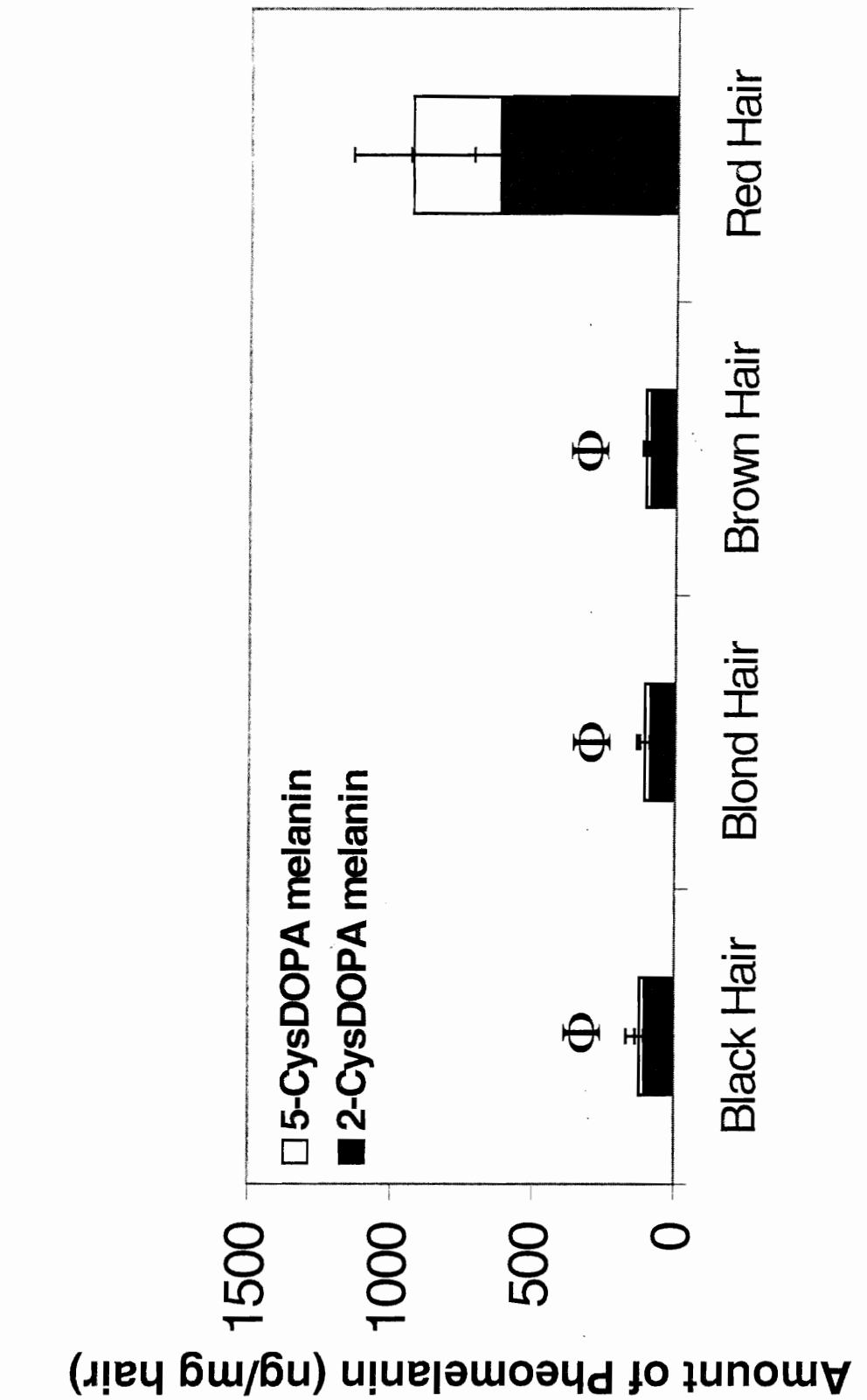
Amount of Pheomelanin (ng/mg hair)
1500
1000
500
0
5-CysDOPA melanin
2-CysDOPA melanin
Φ
Φ
Φ
Black Hair
Blond Hair
Brown Hair
Red Hair

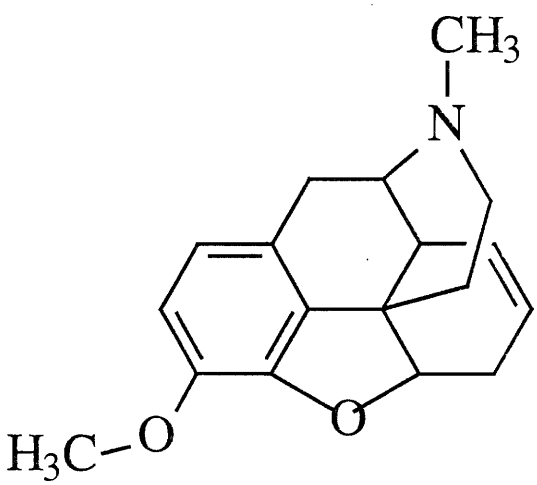

Figure 2.6 *Chemical structure of codeine*

Figure 2.7 *The relationship between codeine incorporation into human hair and eumelanin content.* Codeine concentration is expressed in ng codeine / mg hair. AUC stands for the area under the plasma concentration vs. time pharmacokinetic curve. Dividing the codeine concentration in hair data by plasma AUC normalizes the codeine content of the hair for the amount of drug present in the blood. This procedure makes use of the assumption of a direct linear relationship between blood levels and hair concentrations of codeine, as demonstrated in rats by Gygi *et al.* (146).

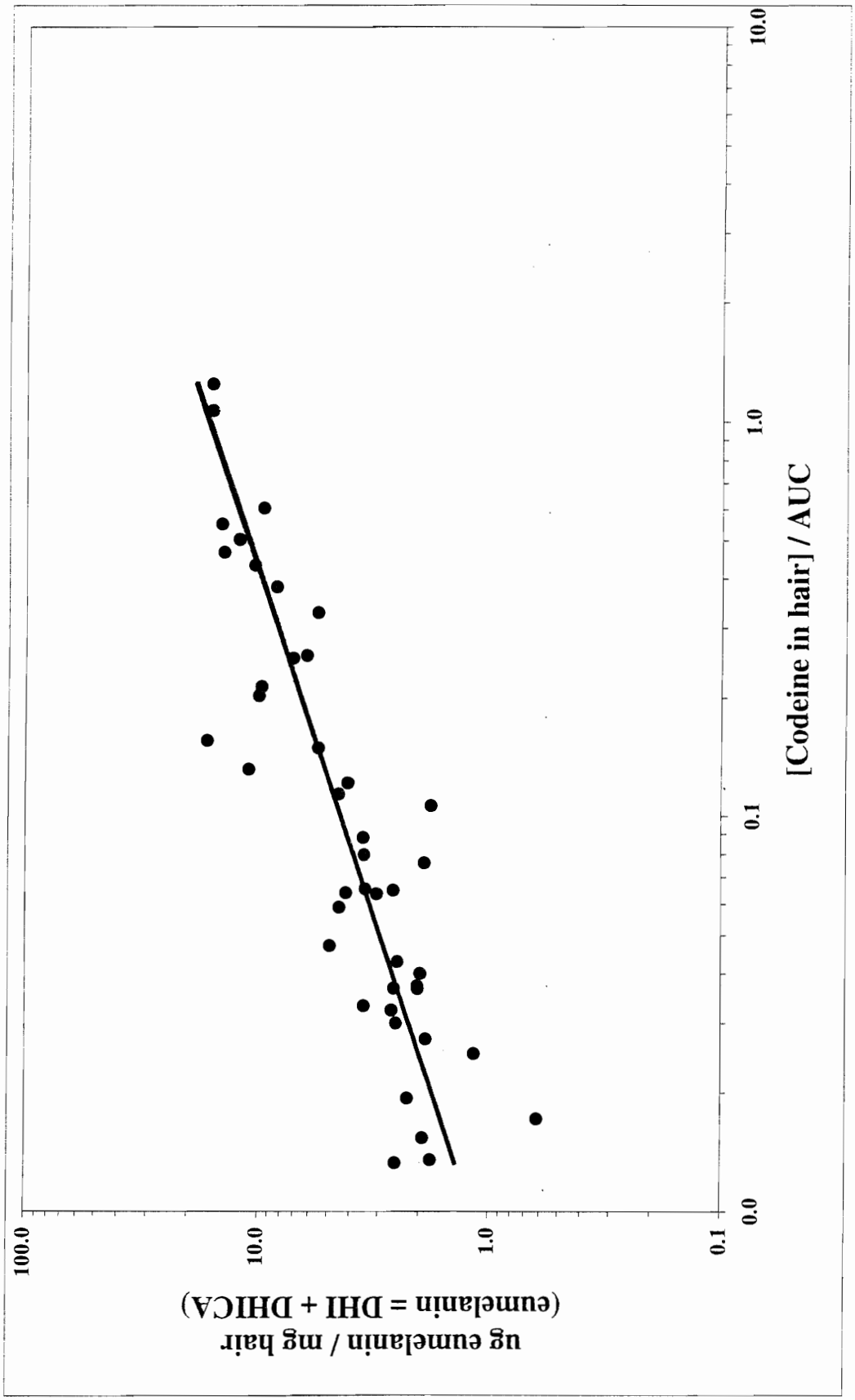
ug eumelanin / mg hair
(eumelanin = DHI + DHICA)
100.0
10.0
1.0
0.1
0.0
0.1
1.0
10.0
[Codeine in hair] / AUC

eumelanin content alone. Pheomelanin content of human hair demonstrates no relationship with codeine content.

Discussion

Several methods have been developed for quantitating the amount of total melanin, eumelanin, and pheomelanin in biological samples (130, 132, 141, 144). The data presented in this study correlated amounts of melanin subtype-specific degradation markers to actual amounts of melanin subtypes in a sample. This was done by determining percent yield values for a given degradation marker from its parent melanin (homopolymer) subtype and using these values on melanin from hair samples to back-calculate how much of each melanin subtype was in the hair. Possible difficulties concerning the validity of the assays such as assay linearity, melanin subtype cross-reactivity, and assay reliability when assessing heteropolymeric melanins were addressed. It must be kept in mind, however, that DHI and DHICA are the major precursors to eumelanin, but eumelanin polymers do not necessarily consist solely of these monomers, even when these are the only monomers used in the synthesis of the polymer. This is due to the fact that hydrogen peroxide, produced in the vicinity of developing melanin polymers during the monomer oxidation process, can partially alter the structure of the forming polymer by oxidatively degrading some of the DHI and DHICA units into carboxylic acid substituted pyrrole units (95, 96). Nevertheless, eumelanins consisting mostly of DHICA units would be expected to have a greater carboxylic acid content than eumelanins consisting mostly of DHI units. (This hypothesis has been confirmed by Novellino *et al.* (95)). In addition, the procedure used to synthesize a melanin can affect the carboxyl content of the resulting melanin (95) which, in turn, may affect yields of

PDCA and PTCA from the resulting polymers. Because of this concern, the melanins used in this study were synthesized via a method that best models the *in vivo* situation. That is, tyrosinase was used as the catalytic enzyme while the reaction was carried out under oxygen in the absence of catalase.

Using the assays and degradation product yield information as described above, it was determined that average black human hair contains approximately 99% eumelanin (60% DHI and 40% DHICA-derived eumelanin) and 1% pheomelanin (80% 2-CysDOPA and 20% 5-CysDOPA-derived pheomelanin); brown and blond hair contain 95% eumelanin and 5% pheomelanin; and red hair contains 67% eumelanin and 33% pheomelanin (Figure 2.5). These data suggest that color determination for black, brown, or blond hair depends more on melanin quantity than eu-/pheomelanin composition, while red hair may arise through an alteration in the melanin synthesis pathway that leads to a greater relative production of pheomelanin. This knowledge must be considered when relating drug-eumelanin or drug-pheomelanin binding data to drug incorporation into hair.

It has been found that yields of degradation markers are different for each subtype of melanin, but that yields are highly reproducible (Table 2.1) and thus can be used to assess the amount of melanin subtypes in a given sample. However, as shown in Table 2.3, some degradation markers are not always produced solely from their primary melanin subtype source, e.g., PTCA is not produced solely from DHICA melanin. Because of consistent yields, and the fact that DHICA-melanin is not cross-reactive, this phenomenon can be accounted for in calculating amounts of melanin subtypes in a sample. This phenomenon is disconcerting given the postulated structures (Figure 2.1)

for melanin subtype precursors, polymers of which have been shown to produce unexpected degradation products. Studies by Napolitano *et al.* (147, 148) have shown that DHI dimers linked at the 2- position can produce both PDCA and PTCA. It is quite interesting to note the 1:1 PDCA:PTCA molar ratio produced from DHI melanin in light of the degradation pathway proposed by Napolitano *et al.* (147) whereby there is a 50% chance of producing either PDCA or PTCA from a 2-4 linked DHI dimer.

Production of PDCA and PTCA from both 5-CysDOPA and 2-CysDOPA pheomelanins is more difficult to explain mechanistically. The production of PDCA and PTCA from pure pheomelanins suggests the presence of indole units in the polymer. This could mean that monomers 1 and/or 2 shown in Figure 2.8 may exist as part of the pheomelanin polymer. Considering the nucleophilic nature of the phenylalanine side chain amino group and the fact that monomers 1 and 2 have not been ruled out as part of the make up of 5-CysDOPA and 2-CysDOPA pheomelanin, the presence of such monomers may explain the production of PDCA and PTCA from pheomelanins. According to Ito *et al.* (149), the existence of monomer 1 in the pheomelanin polymer should be verified by the production of cysteine in hydriodic acid hydrolysates of 5-CysDOPA and 2-CysDOPA pheomelanin. Using HPLC coupled to mass spectrometry (LC/MS) it was demonstrated that no cysteine is produced from 5-CysDOPA and 2-CysDOPA pheomelanin hydriodic acid hydrolysates (data not shown) thus likely ruling out the presence of monomer 1. Monomer 2, however, remains a possibility because it should produce 3AT or AHP upon hydriodic acid hydrolysis and PDCA and PTCA upon alkaline hydrogen peroxide degradation. d' Ischia *et al.* (150) identified monomer 2 (saturated at the 2- position) when cysteine was added to oxidized DOPA. They reported

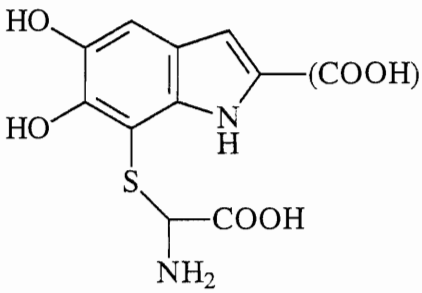

Monomer 1

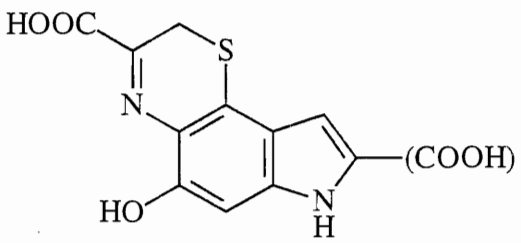

Monomer 2

Figure 2.8 *Chemical structures of monomers 1 and 2*

that this material rapidly autooxidizes to give complex mixtures of yellowish-brown oligomeric materials. The existence of monomer 2 in pheomelanin, however, remains to be proven.

In conclusion, the data presented in this paper provide the means to calculate the amount of each melanin subtype present in a hair sample. As demonstrated in Figure 2.7, a strong relationship exists between codeine incorporation into human hair and eumelanin content. A similar relationship may exist for other basic drugs as well—perhaps providing a means to normalize drug concentrations in hair to eumelanin concentrations so as to eliminate any potential color bias. As testing for drugs in hair becomes a more commonplace procedure, the role of specific melanin subtypes may become more pronounced. Quantitation of melanin subtypes therefore may become critically important in interpreting quantitative drug testing results.

CHAPTER 3

AMPHETAMINE AND N-ACETYLAMPHETAMINE INCORPORATION INTO HAIR: AN INVESTIGATION OF THE POTENTIAL ROLE OF DRUG BASICITY IN HAIR COLOR BIAS[g]

Forensic testing for drugs of abuse in hair has become a popular alternative to traditional urinalysis. Hair color bias, however, presents a problem to fair hair testing. A number of basic drugs including cocaine (66, 151), phencyclidine (69), codeine (65, 152), stanozolol (68), and nicotine (40) have been found to incorporate to a greater extent into dark hair over light colored hair. To develop nonbiased testing procedures, the roles of drug chemistry and hair pigmentation in determining drug concentrations in hair must be understood.

Hair pigment, or melanin, is a polyanionic indolequinone-based polymer that has the potential to interact with positively charged molecules. A number of researchers have suggested that drug-melanin binding through ionic and/or van der Waals interactions between drug molecules and melanin polymers may be responsible for the preferential incorporation of some drugs into pigmented vs. nonpigmented hair (30, 64, 69, 75, 153). Basic drugs are positively charged at physiologic pH. If such drugs are incorporated into

---

[g]Reproduced, with slight modification, from C.R. Borges, D.G. Wilkins, and D.E. Rollins. *J. Anal. Toxicol.* **25:** 221-227 (2001), (the *Journal of Analytical Toxicology*) by permission of Preston Publications. A Division of Preston Industries, Inc.

hair they may bind to melanin and show a preference for incorporation into pigmented vs. non-pigmented hair. Neutral or acidic drugs may only be able to interact with melanin through weak van der Waals forces, thus they are less likely to show a preference for incorporation into pigmented vs. nonpigmented hair. In agreement with this idea, phenobarbital, an acidic drug, does not incorporate preferentially into pigmented vs. non-pigmented rat hair (65). In addition, other evidence indicates that carbamazepine (pKa ~7) does not exhibit a hair color bias in humans (74). Although characterized as a basic drug, a relatively low pKa leaves most of the drug uncharged as it circulates throughout the body.

Ionic interactions with melanin do not provide the only means for a drug to get into hair. In addition to N-AcAp (41) (data shown below), other nonionic compounds such as Δ^9-tetrahydrocannabinol (THC) (33-35, 154), and a large number of steroids such as testosterone (155-157), dehydroepiandosterone (158, 159), 17-β-estradiol (160), and nandrolone (161-163) have been found in hair indicating that melanin may not be the only drug binding site in hair (46, 49, 63).

Amphetamine and N-AcAp have been shown to incorporate into hair (3, 41). This paper describes the use of amphetamine (pKa 9.8) and its nonbasic analog N-AcAp (Figure 3.1) to investigate the role of drug basicity in the hair color bias that is sometimes observed in drug incorporation into hair.

Materials and Methods

Chemicals and Reagents

d-Amphetamine sulfate and d-amphetamine sulfate-d3 were obtained from Sigma (St. Louis, MO). N-AcAp and N-AcAp-d3 were synthesized with acetic anhydride

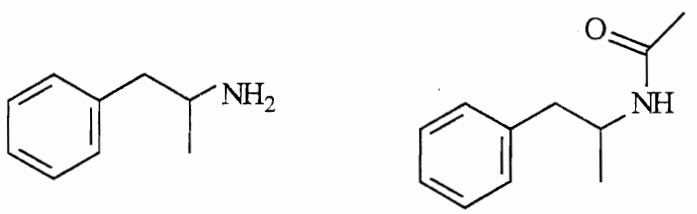

Amphetamine N-Acetylamphetamine

Figure 3.1 *Chemical structures of amphetamine and N-AcAp.*

and acetic anhydride-d6 obtained from Sigma, according to the method of Halmekoski and Saarinen (164). Identities and purity of the crystalline products were verified by mass spectrometry and ^{1}H-NMR (^{1}H-NMR for d0 N-AcAp only) (see Appendix). The melting point of d-N-acetylamphetamine and d-N-acetylamphetamine-d3 was 123-124 °C. N-butyl chloride, chloroform, and methanol (HPLC grade) were obtained from Burdick and Jackson (Muskegon, MI). All other reagent grade chemicals were obtained from Mallinckrodt (St. Louis, MO).

Stock Solutions and Preparation of Standard Curves

Separate stock solutions of amphetamine sulfate and N-AcAp (5 mg/mL) in deionized water and methanol, respectively, were made. (Only the mass of amphetamine from the amphetamine sulfate was accounted for when calculating dilutions.) From stock solutions, working solutions of 0.1, 1, and 10 ng/μL drug in water were made. Daily standard curves were obtained by analyzing hair samples (20 mg) fortified with amphetamine or N-AcAp at 0, 0.1, 0.2, 0.3, 0.5, 1, 2, 3, 5, 10, 25, and 50 ng/mg hair. Quality control (QC) samples (0.3, 3, and 25 ng/mg hair) were prepared daily from working solutions of stock sources different from those used to prepare standard curves.

Animal Protocols

Male LE rats (~150 g) were obtained from Harlan Sprague-Dawley (Indianapolis, IN) and maintained in an environmentally controlled room with a 12-h light-dark cycle and free access to food and water. Animals were housed individually in hanging wire cages to prevent contamination from urine, saliva, bedding, or other rats. Drug free rat hair was obtained by shaving nondosed LE rats. Prior to dosing, the entire dorsal area of

each rat was shaved. d-Amphetamine sulfate or N-AcAp dissolved in normal saline or corn oil, respectively, was administered by intraperitoneal injection once daily at a dose of 10 mg/kg (n=8 for each drug) for 5 days. Regrown hair was shaved and separated into white and black samples 14 days after dosing was started. Hair samples were again collected 28 days after the initial drug administration. Hair was stored at –20 °C before digestion and extraction. Each hair sample was carefully analyzed under a large magnifying glass and any skin flakes present were removed.

Sample Digestion and Extraction

Hair samples were mulched with scissors and then weighed (~20 mg) into separate 16 x 100 silanized glass test tubes. After the addition of 2 ng/mg d3 internal standard, samples were completely solubilized in 2 mL 1 M NaOH overnight at 37 °C. To each sample was added 200 µL concentrated ammonium hydroxide, followed by 4 mL n-butyl chloride : chloroform (4:1). Samples were then mixed for 30 min on a test tube rocker, followed by centrifugation for 10 min at 1800 rpm in an IEC International (Needham Heights, MA) swing bucket centrifuge. The organic layer was transferred to a separate test tube and dried under a gentle stream of air at room temperature. Recoveries of amphetamine and N-AcAp were approximately 80%, thus no significant loss of analyte occurred during evaporation. The dried extracts were reconstituted in 100 µL LC mobile phase for injection.

LC/MS/MS Analysis

HPLC coupled to tandem mass spectrometry (LC/MS/MS) analysis was selected as the analytical technique due to its excellent selectivity and sensitivity as well as its

ability to analyze polar compounds without derivitization. Analysis was performed in positive ion mode on a ThermoQuest TSQ/SSQ 7000 mass spectrometer (Finnigan, San Jose, CA) equipped with an electrospray ionization interface coupled to a Hewlett Packard (Palo Alto, CA) 1100 Series HPLC. Spray voltage was set at 4.5 kV, heated capillary at 250 °C, collision gas at 3.5 mTorr, and collision offset at –25 V. HPLC separation was performed on a Phenomenex (Torrance, CA) Luna 30 x 2.00 mm, 5 μm, C18(2) column under the following conditions: Amphetamine was eluted isocratically with 80% 0.1% formic acid / 20% methanol and monitored at its 136 m/z to 91 m/z transition. Amphetamine-d3 was monitored at its 139 m/z to 92 m/z transition. N-AcAp was eluted isocratically with 40% 0.1% formic acid / 60% methanol and monitored at its 178 m/z to 91 m/z transition. N-AcAp-d3 was monitored at its 181 m/z to 91 m/z transition.

Statistical Analysis

Comparisons between groups were made with a two-tailed Student's t-test assuming homogeneity of variances. Results significant at $p < 0.05$ are reported with relevant approximate p values.

Results

Assay Validation

To validate the analytical method for amphetamine and N-AcAp, intra- and interassay accuracy and intra- and interassay precision were evaluated (Table 3.1). Data for amphetamine and N-AcAp recovery are also included in Table 3.1. Accuracy, precision, and recovery experiments were done with stock solutions separate from those

Table 3.1

Method validation for amphetamine and N-AcAp. Inter assay precision was determined with three runs of three to five samples each. See Results section for explanations of how percentages were calculated.

Amphetamine	n	Target Concentration	%		N-AcAp	n	Target Concentration	%
Intra Assay Accuracy %	n=5	0.3 ng/mg	6.0		Intra Assay Accuracy %	n=5	0.3 ng/mg	3.5
	n=5	3 ng/mg	2.6			n=5	3 ng/mg	3.2
	n=5	25 ng/mg	0.9			n=5	25 ng/mg	6.7
Inter Assay Accuracy %	n=15	0.3 ng/mg	6.6		Inter Assay Accuracy %	n=11	0.3 ng/mg	7.1
	n=15	3 ng/mg	1.5			n=14	3 ng/mg	6.9
	n=15	25 ng/mg	2.8			n=11	25 ng/mg	8.3
Intra Assay Precision % CV	n=5	0.3 ng/mg	7.6		Intra Assay Precision % CV	n=5	0.3 ng/mg	1.8
	n=5	3 ng/mg	0.9			n=5	3 ng/mg	0.7
	n=5	25 ng/mg	1.5			n=5	25 ng/mg	11.8
Inter Assay Precision % CV	n=15	0.3 ng/mg	10.0		Inter Assay Precision % CV	n=11	0.3 ng/mg	7.0
	n=15	3 ng/mg	0.8			n=14	3 ng/mg	1.5
	n=15	25 ng/mg	5.1			n=11	25 ng/mg	5.2
% Recovery	n=5	0.3 ng/mg	85.6		% Recovery	n=5	0.3 ng/mg	74.0
	n=5	3 ng/mg	79.7			n=5	3 ng/mg	81.0
	n=5	25 ng/mg	80.7			n=5	25 ng/mg	80.0

used to prepare standard curves. Accuracy was calculated by dividing the absolute value of the difference between the target concentration and the observed concentration by the target concentration then multiplying by 100 to obtain a percentage. Data are thus read as being accurate to within a certain percentage of the target concentration. Precision was assessed as the percent coefficient of variation from the mean concentration. Recovery was determined by spiking samples with internal standard after extraction and dividing their mean observed concentration by the mean observed concentration of another group of samples to which internal standard was added as described above. Amphetamine and N-AcAp were quantitated by obtaining peak area ratios (d0/d3) and comparing these to a standard curve created in the same manner. Accuracy remained within 8.3% and precision remained within 11.8% at the concentrations studied here. Standard curves were linear from 0 to 50 ng / mg hair and r^2 values were typically 0.99 or higher. The limit of quantitation (LOQ), set at a minimum signal to noise ratio of 5 and quantitation accuracy of 20%, was 0.1 ng drug/mg hair. Recovery of both amphetamine and N-AcAp from the extraction procedure was approximately 80%.

Amphetamine and amphetamine-d3 were monitored with 136 m/z to 91 m/z and 139 m/z to 92 m/z transitions, respectively, and N-AcAp and N-AcAp-d3 were monitored with 178 m/z to 91 m/z and 181 m/z to 91 m/z transitions, respectively. Representative selected reaction-monitoring (SRM) chromatograms for amphetamine and N-AcAp found in rat hair are shown in Figure 3.2. Chromatographic runs were 3 min in length. Hair collected prior to dosing (day 0) contained no detectable drugs. Day 28 hair for both amphetamine and N-AcAp was at or below the LOQ. Analysis of hair collected 14 days after dosing (Figure 3.3) revealed that amphetamine was incorporated into black hair at a

Figure 3.2 *Representative SRM chromatograms for A) amphetamine found in rat hair and B) N-AcAp found in rat hair*

A

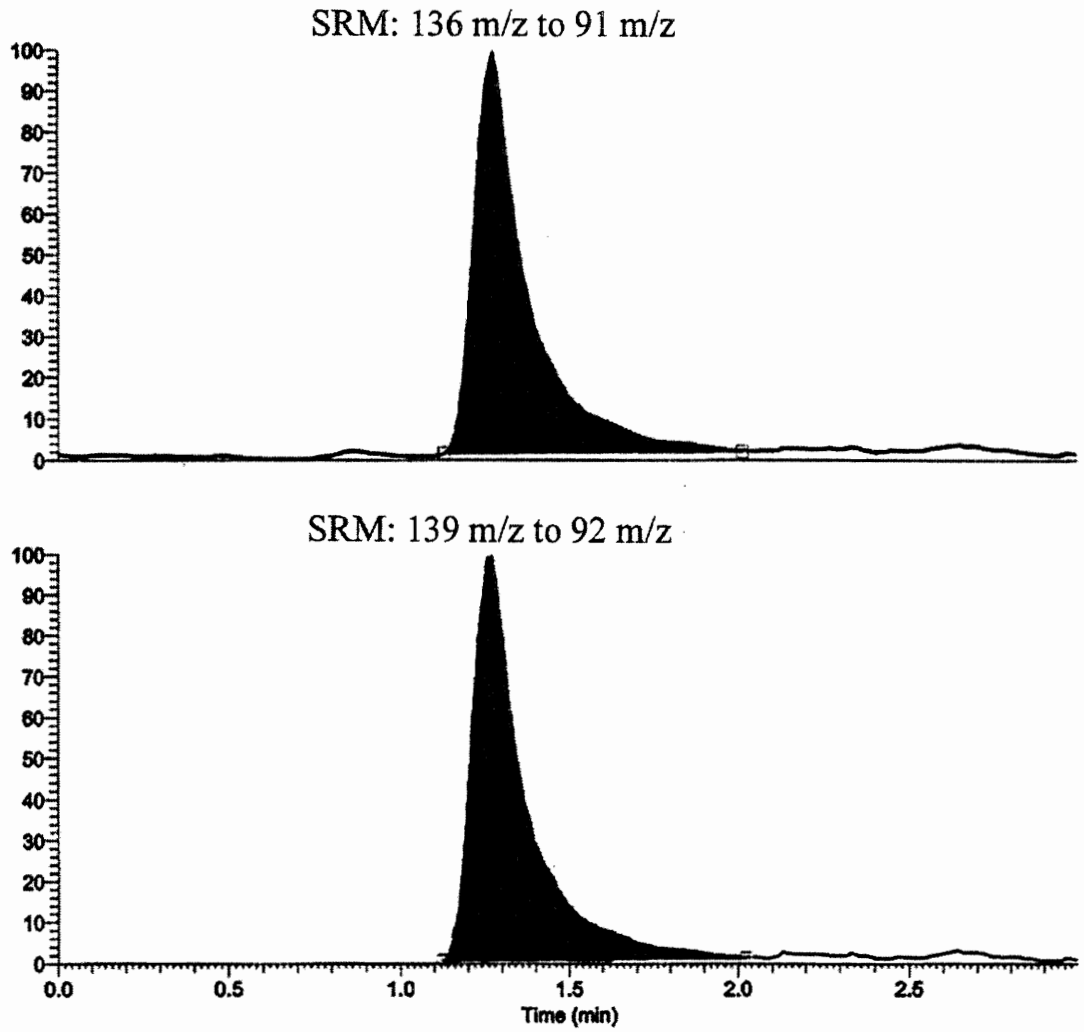
SRM: 136 m/z to 91 m/z
100
90
80
70
60
50
40
30
20
10
0
SRM: 139 m/z to 92 m/z
100
90
80
70
60
50
40
30
20
10
0
0.0
0.5
1.0
1.5
2.0
2.5
Time (min)

B

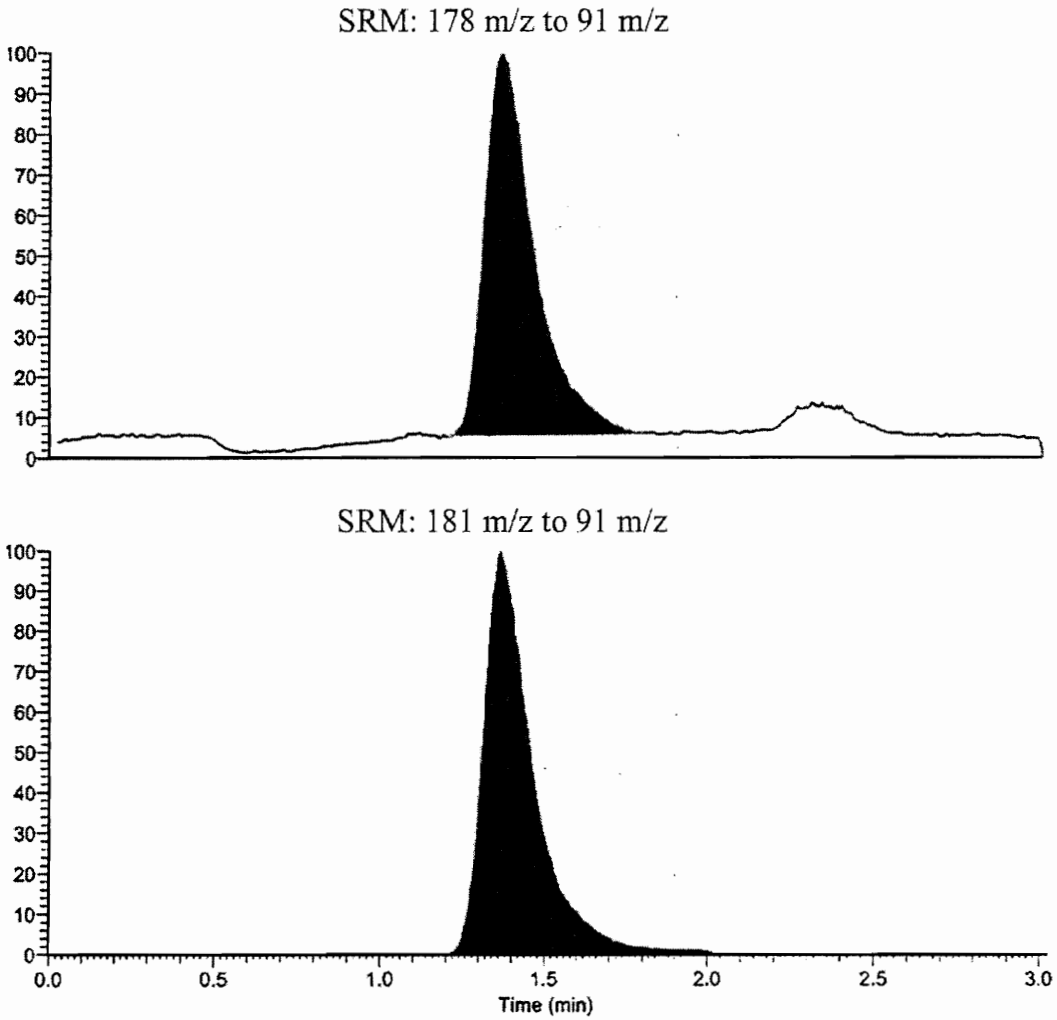
SRM: 178 m/z to 91 m/z
100
90
80
70
60
50
40
30
20
10
0
SRM: 181 m/z to 91 m/z
100
90
80
70
60
50
40
30
20
10
0
0.0
0.5
1.0
1.5
2.0
2.5
3.0
Time (min)

Figure 3.3 *Concentrations of A) amphetamine found in white and black rat hair and B) N-AcAp found in white and black rat hair.* Error bars represent standard deviation. n=8 for each drug. *Significant at $p < 0.001$.

A

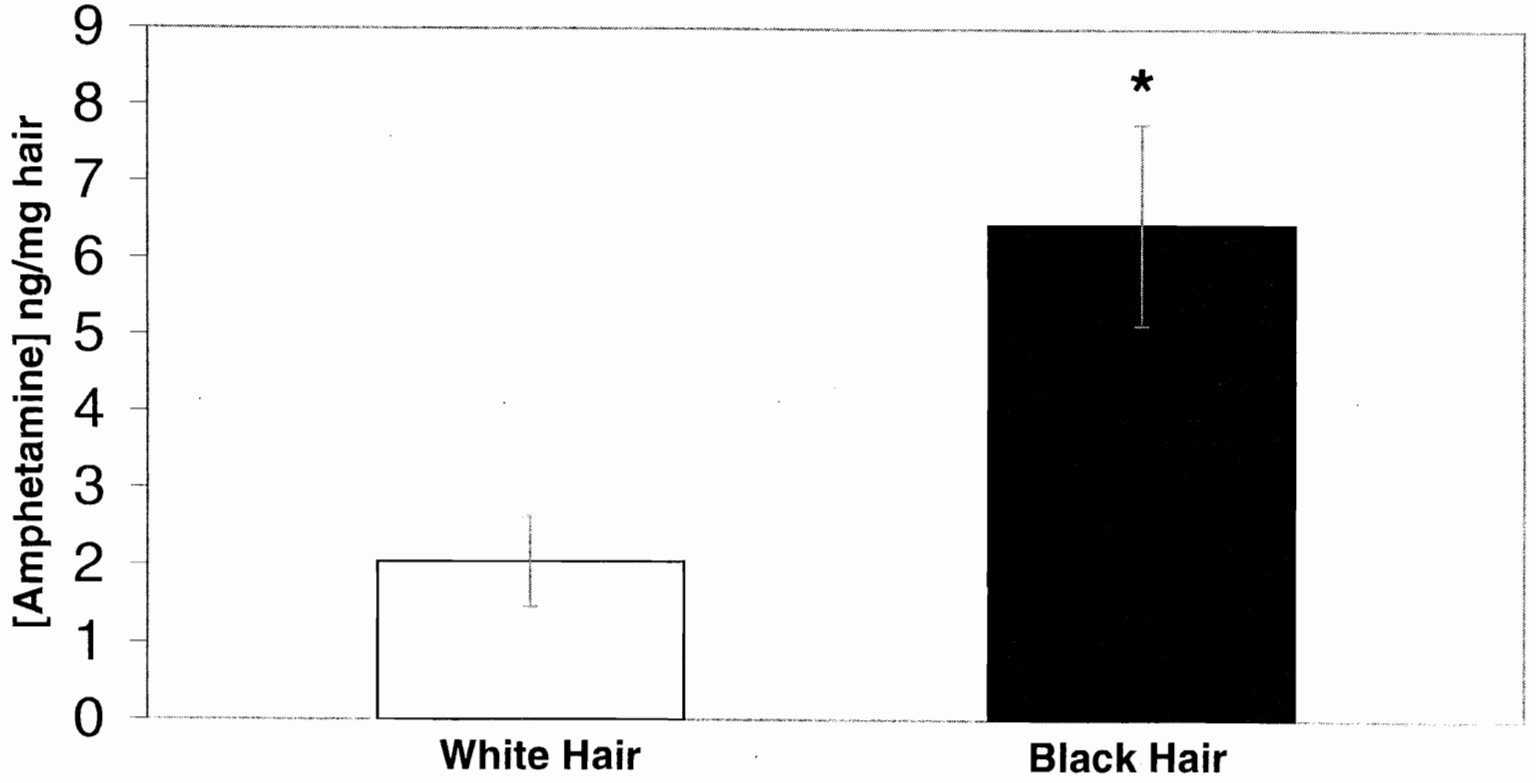

B

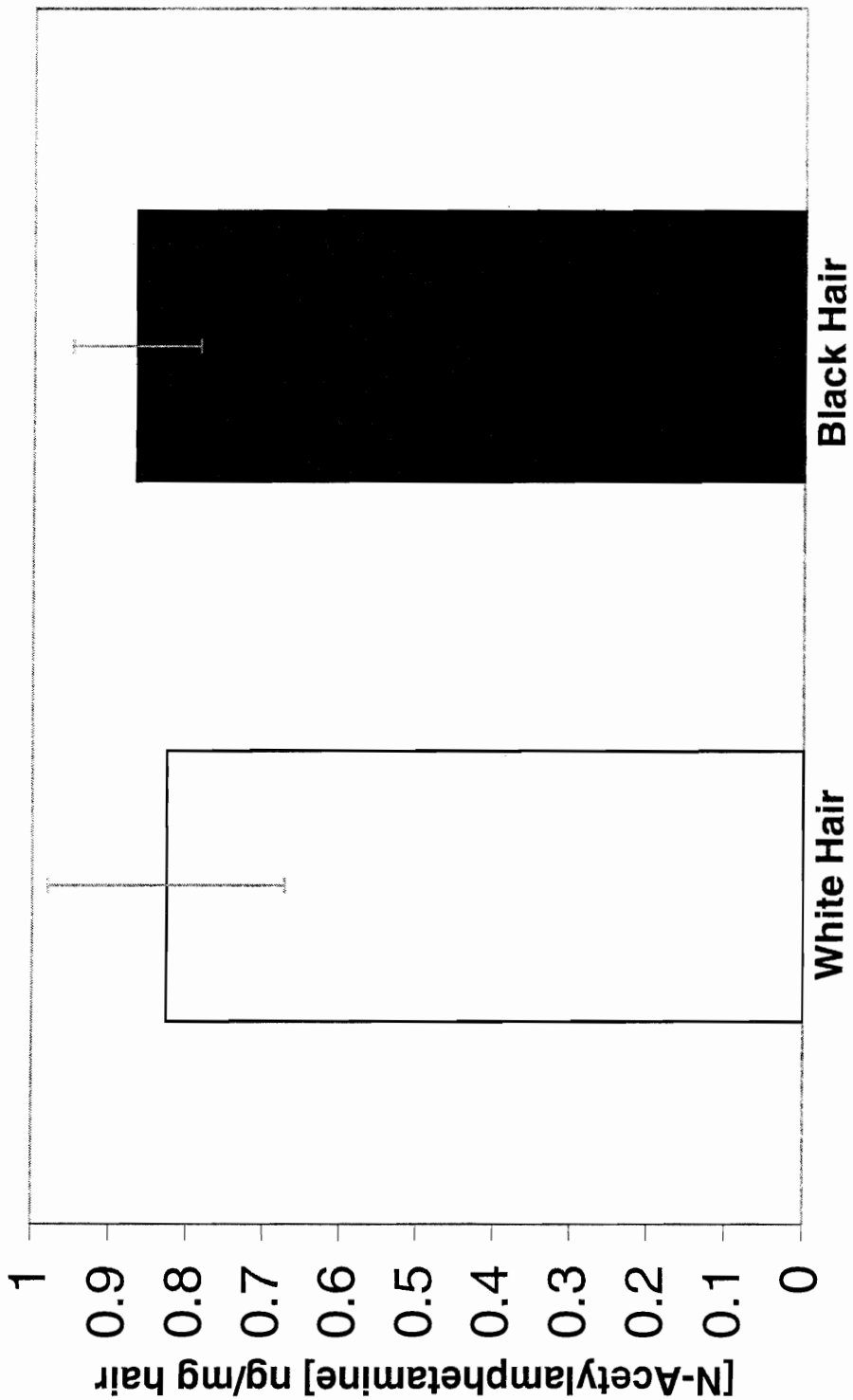
[N-Acetylamphetamine] ng/mg hair
0
0.1
0.2
0.3
0.4
0.5
0.6
0.7
0.8
0.9
1
White Hair
Black Hair

mean concentration of 6.44 ± 1.31 (SD) ng amphetamine / mg hair, an amount significantly different ($p < 0.001$) from that found in white hair (2.04 ± 0.58 ng amphetamine/mg hair) (n=8). In contrast, no difference in N-AcAp content was found between black hair (0.87 ± 0.08 ng N-AcAp/mg hair) and white hair (0.83 ± 0.15 ng N-AcAp/mg hair) from rats dosed with N-AcAp (n=8).

Discussion

Nakahara *et al.* (41, 43, 67, 75) have suggested that drug basicity, which, in theory, leads to drug-melanin binding, is an important characteristic governing the incorporation of a drug into hair. Additional studies have indicated that although drugs do not have to be basic (e.g., phenobarbital) to be highly incorporated into hair (65), drug basicity may play a strong role in the *preferential* incorporation of a given drug into pigmented vs. nonpigmented hair (65, 66, 68, 69, 127, 153). To directly evaluate the role of drug basicity in potential hair color bias, this study employed amphetamine and N-AcAp (a basic drug and its nonbasic analog) to test the hypothesis that a basic drug will show a hair color bias, but that a nonbasic drug will not show a hair color bias. LE rats were chosen for this study because the presence of black and white hair on the same animal helps eliminate black hair vs. white hair drug concentration differences due to additional factors such as species differences and interanimal variability. (Also, by simple visual inspection, no differences were noted between black hair and white hair growth rates on the same animal.) The results of this study clearly demonstrate that drug basicity can lead to a hair color bias, but a lack of basicity appears to eliminate hair color bias. Melanin likely plays the dominant role in the demonstrated hair color bias, but we did not attempt to normalize hair concentrations for melanin content due to the fact that

while there certainly is melanin in black LE rat hair, there are negligible amounts of melanin in white LE rat hair (as determined by the HPLC method of Borges *et al.* (165), chromatograms not shown). Mathematically, normalizing the data in this study to hair melanin content would produce meaningless data. Interestingly, the fact that drugs were incorporated into white LE rat hair demonstrates that melanin is not the only binding location for drugs in hair.

The difference in basicity between amphetamine and N-AcAp represents the most striking contrast between these two drugs, but there is also a difference in lipophilicity, a feature that may be partly responsible for the differences in hair incorporation noted in these studies. However, the greater lipophilicity of N-AcAp is probably not responsible for its lack of a hair color bias or its lesser incorporation into hair regardless of hair color. This is because lipophilicity neither increases melanin binding (see Chapter 4) or overall incorporation into hair, as might be expected according to classical hair incorporation theories.

Evidence for hair color bias also exists for cocaine (66), phencyclidine (69, 128), nicotine (40), cotinine (40), stanozolol (68), and codeine (64, 65) but not for the acidic drug phenobarbital, which shows no hair pigmentation bias whatsoever (65). Melanin consists of polyanionic indolequinonone-based polymers (96) that have been partially degraded into carboxylic acid substituted pyrrole units (95). In theory, the hair color bias demonstrated for basic drugs may be caused by the ionic binding of positively charged, basic drug molecules to negatively charged melanin pigment polymers. *In vitro* drug-melanin binding studies with amphetamine and N-AcAp were also conducted to further test this theory (see Chapter 4).

Some epidemiological evidence (72, 73, 166) has suggested that there is no hair color bias for amphetamines and cocaine. These authors suggest that differences in hair drug concentrations between races are due to differences in drug preferences among the various societal groups rather than due to a hair color bias (defined as the situation where more drug is deposited into darker hair vs. lighter hair, given equal dosing). One primary conclusion is that, "...there is no significant relationship between [hair] color category and likelihood to test positive for cocaine. (166)" Unfortunately, information on exactly which individuals from different races actually ingested the drugs in question is not available in these studies. Hair analysis simply says whether or not there is drug in hair above a certain concentration. As such, there may not be an effective hair color bias. Such epidemiological evidence is derived from a dichotomous hair test outcome, the results of which depend on an established cutoff concentration above which a test result is considered positive. It may be the case that the cutoff concentration is set appropriately so that all (or nearly all) of the individuals taking the drugs in question are found positive regardless of hair color. That is, for (nearly) all users, sufficient drug is incorporated into their hair to produce a positive test outcome regardless of hair color. There may have been no or too few users exposed to a small enough dose for light-haired individuals to test negative and dark-haired individuals to be shown positive for drug use. Importantly, while there may be more drug in dark colored hair, there may still be enough drug in light colored hair to produce a positive result. A recent study by Rollins *et al.* (126) helps to elucidate this matter. Their study demonstrated clear differences between light and dark colored hair concentrations of ofloxacin and codeine for a group of human subjects given the same low therapeutic dose of ofloxacin or codeine. Thus, they

demonstrated hair color biases for both ofloxacin and codeine testing in hair at therapeutic doses. As clearly shown by their results, however, for a given dose, an unfair testing situation only exists if the cutoff concentration is set too high. That is, if the cutoff concentration is set above the mean drug concentration in light hair but below the mean drug concentration in dark hair. While it is necessary to set high enough cutoff concentrations to clearly distinguish from background noise, setting cutoff concentrations as close to background levels as possible will help to make any possible unfair hair color effects as minimal as possible (i.e., there will be fewer individuals in the dose range where a negative test will be produced for light colored hair and a positive test produced for dark colored hair). The likelihood of eliminating an unfair hair-testing situation, however, would have to be determined for each individual drug.

In comparing the overall incorporation of amphetamine vs. N-AcAp in hair, Nakahara *et al.* have demonstrated using dark agouti rats that even though plasma concentrations of N-AcAp are much higher than those of amphetamine (41) (given equal doses), amphetamine is incorporated into hair to a far greater extent than is N-AcAp (41). Their findings regarding amphetamine and N-AcAp in hair were substantiated by this study in LE rats (in both black and white hair). Thus while drug-melanin binding certainly plays a strong role in drug incorporation into hair and determining hair color bias, additional processes such as hair cell drug transport may be important determinants of the amount of a given drug incorporated into hair—pigmentation differences aside. As hair testing for drugs of abuse becomes more commonplace, the relationships between drug and hair cell biochemistry must become better understood to allow for fair and accurate interpretation of drug testing results.

CHAPTER 4

COCAINE, BENZOYLECGONINE, AMPHETAMINE, AND N-ACETYLAMPHETAMINE BINDING TO MELANIN SUBTYPES

Melanin is an indolequinone based polymer that is polyanionic in nature and thought to be capable of binding drugs through both ionic and possibly van der Waals interactions (51, 53). *In vivo*, melanin is formed linked to proteins in organelles known as melanosomes (pigment granules), which are produced in melanocytes. Melanocytes ultimately transfer their melanosomes to keratinocytes where the pigment can be evenly displayed on the body surface or in hair (96, 167). The binding of a wide variety of drugs to melanin both *in vitro* and *in vivo* is well documented (51-53, 55, 79, 168). Because melanin is found throughout the body in areas as diverse as the inner ears, eyes, skin, hair, and brain, the pharmacological and toxicological consequences of drug-melanin binding range from reduction in antibacterial activity (169), induction of drug toxicity (87), and protection from drug toxicity (85, 86), to implications for the origin of Parkinson's disease (77, 78, 80, 88, 89, 170-172).

Our laboratory is primarily interested in drug-melanin binding from the perspective of how it affects drug incorporation into hair. A number of studies have shown that hair pigmentation plays a major role in the concentration of drug incorporated into hair (63, 68, 69, 127). These data suggest that a hair color bias may exist when

testing for drugs of abuse in hair. That is, because more drug is incorporated into the hair of a dark-haired individual, their hair is more likely to be found positive for a drug that binds melanin than is the hair of an individual with light colored hair. While there is some debate as to whether or not melanin can produce an effective "hair color bias" in actual drug testing (72, 73), the fact that drugs can bind to melanin remains uncontested.

To date, the only drugs definitively shown to incorporate to a greater extent in dark hair over light hair have been basic drugs—i.e., drugs that have a positive charge at physiological pH. Negatively charged and neutral drugs such as phenobarbital and N-AcAp specifically investigated for a hair color bias have been shown to lack this phenomenon (42, 65). Such findings suggest that it is the ionic binding between positively charged drug molecules and negatively charged melanin polymers that leads to a greater incorporation of a drug into pigmented vs. nonpigmented hair. In fact, this suspicion is supported by mechanistic studies on the nature of drug-melanin interactions (51, 53).

Melanin, which is ultimately derived from the amino acid tyrosine (Figures 2.1A and 2.1B), can be divided into two types: the black eumelanins and the reddish-brown pheomelanins. These types can be further divided into subtypes: Eumelanins are made up of primarily DHI and DHICA monomers, (Figure 2.1A) and pheomelanins consist of primarily 5-CysDOPA and 2-CysDOPA-derived monomer units (Figure 2.1B). DHI and DHICA are the major precursors of eumelanin, but the polymer does not necessarily consist solely of these monomers. This is due to the fact that hydrogen peroxide, produced in the vicinity of developing melanin polymers, can partially alter the forming polymer by oxidatively degrading some of the DHI and DHICA units into carboxylic

acid substituted pyrrole units (95, 96). Nevertheless, eumelanins consisting mostly of DHICA units would be expected to have a greater carboxylic acid content than eumelanins consisting mostly of DHI units. (This hypothesis has been confirmed by Novellino *et al.* (95)). Because of the significant chemical differences between DHI and DHICA eumelanins and the fact that pheomelanins are substantially chemically different from eumelanins, the binding properties of different melanin subtypes may differ for a given drug.

The purpose of the work presented here was to assess the roles of individual melanin subtypes in binding amphetamine, N-AcAp, cocaine, and BE (Figures 3.1 and 4.1). These drugs were chosen because cocaine (pKa 8.5) exhibits a hair color bias (63, 66) while its zwitterionic chemical congener, BE, has not been shown to exhibit this bias. Similarly, while amphetamine exhibits a hair color bias (42), its nonbasic analog N-AcAp has been shown not to exhibit a hair color bias (42). In addition to the drug-melanin binding studies, attempts were made to begin to elucidate the chemical functional groups on melanin responsible for drug binding. Several model molecules containing one melanin functional group each were analyzed via tandem mass spectrometry for adduct formation with amphetamine and cocaine. The information gleaned from these studies helps to elucidate the important chemical properties of both drugs and melanins that are important for drug-melanin binding and thus for producing a potential hair color bias.

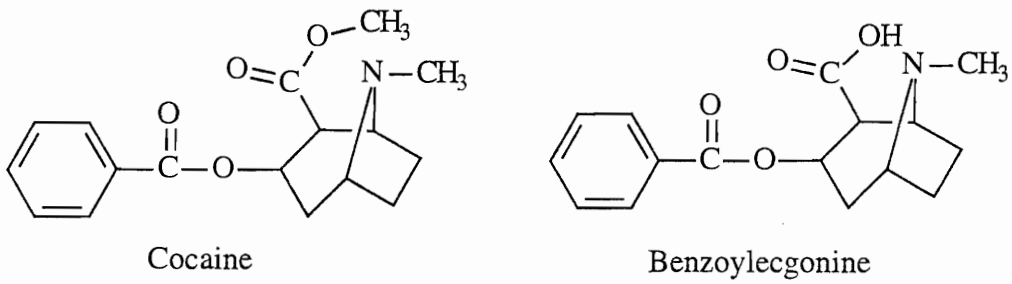

Cocaine Benzoylecgonine

Figure 4.1 *Chemical structures of cocaine and BE*

Materials and Methods

Materials

DHI and DHICA were synthesized as described by Wakamatsu and Ito (142). DHI-melanin and DHICA-melanin were prepared according to the method of Ito *et al.* (144). 5-CysDOPA and 2-CysDOPA were made via the method of Ito *et al.* (143). 5-CysDOPA-melanin and 2-CysDOPA-melanin were prepared as described by Ito and Fujita (141). Mixed eu-/pheomelanin copolymers from DHI and 5-CysDOPA or 2-CysDOPA were also made by the method of Ito and Fujita (141) omitting the acetone wash step. The initial reaction mixture contained 40% DHI and 60% CysDOPA (by mass). Melanin analysis by the method of Borges *et al.* (165) revealed that the copolymers consisted of 80% DHI-melanin and 20% 5-CysDOPA-melanin or 20% 2-CysDOPA-melanin (by mass). ^{3}H-l-(-)-Cocaine was obtained from NEN Life Science Products, Inc. (Boston, MA). ^{3}H-l-(-)-Benzoylecgonine was obtained from Moravek Biochemicals (Brea, CA). Tyrosinase, l-(-)-cocaine hydrochloride, benzoylecgonine tetrahydrate, d-amphetamine sulfate, d-amphetamine-d3 sulfate, and acetic anhydride-d6 were obtained from Sigma (St. Louis, MO). N-AcAp and N-AcAp-d3 were synthesized according to the method of Halmekoski and Saarinen (164), using acetic anhydride-d6 for N-AcAp-d3. Aminopropylsilica (APS) solid phase sorbent was purchased from International Sorbent Technology (Mid Glamorgan, UK). Cytoscint ES liquid scintillation fluid was obtained from ICN Biomedicals, Inc. (Costa Mesa, CA). Buffer salts were obtained from Mallinckrodt (Paris, KY). The structure and purity of all synthetic compounds (except melanins) were confirmed by NMR and mass spectrometry (See Appendix). Matrix assisted laser desorption ionization mass spectrometry (MALDI-

MS) on pure pheomelanin was performed on a PerSeptive Bioscience Voyager-Elite mass spectrometer equipped with a time-of-flight mass analyzer in positive ionization mode using as trans-4-hydroxy-3-methoxycinnamic acid as the sample matrix, by Dr. Vajira Nanayakkara. All other chemicals used are readily available and were of the highest purity available.

Melanin Preparation

Five different melanins were used in these experiments. They included: DHI-melanin, DHICA-melanin, 80% DHI / 20% 5-CysDOPA-melanin (DHI/5-CysDOPA-melanin), 80% DHI / 20% 2-CysDOPA-melanin (DHI/2-CysDOPA-melanin) and 100% 5-CysDOPA-melanin covalently linked to an aminopropylsilica (APS) solid phase sorbent, hereafter referred to as APS-pheomelanin. 5-CysDOPA was covalently attached to the APS sorbent using the same technique that Ibrahim and Aubry (173) used to link tyrosine-derived melanin to APS. Melanins were prepared for binding experiments by repeated homogenizing and washing in 0.066 M potassium phosphate buffer, pH 7.4 (for cocaine and BE binding experiments) or 0.15 M ammonium acetate buffer, pH 7.4 (for amphetamine and N-AcAp binding experiments) until a clear supernatant was obtained. Buffer concentrations were chosen to match the ionic strength of a normal saline solution. Ammonium acetate buffer was used for amphetamine and N-AcAp samples because a volatile buffer was required for LC/MS/MS analysis.

Binding Experiments

For each drug with each melanin, a time course (5, 15, 30, 60, and 90 min) was run to determine the amount of time required for binding equilibrium to be reached.

Time course samples were run at a concentration of 500 pM for cocaine, 2 nM for BE, and 30 nM for amphetamine and N-AcAp. Binding equilibrium was always established by 45 or 60 min. To obtain the binding parameters B_{max} and K_a for each drug-melanin combination, a range of drug concentrations was incubated with each melanin. For cocaine and BE this range included 12 points between 300 pM and 75 μM. For amphetamine and N-AcAp this range included 12 points between 1 nM and 300 μM.

Binding experiments were conducted in silanized 16 x 100 mm glass test tubes by adding the specified amount of drug (dissolved in buffer) to a buffer solution into which had been added 100 μg melanin (from a 1 mg/ml melanin suspension in buffer). The preparatory procedure was the same for all melanins except APS-pheomelanin for which it was necessary to add 3 mg APS-pheomelanin to equal 0.1 mg actual pheomelanin. Incubation was then performed at 37 °C in a vigorously shaking water bath, keeping melanin granules in suspension (325 rpm) for the specified time. For each sample, an analogous sample was incubated in the absence of melanin to serve as a control for any possible background binding. (For APS-pheomelanin samples, blank, or unreacted APS, was used as the background.) Total incubation volumes were 1 mL. At the end of the incubation time, samples were immediately transferred to 1.7 mL microcentrifuge tubes and spun at 14,000 rpm for 90 min at 4 °C. Immediately after centrifugation, 0.6 mL of supernatant was removed and mixed with either 14 mL scintillation fluid (cocaine and BE) or an aliquot of internal standard (amphetamine-d3 or N-AcAp-d3) at approximately one-third the amount of drug used in the incubation. Cocaine and BE samples were then mixed, left to settle overnight, and counted in a Packard 1900CA Tri-carb liquid scintillation counter. Amphetamine and N-AcAp samples were evaporated in a Savant

(Holbrook, NY) Speed-Vac SPD121P concentrator at < 35 °C. Samples were then reconstituted in 100 µL LC mobile phase for analysis.

LC/MS/MS Analysis

Quantitative analysis. LC/MS/MS analysis was performed in positive ion mode on a ThermoQuest (Finnigan, San Jose, CA) TSQ/SSQ mass spectrometer equipped with an electrospray ionization interface coupled to a Hewlett Packard (Palo Alto, CA) 1100 Series HPLC. Spray voltage was set at 4.5 kV, heated capillary at 250 °C, argon collision gas at 3.0 mTorr, and collision offset at –25 V. HPLC separation was performed on a Phenomenex (Torrance, CA) Luna 30 x 2.00 mm, 5 µm, C18(2) column under the following conditions: Amphetamine was eluted isocratically with 85% 0.1% formic acid / 15% methanol and monitored at its 136 m/z to 91 m/z transition. Amphetamine-d3 was monitored at its 139 m/z to 92 m/z transition. N-AcAp was eluted isocratically with 45% 0.1% formic acid / 55% methanol and monitored at its 178 m/z to 91 m/z transition. N-AcAp-d3 was monitored at its 181 m/z to 91 m/z transition.

Qualitative analysis. Qualitative tandem mass spectrometry experiments were performed to determine which melanin functional groups are most important in drug binding. Amphetamine and cocaine were assessed for noncovalent adduct formation with the functional groups on melanin as modeled by oxidized catechol, reduced catechol, deprotonated phthalic acid, and 3-methylindole. Tandem mass spectrometry analyses were carried out on the same instrument as above with the following alterations: Spray voltage was set to 3.5 kV, argon collision gas at 2.0 mTorr, and collision offset varied between –12 and –18 V. Positive ions were monitored for analysis of solutions of drug molecules mixed with oxidized catechol, reduced catechol, and 3-methylindole.

Negative ions were monitored when looking for adducts in mixtures of drugs with phthalic acid. Experiments were carried out by mixing the drug and model compound of interest at 100 μM and 200 μM final concentrations in 0.1% formic acid (unless otherwise specified), respectively, then infusing the mixture into the electrospray source at 10 μL/min with a supplementary HPLC flow of methanol (unless otherwise specified) at 0.05 mL/min. Oxidized catechol was made fresh daily by oxidizing a 0.02 M solution of catechol in water with a few milligrams of Ag_2O. The resulting yellow-brown mixture was then centrifuged at 14,000 rpm in a microcentrifuge at 4 °C for 5 min. The supernatant was then desalted by solid phase extraction as follows: A Waters Sep-Pak C18 solid phase extraction column was conditioned with 3 mL of methanol followed by 3 mL of water. One milliliter of approximately 0.02 M oxidized catechol was applied to the column, which was then washed with 9 mL water. Oxidized catechol was eluted with 2 mL of methanol to obtain a solution of oxidized catechol at approximately 0.01 M. Phthalic acid was kept deprotonated by keeping it in aqueous solution brought to pH 9 with ammonium hydroxide. The supplementary HPLC flow for experiments with phthalic acid was 50% water / 50% methanol at 0.05 mL/min. If an adduct was detected, daughter ion mass spectra were obtained for the parent adduct ion and neutral loss spectra scanning for any expected neutral losses were obtained to confirm the presence of both the drug molecule and the functional group model as part of the parent ion. To confirm adducts, experiments were run with deuterated drugs to confirm expected adduct mass shifts.

Data Analysis

For cocaine and BE the amount of free drug in the form of free fraction of drug was obtained by dividing the counts per min (CPM) for a melanin-containing sample by the CPM for its analogous nonmelanin-containing sample. For amphetamine and N-AcAp this was done by dividing the d0:d3 chromatographic peak area ratio for a melanin-containing sample by the d0:d3 chromatographic peak area ratio for a nonmelanin-containing sample. The bound fraction of drug was then taken as the difference between 1 and the free fraction of drug. The free concentration of drug (in M) was then determined by multiplying the free fraction by the concentration of drug in the sample. The bound concentration of drug (in moles drug/mg melanin) was determined by multiplying the bound fraction by the amount of drug in the sample and dividing this by the amount of melanin in the sample (0.1 mg).

To obtain the binding parameters B_{max} (binding capacity in moles drug / mg melanin) and K_a (binding affinity in M^{-1}), data from a range of drug concentrations were plotted as [Bound] vs. [Free] and analyzed via nonlinear least squares regression analysis using the equation describing drug adsorption to a solid (a Type I Langmuir Isotherm) (174). That is,

$$[B_d] = (B_{max}*K_a*[D])/(1+K_a*[D])$$

where $[B_d]$ is the concentration of bound drug, B_{max} is the maximum binding capacity of the melanin (in moles drug / mg melanin), K_a is the drug-melanin association constant (in M^{-1}), and [D] is the concentration of free drug (in M).

To determine the number of different types of binding sites (n) Scatchard plots were made. Scatchard plots indicated that for drugs that bound to melanin there were generally two types of binding sites, high affinity/low capacity and low affinity/high capacity binding sites. Nonlinear least squares regression analysis provided the low affinity/high capacity binding parameters and the x-intercept and (negative) slope of a Scatchard plot of the low concentration data (first four points) provided the binding parameters for the high affinity/low capacity binding site. Two-tailed Student's t-tests assuming homogeneity of variances were used to compare binding parameters for a drug between melanins.

Results

To investigate the binding of cocaine, BE, amphetamine, and N-AcAp to a variety of different melanin subtypes, drugs were incubated with melanins first at various time points to determine the time required to reach binding equilibrium, then at various concentrations to determine B_{max} and K_a (as described above). Representative selected reaction-monitoring (SRM) chromatograms from analysis of amphetamine and N-AcAp are shown in Figure 4.2. Table 4.1 presents a summary of the binding parameters determined for each drug with each melanin. B_{max} represents binding capacity in moles of drug per mg melanin and K_a represents binding affinity in M^{-1}. Experiments were repeated three times for drugs that bound to melanin and twice for drugs that did not bind to melanin. Out of the four drugs tested for binding to DHI, DHICA, DHI/5-CysDOPA

Figure 4.2 *Representative SRM chromatograms from LC/MS/MS analysis of (A) amphetamine and (B) N-AcAp*

A

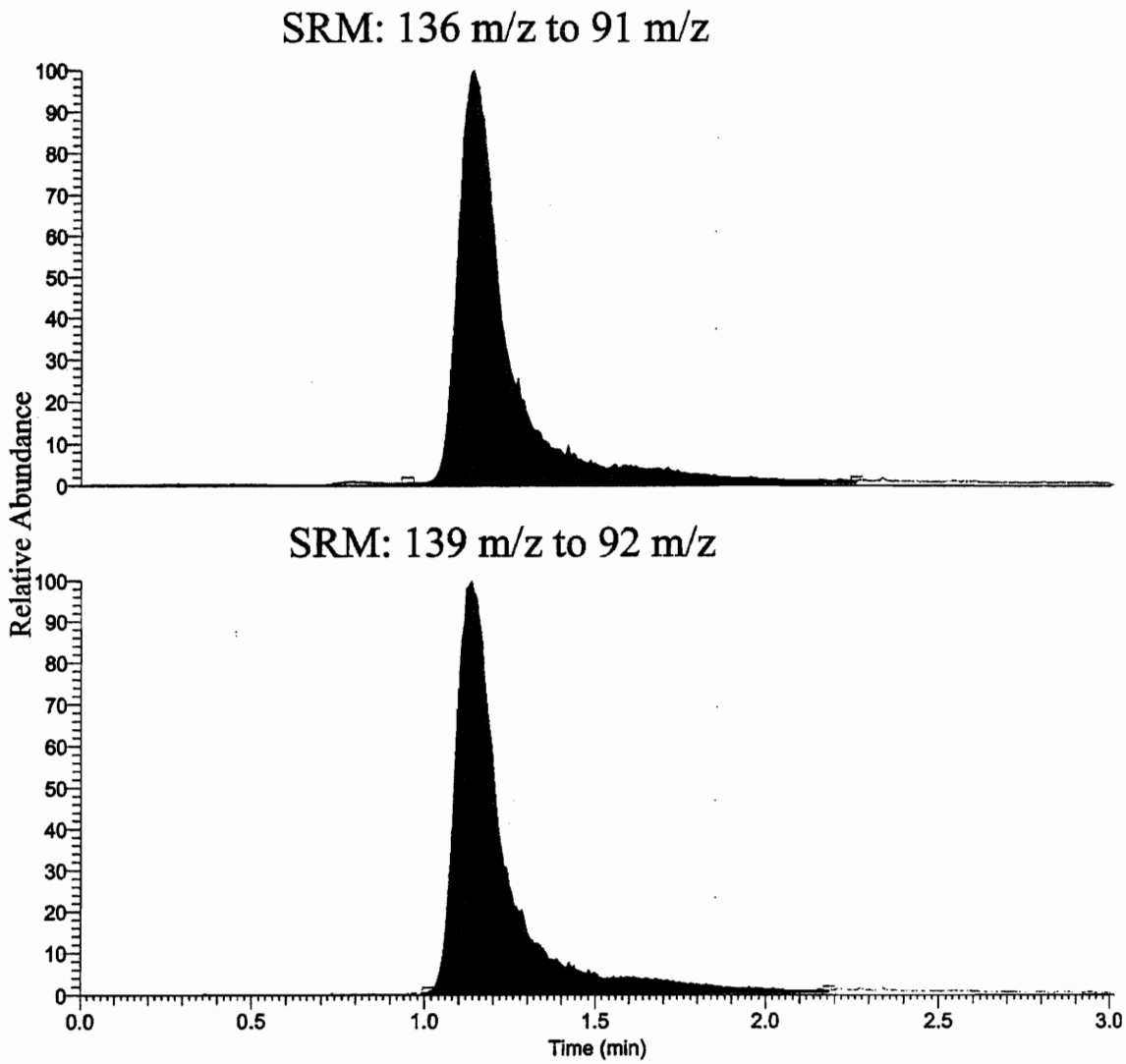
SRM: 136 m/z to 91 m/z
SRM: 139 m/z to 92 m/z
Relative Abundance
Time (min)
0
10
20
30
40
50
60
70
80
90
100
0.0
0.5
1.0
1.5
2.0
2.5
3.0

B

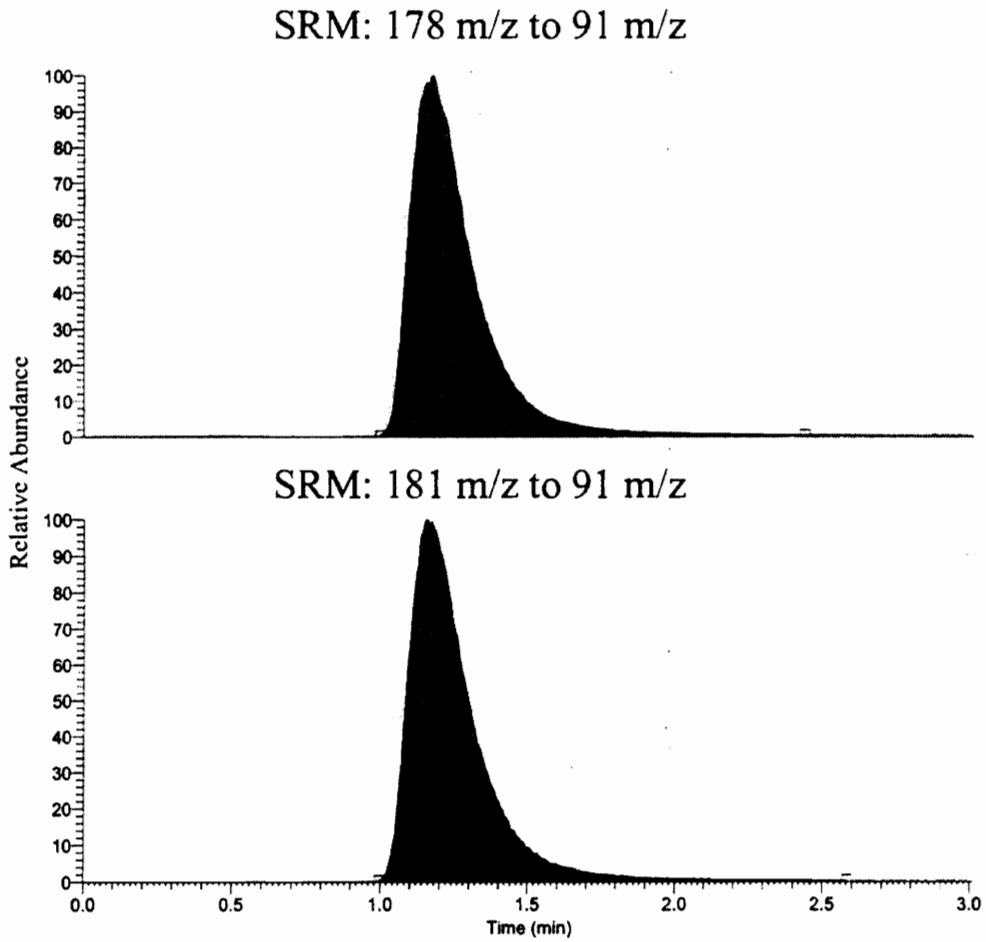
SRM: 178 m/z to 91 m/z
SRM: 181 m/z to 91 m/z
Relative Abundance
Time (min)
0.0
0.5
1.0
1.5
2.0
2.5
3.0

Table 4.1: Drug melanin-subtype binding parameters.[a]

Drug binding to DHI-melanin

	High Affinity / Low Capacity		Low Affinity / High Capacity		
	log Ka	-log Bmax	log Ka	-log Bmax	N = Number of Binding Sites
Cocaine	8.2 ± 0.19	9.5 ± 0.17	4.9 ± 0.039	7.0 ± 0.078	2
Amphetamine	6.6 ± 0.40	9.3 ± 0.35	3.9 ± 0.34	7.0 ± 0.25	2

Drug binding to DHICA-melanin

	High Affinity / Low Capacity		Low Affinity / High Capacity		
	log Ka	-log Bmax	log Ka	-log Bmax	N = Number of Binding Sites
Cocaine	7.8 ± 0.14	9.6 ± 0.16	4.5 ± 0.29	7.1 ± 0.082	2
Amphetamine	7.2 ± 1.2	9.9 ± 1.2	NB[b]		1

[a] Ka in units of M^{-1}. Bmax in units of mol drug/mg melanin. n=3 for all points except n=2 for NBs and n=4 for Ap-DHI-melanin and Ap-80% DHI / 20% 2-CysDOPA-melanin binding studies.

[b] NB indicates no binding observed.

Drug binding to 80% DHI / 20% 5-CysDOPA-melanin

	High Affinity / Low Capacity		Low Affinity / High Capacity		
	log Ka	-log Bmax	log Ka	-log Bmax	N = Number of Binding Sites
Cocaine	8.0 ± 0.31	9.5 ± 0.29	[c]4.3 ± 0.23	6.8 ± 0.21	2
Amphetamine	COMP[d]		4.1 ± 0.32	7.1 ± 0.25	2

Drug binding to 80% DHI / 20% 2-CysDOPA-melanin

	High Affinity / Low Capacity		Low Affinity / High Capacity		
	log Ka	-log Bmax	log Ka	-log Bmax	N = Number of Binding Sites
Cocaine	8.2 ± 0.048	9.6 ± 0.061	[c]4.4 ± 0.17	6.9 ± 0.16	2
Amphetamine	COMP[d]		3.7 ± 0.32	6.9 ± 0.29	2

[a] Ka in units of M^{-1}. Bmax in units of mol drug/mg melanin. n=3 for all points except n=2 for NBs and n=4 for Ap-DHI-melanin and Ap-80% DHI / 20% 2-CysDOPA-melanin binding studies.

[b] NB indicates no binding observed.

[c] Indicates a significant difference ($p < 0.05$) from DHI-melanin.

[d] COMP inidcates competition from buffer cations.

DHI/2-CysDOPA, and 5-CysDOPA melanins, only cocaine and amphetamine were found to bind to melanins. BE and N-AcAp did not bind to any of the melanins in this study. In addition, cocaine and amphetamine were found not to bind to the 5-CysDOPA-melanin (when APS was used as a measure of background binding, data not shown). As a positive control for the APS-linked 5-CysDOPA pheomelanin binding studies, L-DOPA-derived melanin was linked to the APS solid phase and found to bind cocaine with similar characteristics as "free" L-DOPA melanin.

For most of the (tested) drug-melanin binding interactions, there appeared to be two different binding sites; a high affinity/low capacity binding site and a low affinity/high capacity binding site. The concave nature of Scatchard plots derived from binding data demonstrated this to be the case. A representative Scatchard plot for cocaine binding to DHI-melanin is provided in Figure 4.3. Note that a group of data points appears to run along the y-axis and another group appears to run more parallel with the x-axis. The former section represents the high affinity/low capacity binding site (B_{max} and K_a values were determined by the x-intercept and (negative) slope of the section, respectively), while the latter section represents the low affinity/high capacity binding site. Because linearized (double reciprocal) equations and their associated plots tend to skew the relative error of the smallest plot values by disproportionately relying upon them as the major determinants of plot slope and intercept values, B_{max} and K_a values for the low affinity/high capacity binding sites (a region defined by higher concentration data points) were determined through nonlinear least squares regression analysis as discussed above and demonstrated in Figure 4.4.

Figure 4.3 *Scatchard plot for cocaine binding to DHI-melanin.* Two linear sections are present, indicating two different types of binding sites. Error bars indicate standard deviation. N = 3.

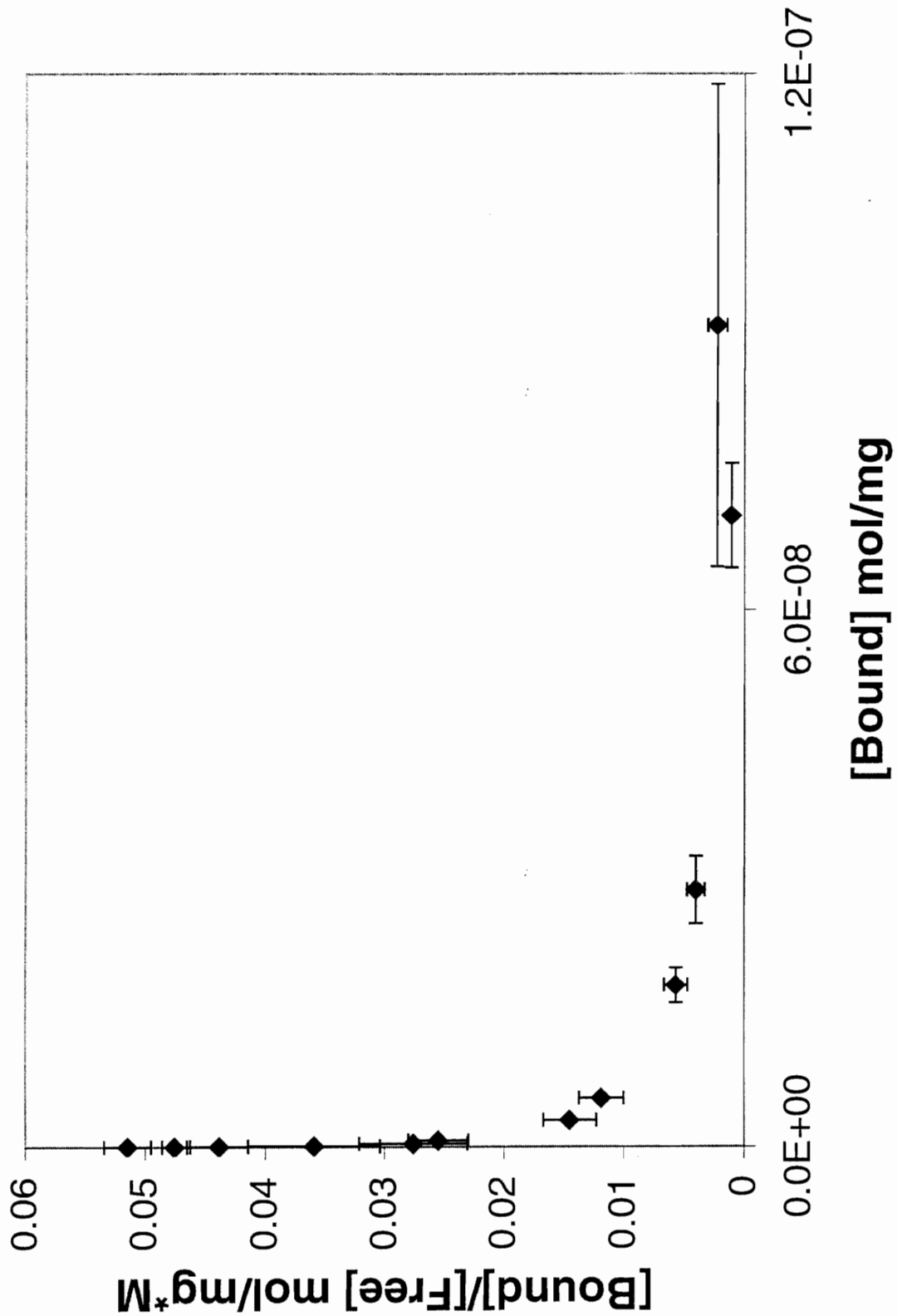
[Bound]/[Free] mol/mg*M
0.06
0.05
0.04
0.03
0.02
0.01
0
0.0E+00
6.0E-08
1.2E-07
[Bound] mol/mg

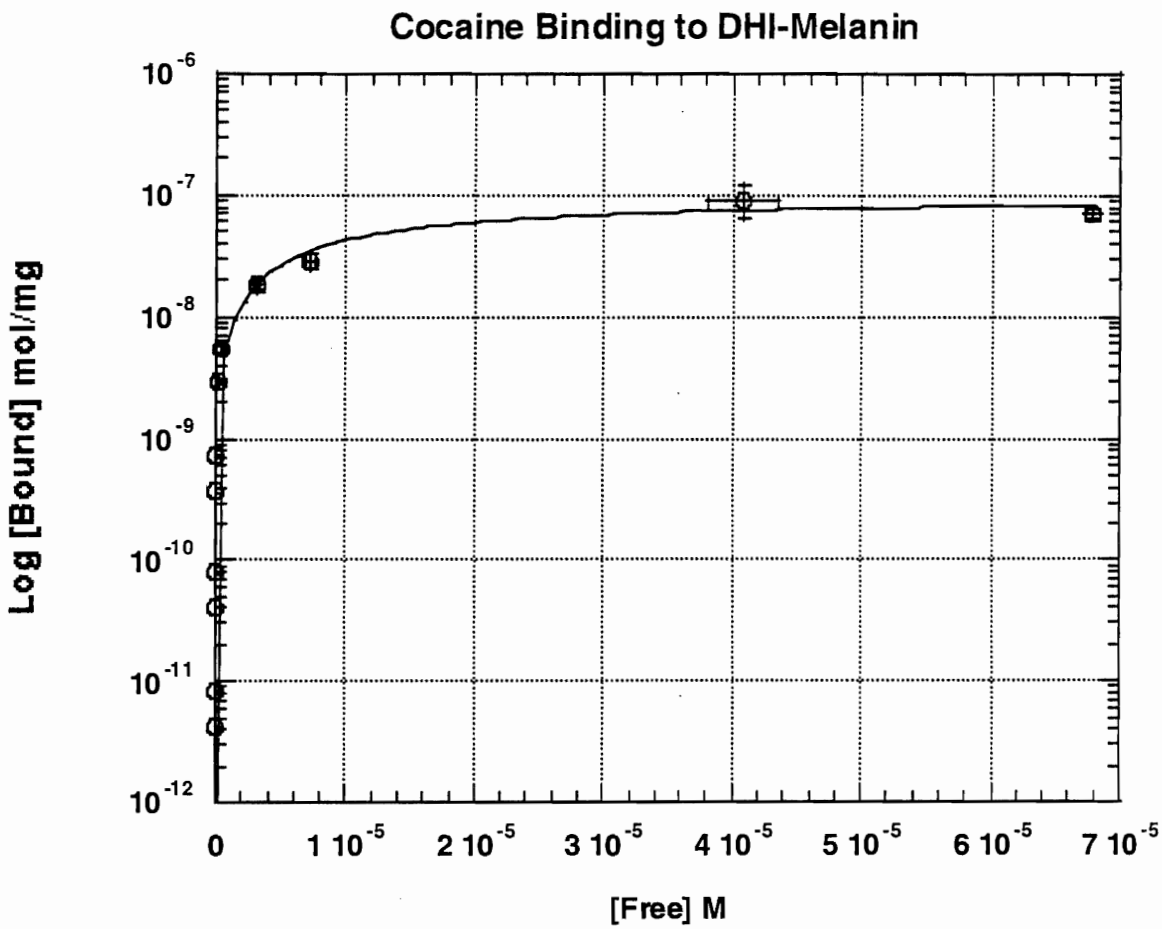

Figure 4.4 *Hyperbolic binding data plot for cocaine binding to DHI-melanin.* Such plots were used to perform nonlinear least squares regression analysis and determine B_{max} and K_a values for the low affinity/high capacity binding sites. Due to the wide range of drug concentrations used, data are plotted on a semilog scale so that most of the data points do not appear to be clustered at the origin. Error bars indicate standard deviation. n = 3.

As shown in Table 4.1, there were relatively few significant differences in the binding parameters for a given drug to the different melanin subtypes. The major difference was that none of the drugs that bound to eumelanins and mixed eu-/pheomelanins bound to pure (APS linked) pheomelanin. A direct comparison of K_a values between drugs is not legitimate due to the fact that different buffer systems were used. K_a data are not directly comparable because different buffer cations may compete differently for melanin binding sites and thus alter the K_a values that may have been observed if the binding studies had been conducted in identical buffer systems. Comparison of binding parameters between cocaine and amphetamine analogs, however, was not a goal of this study—as this was done previously for cocaine and amphetamine (55). Except in cases where binding data could not be assessed for amphetamine, B_{max} values for cocaine and amphetamine were similar (Table 4.1). This is in agreement with Shimada and co-worker's data (55).

Competition for melanin binding from buffer cations, as indicated by a convex Scatchard plot (51) (Figure 4.5), was found to occur for amphetamine binding to mixed eu-/pheomelanins, but not to pure eumelanins. When binding experiments were conducted in the absence of buffer, the apparent competition from buffer cations was eliminated and a concave Scatchard plot was demonstrated. The only other significant difference between melanins was the lower binding affinity of cocaine to the low affinity/high capacity binding site of the mixed eu-/pheomelanins compared to the analogous site on pure eumelanins (Student's t-test, $p < 0.05$).

Noncovalent amphetamine and cocaine adducts with oxidized catechol, reduced catechol, deprotonated phthalic acid, and 3-methylindole were searched for by tandem

Figure 4.5 *Scatchard plot for amphetamine binding to a mixed eu-/pheomelanin (80% DHI / 20% 5-CysDOPA-melanin).* Due to the wide range of drug concentrations used, data are plotted on a semilog scale so that lower x-axis values can be distinguished from each other. The convex shape indicates competition for binding from buffer cations. Error bars indicate standard deviation. n = 3

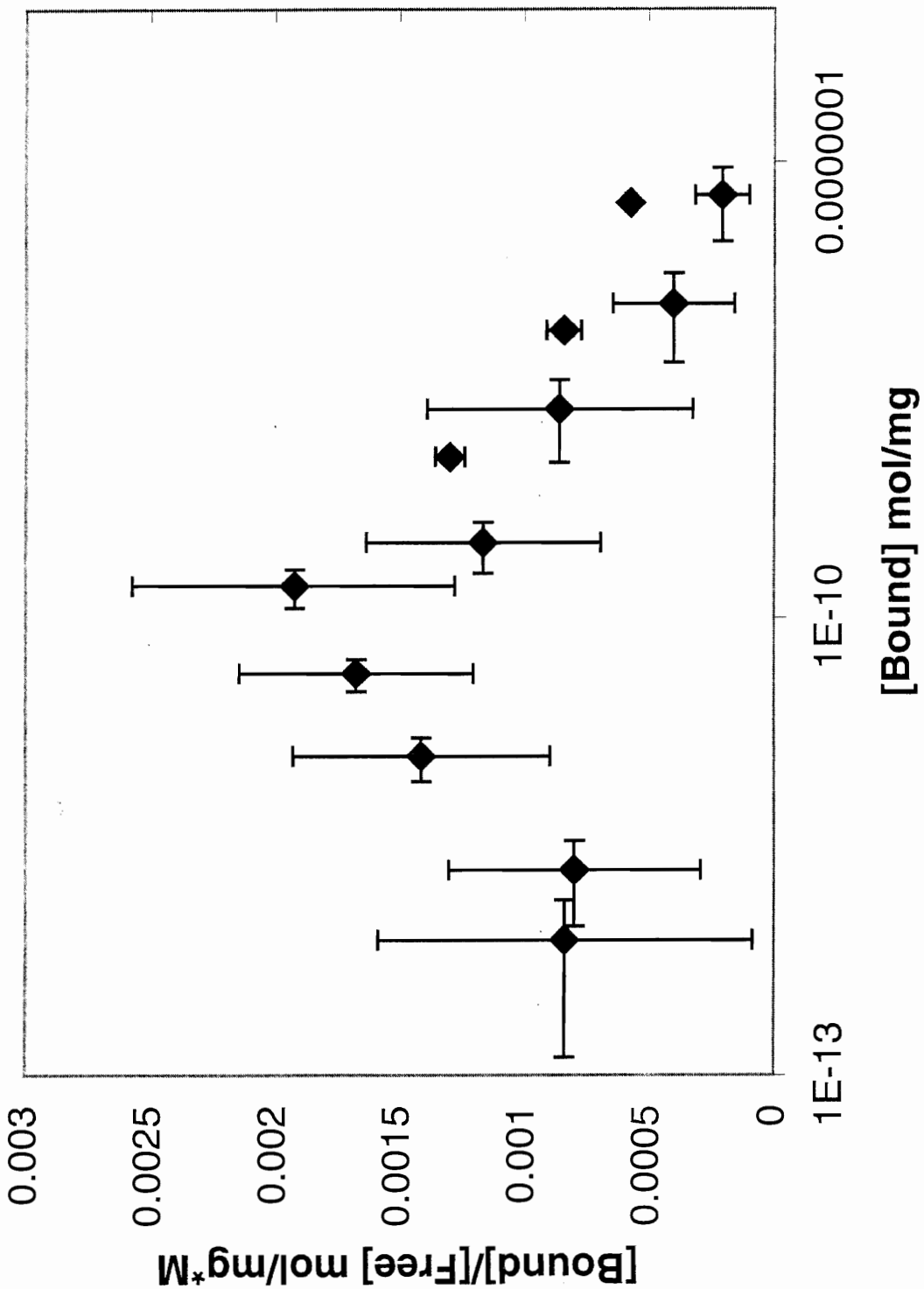
0.003
0.0025
0.002
0.0015
0.001
0.0005
0
[Bound]/[Free] mol/mg*M
1E-13
1E-10
0.0000001
[Bound] mol/mg

mass spectrometry as a means of assessing which chemical functional groups on melanin are most important for drug binding. Mass spectra shown in Figure 4.6 show the peaks corresponding to the only drug-functional group adduct observed; that of amphetamine with a covalent dimer of oxidized catechol (350 m/z) (Figure 4.7). (Other peaks in the single stage spectra below 130 m/z and at 332 m/z and 360 m/z are artifacts from the solvents employed.) The proposed structure shows a 3-3' linkage between the monomers as this seems the most likely candidate given that monomers of oxidized catechol do not form adducts with amphetamine; i.e., the oxygen atoms of the two monomers need to be in close proximity to each other to effect adduct formation. Other linkages such as 3-4' and 4-4', as well as neutral semiquinone radicals may be involved in adduct formation, but it is impossible to determine from the data obtained. Mass spectra shown in Figure 4.6 (D)-(F) demonstrate the mass shift of the adduct observed when amphetamine-d3 was employed in the study instead of amphetamine. MS/MS daughter ion and neutral loss spectra in Figure 4.6 (B)-(C) and (E)-(F) also show that amphetamine is part of the parent ion and that the covalent dimer of oxidized catechol (neutral 214 amu) is lost whether the experiment was performed with amphetamine or amphetamine-d3. Amphetamine in solution with reduced catechol produced no peaks that would correspond to amphetamine adduct formation with reduced catechol or a reduced catechol dimer.

Discussion

Binding of cocaine and amphetamine to synthetic L-DOPA derived melanin has been demonstrated previously (55, 56). Data from Shimada *et al.* (55) obtained from drug binding studies to L-DOPA melanin in 0.1 M potassium phosphate buffer, pH 7.4, indicate log K_a and $-\log B_{max}$ values for (±)-cocaine of 5.9 and 8.6, respectively, and for

Figure 4.6 *Mass spectra providing evidence for the amphetamine—oxidized catechol dimer adduct.* (A) through (C) represent spectra obtained from a 0.1% formic acid solution containing 100 μM amphetamine and ~200 μM oxidized catechol. (D) through (F) represent spectra obtained from a 0.1% formic acid solution containing 100 μM amphetamine-d3 and ~200 μM oxidized catechol. Single stage mass spectrum (A), MS/MS of 350 m/z (B), neutral loss scan for 214 amu (C), single stage mass spectrum (D), MS/MS of 353 m/z (E), and neutral loss scan for 214 amu (F).

A

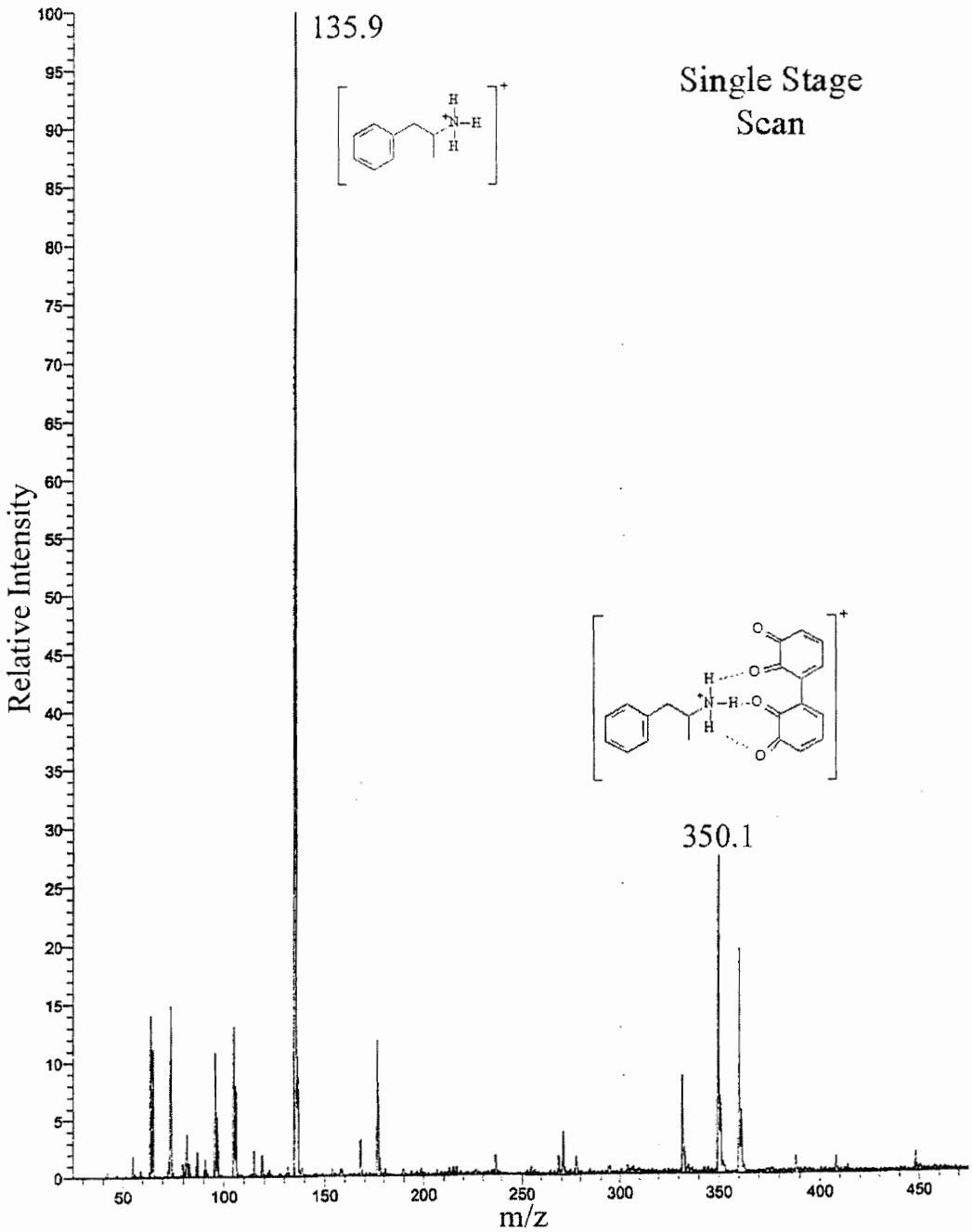
135.9
Single Stage
Scan
350.1
Relative Intensity
m/z
100
95
90
85
80
75
70
65
60
55
50
45
40
35
30
25
20
15
10
5
0
50
100
150
200
250
300
350
400
450

B

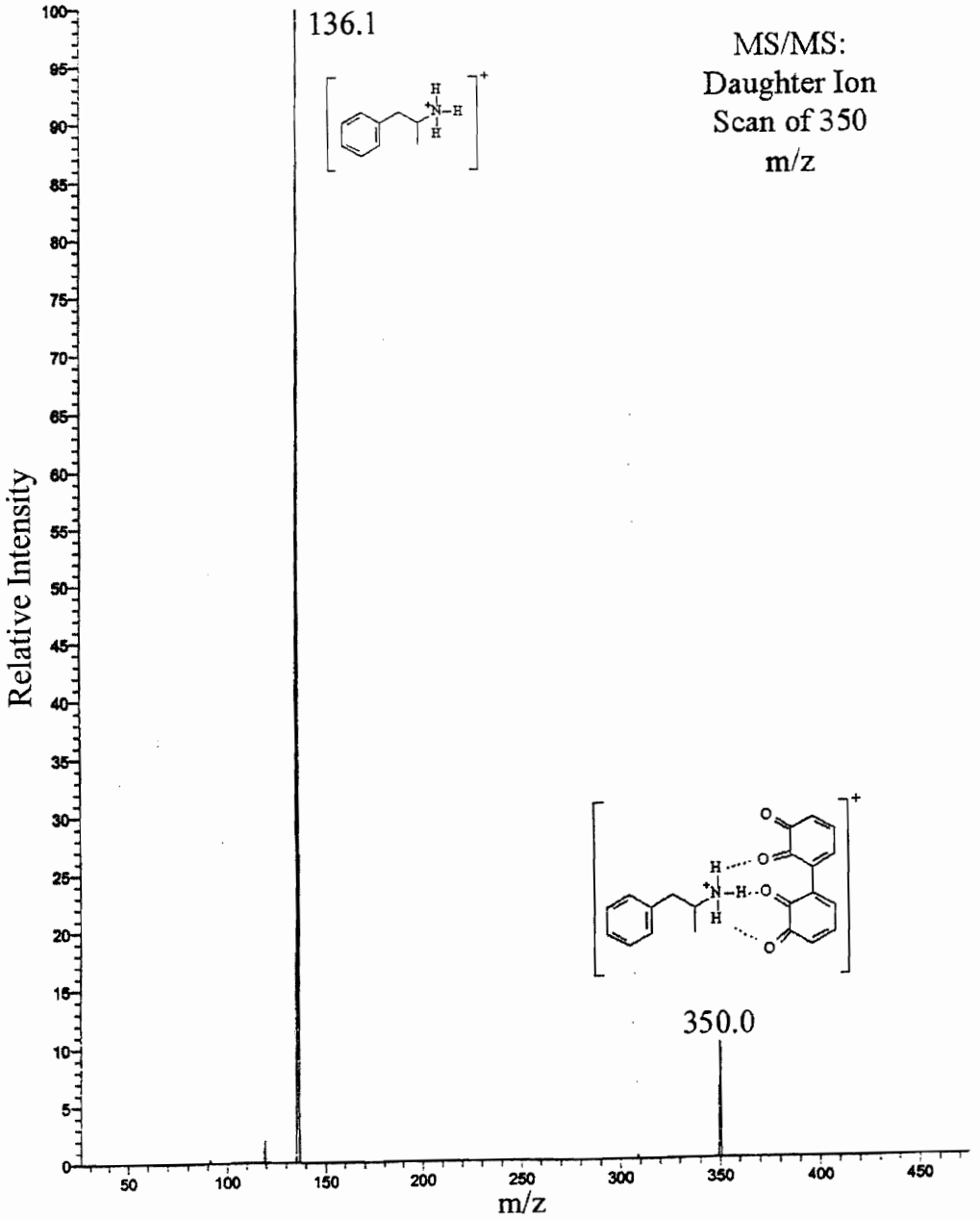
136.1
MS/MS:
Daughter Ion
Scan of 350
m/z
Relative Intensity
350.0
m/z

C

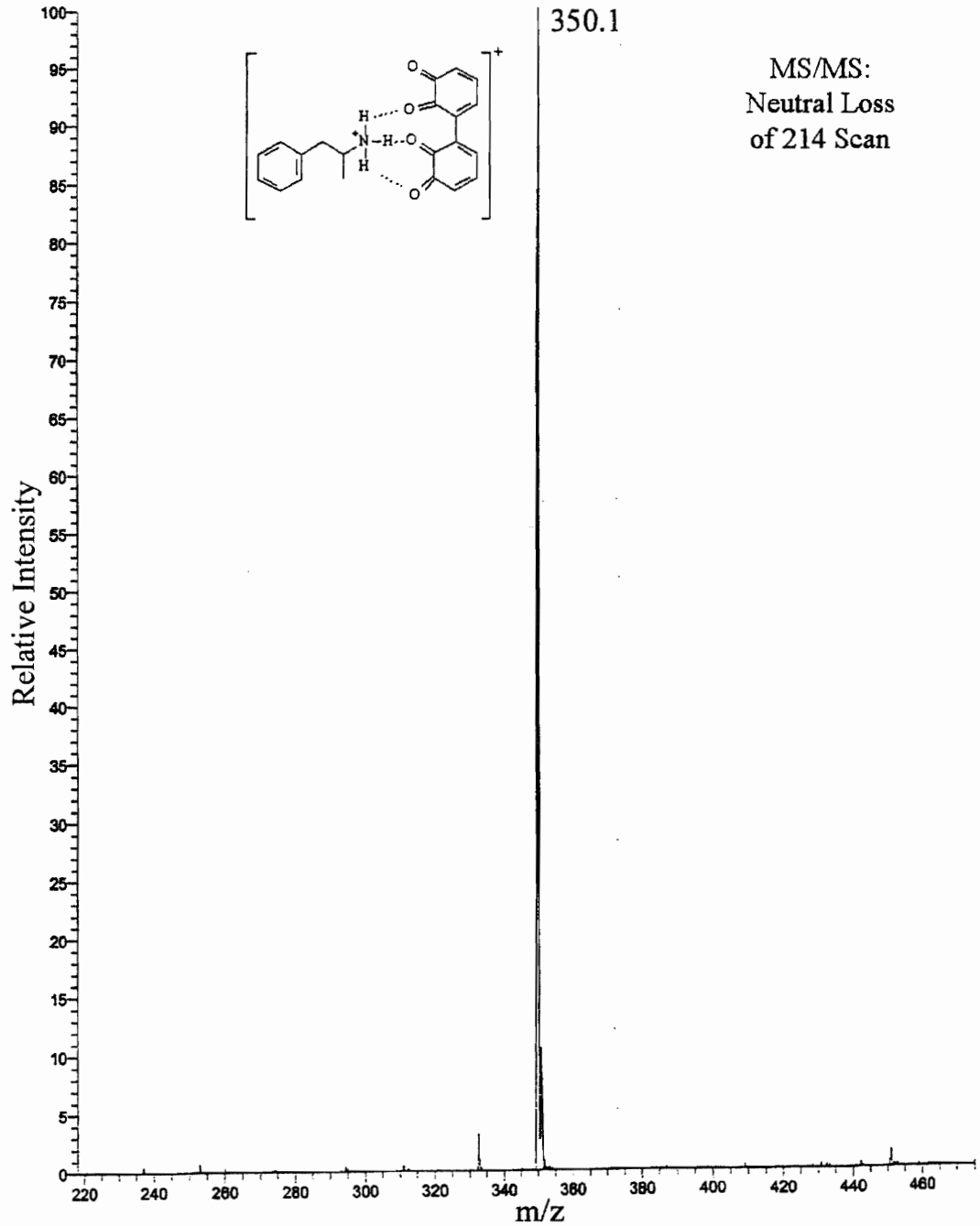
350.1
MS/MS:
Neutral Loss
of 214 Scan
Relative Intensity
m/z
100
95
90
85
80
75
70
65
60
55
50
45
40
35
30
25
20
15
10
5
0
220
240
260
280
300
320
340
360
380
400
420
440
460

D

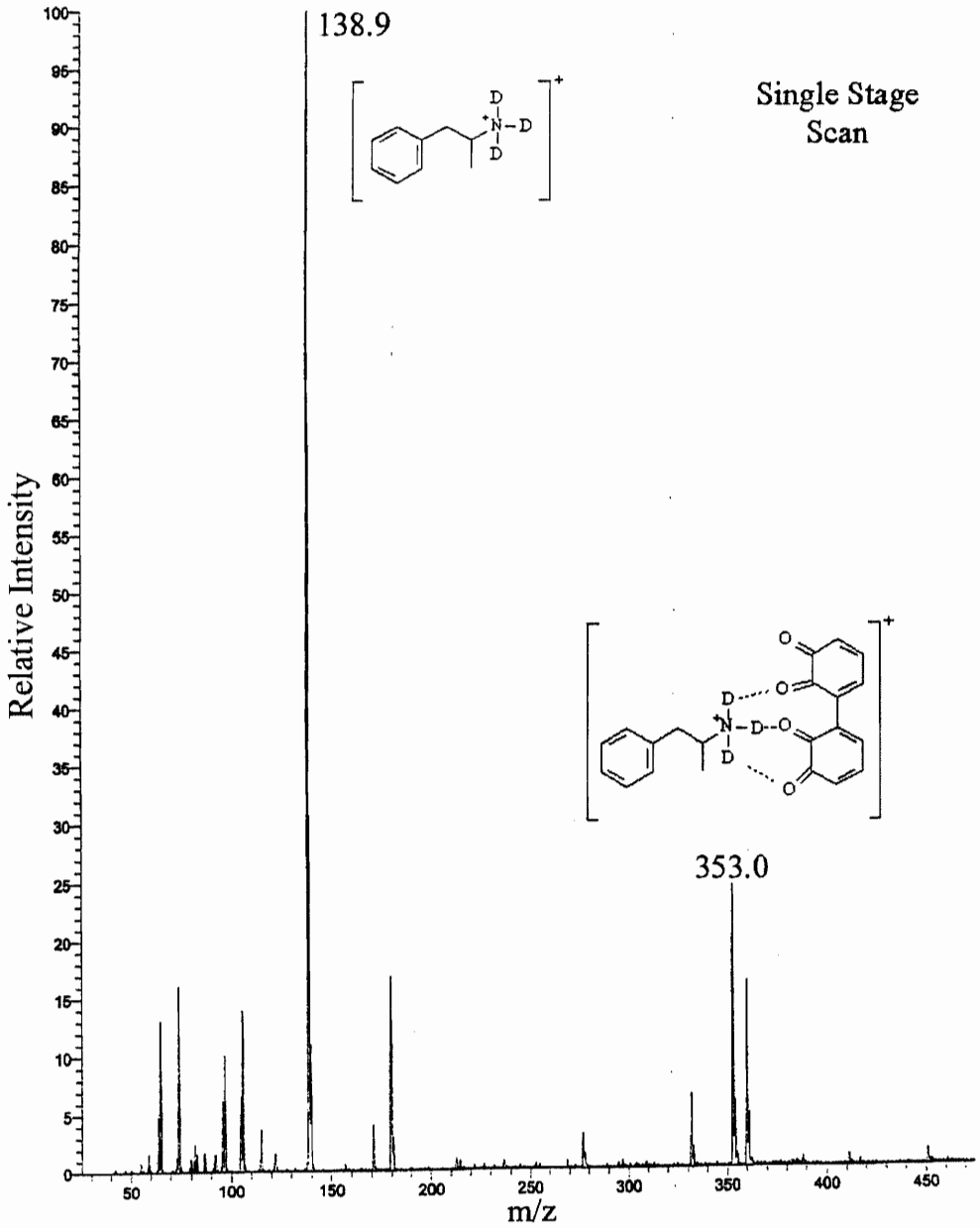
138.9
Single Stage
Scan
353.0
Relative Intensity
m/z
100
95
90
85
80
75
70
65
60
55
50
45
40
35
30
25
20
15
10
5
0
50
100
150
200
250
300
350
400
450

E

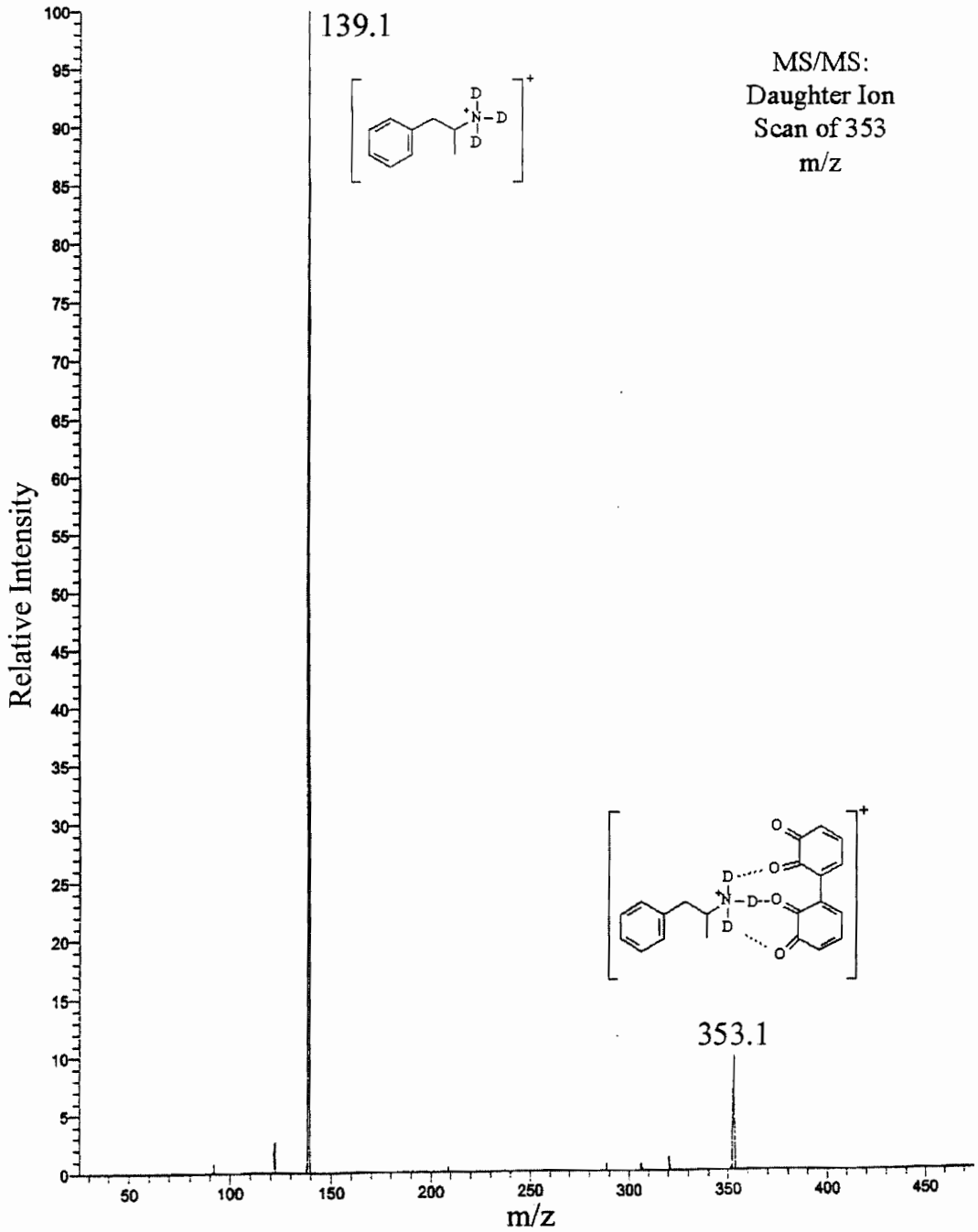
139.1
MS/MS:
Daughter Ion
Scan of 353
m/z
353.1
Relative Intensity
m/z
100
95
90
85
80
75
70
65
60
55
50
45
40
35
30
25
20
15
10
5
0
50
100
150
200
250
300
350
400
450

F

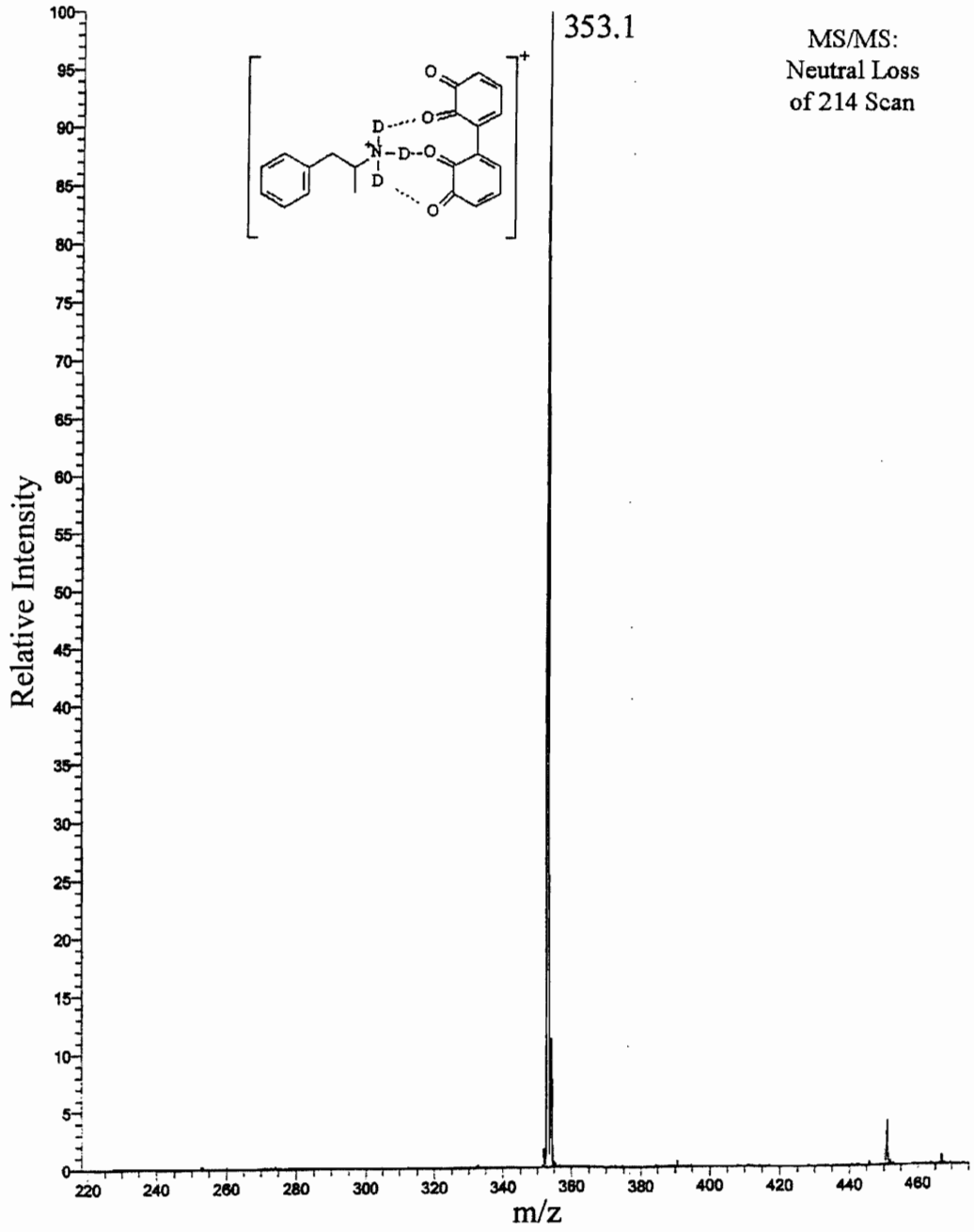
353.1
MS/MS:
Neutral Loss
of 214 Scan
Relative Intensity
m/z
100
95
90
85
80
75
70
65
60
55
50
45
40
35
30
25
20
15
10
5
0
220
240
260
280
300
320
340
360
380
400
420
440
460

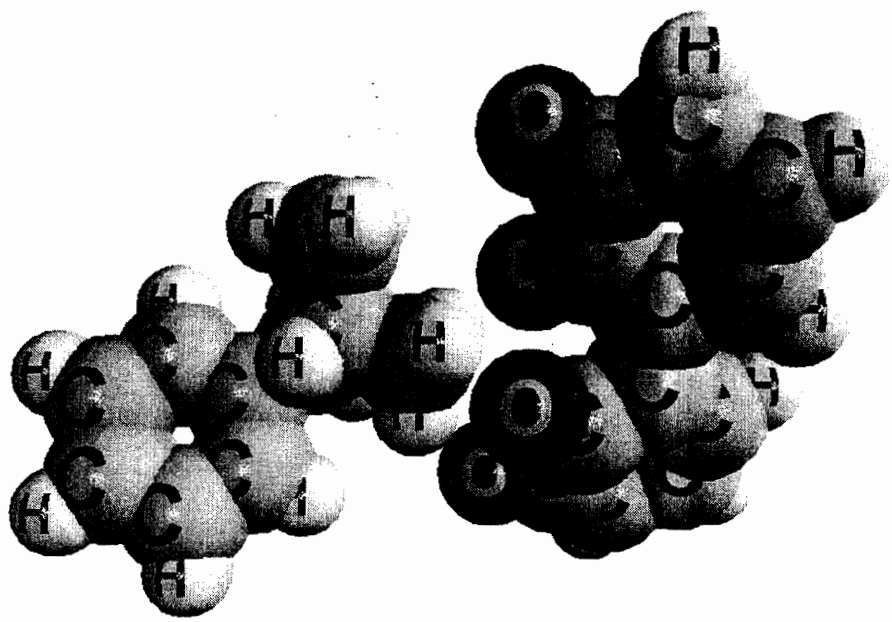

Figure 4.7 *Proposed amphetamine—oxidized catechol dimer adduct as detected by tandem mass spectrometry.* Energy minimized spacefill diagram showing the interaction of positively charged amphetamine with the oxidized catechol dimer.

(+)-amphetamine of 5.4 and 8.7, respectively. The data of Shimada *et al.* were obtained through the use of double reciprocal plots, which only reveal binding data for the high affinity/low capacity binding site. A direct comparison between their K_a data and ours is not legitimate due to the fact that different buffer systems were used, but it can be seen from Table 4.1 that their B_{max} values are reasonably close to the values obtained in this study. The greater ionic strength of their buffer system relative to ours, however, suggests that they should observe lower apparent K_a values—which they did.

Because cocaine and amphetamine have previously been found to bind to melanin, it was not surprising to find that these drugs bind to most of the melanin subtypes in this study. The chemical congeners of cocaine and amphetamine, BE and N-AcAp, respectively, however, were found not to bind to any type of melanin at all. This information provides clues as to what chemical features are important for drug-melanin binding. The structural difference between cocaine and BE is a methyl ester vs. a carboxylic acid. Based on suspected mechanisms of drug-melanin binding (51, 53), the electronic properties of a methyl ester are unlikely to be important for drug-melanin binding. Rather, the positive charge on the nitrogen of cocaine (pKa 8.5) is most likely to be responsible for the drug's binding to melanin. For BE, the introduction of a negative charge in the same molecule could render the positively charged nitrogen much less available for ionic binding with the negatively charged melanin polymer. In a similar scenario, the acetyl group of N-AcAp makes the amphetamine molecule nonbasic and thus not charged at physiologic pH. Again, it can be seen that the effective removal of a positive charge renders the drug molecule unable to bind to melanin.

Assuming the importance of a positively charged drug molecule for binding to melanin it is expected that the greater number of negatively charged atoms in the melanin polymer, the more positively charged drug molecules would bind to it (i.e., B_{max} should increase). As stated in the introduction, a comparison of DHI and DHICA monomers suggests that DHICA melanin should have a greater carboxylic acid content (and thus stronger anionic nature) than DHI melanin. This idea was confirmed by Novellino *et al.* (95) when it was demonstrated that DHICA melanin produces twice as much CO_2 as DHI melanin upon acid catalyzed thermal decarboxylation of the melanin pigments. Thus it was expected that DHICA melanin would have a larger capacity (B_{max}) for binding a given positively charged drug than DHI melanin. This was found not to be the case. Reasons for this are not certain, but there are a several possibilities. First, it may be possible that the carboxylic acid group is not responsible for cocaine or amphetamine binding, which seems unlikely given the mechanistic evidence for ionic binding interactions (51, 53). Second, a simple visual inspection (as well as visible wavelength optical absorbance—data not shown) of the homogenized DHI and DHICA melanin suspensions revealed that for a given mass/volume concentration of melanin in aqueous suspension, DHI melanin has more surface area (is finer and less grainy) than DHICA melanin. This may render a relatively significant portion of the carboxylic acid groups in DHICA melanin unable to interact with solvent molecules and thus unable to bind to drug present in solution.

Drug molecules seem to bind best if they are positively charged, regardless of whether or not they have a hydrophobic region such as a phenyl group (compare amphetamine and N-AcAp binding). In addition, a simple nickel (II) cation can display

the same complex (multi-site) binding characteristics as a structurally more complex drug molecule (51). This study and those of others (51, 53) suggest that there must be two separate sites on melanin that are capable of binding a positively charged ion or molecule. It has been previously suggested that the ortho-semiquinone free radical centers in melanin can bind doubly and triply charged cations forming chelate complexes (83). This could account for one of the binding sites for Ni^{2+}, but due to the fact that nitrogen atoms within organic molecules cannot act as the guest of a chelation complex, it cannot account for the binding of drug molecules.

Tandem mass spectral analysis of a solution of amphetamine mixed with oxidized catechol (Figure 4.6) strongly suggests that amphetamine can interact with the orthoquinone groups on oxidized indolequinone units of melanin. Interestingly, amphetamine was not found to complex with oxidized catechol monomers. This suggests that melanin secondary structure may play an important role in drug-melanin binding. This hypothesis is supported by the fact that cocaine did not form any adducts with oxidized catechol as amphetamine did, even though cocaine also demonstrates biphasic (two-site) binding to melanin. Molecular dynamics energy minimization experiments using the ChemSite ChemDemo program with a bath temperature of 300 K, an integration time step of 1 fs, total time of 10 ps, 100 equilibration steps, and non-bonded interaction cutoff distance of 10 Å show that the hydrogens attached to the primary amine of amphetamine intercalate between the oxygens of the dimerized oxidized catechol molecule and likely form three separate hydrogen bonds as depicted in Figure 4.7. The fact that cocaine did not form adducts with oxidized catechol is consistent with this model, because the positively charged tertiary amine of cocaine could not intimately

interact with the oxidized catechol dimer in the same manner as amphetamine due to steric hindrance. Based on the data obtained in these studies in conjunction with the investigations of others, it seems that the high affinity/low capacity binding site for basic drugs with melanin arises from an interaction of the positively charged drug molecule with appropriately shaped, electron dense, secondary structures of the melanin polymer. Evidence that this may be the high affinity/low capacity binding site also comes from Stepien and Wilczok (53) who demonstrated that adding a substantial amount of ethanol (20-50%) to a binding experiment selectively eliminates the high affinity/low capacity binding site. The presence of an organic solvent capable of forming hydrogen bonds could disrupt melanin secondary structure and compete with drug molecules for hydrogen bonding interactions with melanin. Evidence that a positive ionic charge on the drug molecule is an important facet of the high affinity/low capacity binding site was presented by Stepien and Wilczok (53) when it was shown that the binding affinity of this site decreases in the presence of high concentrations of sodium cations. In addition, Larsson *et al.* (50) demonstrated the complete elimination of paraquat binding under very acidic conditions. Extreme acidity could alter both the chemical nature and secondary structure of melanin in addition to providing binding competition, completely obliterating any significant drug-melanin interactions. In agreement with their observations, we were able to completely eliminate amphetamine binding to DHI melanin in 1 M HCl (data not shown). Thus, appropriately shaped, electron dense, melanin secondary structures within the melanin polymer could account for the high affinity/low capacity drug-melanin binding site.

Other evidence (51, 53) suggests that the other binding site can be accounted for by an ionic interaction—an interaction between the numerous carboxylic acid groups on melanin and positively charged drug molecules. Again, buffer cation competition for binding (51, 53) shows that both binding sites are sensitive to the ionic charge state of the drug molecule. Furthermore, using theoretical linear solvation energy relationships, Lowrey *et al.* (61) derived an equation for drug-melanin interactions that supports a charge transfer model. The fact that we were unable to observe drug-phthalic acid non-covalent adducts via mass spectrometry does not refute the carboxylic acid functional groups of melanin as participants in drug binding. Such interactions may be too weak to observe using this technique.

Finally, the participation of van der Waals interaction in some drug-melanin binding, however, cannot be discounted. Larsson and Tjalve (51) showed that the binding of chlorpromazine and chloroquine could not be completely depressed even in 2 M HCl. Under these acidic conditions, all negative charges on melanin would be eliminated. Interestingly, Larsson and Tjalve demonstrated two binding sites for nickel (II) and paraquat, and their evidence suggested the presence of three binding sites for chlorpromazine and chloroquine. Thus, for certain (possibly more planar and hydrophobic) compounds, van der Waals binding interactions with melanin may occur.

Based on structural studies, there are far more carboxylic acid groups present on melanin than there are orthoquinone or special secondary structure sites available for interacting with drug molecules (95, 96). This fact supports our assertion that the high affinity/low capacity binding site is probably derived from appropriately shaped, electron dense, melanin secondary structures within the melanin polymer, and the low

affinity/high capacity binding site consists of an ionic interaction between negatively charged carboxylic acid groups on melanin and positively charged drug molecules. In theory, it is possible for multiple hydrogen bonds to be stronger than single ionic bonds, given that hydrogen bonds range in energy from 10-40 kJ/mol and ionic bonds range in energy from 100-1000 kJ/mol (175). It must be kept in mind, however, that the sites discussed above for the binding of basic drugs to melanin have not been absolutely proven. They still remain speculative based on the binding observations of these and other studies.

The complete lack of cocaine and amphetamine binding to pure (APS linked) pheomelanin was an unexpected result, especially given the findings of Mars and Larsson (57) showing that synthetic pheomelanin is capable of binding a number of drugs. The apparent contradiction between their study and ours may be mostly resolved by two pieces of information. First, their pheomelanin may have contained a significant number of eumelanic monomer units due to the fact that L-DOPA in the presence of cysteine was used as the starting material for pheomelanin synthesis, and they did not obtain pheomelanin with a 38% w/w concentration of cysteine (the theoretical maximum for a 1:1 molar cysteine to L-DOPA incorporation ratio). The 1:1 cysteine to L-DOPA molar ratio was built-in to our pheomelanin due to the fact that the polymerization reaction was started with 5-CysDOPA. The former pheomelanin is probably a more biologically relevant pheomelanin, but we were interested in defining the drug binding properties of a theoretically "pure" pheomelanin, for which we believe our melanin is a more accurate model. Second, at least one carboxylic acid group from each purely pheomelanin polymer was converted to an amide for the sake of linking the pheomelanin polymer to

the APS solid phase. The elimination of carboxylic acid group(s) from the pheomelanin polymer is expected to decrease the ability of the polymer to bind basic drugs. If the pheomelanin polymer was excessively large and was known to be linked to the APS solid phase by only one amide bond, then the binding of drugs to pheomelanin may not have been inhibited by the attachment of pheomelanin to APS solid phase. The pheomelanin polymers synthesized for this study, however, are suspected to be no bigger than trimers of benzothiazine units. This suspicion comes from the fact that the pure pheomelanin is soluble in slightly basic aqueous medium and matrix assisted laser desorption ionization mass spectrometry (MALDI-MS) analysis of the pheomelanin indicates molecular weights no bigger than would be formed by trimers (data not shown).

With respect to drug incorporation into hair, it is intriguing to note that cocaine and amphetamine bind to melanins, but BE and N-AcAp do not. Cocaine and amphetamine have both been shown to have a hair color bias (42, 66), that is, in a black and white animal model more of both of these drugs were found in black hair than in white hair on the same animal. BE and N-AcAp both minimally incorporate into hair, regardless of their high plasma area under the concentration vs. time curves (AUCs) (41, 66) and N-AcAp has been shown not to exhibit a hair color bias (42). If drug-melanin binding is responsible for observed hair color biases, which appears to be the case since the only difference between black and white hair on the same animal is the presence of pigment in some hairs and the lack of it in others, then it may be possible to correct for this bias by normalizing drug concentrations found in hair by the eumelanin content of that hair. Evidence that this may be an appropriate correction comes from a study by

Rollins *et al.* (126) where interindividual differences in codeine concentrations in hair could be mostly accounted for by the eumelanin content of the hair.

CHAPTER 5

INFLUX AND EFFLUX OF AMPHETAMINE, N-ACETYLAMPHETAMINE, COCAINE, AND BENZOYLECGONINE IN KERATINOCYTES, PIGMENTED MELANOCYTES, AND NONPIGMENTED MELANOCYTES

Testing for drugs of abuse in hair has become a widely accepted alternative to traditional urinalysis (112, 176). Unfortunately, there are still a few potentially confounding variables involved in hair testing. Such variables include the role of environmental contamination in hair testing and adequacy of laboratory wash procedures designed to remove externally deposited drug, the role(s) of bleaching and/or other chemical treatments on the outcome of a hair test, and the role of hair pigment in drug incorporation into hair. The studies described here focus on two major aspects of the latter variable; the role of hair pigmentation in producing a hair color bias in drug incorporation into hair (which has been observed for many basic drugs including cocaine (66, 151), codeine (65, 152), amphetamine (42), phencyclidine (69), stanozolol (68), and nicotine (40)) and the fundamental physiological issue of cellular selectivity in hair cell drug uptake.

Despite the widespread utilization of hair as a matrix for drug detection, hair color bias (defined as the greater incorporation of a drug into darker hair over lighter hair, given equal blood plasma pharmacokinetics) still presents a major obstacle to fair hair

testing. In theory, given the same dose and route of administration, a dark haired individual may produce a positive drug test and a light haired individual may produce a negative drug test, if the cutoff concentration used to define a positive test happens to be established between the concentrations observed in the two specimens. Black hair pigment, or eumelanin, is a polyanionic indolequinone based polymer that has the capacity to bind positively charged (usually basic) drug molecules through what are thought to be both ionic and non-ionic interactions (30, 51-53, 55, 64-66, 69, 75, 76, 79, 153). This binding, and thus accumulation of the drug on melanin, is thought to produce the hair color bias. According to this theory, neutral or acidic drugs that do not bind melanin should not exhibit a hair color bias. This has been documented *in vivo* for the neutral drug N-AcAp (42, 76). Additional support for this theory is provided by phenobarbital, an acidic drug that does not show a hair color bias (65). Further evidence from carbamazepine, a basic drug with a low pKa (7.0; predominately uncharged at physiologic pH), also helps bolster this theory (74). The studies presented below employed the basic drug amphetamine and its nonbasic analog N-AcAp to examine the phenomenon of hair color bias at the cellular level by studying uptake and efflux into and out of pigmented melanocytes (PM) and nonpigmented melanocytes (NPM).

Amphetamine and cocaine are more highly incorporated into rat hair than BE and N-AcAp, respectively (41, 42, 66) regardless of whether hair is pigmented or non-pigmented. From the traditional pharmacologic point of view, based on the idea that passive diffusion plays a large role in the cellular uptake of small molecule xenobiotics and that nonpolar, uncharged molecules can diffuse into cells much more readily than their polar, charged counterparts, these data are counterintuitive and unexpected.

Bewilderment increases when drug plasma concentrations are taken into account: Given equal dosing in dark agouti rats, the plasma area under the concentration vs. time curve (AUC) is about four times greater for N-AcAp than it is for amphetamine (41) and that of BE is about twice as large as cocaine (66). There are at least two possible explanations for this seemingly conflicting data. First, N-AcAp and BE are highly protein bound and essentially unable to be taken into hair cells, or second, the hair cells have a transport system in place that permits the selective uptake of amphetamine and cocaine, but the relative exclusion of N-AcAp and BE. The former possibility was investigated and excluded in these studies—see Discussion for further details on this matter.

Amphetamine and N-AcAp, and cocaine and BE (Figures 3.1 and 4.1) were employed as model basic (and extensively incorporating) and nonbasic[h] (and low-level incorporating) pairs of drugs, respectively, to further document the roles of drug basicity in hair color bias and cellular selectivity in hair cell drug transport. Influx and efflux of amphetamine and N-AcAp were examined in keratinocytes, pigmented melanocytes (PM), and nonpigmented melanocytes (NPM) and influx and efflux of cocaine and BE were examined in PM and NPM. By sheer number, keratinocytes are the major cell type that makes up hair. In fact, under normal circumstances melanocytes merely transfer their melanin granules to keratinocytes prior to the movement of keratinocytes up into the growing hair shaft (93, 98-102). Thus, because of their major role in hair construction, keratinocytes were initially included in these studies along with the PM and NPM.

---

[h] BE is, technically, a basic drug. However, it also contains an acidic functional group and thus is a zwitterion and neutral at physiologic pH. With regard to hair incorporation and melanin binding, BE behaves relative to cocaine much as N-AcAp does to amphetamine. This may be due to formation of an intramolecular five-membered-ring ionic bond which could decrease BE's capacity to behave as a typical basic drug.

Materials and Methods

Chemicals and Reagents

N-AcAp and N-AcAp-d3 were synthesized from d-amphetamine sulfate according to the method of Halmekoski and Saarinen (164) using acetic anhydride and deuterated acetic anhydride, respectively. Purity was verified by mass spectrometry and/or NMR. d-Amphetamine sulfate, d-amphetamine-d3, l-(-)-cocaine hydrochloride, benzoylecgonine tetrahydrate sulfate, phorbol 12-myristate 13-acetate (TPA), glutamine, phenol red, phenylthiocarbamide were purchased from Sigma (St. Louis, MO). Cocaine-d8 (100 μg/mL) was obtained from High Standard Products (Inglewood, CA), and BE-d3 (100 μg/mL) was obtained from Cerriliant (Austin, TX). Keratinocyte Growth Media (KGM) was purchased from Clonetics, a division of Cambrex (East Rutherford, NJ). RPMI 1640 cell culture media, penicillin/streptomycin, and fetal calf serum were purchased from Life Technologies/Invitrogen (New York, NY). A bicinchoninic acid protein assay kit was purchased from Pierce (Rockford, IL). Centrifree ultrafiltration devices with Ultracel YMT membranes for performing plasma protein binding studies were purchased from Millipore (Bedford, MA). Bond Elute Certify solid phase extraction cartridges were obtained from Varian (Harbor City, CA). All other reagents were purchased in the highest purity form available.

Cell Lines and Culture

Cynthia Jorgensen and Dr. Gerald Krueger from the Department of Dermatology at the University of Utah kindly provided keratinocytes. The keratinocytes had been isolated from neonatal foreskins and immortalized as described previously (177).

Keratinocytes were routinely cultured in KGM. Melan-a melanocytes, isolated from C57BL/6 melanoblasts as described elsewhere (178), were generously donated by Simon Hill and Dr. Dorothy Bennett of the Department of Anatomy, St. George's Hospital Medical School, London. Melan-a melanocytes were cultured in supplemented RPMI 1640 media containing penicillin (100,000 U/L), streptomycin (100 mg/L), glutamine (2 mM), TPA (200 nM), extra phenol red (5 μg/mL), 10 mM HCl, and 10% fetal bovine serum in a humidified 5% CO_2 atmosphere at 37°C. Melan-a cells were made nearly amelanotic by culturing the cells in 200 μM phenylthiocarbamide, a tyrosinase inhibitor, for two to three passages before experimentation. Melanocytes were tested for mycoplasma contamination through submission to Bionique Testing Laboratories, Inc. (Saranac Lake, NY) and found to be negative for mycoplasma.

Influx Experiments

Drug influx experiments were carried out in standard 25 cm^2 "T25" cell culture flasks. Drugs were diluted into prewarmed cell culture media lacking serum. Culture media was removed from the cells and 5 mL drug containing media was introduced and kept on the cells for the desired time period at the desired temperature (usually in the incubator at 37 °C). After the desired time had elapsed the media was quickly removed by aspiration, and the cells were washed very rapidly three consecutive times with 5 mL (per rinse) of ice-cold phosphate buffered saline (PBS). Cells were then dissolved in 2.5 mL of 0.1 M NaOH (for amphetamine and N-AcAp) or in 0.1 M potassium phosphate buffer, pH 5.0 containing 1% Triton X-100 (for cocaine and BE). Thirty microliters of 10 μM deuterated drug was then added to the solution to serve as an internal standard for quantitation. To ensure complete dissolution of the cells, flasks were scraped with a cell

scraper prior to transfer of the cell lysate to a silanized glass test tube for protein assay and extraction (see Sample Preparation below). Cell viability was assessed for each drug treatment via the trypan blue dye exclusion and cell counting assay. Viability was greater than 90% for all treatments.

Efflux Experiments

The time required to establish equilibrium uptake was first determined with influx experiments. For amphetamine and cocaine, equilibrium uptake was determined to be well established by 30 min. Thus, to begin an efflux experiment, cells were pre-loaded with drug for 30 min in the same manner as an influx experiment. At 30 min elapsed influx time, drug-containing media was removed and the cells were rinsed three times with 5 mL of ice-cold PBS. Five milliliters of prewarmed serum free and drug free media was then added to the cells and the cells were incubated at 37°C for a set efflux time. When the set efflux time had elapsed, the media was collected and temporarily placed in a plastic beaker. Cells were then rinsed three times with 5 mL ice-cold PBS and set aside to be analyzed for the amount of drug remaining in the cells in the same manner as the influx experiments as described above. At a convenient time within 2 hrs, 4.25 mL of media collected from the efflux experiment was quantitatively transferred to a silanized glass test tube to which was added 30 μL of 10 μM deuterated analog to serve as an internal standard for quantitation.

Sample Preparation

Influx experiments. To normalize the amount of drug taken up by the cells in a given flask for the number of cells in the flask, a bicinchoninic acid protein assay was

performed on 25 µL of cell lysate to determine the amount of protein contained in the flask. Protein assays were performed in duplicate. For keratinocytes, the protein assay was performed directly on the cell lysates. For melanocytes, melanin was first precipitated by bringing 60 µL of cell lysate to pH ~5 (if necessary) with 10 µL of 0.5 M HCl, then spinning samples in a microcentrifuge at 4 °C for 15 min. Supernatant was then directly analyzed for protein content.

For amphetamine and N-AcAp samples, 300 µL of 2 M HCl was added to each lysate to bring the pH to between 1 and 2 to completely denature any intact proteins. Then 200 µL of 3.1 M NaOH was added to bring the pH to 12-13. This was followed by the addition of 200 µL concentrated NH_4OH. Samples were then extracted by addition of 5 mL of n-butyl chloride:chloroform (4:1) to the lysate, mixing for 30 min, centrifuging at 2000 rpm for 10 min, then removing the organic layer to a separate test tube. Organic extracts were then dried under a gentle stream of air at < 30°C and reconstituted in 100 µL of 0.1 % formic acid for injection onto the LC/MS/MS instrument.

Cocaine and BE samples were extracted with Bond Elute Certify solid phase extraction cartridges as follows: Columns were preconditioned with 2 mL methanol followed by 2 mL 0.1 M potassium phosphate buffer, pH 6.0. Following sample application, columns were rinsed with 6 mL water, 3 mL 0.1 M HCl, and 9 mL methanol after which columns were dried for 5 min. Cocaine and BE were eluted from the columns with 2 mL of fresh methylene chloride : isopropanol (80:20) containing 2% concentrated ammonium hydroxide. Samples were evaporated under a gentle stream of air at less than 40 °C then reconstituted in 100 µL 0.1% formic acid for LC/MS/MS

analysis. Daily standard curve and quality control samples for all drugs were extracted in the appropriate analogous manner.

Efflux experiments. Serum free cell culture media samples from efflux experiments were extracted in the same manner as influx cell lysate samples, but 300 µL of 3.1 M NaOH was required to raise the pH to 12-13 prior to liquid-liquid extraction. The pH of cocaine and BE containing cell culture media efflux samples was adjusted to ~5 with HCl prior to solid phase extraction.

Plasma protein binding experiments. Fresh human serum (BE) or plasma (N-AcAp) was obtained from healthy, drug-free volunteers after an overnight fast. To 485 µL serum or plasma was added 15 µL drug solution containing ^{3}H-BE (36 nCi) or N-AcAp to make final serum concentrations of 6 nM to 600 µM. Samples were incubated at room temperature for 30 min. One hundred microliters of the sample were then set aside for analysis to obtain a quantitative value for total drug in solution. (In the case of N-AcAp, 200 µL N-AcAp-d3, concentrated to give 1/3 the total amount of N-AcAp used in the original sample, was then added to the 100 µL whole plasma sample as an internal standard.) With the other half of the sample, free drug was then separated from protein bound drug through the use of Centrifree ultrafiltration devices with Ultracel YMT membranes (30,000 Da cut-off) spun at an average g-force of 1447 × g for 15 min to separate serum from ultrafiltrate. (The molecular weight cutoff of these devices is low enough to exclude albumin and alpha-1-acid glycoprotein, the two most significant drug binding plasma proteins.) One hundred microliters of ultrafiltrate were then collected (and in the case of N-AcAp internal standard added, as above, for quantitation) for analysis. BE samples were then analyzed as described below. N-AcAp samples were

extracted with Bond Elute Certify solid phase extraction cartridges as follows: To a 300 µL sample (including internal standard) was added 700 µL 0.1 M potassium phosphate buffer, pH 6.0. A column was preconditioned with 2 mL methanol, followed by 3 mL of the potassium phosphate buffer. Samples were then applied and columns were rinsed with 1 mL water, 1 mL of 0.1 M acetic acid, and again with 1 mL water then dried for 5 min. Samples were then eluted with 3 mL of methanol : 5 M HCl (20:1), dried in a Savant Speed-Vac sample concentrator, and reconstituted in LC mobile phase for analysis. As positive binding controls, cocaine and amphetamine were analyzed in analogous manners as BE and N-AcAp, respectively. Positive control data were comparable to literature values (179, 180).

Sample Analysis

Quantitative drug analysis was carried out on influx and efflux samples using a ThermoQuest TSQ/SSQ triple stage quadrupole tandem mass spectrometer in selected reaction monitoring (SRM) mode coupled to a Hewlett Packard (Palo Alto, CA) 1100 series HPLC. LC/MS/MS was selected as the analytical technique because of its excellent selectivity, sensitivity, and quantitative ability as well as its ability to analyze polar compounds without derivitization. (In addition, analysis by this technique as compared to the use of radiolabeled drugs allows determination and quantitation of the drug itself within cells, not accumulation of data that is ambiguous with respect to the actual identity of the influxed (or effluxed) molecule.) Samples were injected onto a Metachem Metasil Basic 3 µm particle size 30 x 2.0 mm HPLC column. For optimal chromatography, the following gradient was run for amphetamine samples: From 0-2.2 min. composition was held at 98% 0.1% formic acid / 2% methanol at a flow rate of 0.2

mL/min. Composition was then ramped to 40% aqueous / 60% organic over 0.1 min and held until 6.4 total min when composition was ramped back to 98% aqueous / 2% organic and flow rate to 0.4 mL/min over 0.1 min and held until 12.5 min at which time the flow rate was ramped to 0.2 mL/min over 0.1 min and held until 14.5 min at which time the next sample was injected. Using the same mobile phases, N-AcAp was analyzed with the following gradient: From 0.1 to 5.0 min composition was ramped from 98% aqueous / 2% organic to 10% aqueous / 90% organic and held until 8.9 min at which time the composition and flow rate were changed to 98% aqueous / 2% organic and 0.4 mL/min, respectively, over 0.1 min. These conditions were held until 14.0 min when initial condition were re-established over 0.1 min and held until 15.5 min when the next sample was injected. Cocaine and BE were eluted from the same column under the following conditions: From 0 to 1.0 min composition was held at 98% 0.1% formic acid / 2% acetonitrile (at a 0.2 mL/min flow rate) at which time it was quickly ramped to 90% organic over 0.1 min and held until 6.9 min. Over 0.1 min composition was shifted back to original conditions and flow rate to 0.4 mL/min. At 11.4 min flow rate was changed back to 0.2 mL/min over a 0.1 min time range. These conditions were held for another min until the next sample was injected. Ionization was effected with an electrospray ionization source in positive ion mode with the spray voltage set at 4.5 kV. The heated capillary was set at 250 °C, collision gas at 3.0 mTorr, and collision offset at –20 V (for amphetamine and N-AcAp) and –24 V for cocaine and BE. SRM m/z transitions monitored were as follows: Amphetamine (136 m/z to 91 m/z), amphetamine-d3 (139 m/z to 92 m/z), N-AcAp (178 m/z to 91 m/z), N-AcAp-d3 (181 m/z to 91 m/z), cocaine

(304 m/z to 182 m/z), cocaine-d8 (312 m/z to 185 m/z), BE (290 m/z to 168 m/z), and BE-d3 (293 m/z to 171 m/z).

Prepared serum or plasma and ultrafiltrate samples were either analyzed via scintillation counting (BE, with correction for protein quenching of signal) or LC/MS/MS as described above.

Eumelanin assays were performed as previously described in Chapter 2 on one sample from each cell category (i.e., pigmented or nonpigmented) from each experiment and normalized for protein content so that approximate melanin quantities in the rest of the flasks containing that cell category in that experiment could be calculated. The use of phenylthiocarbamide as a tyrosinase inhibitor produced NPM that contained as little as 160 μg eumelanin/mg protein compared to cells cultured in the absence of phenylthiocarbamide which contained as much as 6400 μg eumelanin/mg protein.

Data Analysis

Quantitative analysis was performed by calculating drug to internal standard SRM chromatogram peak area ratios and comparing them to a standard curve generated in the same way using known amounts of drug. For each influx time point, an analogous negative control sample was run in which no cells had been cultured in the flask. This was done to determine the background level of drug adhered to the flask alone and removed by the collection procedure. The amount of drug adhered to the flask was subtracted out of the value determined for the cellular uptake sample. Generally this had very little to no effect on the data produced as the amount of drug taken up by cells greatly exceeded (>>10 fold) the amount of drug adhered to the flask alone. For influx experiments the amount of drug taken up by a flask of cells was divided by the amount of

protein in that flask of cells and plotted against time. For efflux experiments, the amount of drug effluxed out of the cells and the amount of drug remaining in the cells were added together to obtain the total amount of drug originally taken up (after 30 min of influx) by the cells. This sum was then divided by the amount of drug remaining in the cells to obtain the fraction of influxed drug remaining in the cells and plotted against time.

Results

Time courses of influx and efflux were carried out so that both initial rates and uptake amounts at equilibrium could be approximated. Initial influx or efflux was always established very quickly, i.e., in a matter of a few min or less. Typical SRM chromatograms obtained from cell uptake/efflux experiments for the purpose of drug quantitation are shown in Figure 5.1A-D. No smoothing algorithms or special chromatographic processing was performed. Drug to internal standard peak area ratios were used for quantitation. In the figures that follow, each data point is determined from a separate flask of cells. No two data points were obtained from one flask of cells. Figures 5.2A-B depict time courses for influx of 1 μM amphetamine or cocaine into keratinocytes, PM, and NPM. Each time course was repeated twice. Initial influx was completed in nonpigmented cells by 60 s, but in pigmented cells it was completed and influx equilibrium was established by 15 min. Eumelanin content had a dramatic effect on the equilibrium influx amount of amphetamine and cocaine taken up into pigmented vs. NPM. Keratinocytes take up the least amount of amphetamine on a per mg of protein basis. However, it is important to realize that per flask, keratinocytes produce about five times as much protein as melanocytes, thus decreasing their apparent relative uptake amounts by a factor of 5. An expanded plot of the keratinocyte influx data is seen in

Figure 5.1 *SRM chromatograms of (A) amphetamine, (B) N-AcAp, (C) cocaine, and (D) BE from cell lysates.*

A

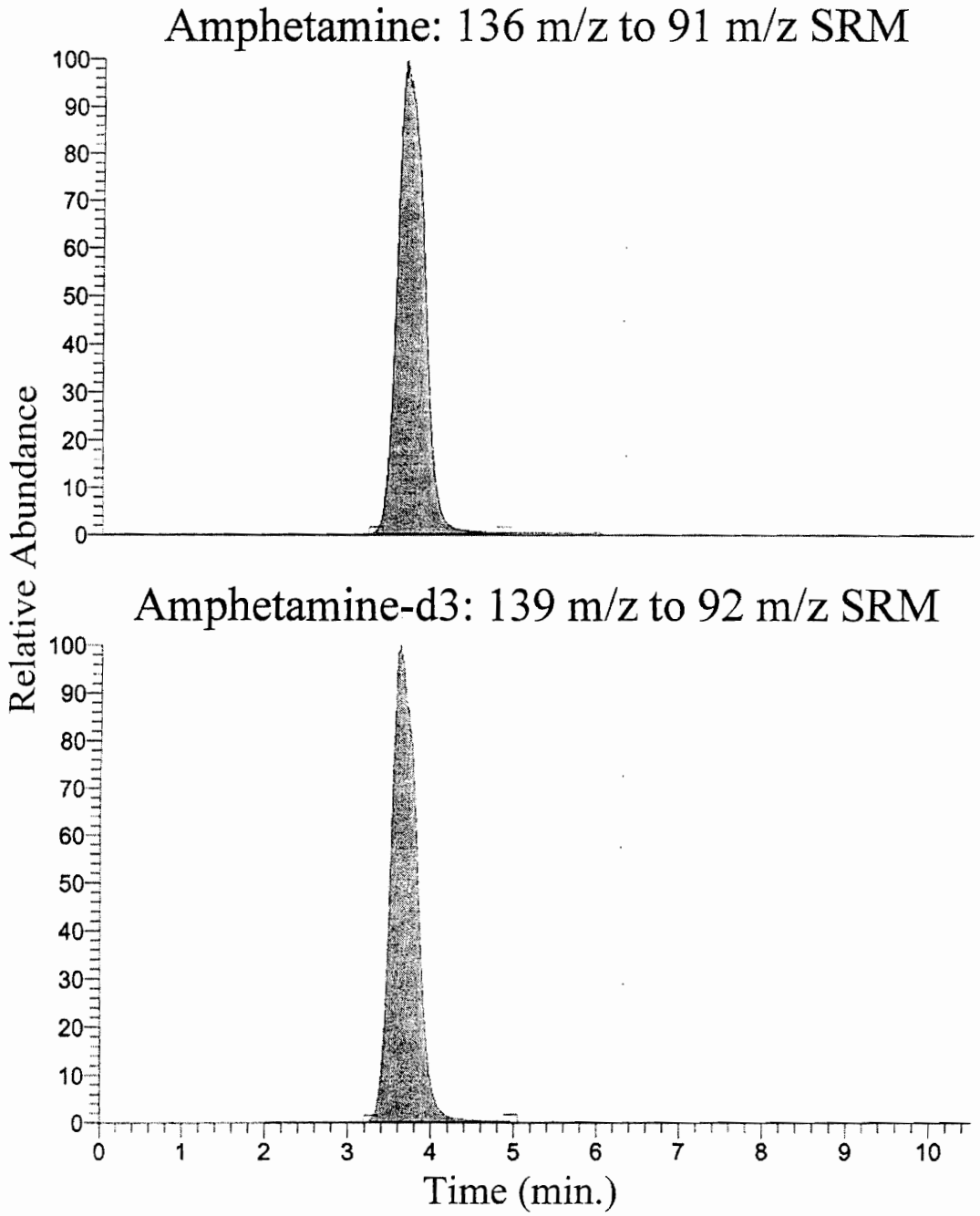
Amphetamine: 136 m/z to 91 m/z SRM
Amphetamine-d3: 139 m/z to 92 m/z SRM
Relative Abundance
Time (min.)
0
10
20
30
40
50
60
70
80
90
100
0
1
2
3
4
5
6
7
8
9
10

B

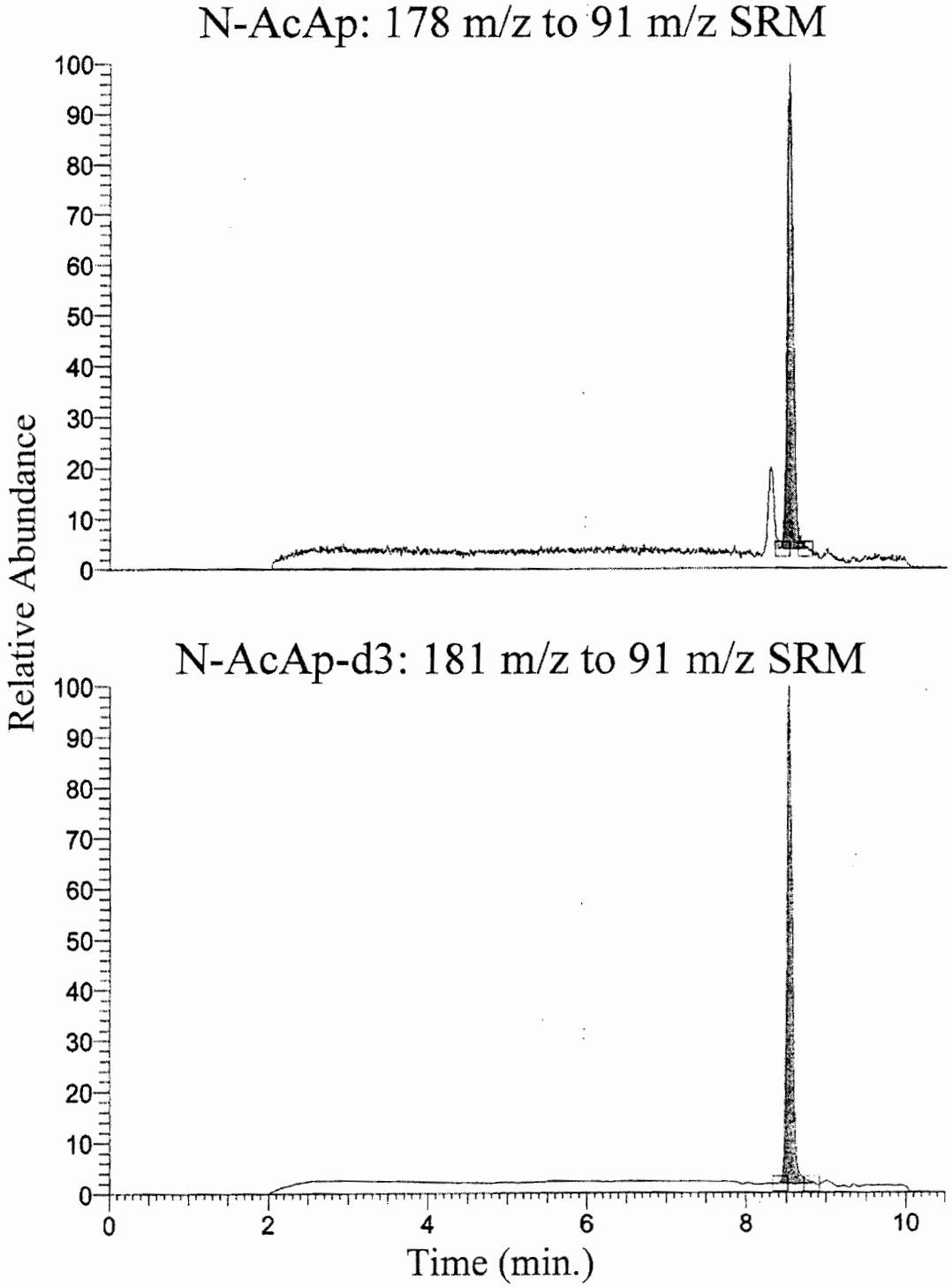
N-AcAp: 178 m/z to 91 m/z SRM
N-AcAp-d3: 181 m/z to 91 m/z SRM
Relative Abundance
Time (min.)
0
10
20
30
40
50
60
70
80
90
100
0
2
4
6
8
10

C

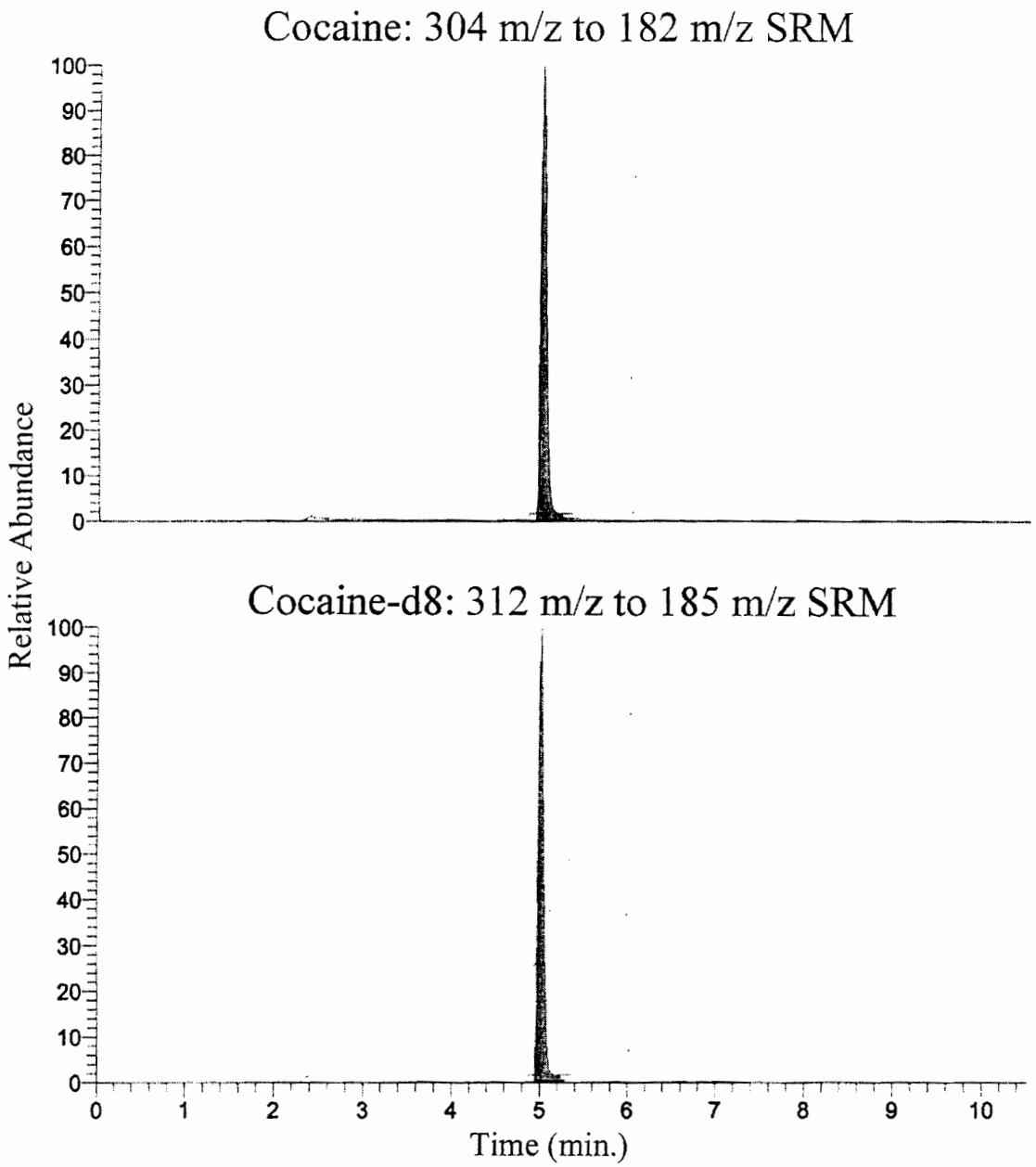
Cocaine: 304 m/z to 182 m/z SRM
Cocaine-d8: 312 m/z to 185 m/z SRM
Relative Abundance
Time (min.)
0
10
20
30
40
50
60
70
80
90
100
0
1
2
3
4
5
6
7
8
9
10

D

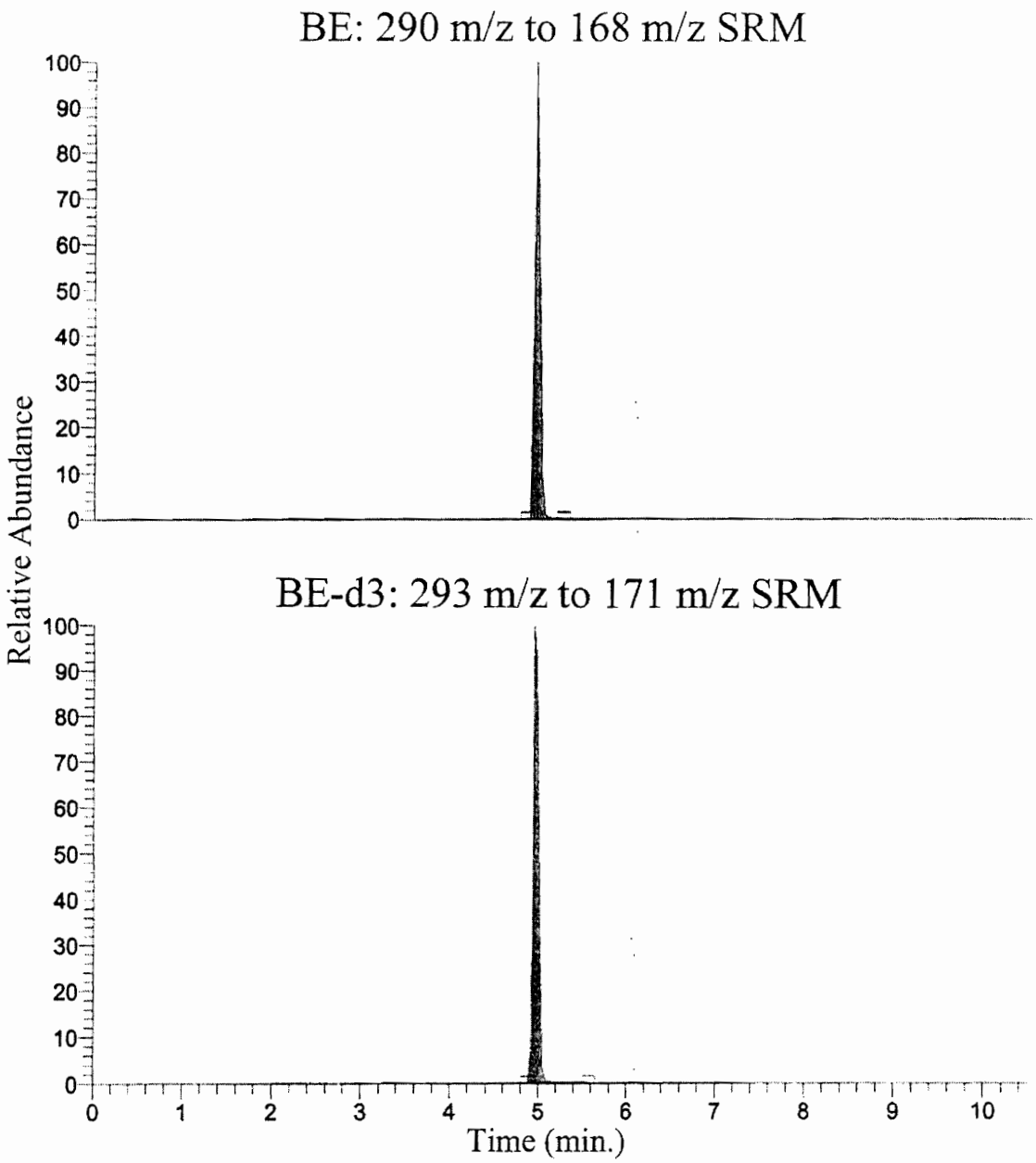
BE: 290 m/z to 168 m/z SRM
BE-d3: 293 m/z to 171 m/z SRM
Relative Abundance
Time (min.)
0
10
20
30
40
50
60
70
80
90
100
0
1
2
3
4
5
6
7
8
9
10

Figure 5.2 *Influx of (A) 1 μM amphetamine and (B) 1 μM cocaine into keratinocytes, pigmented melanocytes (PM) and nonpigmented melanocytes (NPM) over time.* #1 and #2 designate the first and second repetitions of an experiment. For ease of reference, eumelanin content in μg eumelanin / mg protein is expressed in the legend. Initial data points were at 15, 30, 45, and 60 seconds. Keratinocyte data points represent the average of two determinations while the error bars represent the actual data points. Each experiment with melanocytes is displayed as an individual series.

A

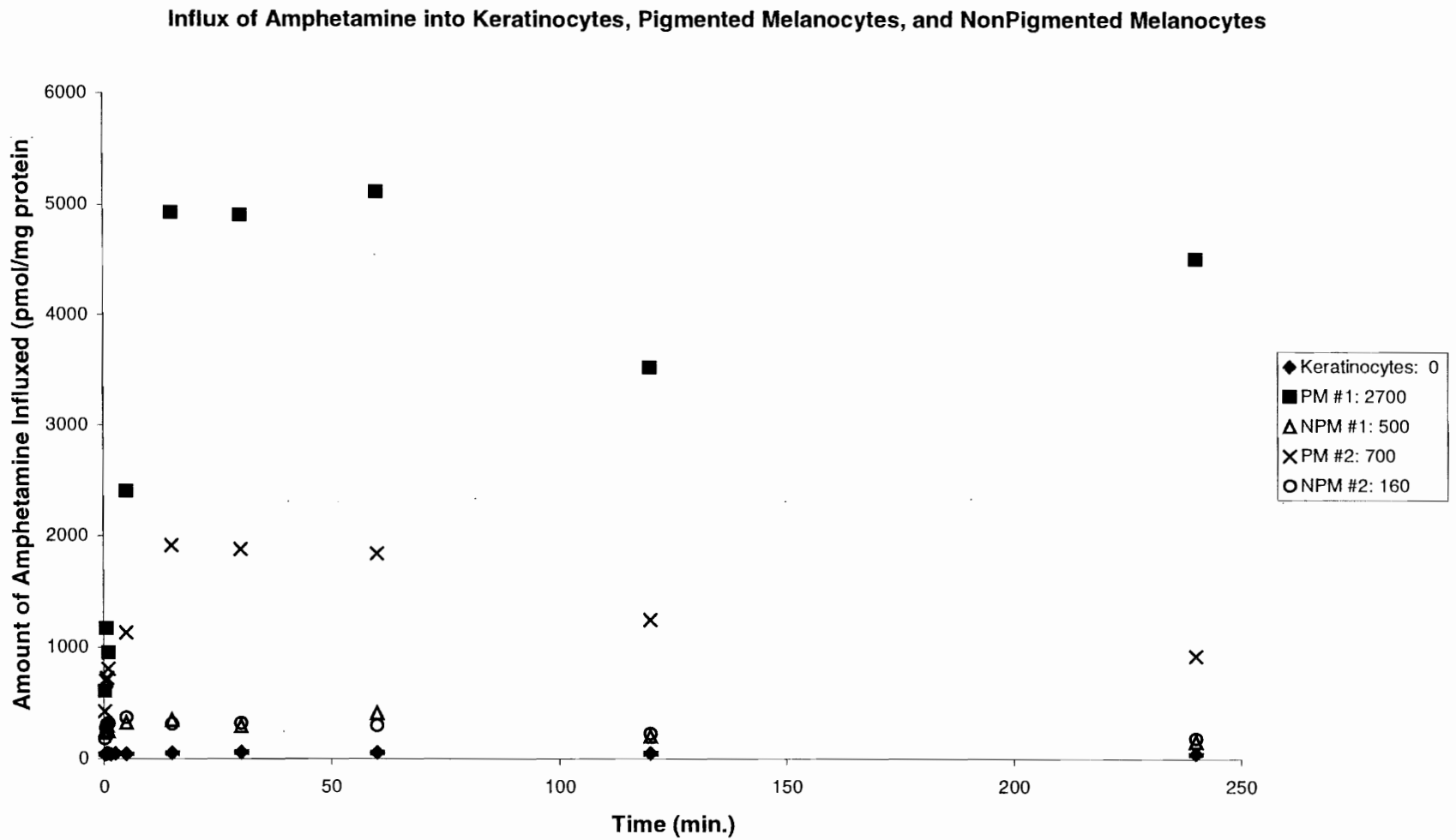
Influx of Amphetamine into Keratinocytes, Pigmented Melanocytes, and NonPigmented Melanocytes
Amount of Amphetamine Influxed (pmol/mg protein
6000
5000
4000
3000
2000
1000
0
0
50
100
150
200
250
Time (min.)
Keratinocytes: 0
PM #1: 2700
NPM #1: 500
PM #2: 700
NPM #2: 160

B

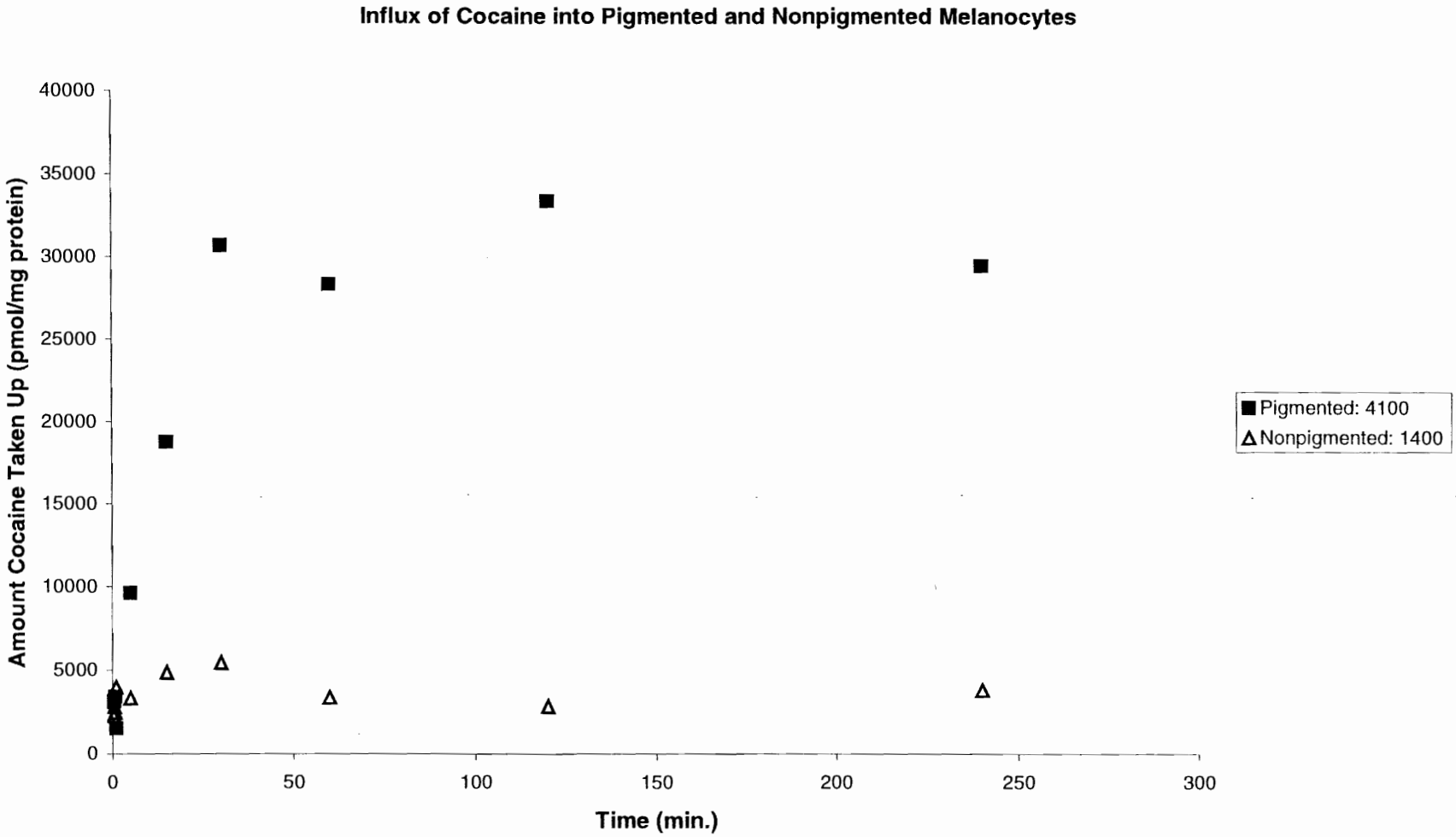
Influx of Cocaine into Pigmented and Nonpigmented Melanocytes
Amount Cocaine Taken Up (pmol/mg protein)
40000
35000
30000
25000
20000
15000
10000
5000
0
0
50
100
150
200
250
300
Time (min.)
Pigmented: 4100
Nonpigmented: 1400

Figure 5.3. The initial influx phase for amphetamine uptake into keratinocytes (and non-pigmented melanocytes) is very difficult to assess visually from a graphical representation when experiments are run at 37 °C. To determine if initial uptake of amphetamine into keratinocytes is linear, the experiment was performed with media at 4 °C. At this temperature, uptake is linear for at least 5 min (Figure 5.4).

To evaluate the effect of melanin content on amphetamine and cocaine uptake, the data for influx of amphetamine into PM and NPM were normalized for melanin content (Figures 5.5A-B). This procedure shifts the amphetamine influx data such that most of the data from the least pigmented cells (NPM #2, 160 μg eumelanin/mg protein) is greater than that of most of the data from the deepest pigmented cells (PM#1, 2700 μg eumelanin/mg protein). This demonstrates the strong effect that eumelanin has on cellular amphetamine uptake. Similarly, once normalized for cellular eumelanin content, cocaine influx data for PM and NPM move closer together.

Based on the influx data, it was determined that influx equilibrium of amphetamine and cocaine was well established for all cell lines by 30 min. Thus, efflux experiments were run by first preloading cells for 30 min with drug. Efflux of amphetamine and cocaine from keratinocytes, PM, and NPM over time is shown in Figure 5.6A-B. Keratinocytes and NPM quickly efflux the amphetamine, but PM are slow to efflux and retain about 40% of influxed amphetamine, if efflux media is not refreshed. If efflux media is refreshed with drug free media periodically, PM will eventually redistribute essentially all amphetamine back into the media (Figure 5.7). There is a difference in the efflux pattern for cocaine between PM and NPM, and in the experiments conducted here NPM still retained about 40% of the influxed cocaine. This

Figure 5.3 *Expanded view of amphetamine influx into keratinocytes.* Data points represent the average of two determinations while the error bars represent the actual data points.

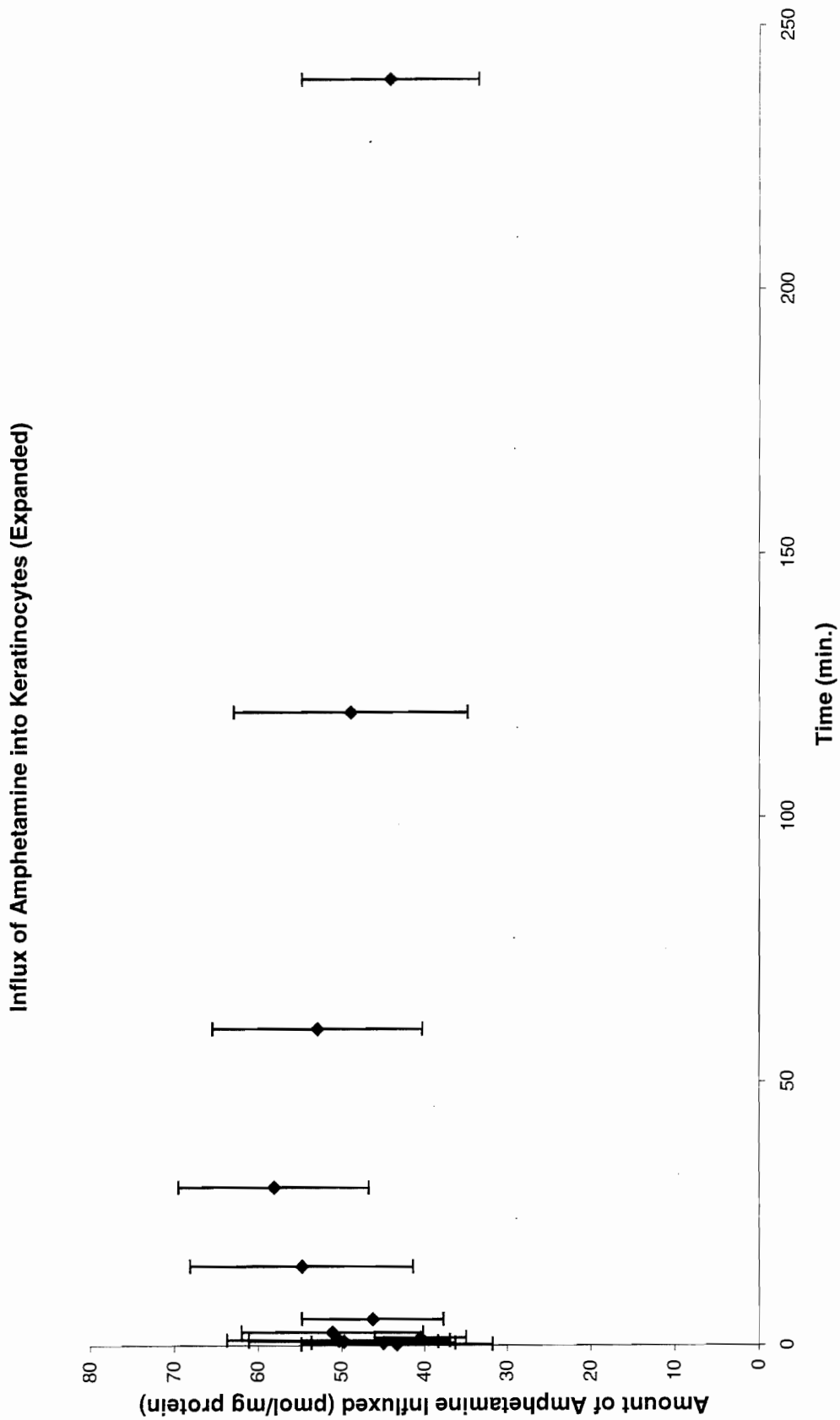
Influx of Amphetamine into Keratinocytes (Expanded)
Amount of Amphetamine Influxed (pmol/mg protein)
0
10
20
30
40
50
60
70
80
0
50
100
150
200
250
Time (min.)

Figure 5.4 *Initial influx of amphetamine into keratinocytes at 4 ℃*

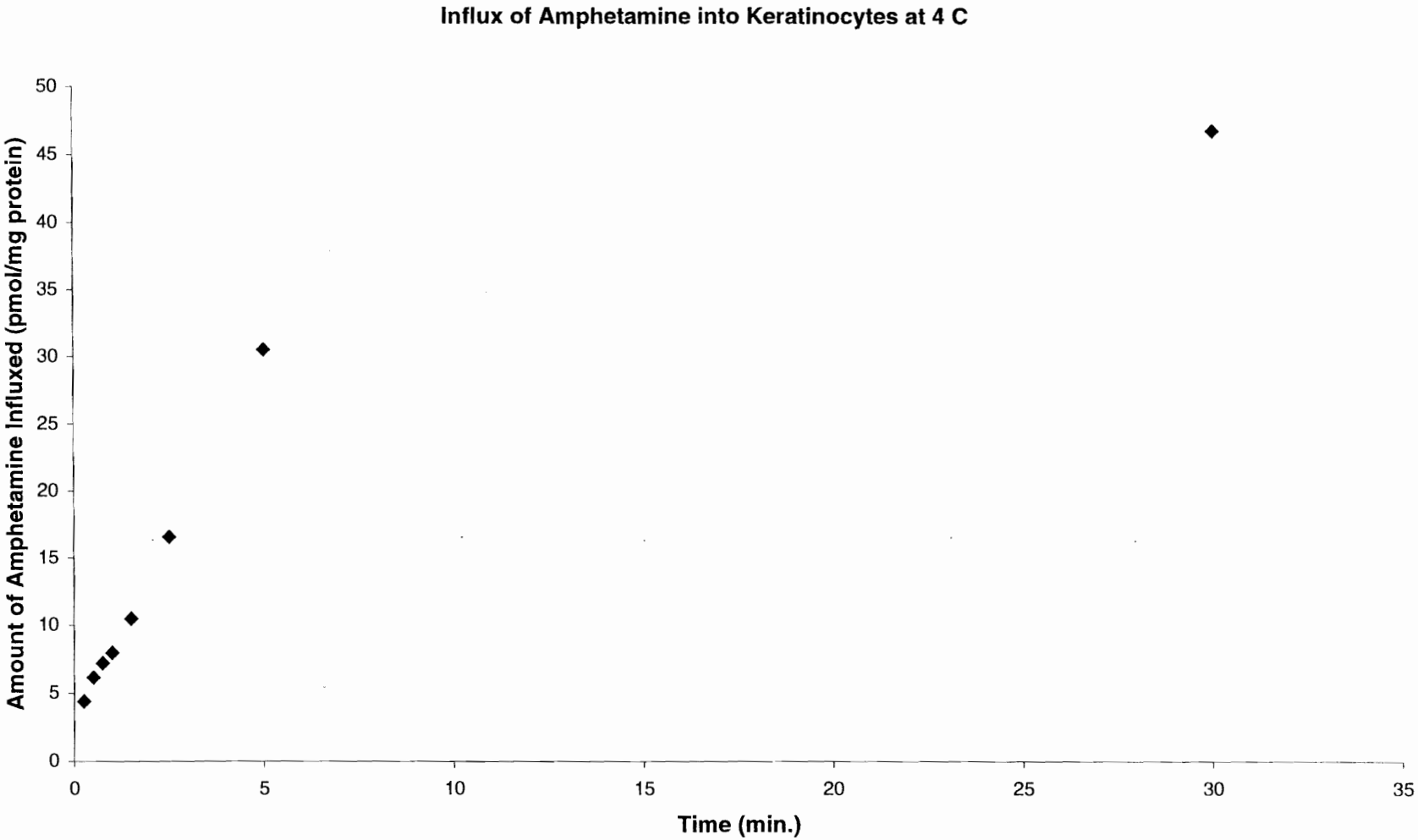
Influx of Amphetamine into Keratinocytes at 4 C
Amount of Amphetamine Influxed (pmol/mg protein)
0
5
10
15
20
25
30
35
40
45
50
0
5
10
15
20
25
30
35
Time (min.)

Figure 5.5 *Influx of (A) amphetamine and (B) cocaine into pigmented melanocytes (PM) and nonpigmented melanocytes (NPM) normalized for eumelanin content.* (Eumelanin content is also expressed in the legend in units of μg eumelanin / mg protein.)

A

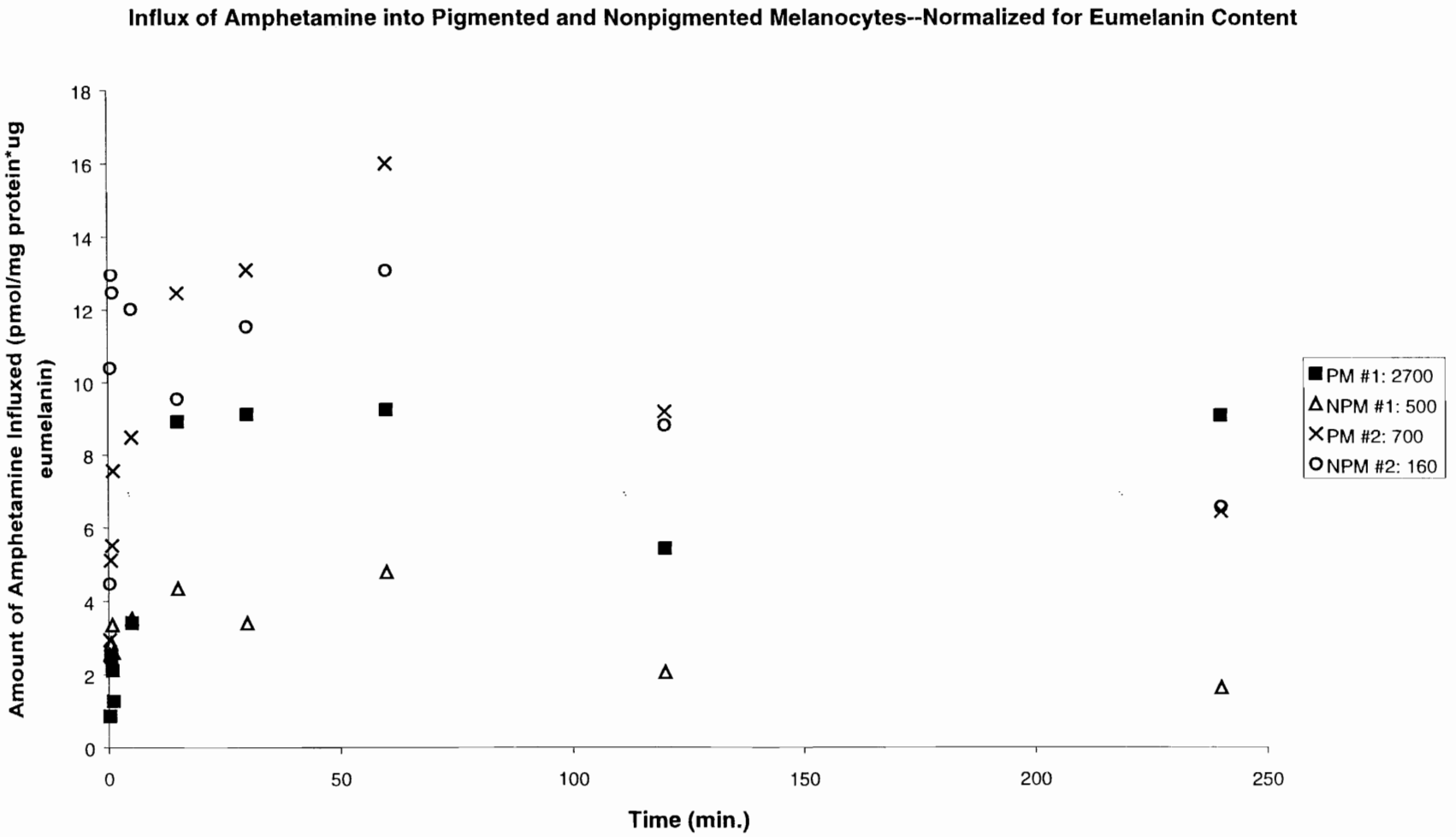
Influx of Amphetamine into Pigmented and Nonpigmented Melanocytes--Normalized for Eumelanin Content
Amount of Amphetamine Influxed (pmol/mg protein*ug eumelanin)
Time (min.)
0
2
4
6
8
10
12
14
16
18
0
50
100
150
200
250
PM #1: 2700
NPM #1: 500
PM #2: 700
NPM #2: 160

B

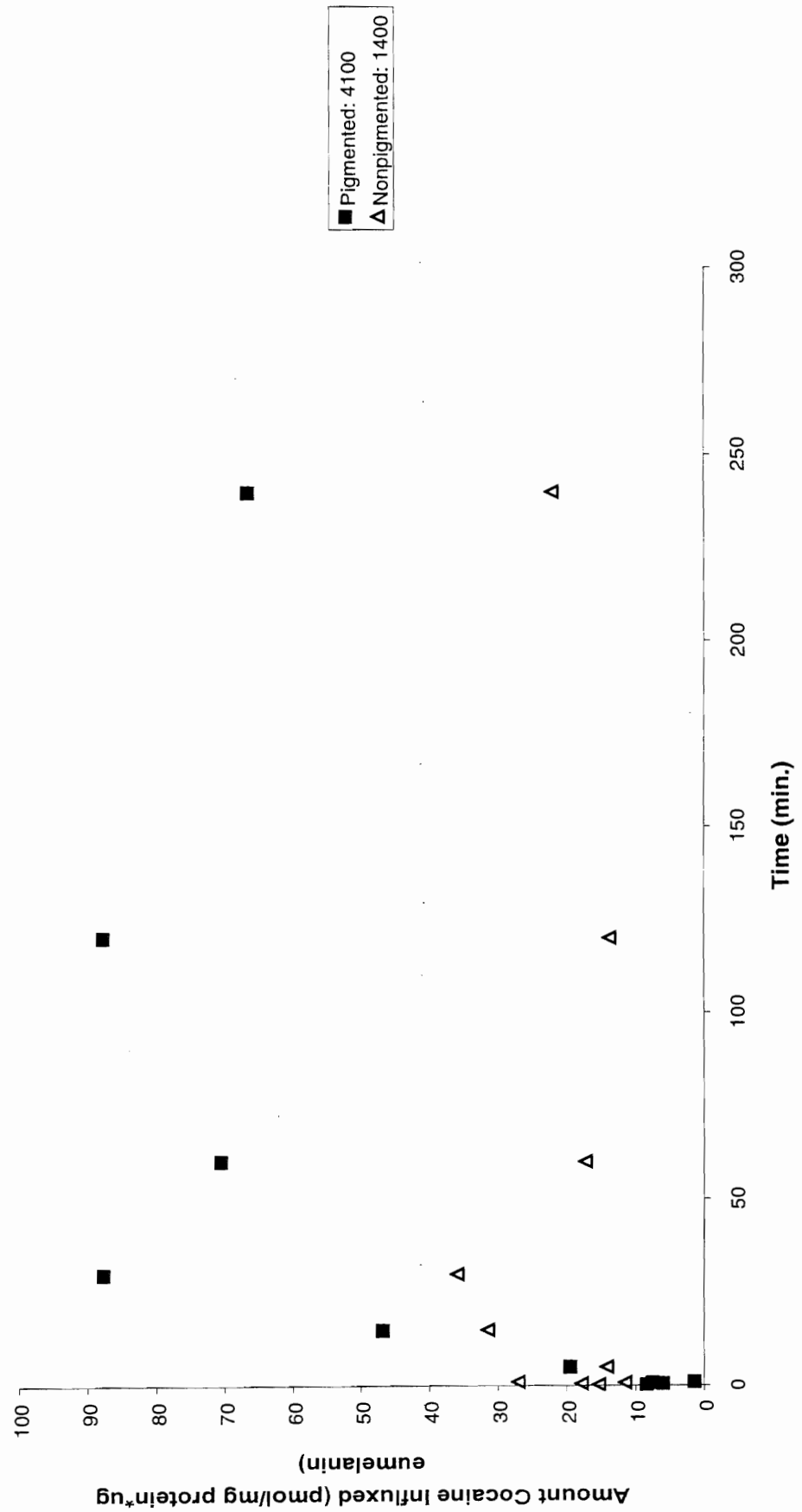
Cocaine Uptake by Pigmented and Nonpigmented Melanocytes--Normalized for Eumelanin Content
Pigmented: 4100
Nonpigmented: 1400
Amount Cocaine Influxed (pmol/mg protein*ug eumelanin)
Time (min.)
0
10
20
30
40
50
60
70
80
90
100
0
50
100
150
200
250
300

Figure 5.6 *Efflux of (A) amphetamine and (B) cocaine from keratinocytes, pigmented melanocytes (PM), and nonpigmented melanocytes (NPM) over time.* #1 and #2 designate the first and second repetitions of an experiment. For ease of reference, eumelanin content in μg eumelanin / mg protein is expressed in the legend. Initial data points were at 15, 30, 45, and 60 seconds. Keratinocyte data points represent the average of two determinations while the error bars represent the actual data points. Each experiment with melanocytes is displayed as an individual series.

A

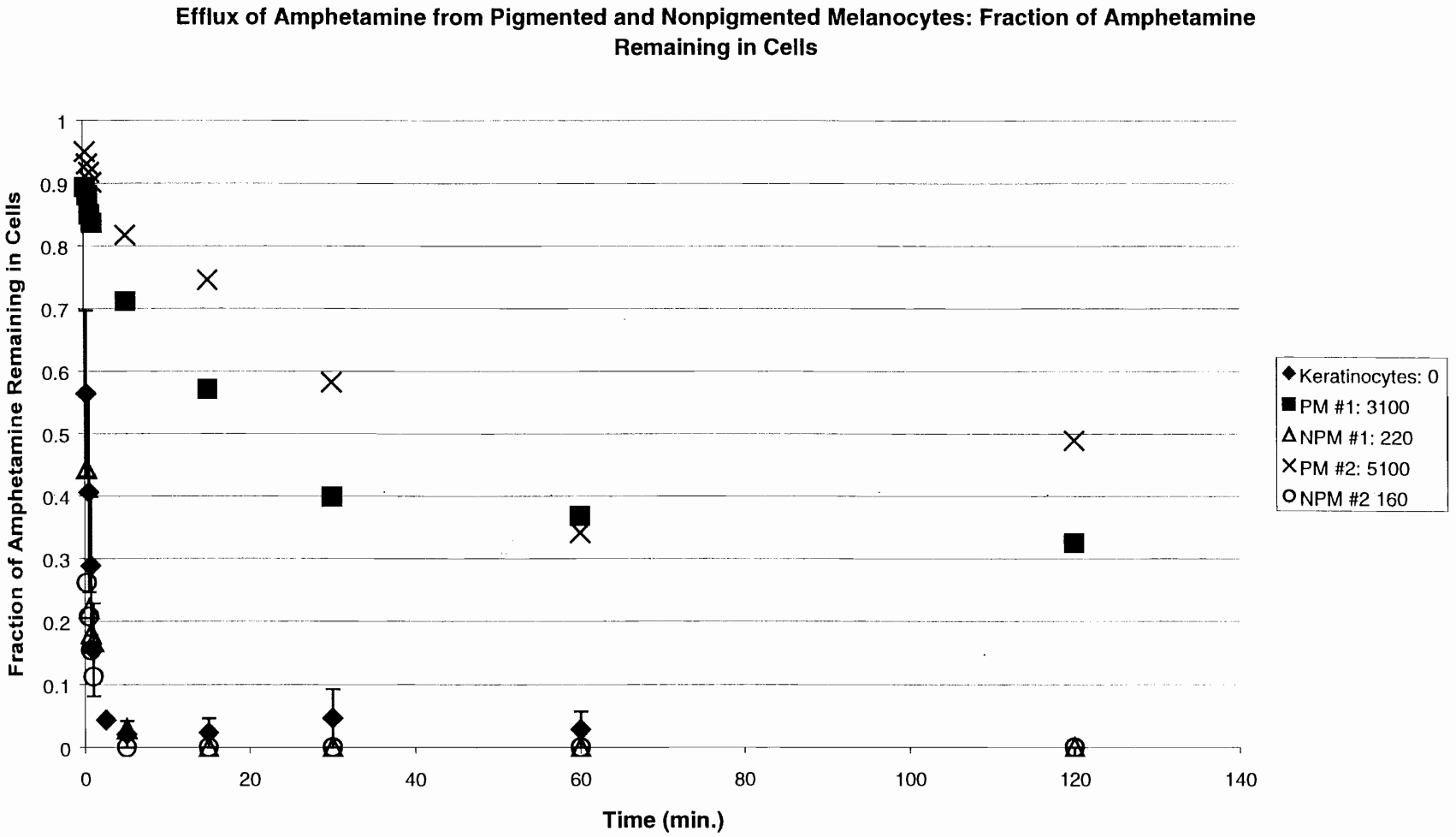
Efflux of Amphetamine from Pigmented and Nonpigmented Melanocytes: Fraction of Amphetamine Remaining in Cells
Fraction of Amphetamine Remaining in Cells
1
0.9
0.8
0.7
0.6
0.5
0.4
0.3
0.2
0.1
0
0
20
40
60
80
100
120
140
Time (min.)
Keratinocytes: 0
PM #1: 3100
NPM #1: 220
PM #2: 5100
NPM #2 160

B

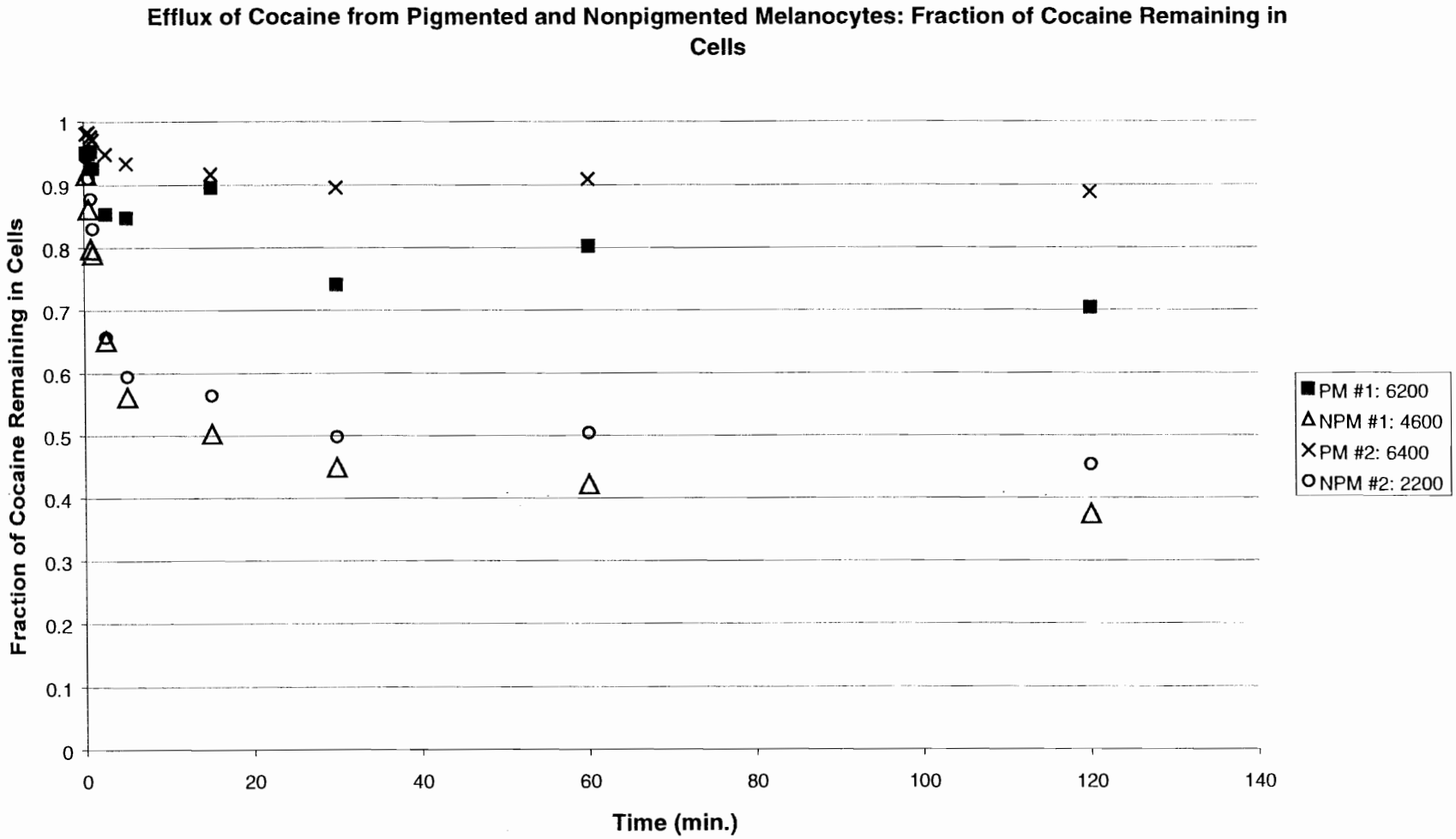
Efflux of Cocaine from Pigmented and Nonpigmented Melanocytes: Fraction of Cocaine Remaining in Cells
Fraction of Cocaine Remaining in Cells
1
0.9
0.8
0.7
0.6
0.5
0.4
0.3
0.2
0.1
0
0
20
40
60
80
100
120
140
Time (min.)
PM #1: 6200
NPM #1: 4600
PM #2: 6400
NPM #2: 2200

Figure 5.7 *Efflux of amphetamine from pigmented melanocytes when efflux media is refreshed every 30 min.* Data are shown fit to a natural logarithmic decay curve.

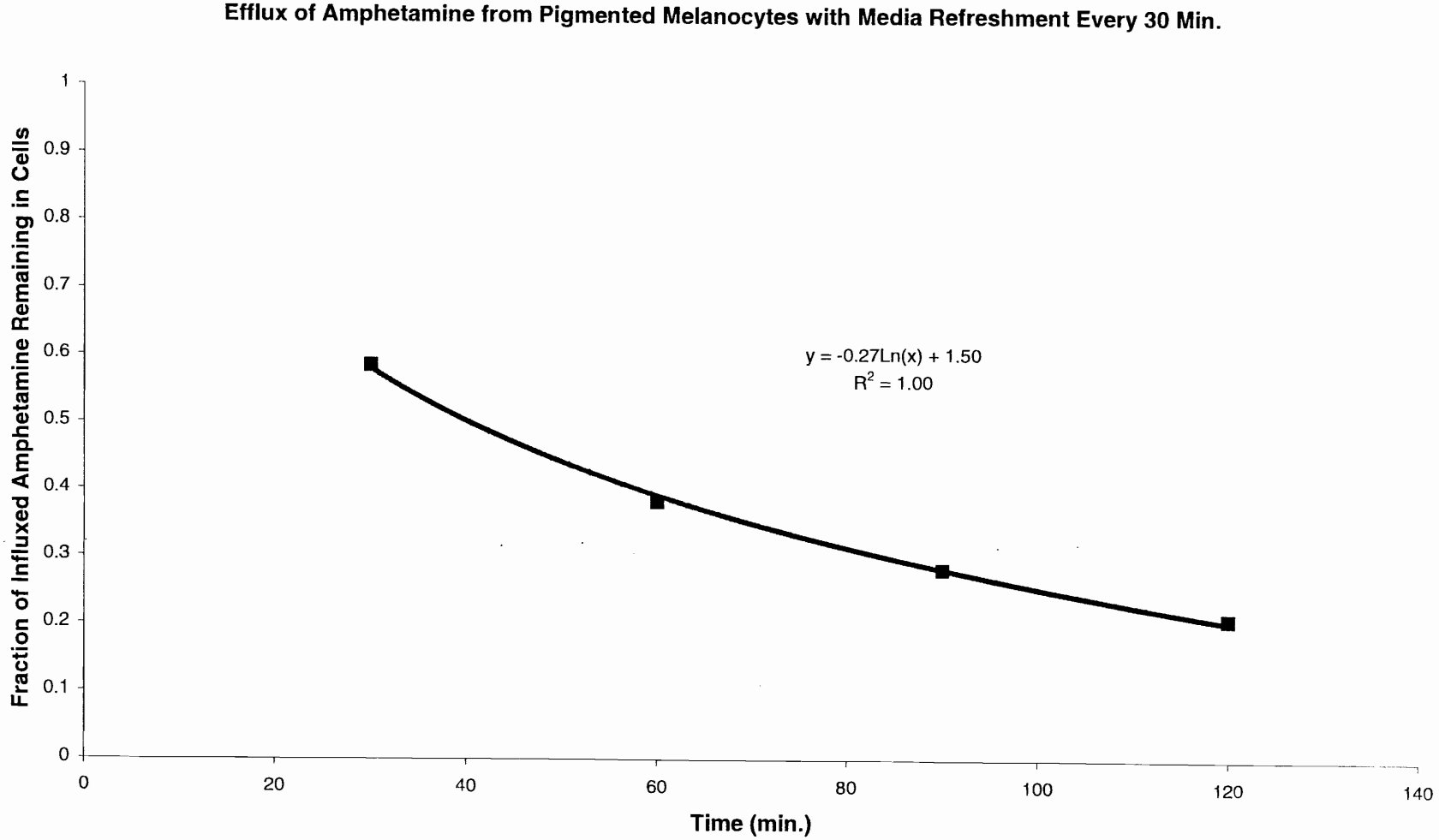
Efflux of Amphetamine from Pigmented Melanocytes with Media Refreshment Every 30 Min.
Fraction of Influxed Amphetamine Remaining in Cells
1
0.9
0.8
0.7
0.6
0.5
0.4
0.3
0.2
0.1
0
y = -0.27Ln(x) + 1.50
R2 = 1.00
0
20
40
60
80
100
120
140
Time (min.)

may be due to the fact that the "nonpigmented" cells used in this particular experiment displayed some pigmentation (4600 μg eumelanin/mg protein), even though they were less pigmented than their "pigmented" counterparts (6200 μg eumelanin/mg protein) from the same experiment.

In contrast to amphetamine, N-AcAp is not readily incorporated into keratinocytes, PM, or NPM—even at 10 times the concentration. Figure 5.8A-B shows the total (nonbackground subtracted) uptake of 10 μM N-AcAp and net (background subtracted) 10 μM BE uptake into the cells. None of the N-AcAp data points are greater than five times the background uptake of an empty flask and thus cannot be attributed unequivocally to actual cellular uptake. Melanocyte uptake of N-AcAp appears greater than that of keratinocytes due to normalization of the data for protein content. (As stated above, a flask of keratinocytes contains about five times as much protein as a flask of melanocytes.)

BE influx data is inconsistent relative to the patterns of other influx data, but it does suggest that there is no effect of cellular pigmentation on the amount of BE taken up into melanocytes. To confirm this finding, experiments were conducted to assess the efflux of BE from PM and NPM. Results (Figure 5.9) indicate that BE is effluxed from NPM a little faster than from PM, and BE is totally removed from both PM and NPM by 60 min. Thus no pigmentation bias was observed for BE.

Serum or plasma protein binding of BE and N-AcAp was found to be relatively minor (Figures 5.10A and B). BE did not bind to serum proteins at all, and N-AcAp was at most only 40% bound to plasma proteins. The peculiar concave nature of the N-AcAp plasma protein binding curve produces a convex Scatchard plot—a feature suggestive of

Figure 5.8 *Influx of (A) 10 μM N-AcAp and (B) 10 μM BE into keratinocytes, pigmented melanocytes (PM), and nonpigmented melanocytes (NPM).* For (A) N-AcAp, none of the data points are greater than five times the background uptake of an empty flask and thus cannot be officially counted as actual cellular uptake. Keratinocyte data appear lower due to the greater protein content of keratinocytes. For (B) BE, all data points are greater than 10 times background uptake levels.

A

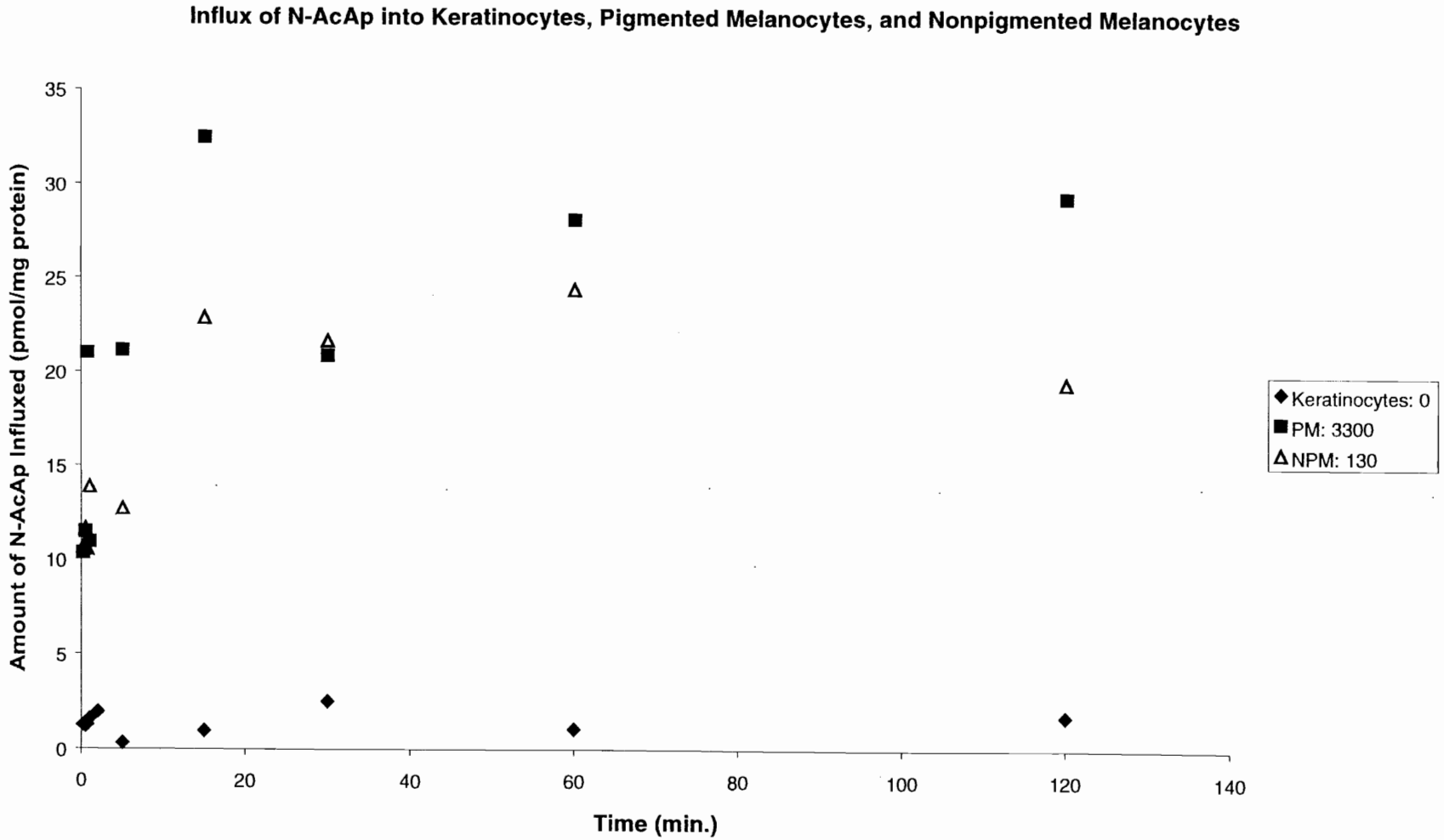
Influx of N-AcAp into Keratinocytes, Pigmented Melanocytes, and Nonpigmented Melanocytes
Amount of N-AcAp Influxed (pmol/mg protein)
35
30
25
20
15
10
5
0
0
20
40
60
80
100
120
140
Time (min.)
Keratinocytes: 0
PM: 3300
NPM: 130

B

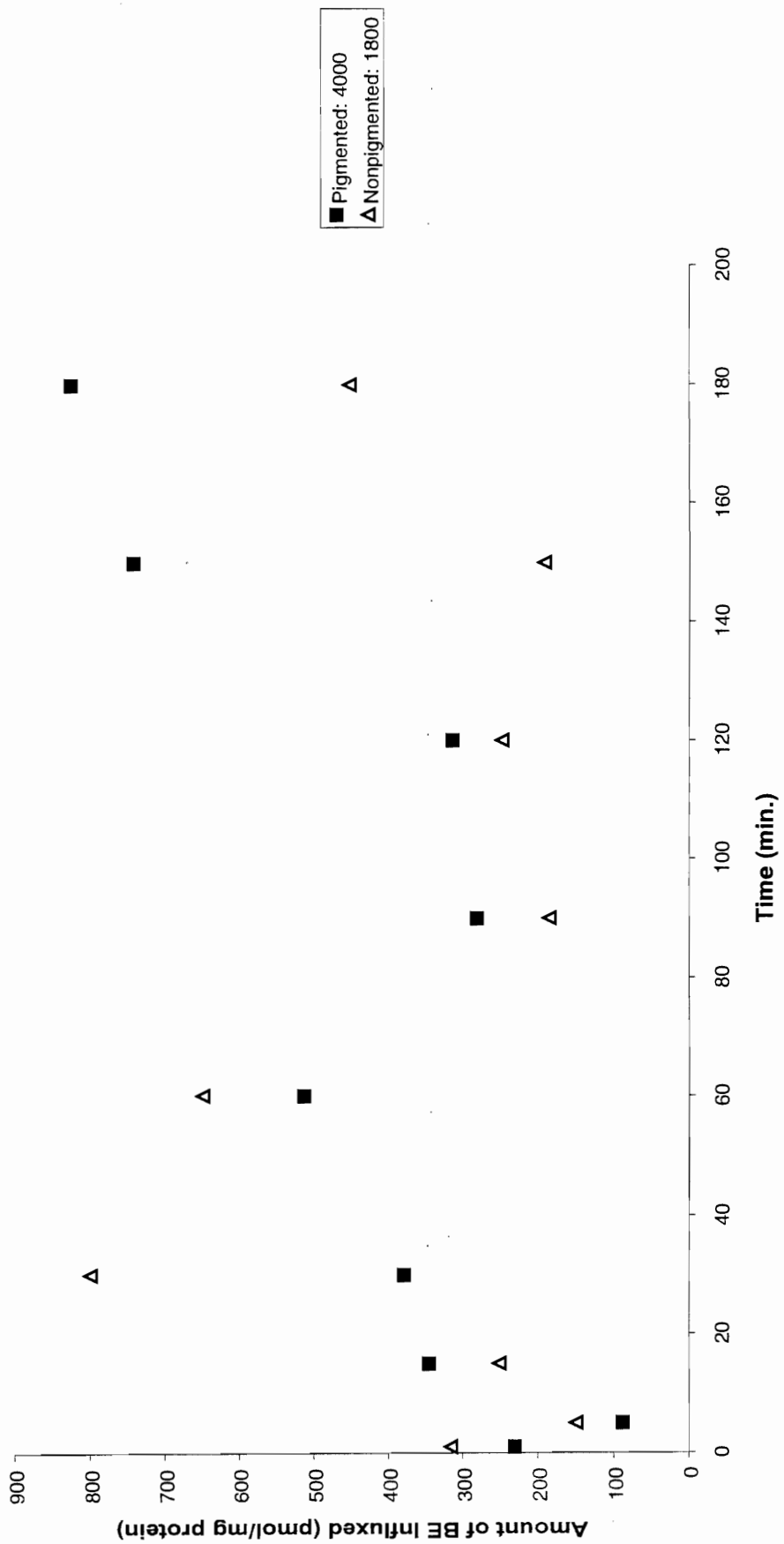
Influx of BE into Pigmented and Nonpigmented Melanocytes
Pigmented: 4000
Nonpigmented: 1800
Amount of BE Influxed (pmol/mg protein)
Time (min.)
0
100
200
300
400
500
600
700
800
900
0
20
40
60
80
100
120
140
160
180
200

Figure 5.9 *Efflux of BE from pigmented melanocytes (PM) and nonpigmented melanocytes (NPM) over time.* For ease of reference, eumelanin content in μg eumelanin / mg protein is expressed in the legend.

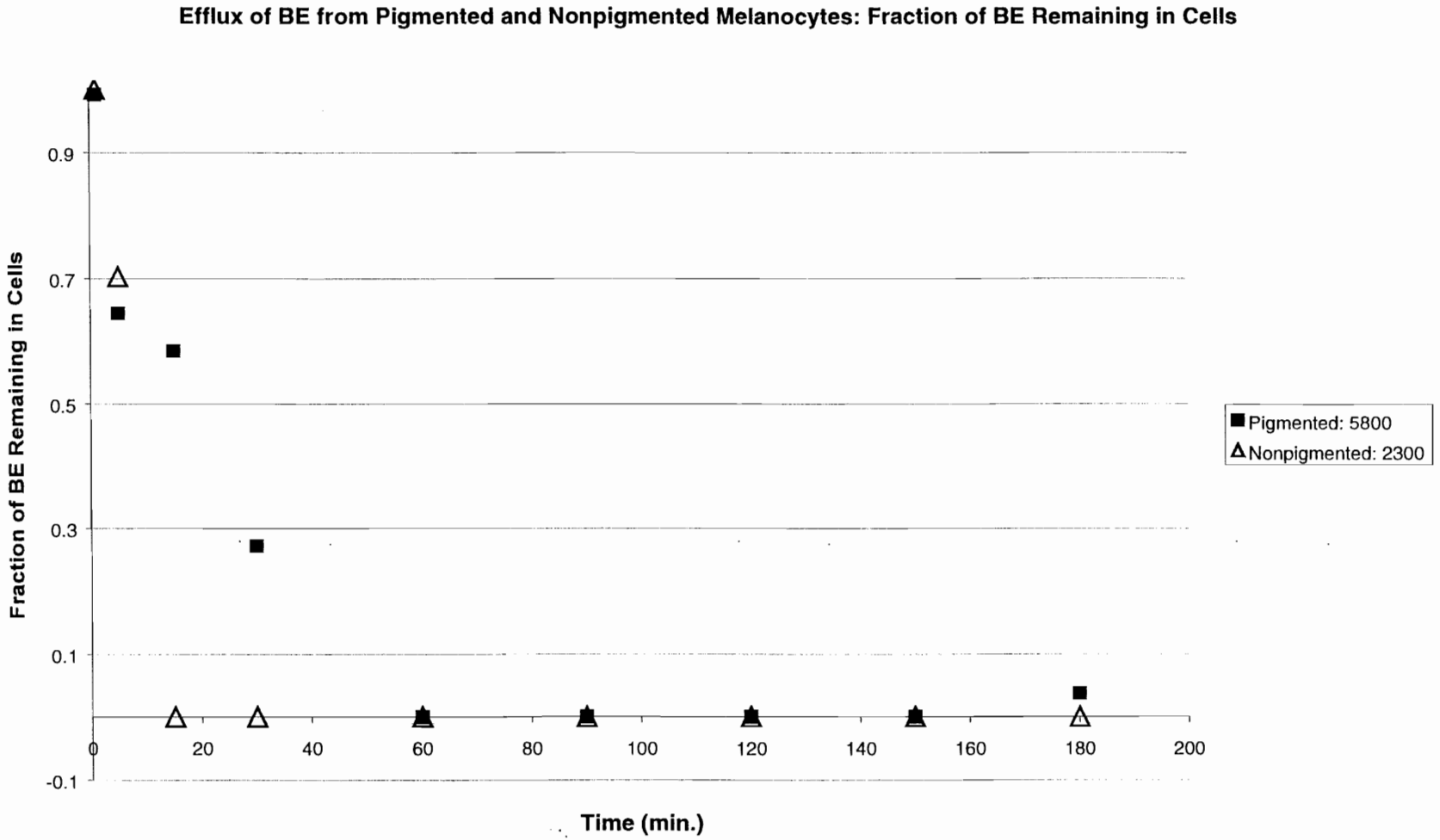
Efflux of BE from Pigmented and Nonpigmented Melanocytes: Fraction of BE Remaining in Cells
Fraction of BE Remaining in Cells
0.9
0.7
0.5
0.3
0.1
-0.1
0
20
40
60
80
100
120
140
160
180
200
Time (min.)
Pigmented: 5800
Nonpigmented: 2300

Figure 5.10 *Serum and plasma protein binding of (A) BE and (B) N-AcAp, respectively.* Data points represent the average of two determinations while the error bars represent the actual data points.

A

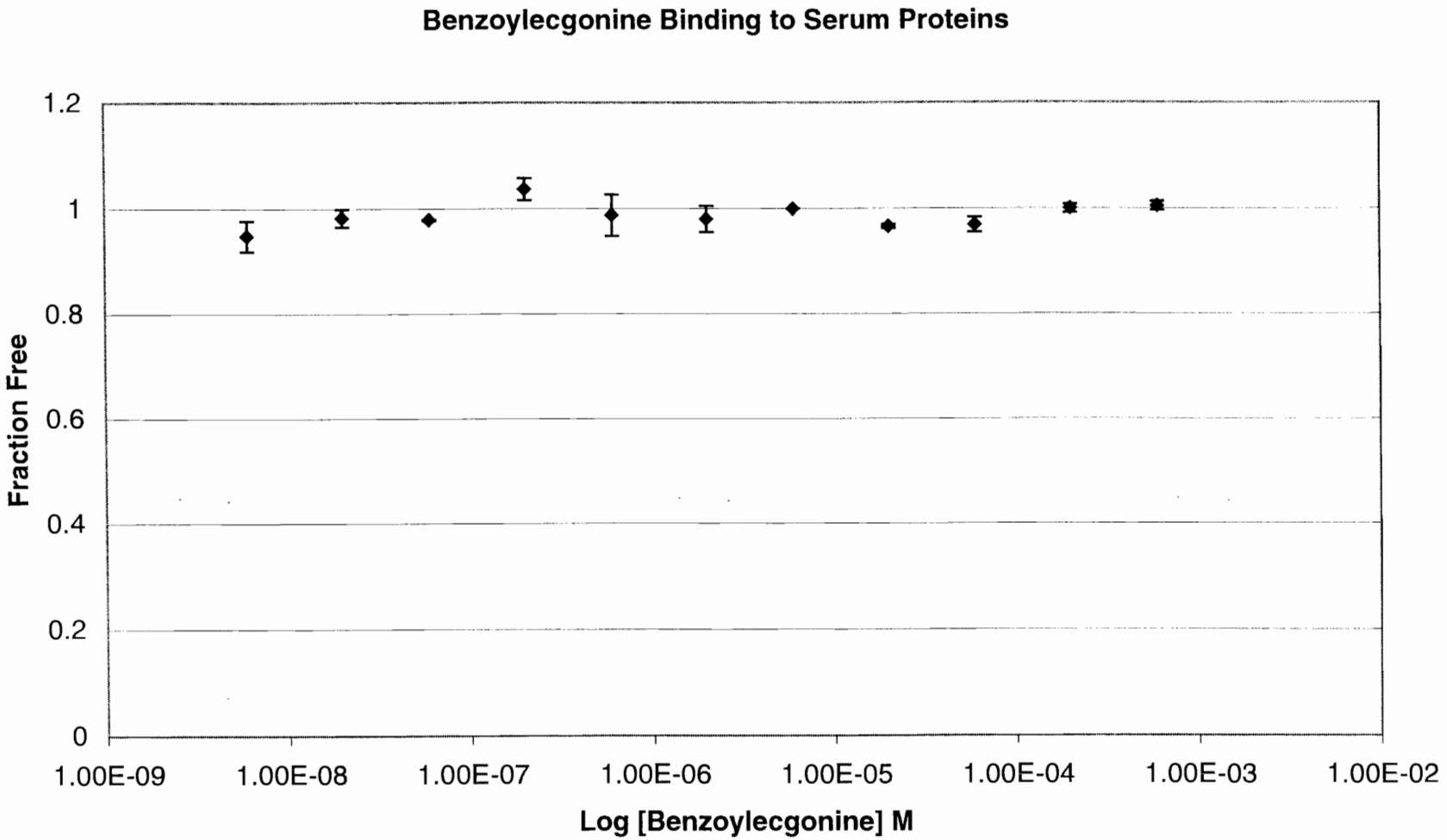
Benzoylecgonine Binding to Serum Proteins
Fraction Free
1.2
1
0.8
0.6
0.4
0.2
0
1.00E-09
1.00E-08
1.00E-07
1.00E-06
1.00E-05
1.00E-04
1.00E-03
1.00E-02
Log [Benzoylecgonine] M

B

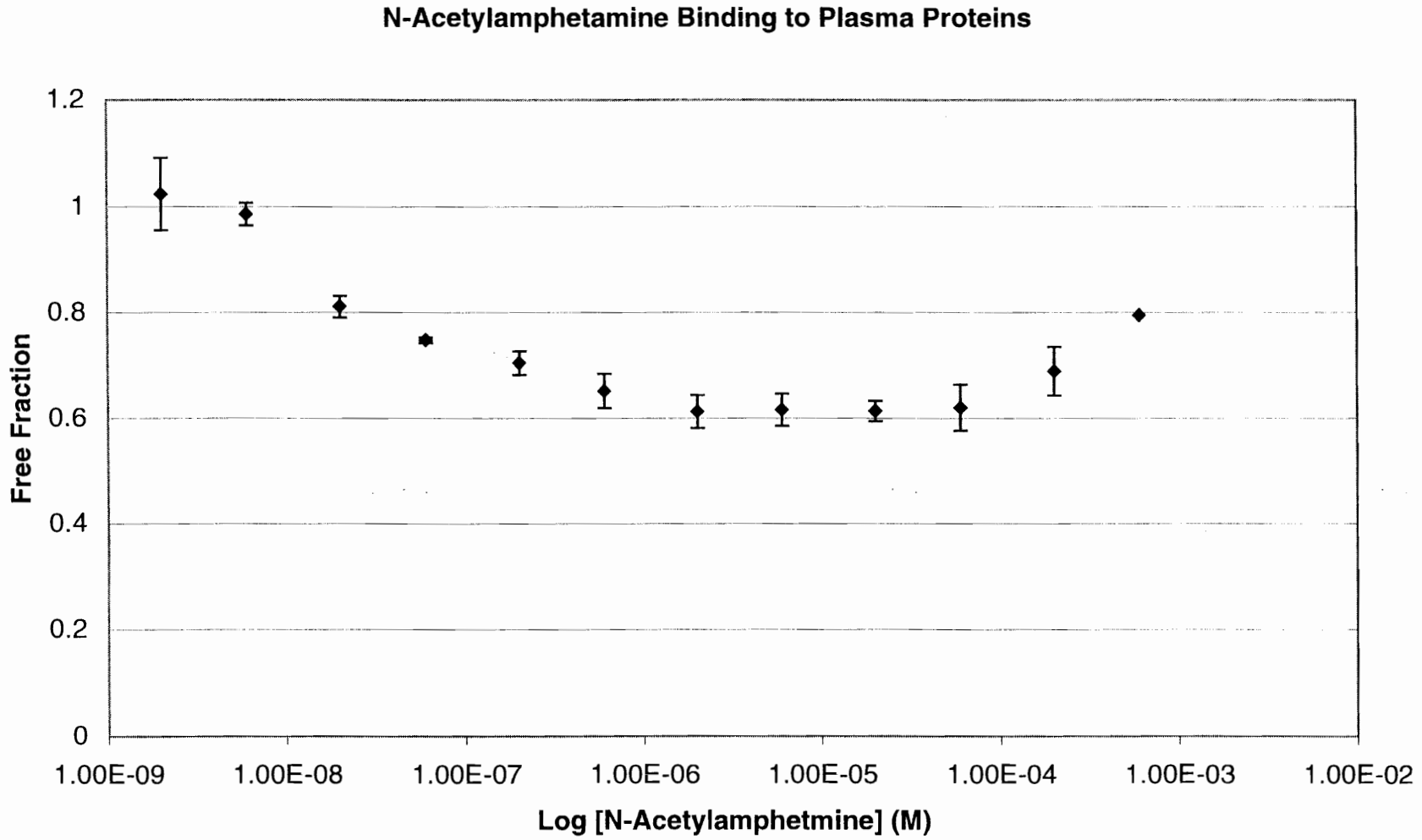
N-Acetylamphetamine Binding to Plasma Proteins
Free Fraction
1.2
1
0.8
0.6
0.4
0.2
0
1.00E-09
1.00E-08
1.00E-07
1.00E-06
1.00E-05
1.00E-04
1.00E-03
1.00E-02
Log [N-Acetylamphetmine] (M)

cooperative binding.

Discussion

Various models have been used that assess the potential hair color bias of specific drugs. These include drug-melanin binding studies (50-53, 55, 76, 78, 79, 168), animal *in vivo* incorporation studies (specifically with black and white Long-Evans rats) (40, 42, 65, 66, 69, 181), and human *in vivo* incorporation studies (126, 152, 182). Taken together, these data suggest that basic drugs with pKa values greater than physiologic pH will exhibit a hair color bias, while net neutral or acidic drugs will not. The studies presented here were designed to further test this hypothesis with yet another model of drug incorporation into hair—specifically, hair cell drug transport.

The initial influx and efflux of amphetamine and cocaine into or out of the keratinocytes, PM, and NPM is very rapid, ending within a matter of a min or two for nonpigmented cells, and within a matter of about 15 min for PM. However, the data acquired in these studies do not make an absolute distinction as to whether drug is transported into cells or simply adheres to the outside of cells in the flask. (Keratinocyte data, e.g., are ambiguous in this matter.) Differences between PM and NPM, however, suggest that amphetamine and cocaine are actually entering melanocytes since melanin is contained on the inside of cells and appears to have a strong effect on the uptake and efflux of amphetamine and cocaine from melanocytes. These data suggest a model of quick initial transport into or out of cells with an extended time period required for accumulation of drug onto or removal of drug from melanin. Equilibrium rate constants for cellular transport and drug-melanin binding thus determine the time frame for the whole process.

Perhaps the most striking aspect of these studies is the influence of melanin on amphetamine and cocaine influx and efflux. As evidenced in Figure 5.2, PM accumulate much greater amounts of amphetamine or cocaine at equilibrium than do NPM. In addition to the fact that the only difference between these two cell lines is inhibition of tyrosinase and thus a dramatic reduction of eumelanin content in one line; normalization of these data for cellular eumelanin content—i.e., dividing drug uptake (pmol/mg protein) by the eumelanin content of the cells (μg eumelanin) (Figure 5.5) also strongly supports the notion that drug-melanin binding and accumulation of drug on melanin is the reason for greater uptake of the basic drugs by PM than NPM. There may still appear to be some difference between PM and NPM influx of amphetamine and cocaine after the data is normalized for eumelanin content, but these differences can be attributed to experimental variability, as the differences between PM and NPM are much less on both an absolute and relative scale once uptake data are normalized for eumelanin content. In addition, once data are normalized for eumelanin content, NPM data points are not distinguishable from PM data points. Likewise, these same reasons explain the rapid and complete efflux of amphetamine and cocaine from nonpigmented cells, and the slow and incomplete efflux of the drugs from pigmented cells. The fact that efflux of amphetamine from PM is a slow, but equilibrium-mediated process is demonstrated by the evidence in Figure 5.7, which shows that if cells are continuously exposed to an amphetamine free extracellular environment, amphetamine will eventually be exported into the extracellular fluid.

Interestingly, with respect to the cellular melanin content and melanin binding constants of eumelanin for amphetamine, the average amount of amphetamine taken up

into PM is approximately $2.0x10^{-9}$ mol / mg eumelanin. This value falls between the low capacity ($1.3x10^{-10}$ mol / mg eumelanin) and high capacity ($1x10^{-7}$ mol / mg eumelanin) maximal binding parameters for amphetamine to eumelanin (see Chapter 4). Likewise, the average amount of cocaine taken up by PM at equilibrium is $7.3x10^{-9}$ mol / mg eumelanin, which also fits between the low and high capacity maximal binding parameters for cocaine to eumelanin (see Chapter 4). These observations reinforce the idea that the level of influx of amphetamine into pigmented cells is directly related to cellular eumelanin content due to amphetamine binding to the eumelanin polymers.

In addition to the capability to address issues of hair color bias, these cellular models also allow an investigation into hair cell selectiveness in drug transport. A previous study by Nakahara and Kikura (41) showed that when Dark Agouti rats are given amphetamine or N-AcAp at the same dose, the plasma area under the concentration vs. time curve (AUC) for N-AcAp is about four times greater than that of amphetamine. Analogously, Hubbard *et al.* (66) found that the AUC for BE is about twice that of cocaine after systemic administration of cocaine. A unique finding of these two studies was that the amount of amphetamine or cocaine found in hair is much greater than the amount of N-AcAp or BE found in hair; both in the above studies and in one of our previous studies (42). This is inconsistent with predictions based on a classical diffusion model of cellular uptake. At least two possibilities can account for this apparent discrepancy: Either N-AcAp and BE are highly protein bound and essentially unable to be taken into hair cells, or the hair cells have a transport system in place that permits the selective uptake of amphetamine and cocaine, but the relative exclusion of N-AcAp and BE. To test the former possibility, drug-plasma protein binding studies were conducted

with N-AcAp and BE prior to conducting the cell transport studies. The binding studies conducted across the complete range of physiologically relevant BE and N-AcAp plasma concentrations excluded the former possibility by demonstrating that BE is not bound to serum proteins (compared to 80-55% binding for cocaine across physiologically relevant serum concentrations(179)) and N-AcAp is at maximum only 40% bound to plasma protein (compared to amphetamine's binding of about 20% across physiologically relevant plasma concentrations (180)). Thus the *free*-drug-in-plasma AUC (free AUC) ratios between cocaine and BE and amphetamine and N-AcAp remain substantially less than one. Specifically, based on a assimilation of the plasma AUC data of Hubbard *et al.* (66) and the cocaine serum protein binding data of Parker *et al.* (179) with the data presented here, the cocaine : BE free AUC ratio was approximately 0.06-0.21. Also, based on a comparison Nakahara and Kikura's data (41) and the data presented here, the amphetamine : N-AcAp free AUC ratio reached a maximum of only 0.33.

These studies examining the influx of amphetamine, cocaine, N-AcAp, and BE into hair-related cells firmly support the hypothesis that hair cells do not simply take up drugs available in the plasma following a simple diffusion model. Even at a 10-fold greater concentration than amphetamine, N-AcAp still is not transported into keratinocytes or melanocytes. Likewise, also at a 10-fold greater concentration, BE is still influxed to a much lesser extent than cocaine. Inconsistencies in BE influx data may indicate that BE is simply adhering to the outside of the cells. As mentioned previously, unless a pigment bias is observed, these experiments cannot distinguish between uptake and simple adherence to the outside of cells. If BE is simply associating with the outside of the cells, quantitative levels of BE may be quite sensitive to minor inconsistencies

during the PBS wash phase of the experiment. If simple diffusion were responsible for uptake of these drugs into hair cells, then even given the same AUC (or cellular exposure) one would still expect greater amounts of N-AcAp to be incorporated into the hair cells because it is the more nonpolar, uncharged compound. However, although N-AcAp was found in the hair of systemically dosed rats (42), our current study did not demonstrate cellular transport of N-AcAp into keratinocytes or melanocytes. As stated above, while absolute signals from N-AcAp in our influx samples were far above quantitation limits, they were low relative to background noise from drug adherence to the flask. Background signal of N-AcAp from drug adhered to the flasks was not high; at 10 μM, the background was just slightly lower than that of amphetamine at 1 μM. Thus the nuances of the experimental conditions themselves may preclude an assessment of the precise extent of cellular uptake of N-AcAp. One could make the argument that because the N-AcAp influx data for melanocytes fit hyperbolic regression curves, modeling simple facilitated transport (KaleidaGraph, Synergy Software) with R^2 values between 0.80 and 0.85, that there may be some actual cellular transport. However, again, because of the low signal to background ratio of the data, we prefer not to draw such conclusions with certainty.

Specific cellular transport processes appear to be operational for amphetamine and cocaine. However, no mechanistic studies were conducted here to determine the exact mode of transport. Linear initial transport regions are vital to such studies, thus in an effort to observe them, an amphetamine influx experiment into keratinocytes was run at 4 °C (Figure 5.4). This technique slowed the initial transport process sufficiently for linear rates to be observed for a significant time period. Thus, such a cooling technique

may be of value in future mechanistic studies on the mode of amphetamine (and possibly cocaine) transport into hair forming cells.

Cellular transport models, such as those employed in this study, may be valuable tools to help predict hair incorporation properties and potential color biases, but they are not without their limitations. For example, the model is not a whole animal system and does not contain the complex variety of cellular interactions between different cell types, as would be the case in a living animal. Thus data obtained may not reflect *in vivo* reality in all cases. In addition, the cells used in these studies were not hair follicle-derived due to viability and pigmentation limitations involved with such specialized cells. As such, data obtained from such cells cannot reliably be used as an absolute predictor of the hair incorporation properties of any given drug, but must be used in conjunction with supporting data from other models of drug incorporation into hair.

In conclusion, the data presented in this chapter demonstrate the dramatic effects of cellular pigmentation and transport selectivity on the uptake and retention of basic and highly (hair) incorporating drugs in comparison to their nonbasic and low-level incorporating congeners.

CHAPTER 6

SUMMARY AND SIGNIFICANCE

Summary

The results presented in this dissertation are summarized with the following statements:

1. PDCA and PTCA, markers for DHI and DHICA eumelanin units, respectively, are produced in 0.37% and 4.8% yields, respectively, when melanins are subjected to alkaline hydrogen peroxide degradation.
2. 3AT and AHP, markers for 2-CysDOPA and 5-CysDOPA, respectively, are produced in 16% and 23% yield, respectively, when subjected to hydriodic acid hydrolysis.
3. Indole based monomer units are present in pheomelanin, not just eumelanin.
4. On a mass basis, black human hair contains approximately 99% eumelanin and 1% pheomelanin, brown and blond hair contain 95% eumelanin and 5% pheomelanin; and red hair contains 67% eumelanin and 33% pheomelanin.
5. Codeine incorporation into human hair after oral administration is directly proportional to the amount of eumelanin, but not pheomelanin, in the hair.
6. Amphetamine (a basic, positively charged drug at physiologic pH) shows a hair color bias and is more highly incorporated into hair than is N-AcAp (amphetamine's nonbasic, neutral analog) which lacks a hair color bias. This

occurs despite the fact that the *free* plasma AUC for N-AcAp is about 3-fold that of amphetamine.

7. Amphetamine and cocaine, two basic, positively charged drugs that show a hair color bias, bind to eumelanins and mixed eu-/pheomelanins to varying degrees, but not to pure pheomelanin. BE and N-AcAp, net neutral drugs that do not show a hair color bias, do not to bind to any type of melanin.
8. Melanin subtypes (beyond the eu-/pheomelanin distinction) do not appear to be important predictors of drug-melanin binding.
9. Multiple hydrogen bonding interactions between basic drug molecules and melanin, made possible by eumelanin secondary structure, likely comprise the high affinity/low capacity melanin binding site, while ionic interactions between positively charged, basic drug molecules and negatively charged melanin likely comprise the low affinity/high capacity melanin binding site.
10. Cultured melanocytes, when pigmented, show an influx bias for amphetamine and cocaine, but this was shown not to be the case for N-AcAp and BE.
11. PM are much slower to efflux amphetamine and cocaine, and do so less completely than NPM.
12. Based on amphetamine and cocaine data, cultured melanocytes appear to be an appropriate model for predicting hair color biases and relative hair incorporation between drugs.
13. Classic passive diffusion models are not predictive of the relative levels of incorporation of amphetamine, N-AcAp, cocaine, or BE into hair.

Significance

Determination of percent yields of melanin subtype degradation markers permit the direct assessment of the mass amount of each melanin subtype in a hair sample. Such information allows data (i.e., on drug incorporation into hair) to be normalized for actual melanin content—normalization for marker content or a nonspecific melanin content based on one type of natural melanin (e.g., sepia melanin) is no longer necessary. Unexpected findings in the course of these investigations provided evidence of indole units from pure pheomelanin polymers. These data call for a revision of the classic structure of pure pheomelanin as a solely benzothiazine-based polymer. Application of the data derived from the study of synthetic model melanins suggests that the total amount of melanin in hair is a more important predictor of hair color than is the mass ratio between eumelanin and pheomelanin in hair. In addition, the data show that hair eumelanin content is more important than pheomelanin content in regulating the incorporation of codeine into hair. The drug-melanin binding data with amphetamine and cocaine presented in Chapter 4 demonstrate that this is true for other basic drugs as well. In addition, mass spectral studies presented in Chapter 4 shed new light on the confounding nature of the chemical binding interaction between drugs and melanin.

Hair incorporation data (presented in Chapter 3) for amphetamine and N-AcAp emphasize the importance of basicity in hair color bias and, coupled with the plasma pharmacokinetic data of Nakahara and Kikura (41), suggest that passive diffusion is not an appropriate mechanism for incorporation of these drugs into hair. These conclusions are strongly bolstered by the cellular transport data in Chapter 5 that demonstrates plentiful uptake (and a hair color bias) for amphetamine, but negligible uptake for N-

AcAp, even at 10 times the concentration of amphetamine. Efflux data, if an appropriate model for part of the drug-incorporation-into-hair process, illustrate how drugs that show a hair color bias by binding to melanin are retained in hair forming cells to a much greater extent and for a much longer time than their chemical congeners that lack a hair color bias. The implications gleaned from cellular transport data on amphetamine and N-AcAp are further supported by cocaine and BE, two additional drugs that have analogous hair incorporation characteristics to amphetamine and N-AcAp.

Drug pairs with chemical properties similar to the ones used in these studies would be expected to incorporate into hair, bind to melanin, and undergo cellular transport in analogous manners. Further studies on basic, but uncharged molecules such as diazepam, pKa 3.3, would further elucidate the role of charge state in hair color bias.

In conclusion, the data presented in this dissertation demonstrate that amphetamine and cocaine exhibit hair color biases, and do so through non-diffusion-mediated cellular uptake and subsequent retention via a mechanism of eumelanin binding.

APPENDIX

The data presented in this appendix are nuclear magnetic resonance (NMR), mass spectral (MS), and ultraviolet (UV) spectral data that support the identities of chemicals synthesized as they were needed for the work presented in this dissertation.

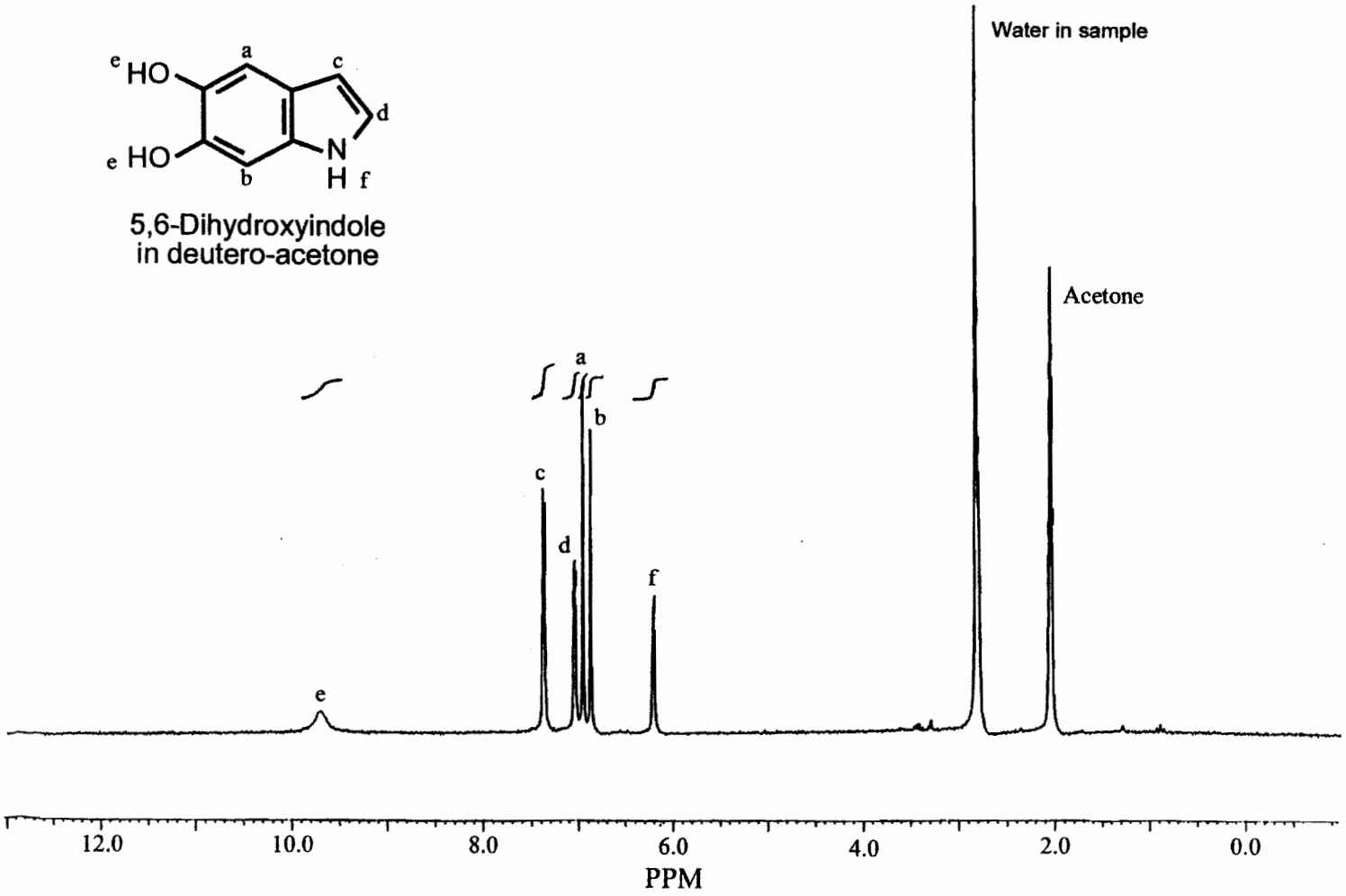
e HO
a
c
d
e HO
b
N
H f
5,6-Dihydroxyindole
in deutero-acetone
Water in sample
Acetone
a
b
c
d
f
e
12.0
10.0
8.0
6.0
4.0
2.0
0.0
PPM

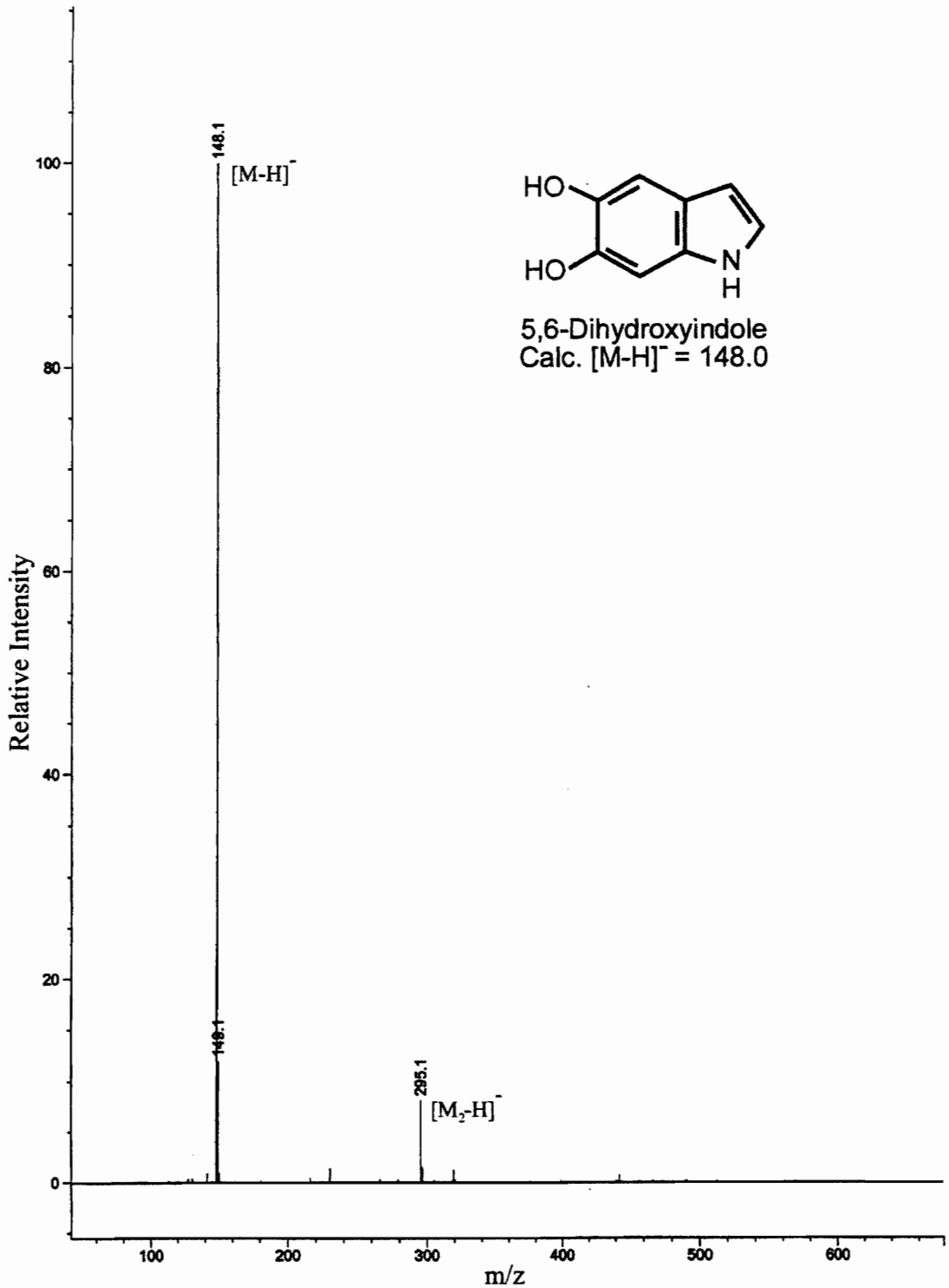
148.1
[M-H]⁻
HO
HO
N
H
5,6-Dihydroxyindole
Calc. [M-H]⁻ = 148.0
Relative Intensity
100
80
60
40
20
0
148.1
295.1
[M2-H]⁻
100
200
300
400
500
600
m/z

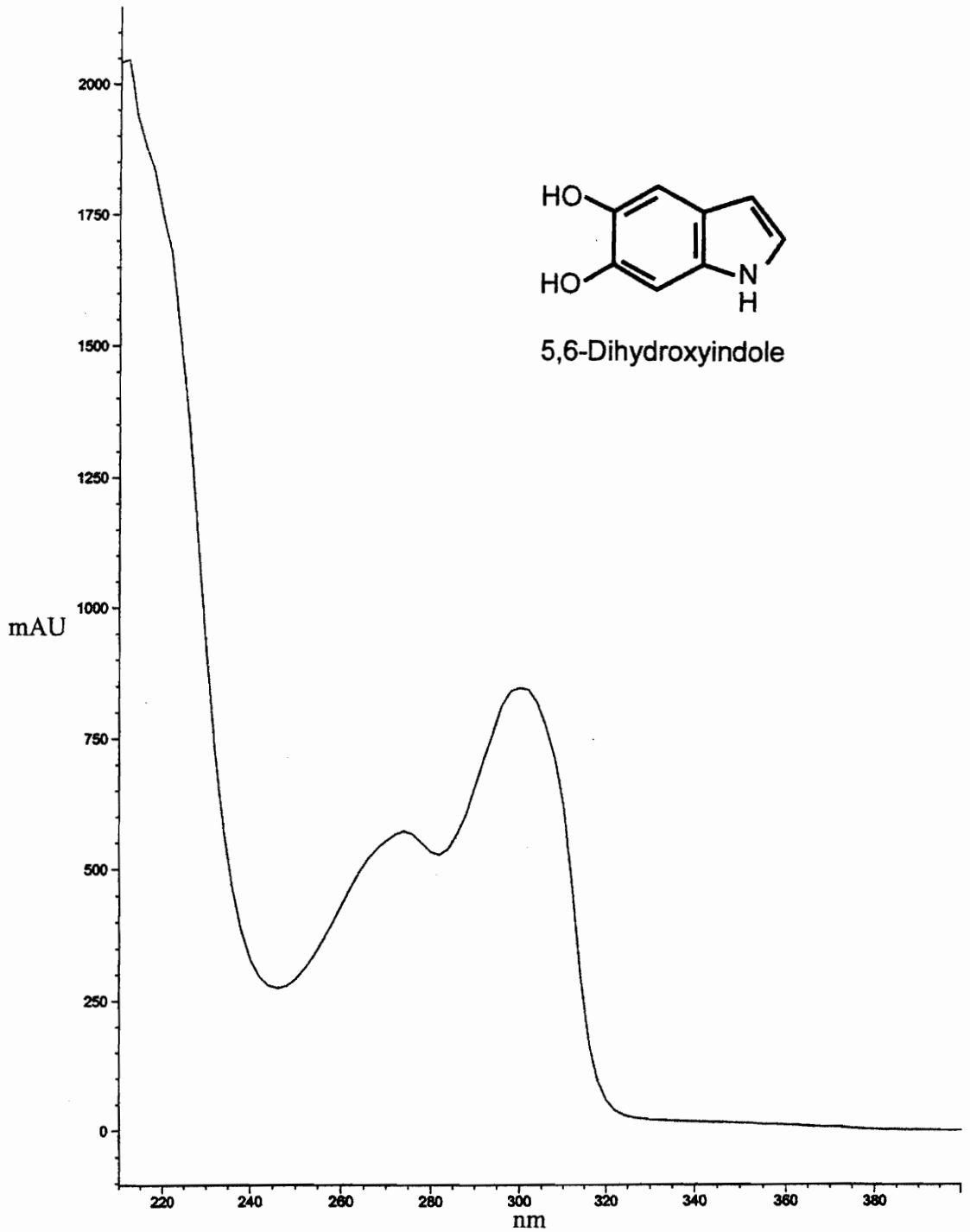
HO
HO
N
H
5,6-Dihydroxyindole
mAU
2000
1750
1500
1250
1000
750
500
250
0
220
240
260
280
300
320
340
360
380
nm

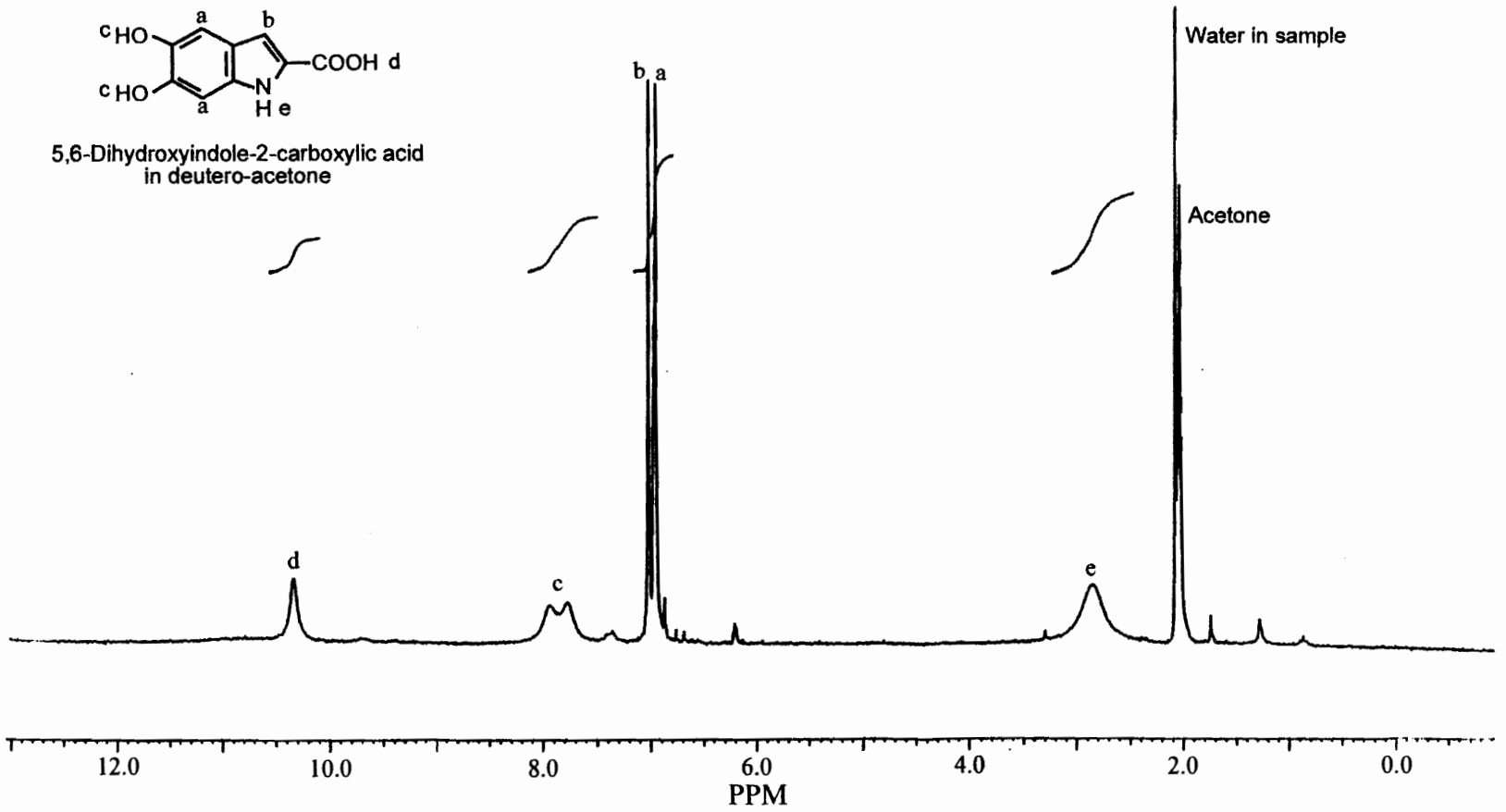
c HO
a
b
COOH d
c HO
a
N
H e
5,6-Dihydroxyindole-2-carboxylic acid
in deutero-acetone
b a
Water in sample
Acetone
d
c
e
12.0
10.0
8.0
6.0
4.0
2.0
0.0
PPM

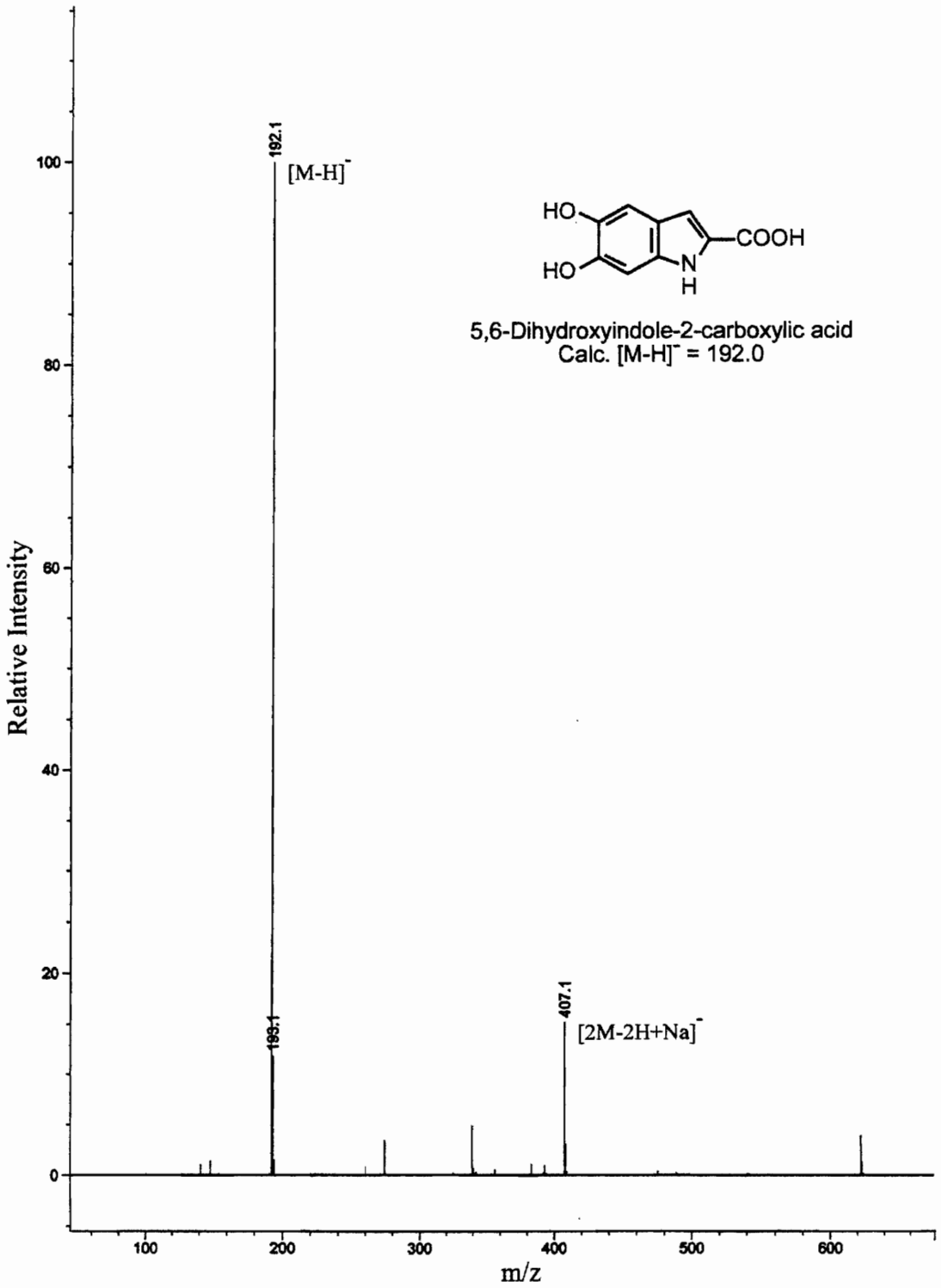
192.1
[M-H]⁻
HO
HO
COOH
N
H
5,6-Dihydroxyindole-2-carboxylic acid
Calc. [M-H]⁻ = 192.0
193.1
407.1
[2M-2H+Na]⁻
Relative Intensity
m/z
0
20
40
60
80
100
100
200
300
400
500
600

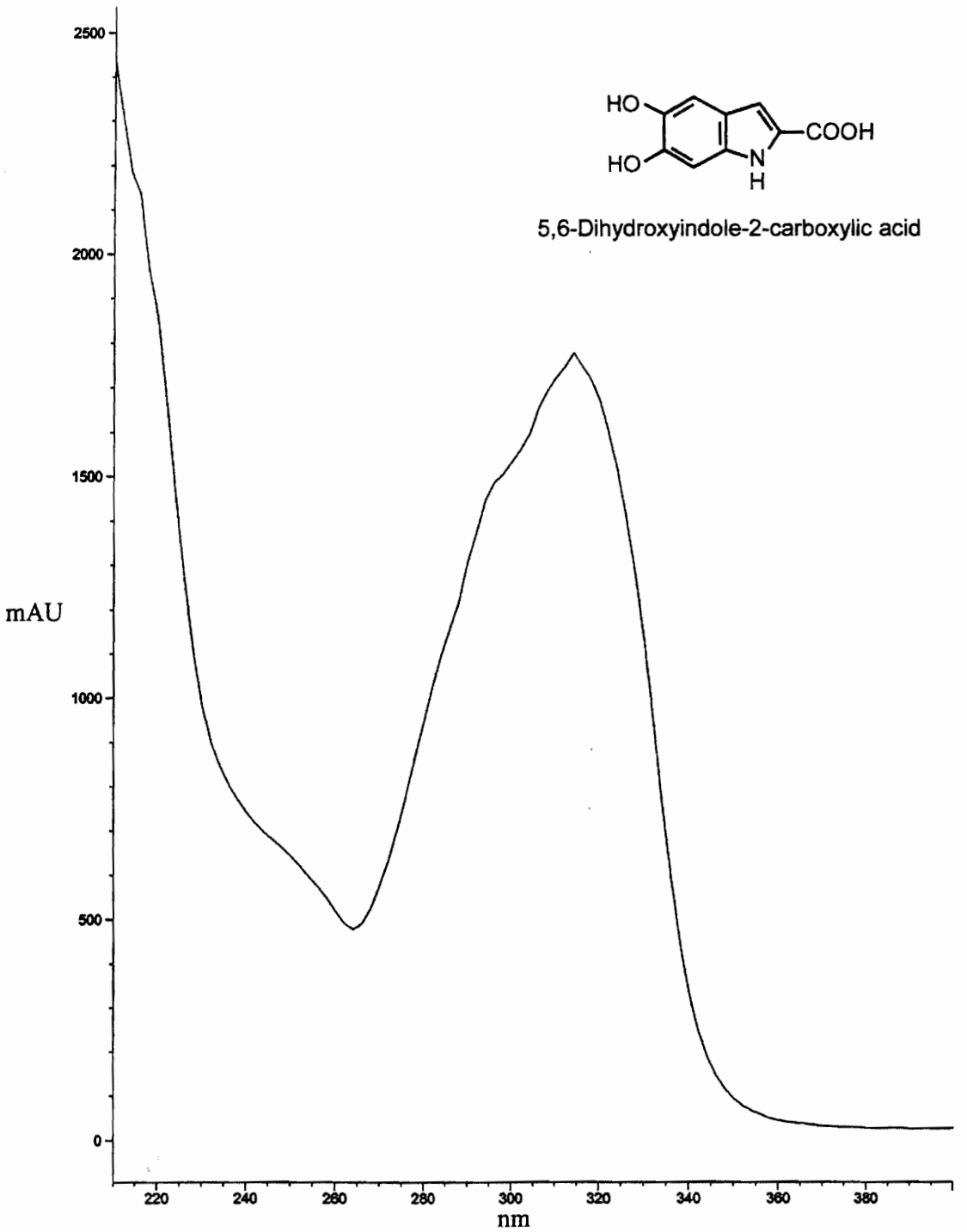
HO
HO
COOH
N
H
5,6-Dihydroxyindole-2-carboxylic acid
mAU
2500
2000
1500
1000
500
0
220
240
260
280
300
320
340
360
380
nm

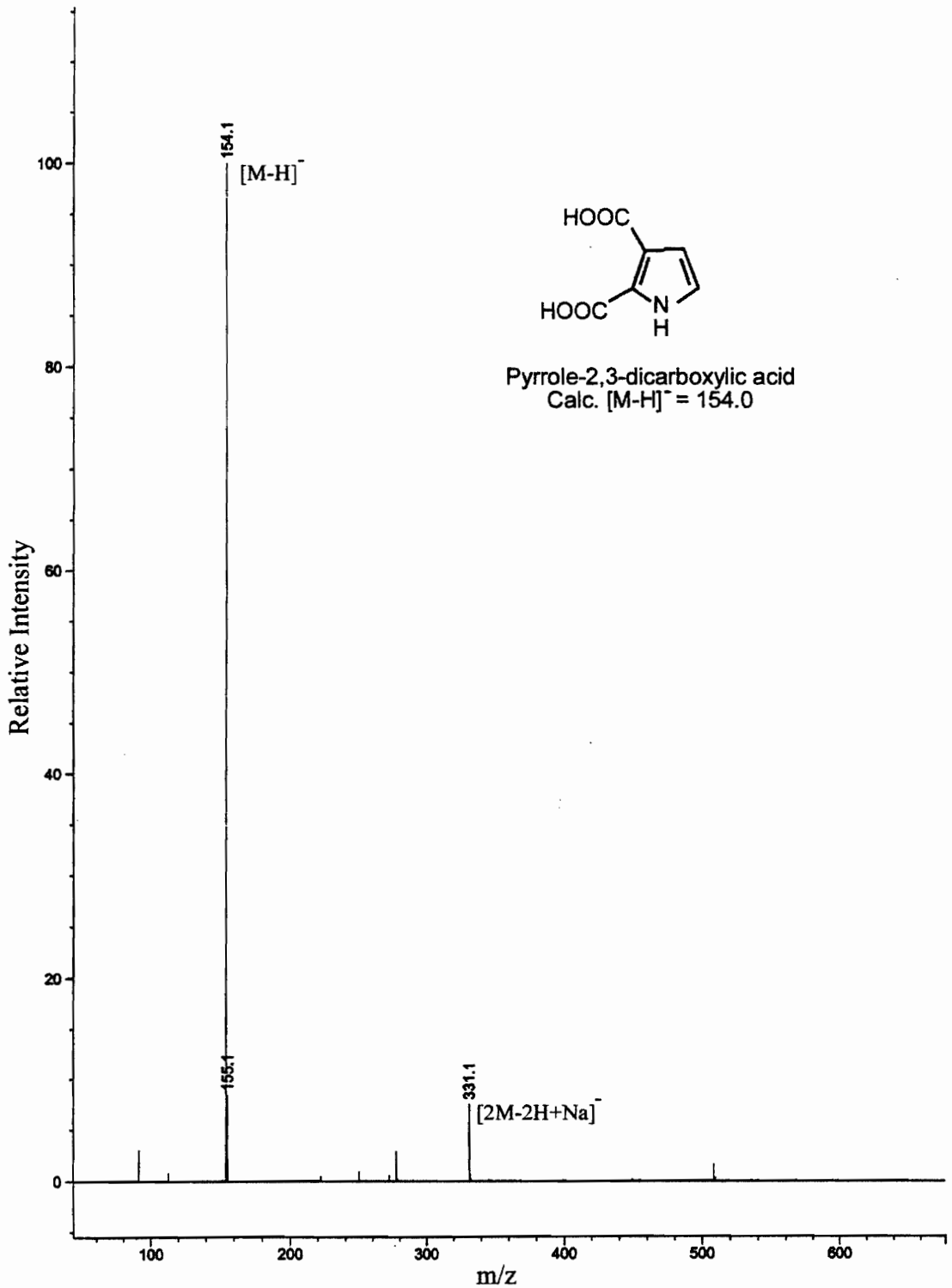
154.1
[M-H]⁻
HOOC
HOOC
N
H
Pyrrole-2,3-dicarboxylic acid
Calc. [M-H]⁻ = 154.0
Relative Intensity
155.1
331.1
[2M-2H+Na]⁻
m/z
0
20
40
60
80
100
100
200
300
400
500
600

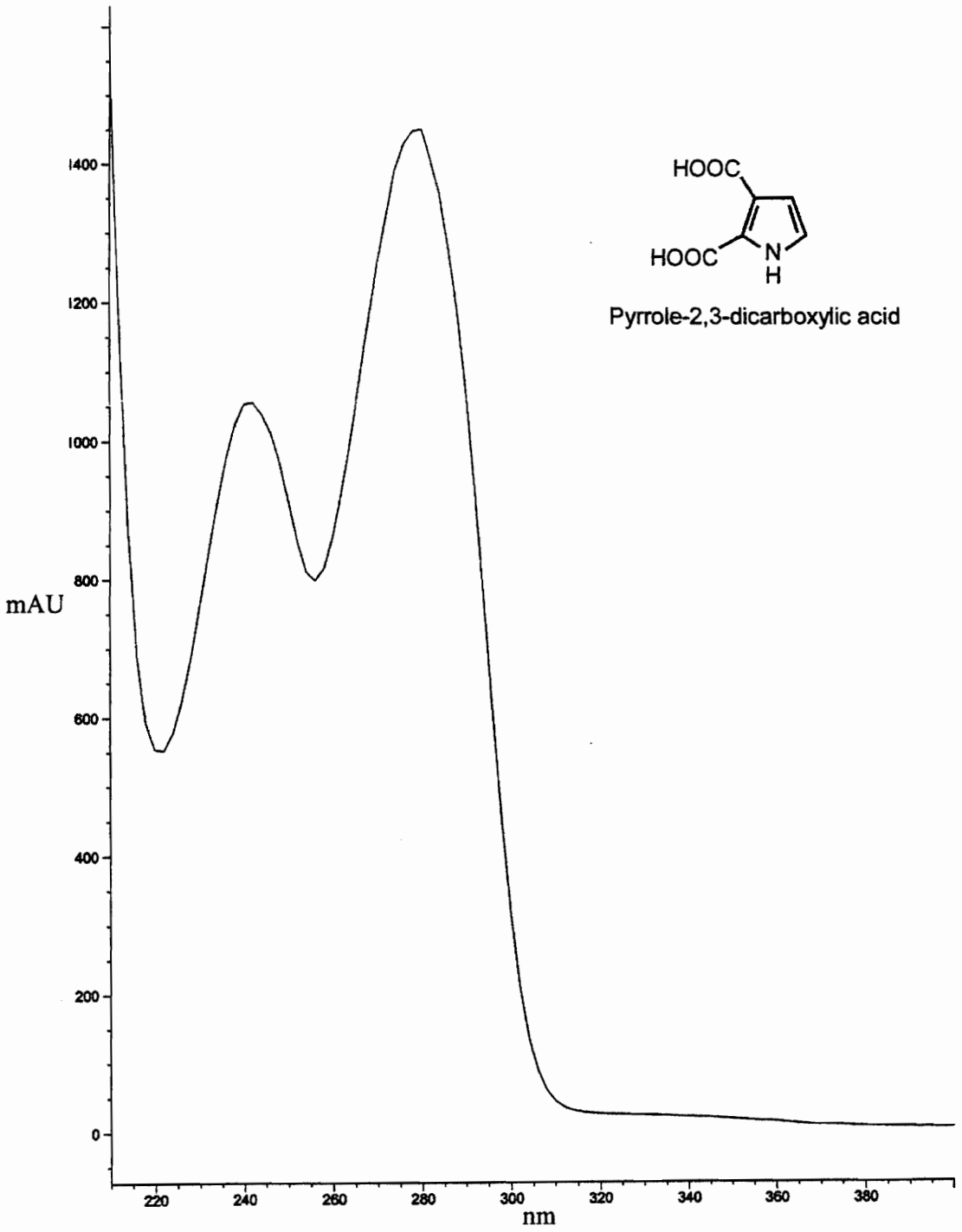
HOOC
HOOC
N
H
Pyrrole-2,3-dicarboxylic acid
mAU
1400
1200
1000
800
600
400
200
0
220
240
260
280
300
320
340
360
380
nm

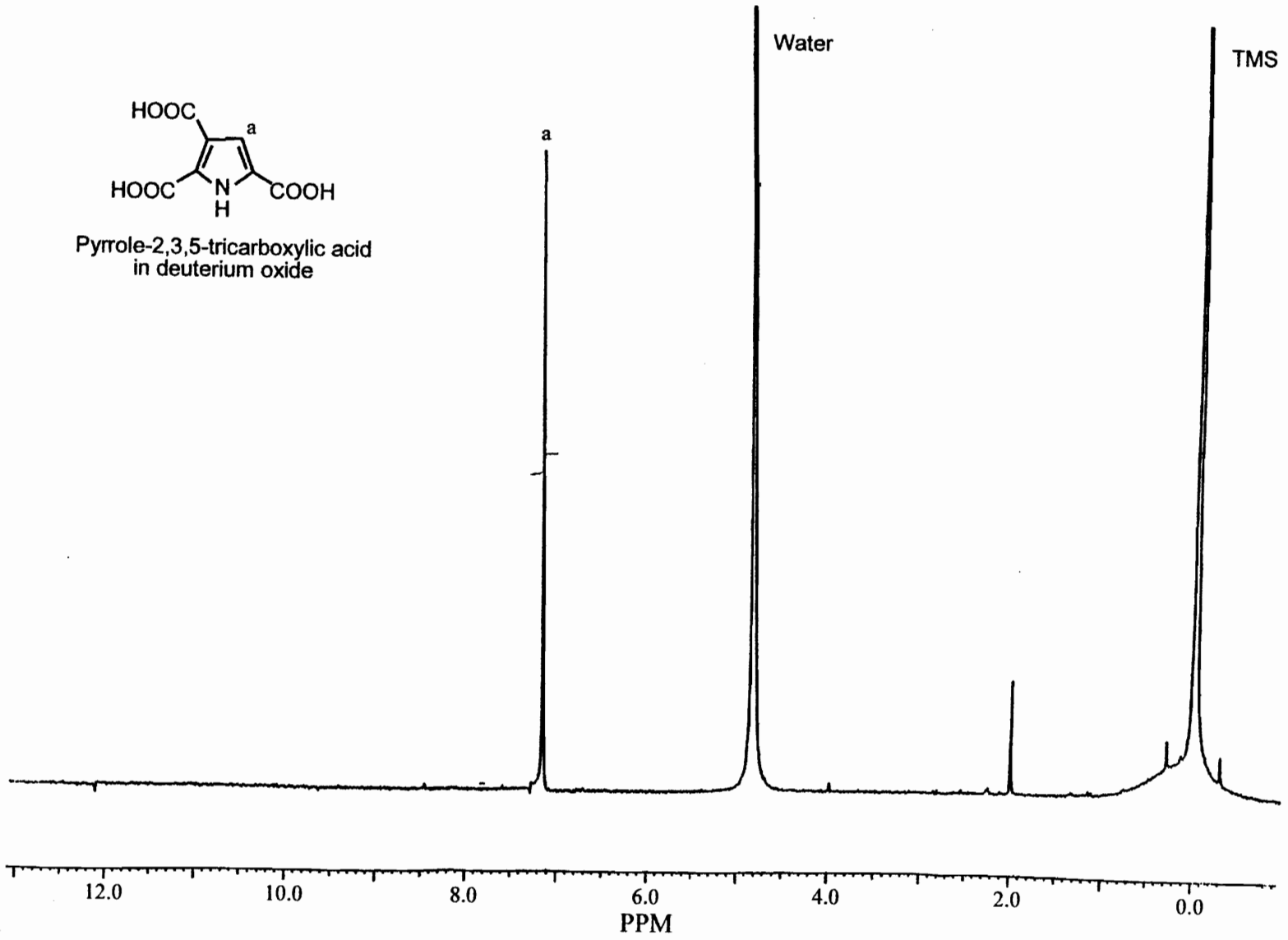
HOOC
a
HOOC
N
H
COOH
Pyrrole-2,3,5-tricarboxylic acid
in deuterium oxide
a
Water
TMS
12.0
10.0
8.0
6.0
4.0
2.0
0.0
PPM

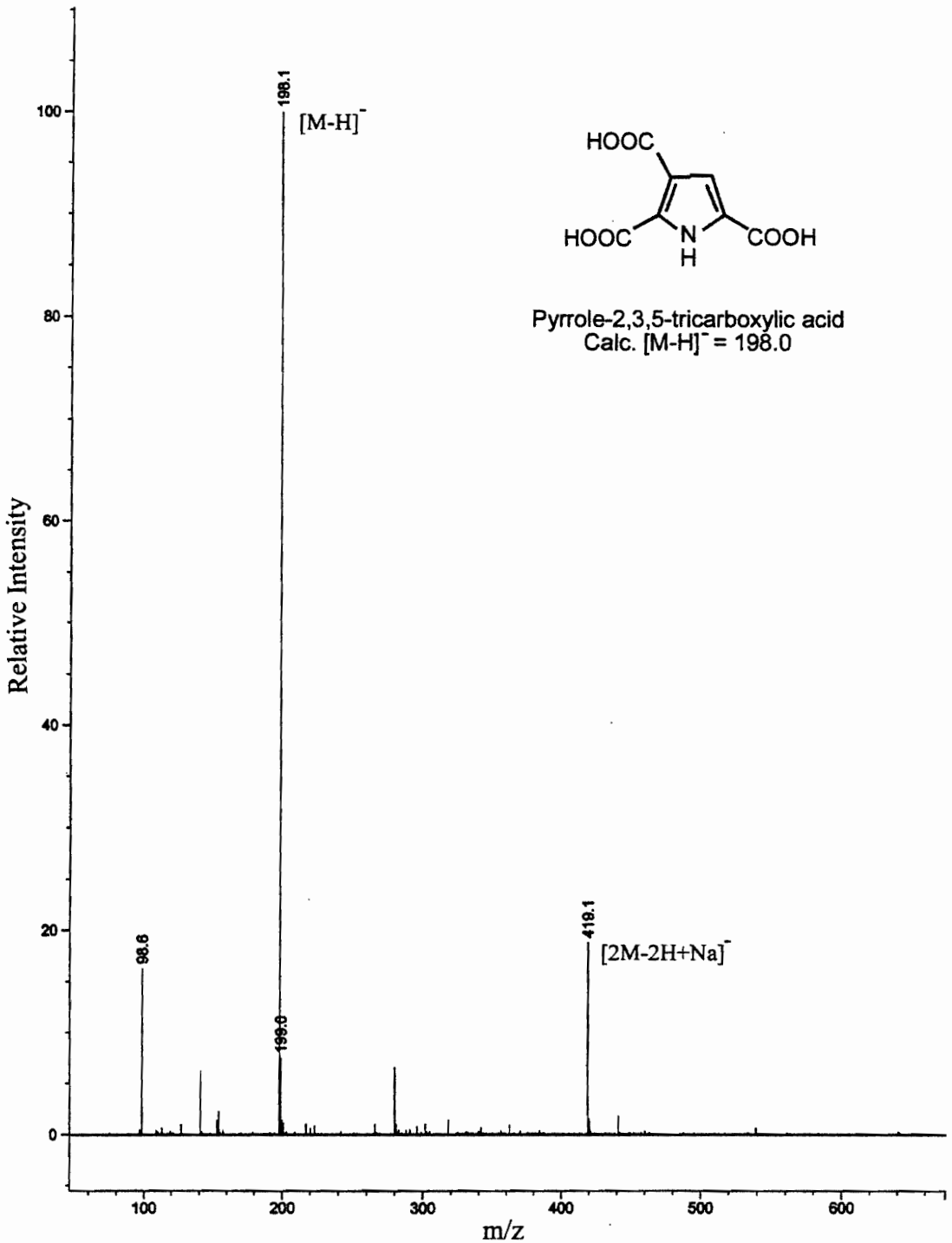
198.1
[M-H]⁻
HOOC
HOOC
N
H
COOH
Pyrrole-2,3,5-tricarboxylic acid
Calc. [M-H]⁻ = 198.0
Relative Intensity
100
80
60
40
20
0
98.6
199.0
419.1
[2M-2H+Na]⁻
100
200
300
400
500
600
m/z

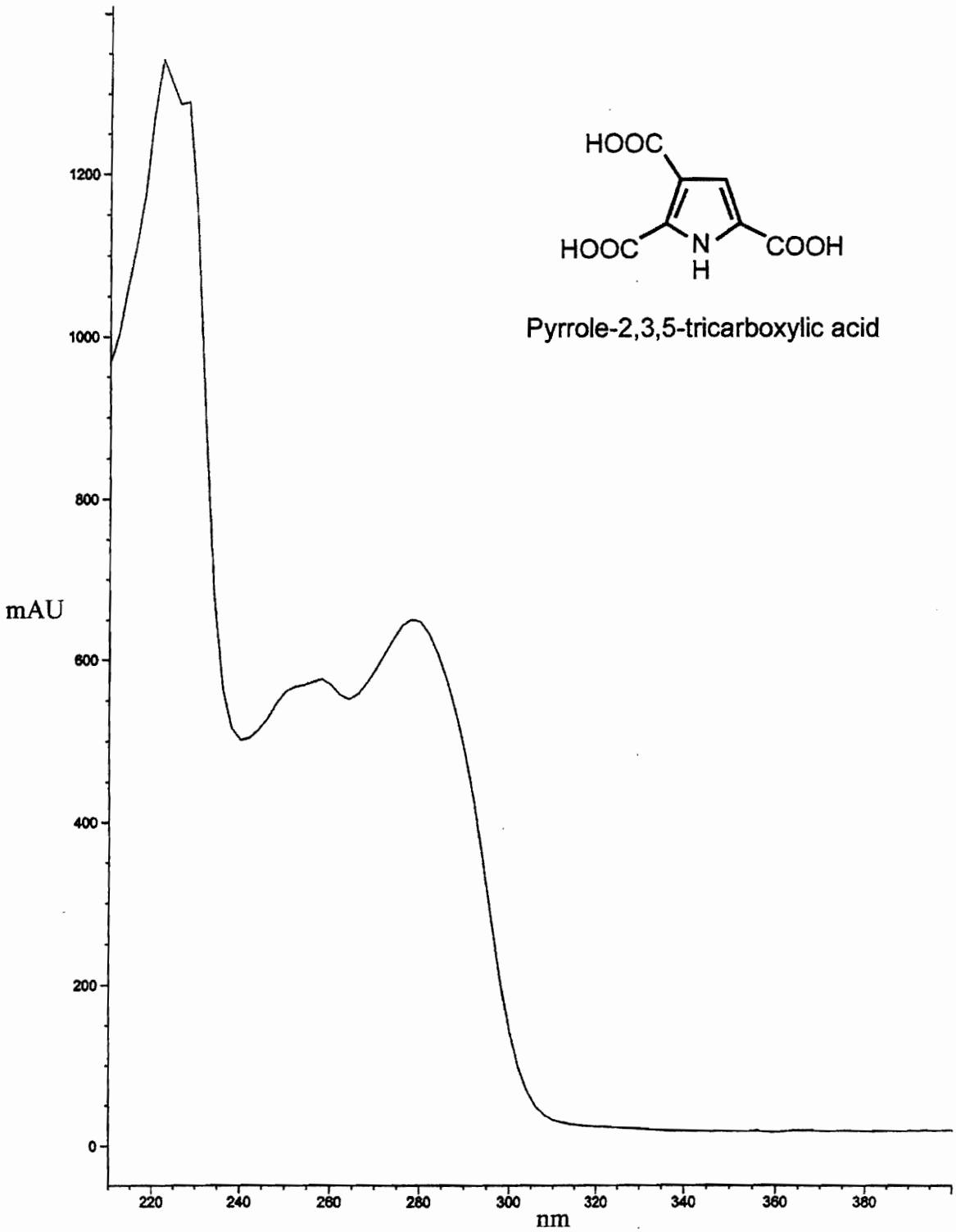
HOOC
HOOC
N
H
COOH
Pyrrole-2,3,5-tricarboxylic acid
mAU
1200
1000
800
600
400
200
0
220
240
260
280
300
320
340
360
380
nm

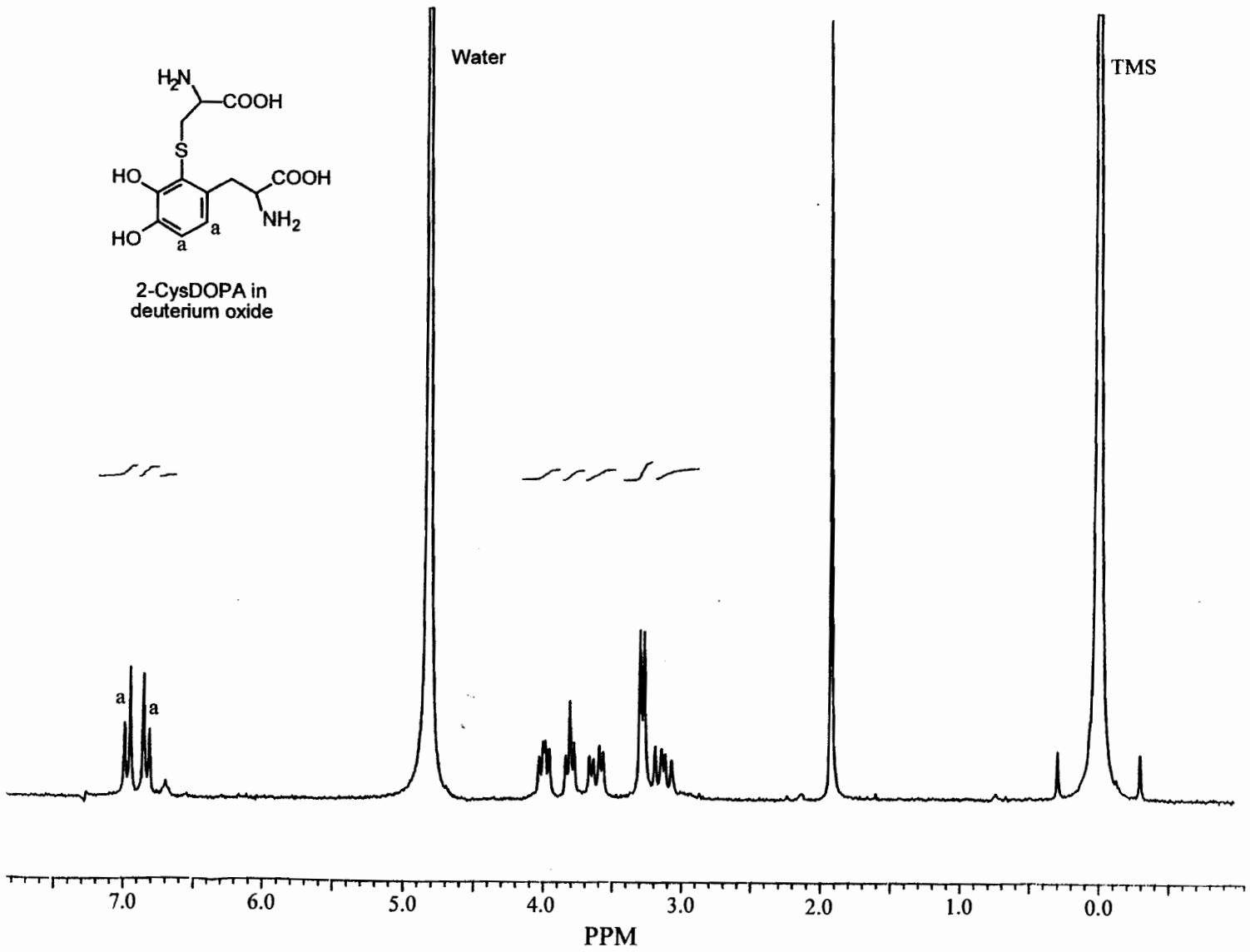
Water
TMS
2-CysDOPA in
deuterium oxide
a
a
7.0
6.0
5.0
4.0
3.0
2.0
1.0
0.0
PPM

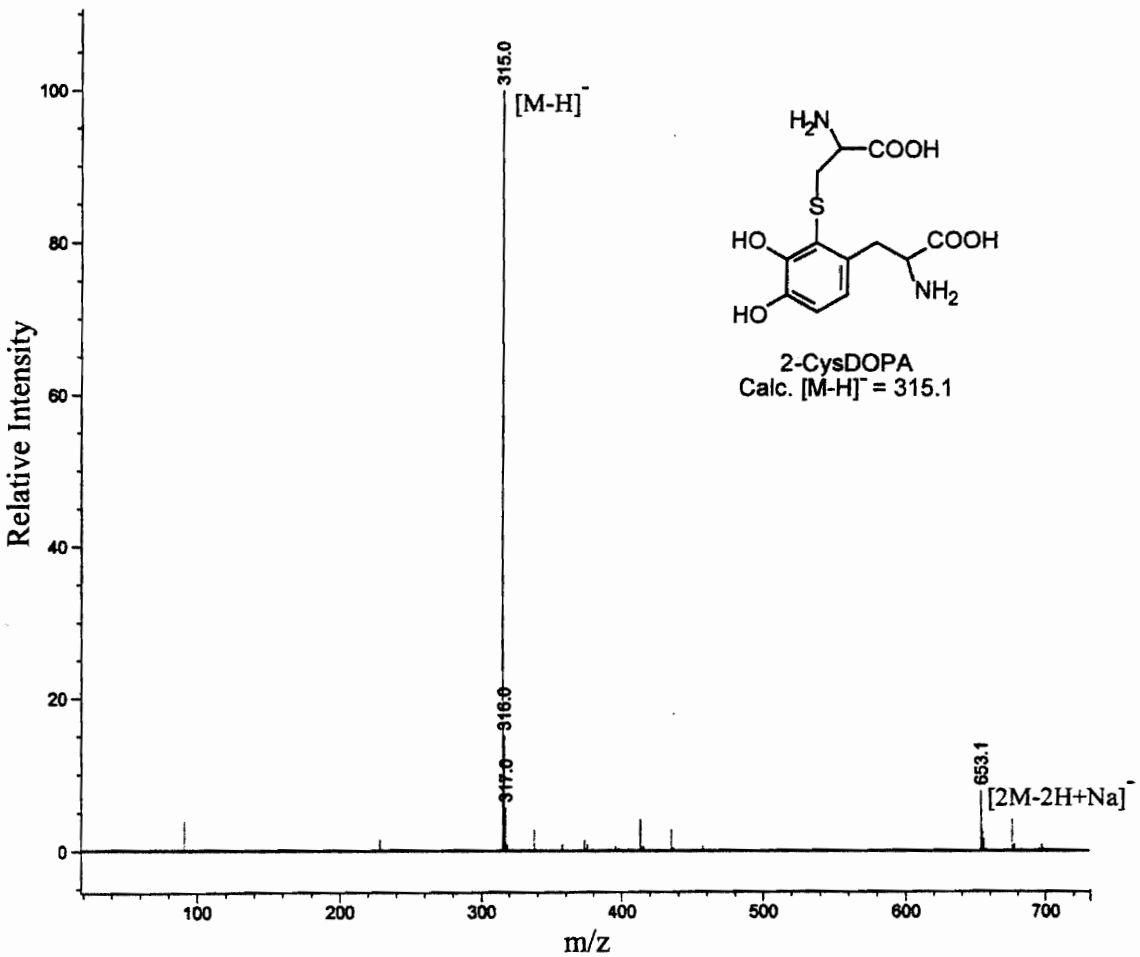
315.0
[M-H]⁻
316.0
317.0
653.1
[2M-2H+Na]⁻
Relative Intensity
m/z
100
80
60
40
20
0
100
200
300
400
500
600
700
H2N
COOH
S
HO
COOH
NH2
HO
2-CysDOPA
Calc. [M-H]⁻ = 315.1

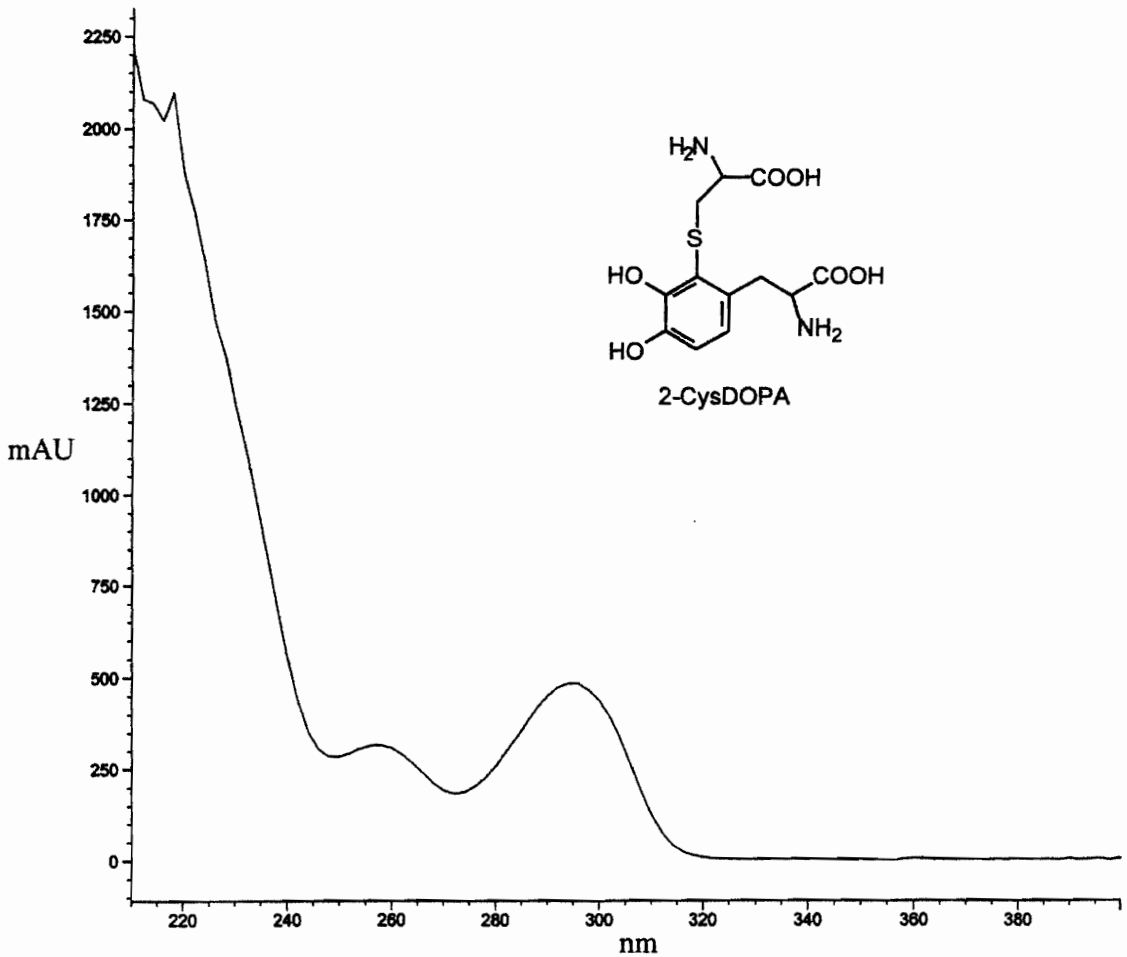
2250
2000
1750
1500
1250
1000
750
500
250
0
mAU
220
240
260
280
300
320
340
360
380
nm
H2N
COOH
S
HO
COOH
NH2
HO
2-CysDOPA

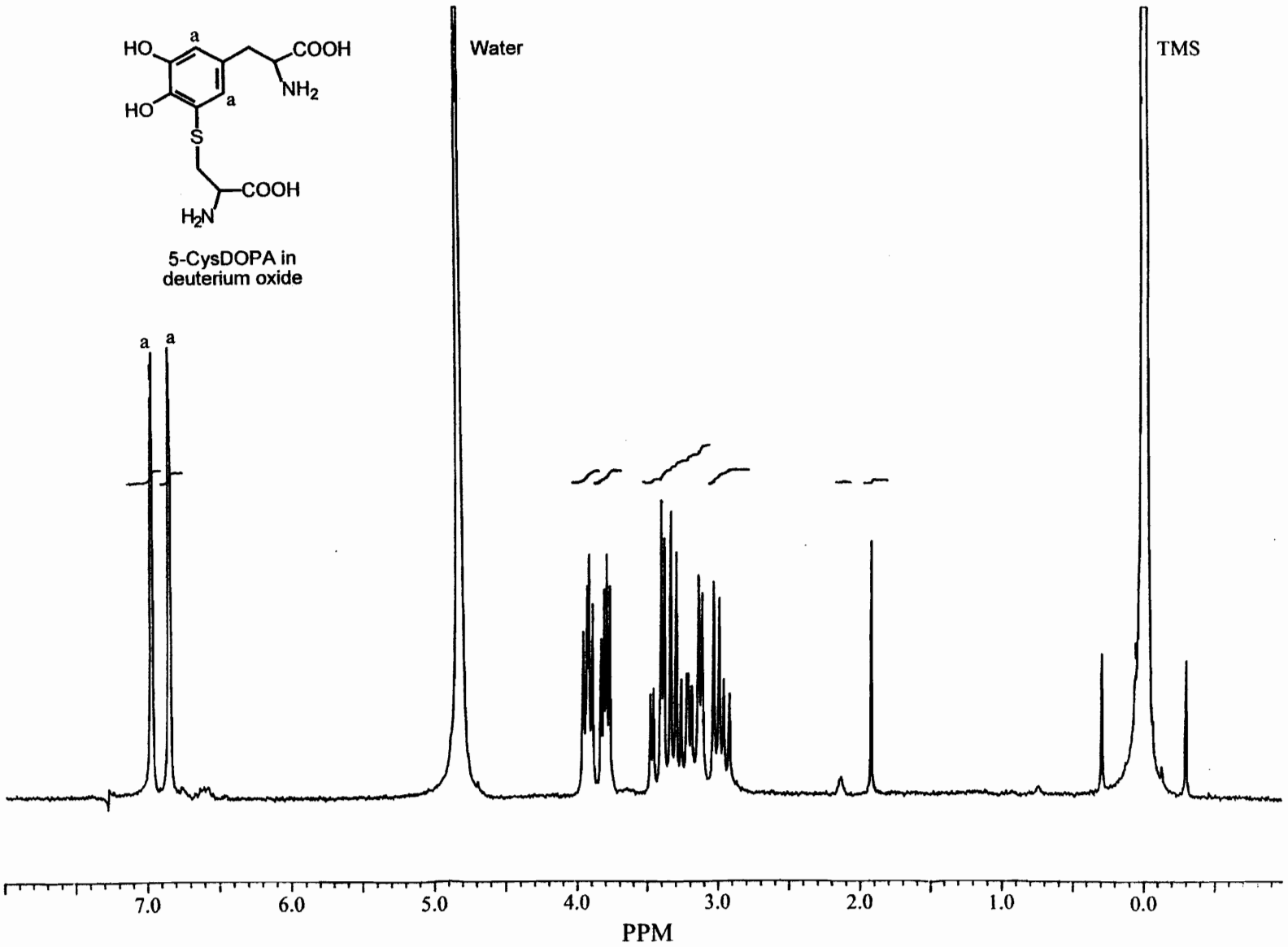
HO
a
COOH
NH2
HO
a
S
COOH
H2N
5-CysDOPA in
deuterium oxide
a
a
Water
TMS
7.0
6.0
5.0
4.0
3.0
2.0
1.0
0.0
PPM

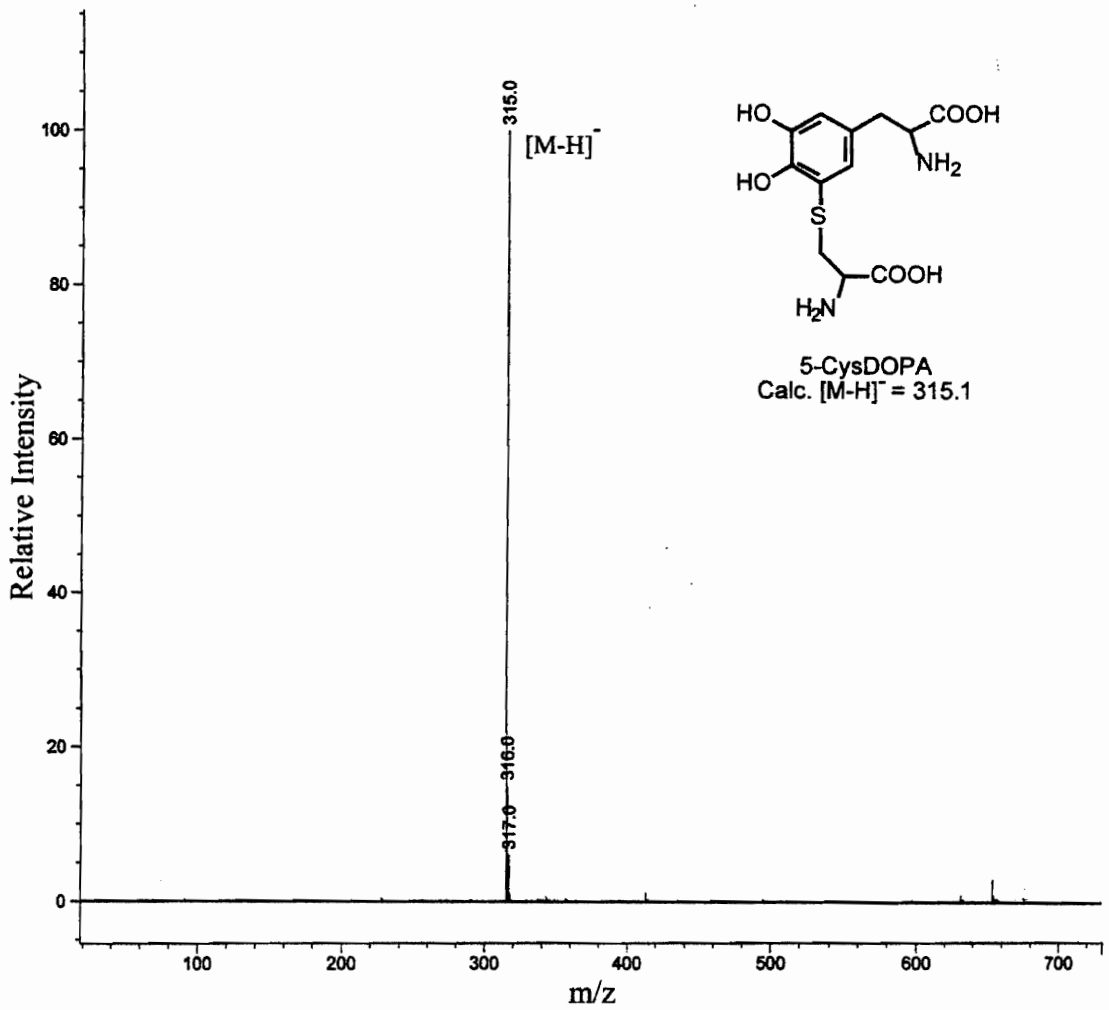
315.0
[M-H]⁻
316.0
317.0
Relative Intensity
m/z
100
80
60
40
20
0
100
200
300
400
500
600
700
HO
HO
COOH
NH2
S
COOH
H2N
5-CysDOPA
Calc. [M-H]⁻ = 315.1

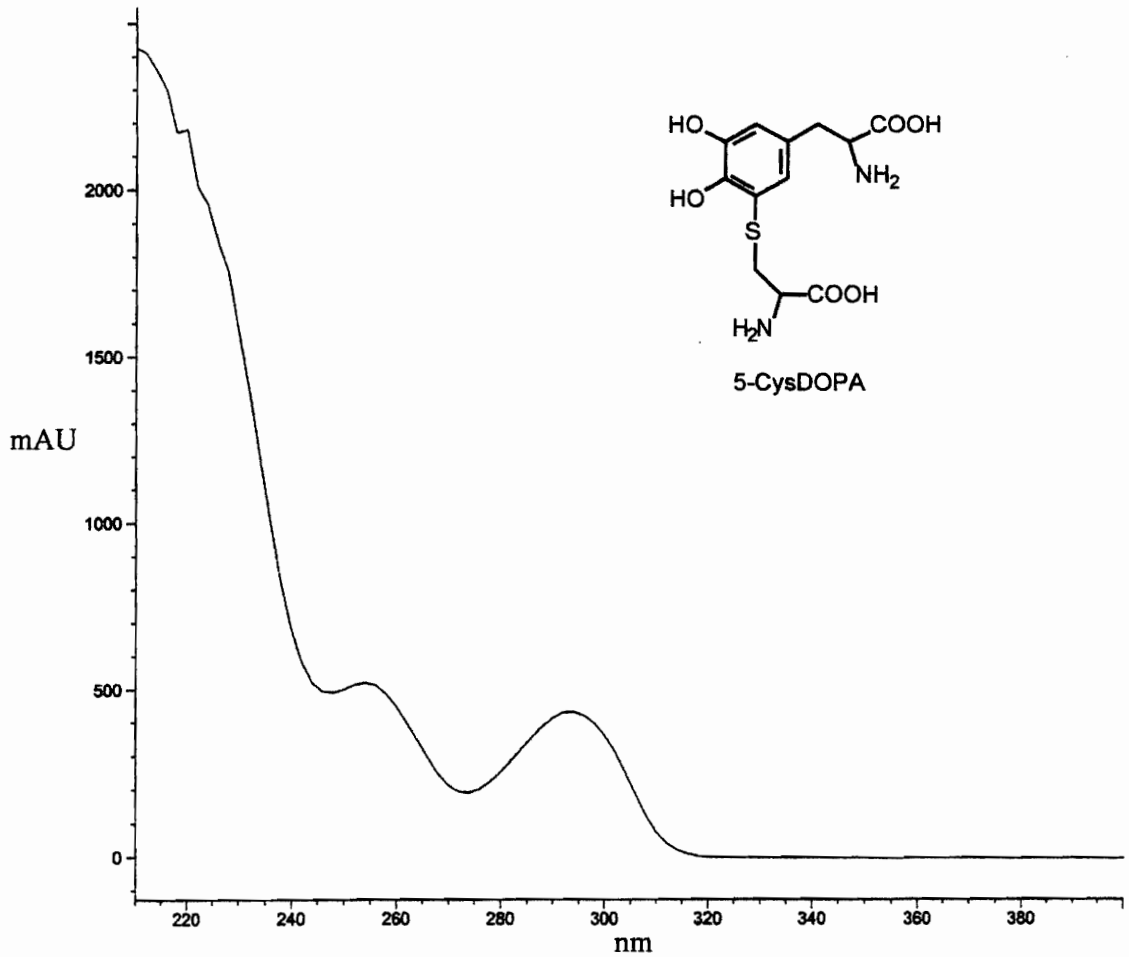
HO
HO
COOH
NH2
S
COOH
H2N
5-CysDOPA
mAU
2000
1500
1000
500
0
220
240
260
280
300
320
340
360
380
nm

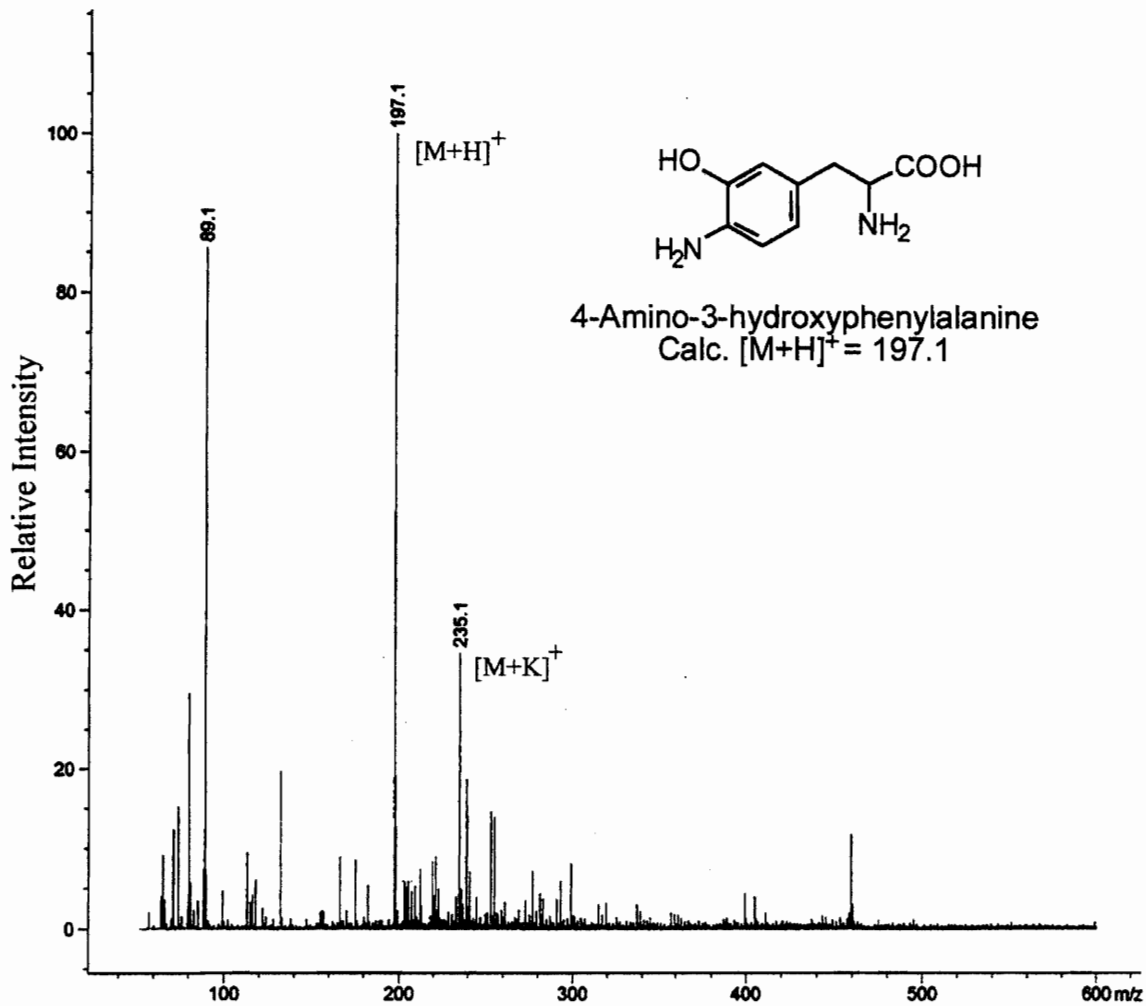
Relative Intensity
100
80
60
40
20
0
89.1
197.1
[M+H]+
235.1
[M+K]+
100
200
300
400
500
600 m/z
HO
COOH
NH2
H2N
4-Amino-3-hydroxyphenylalanine
Calc. [M+H]+ = 197.1

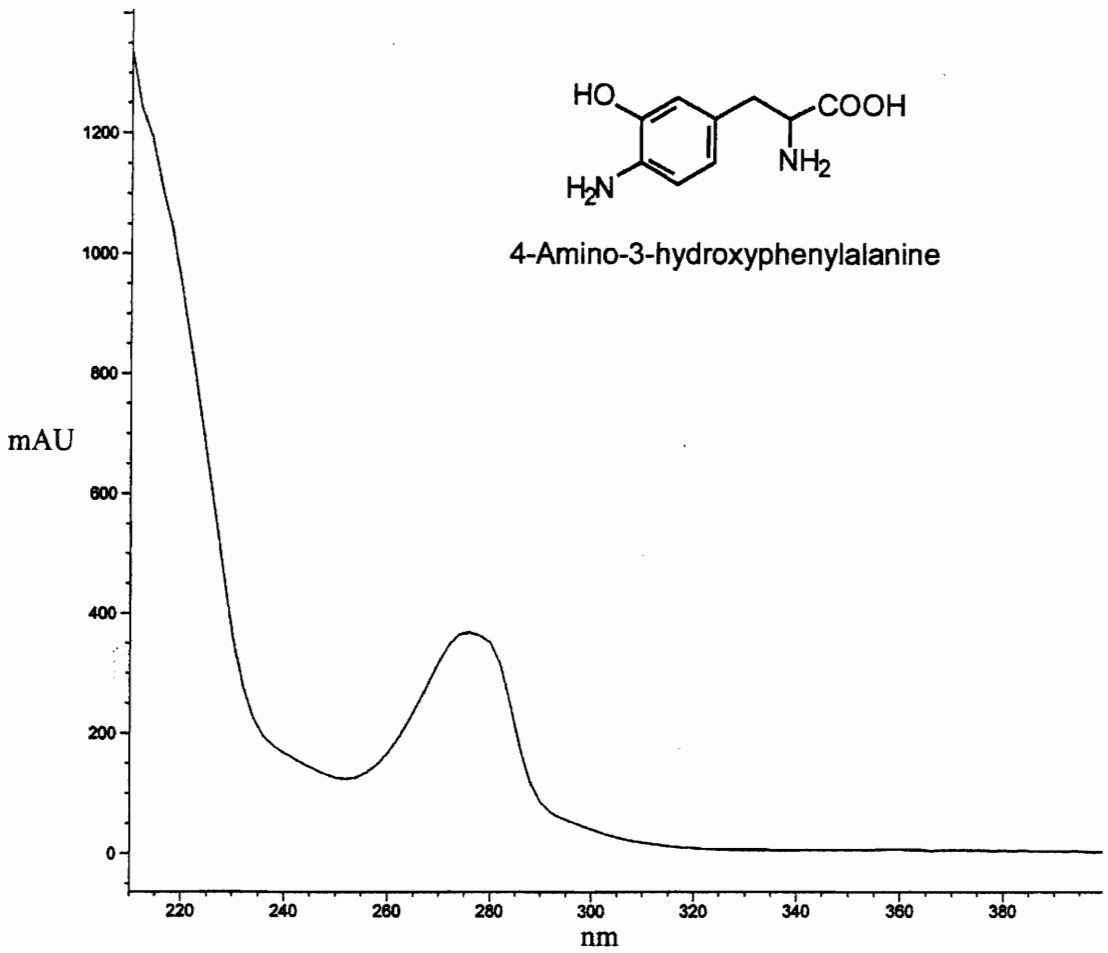
HO
COOH
NH2
H2N
4-Amino-3-hydroxyphenylalanine
mAU
1200
1000
800
600
400
200
0
220
240
260
280
300
320
340
360
380
nm

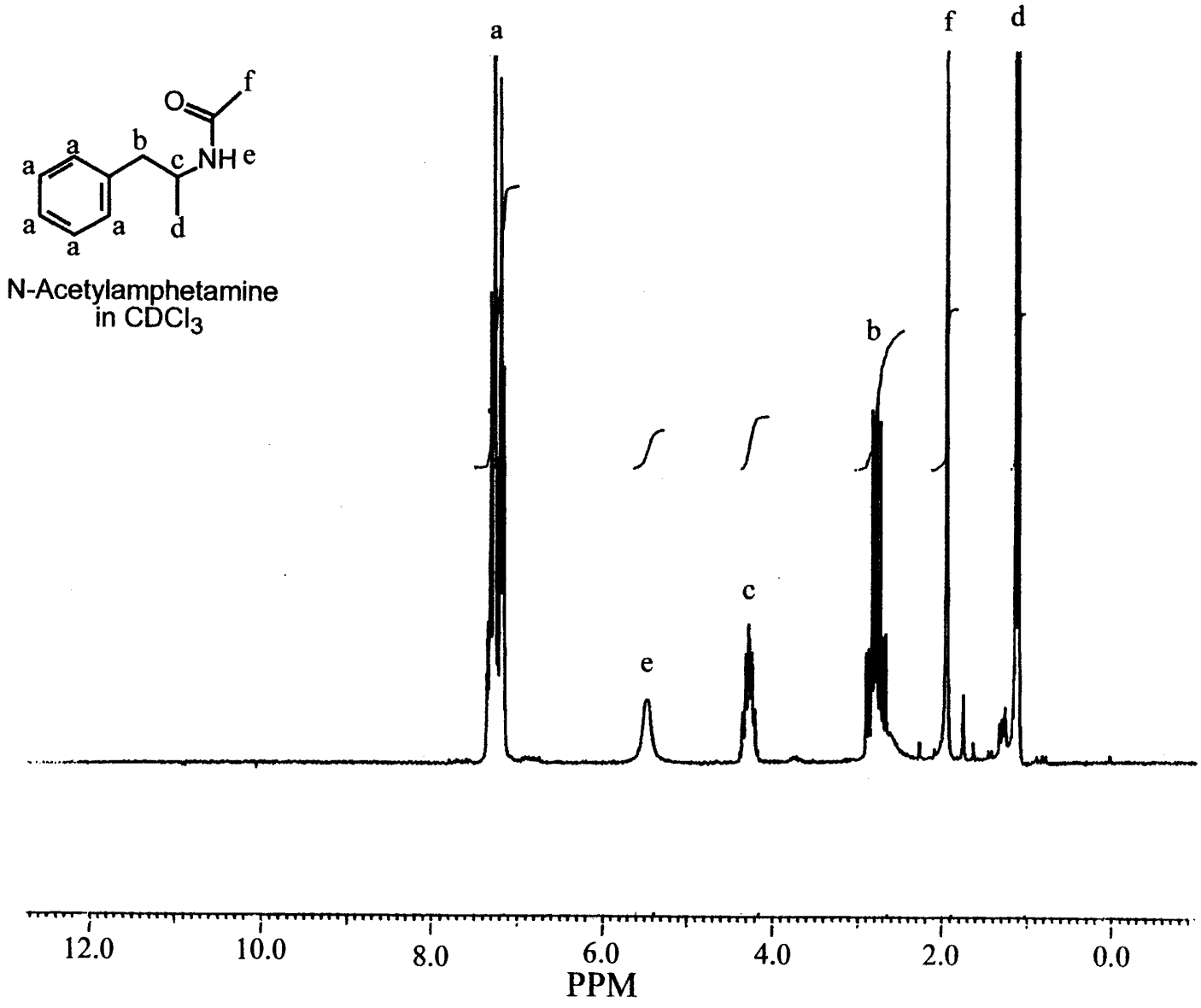

N-Acetylamphetamine
in $CDCl_3$

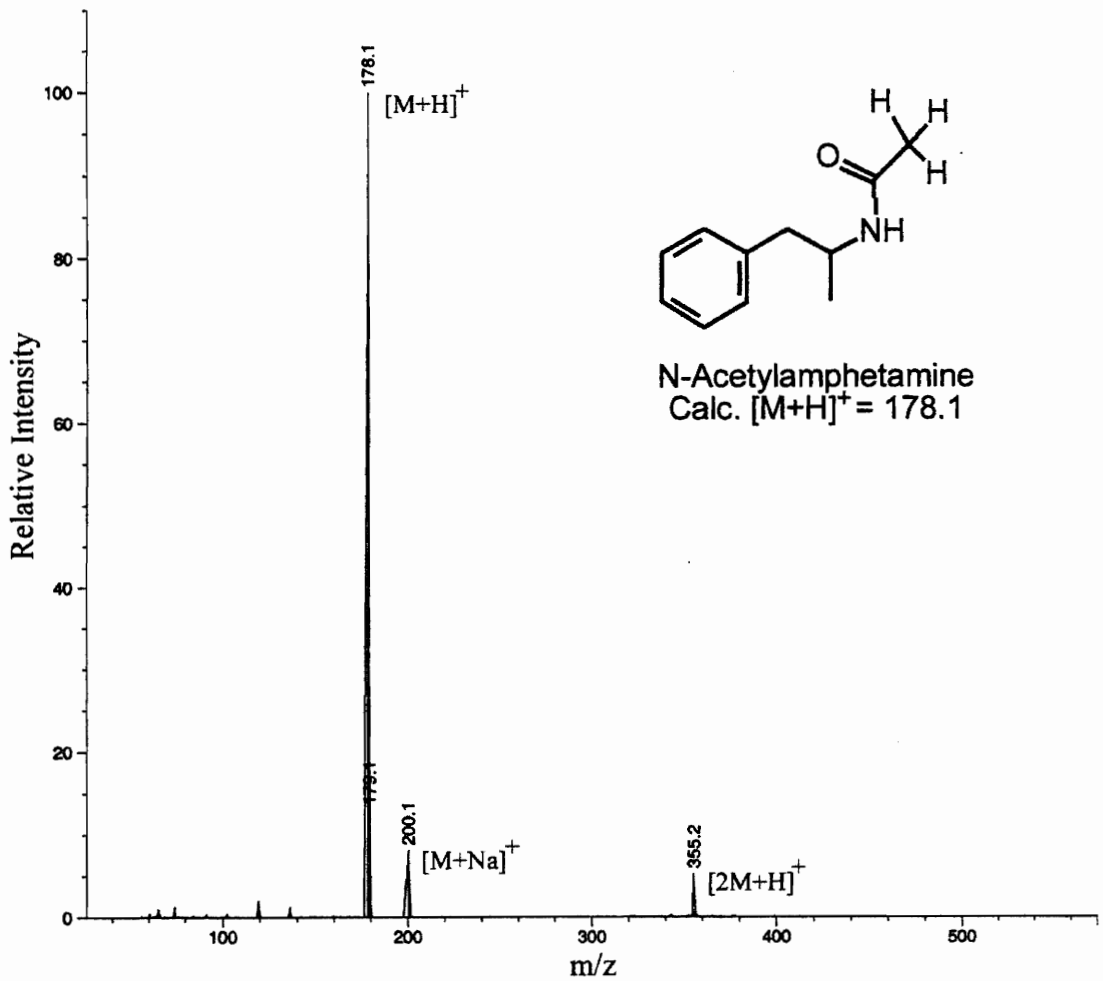
178.1
[M+H]+
179.1
200.1
[M+Na]+
355.2
[2M+H]+
Relative Intensity
m/z
100
80
60
40
20
0
100
200
300
400
500
H
H
H
O
NH
N-Acetylamphetamine
Calc. [M+H]+ = 178.1

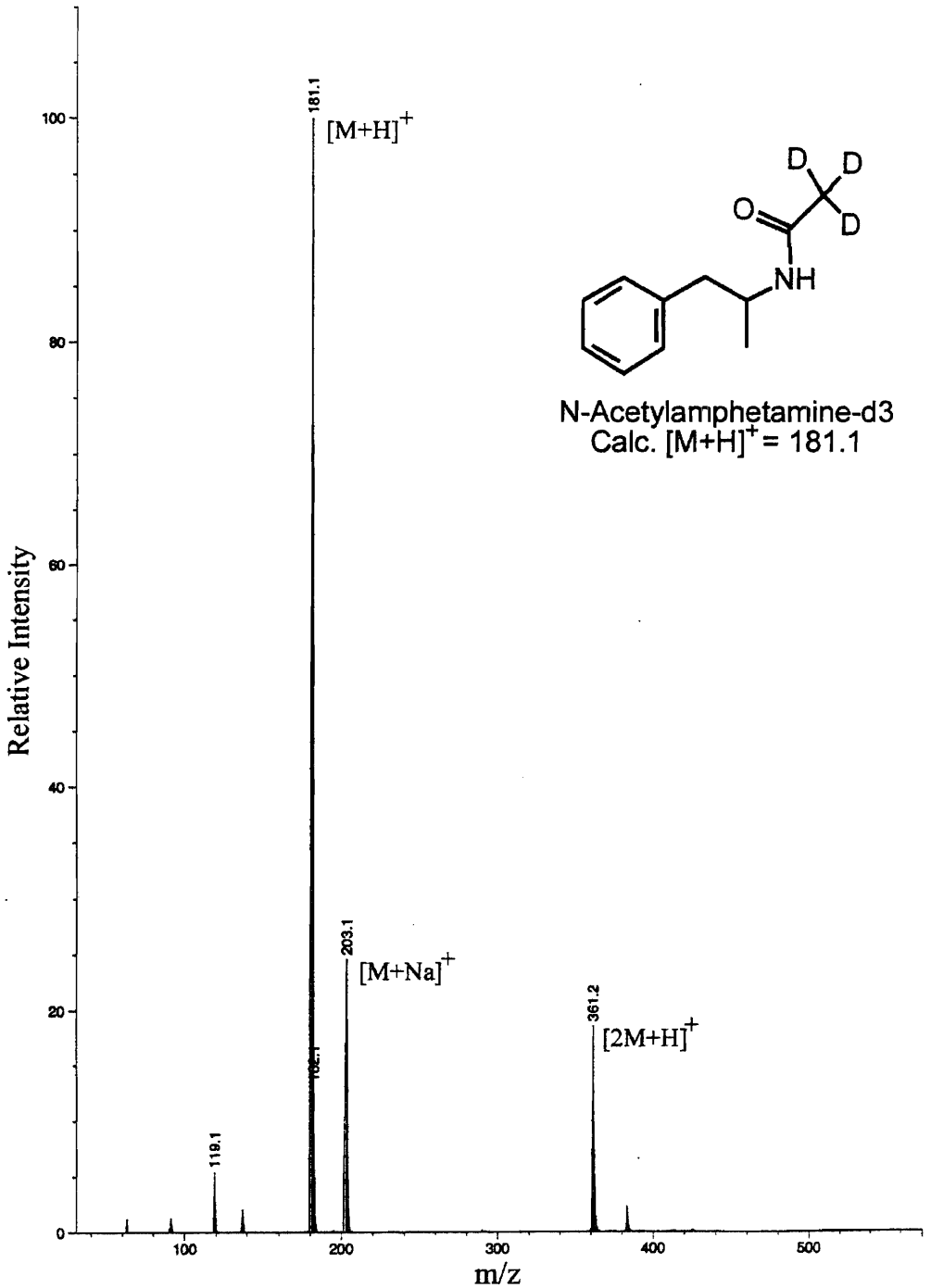
181.1
[M+H]+
203.1
[M+Na]+
361.2
[2M+H]+
118.1
Relative Intensity
m/z
D
D
D
O
NH
N-Acetylamphetamine-d3
Calc. [M+H]+ = 181.1

REFERENCES

1. Casper, J. L. Praktisches Handbuch der Gerichtlichen Medizin., Vol. 2, pp. 1857-1858. Berlin: A. Hirschwald, 1858.

2. Goldblum, R. W., Goldbaum, L. R., and Piper, W. N. Barbiturate concentrations in the skin and hair of guinea pigs. J. Invest. Dermatol. *22:* 121-128, 1954.

3. Harrison, W. H., Gray, R. M., and Solomon, L. M. Incorporation of D-amphetamine into pigmented guinea-pig hair. Br J Dermatol. *91:* 415-418, 1974.

4. Maugh, T. H. Hair: a diagnostic tool to complement blood serum and urine. Science. *202:* 1271-1273, 1978.

5. Fletcher, D. J. Hair analysis. Proven and problematic applications. Postgrad Med. *72:* 79-81, 84, 87-78, 1982.

6. Hambidge, K. M. Hair analyses: worthless for vitamins, limited for minerals. Am J Clin Nutr. *36:* 943-949, 1982.

7. Sky-Peck, H. H. Distribution of trace elements in human hair. Clin Physiol Biochem. *8:* 70-80, 1990.

8. Contiero, E. and Folin, M. Trace elements nutritional status. Use of hair as a diagnostic tool. Biol Trace Elem Res. *40:* 151-160, 1994.

9. Seidel, S., Kreutzer, R., Smith, D., McNeel, S., and Gilliss, D. Assessment of commercial laboratories performing hair mineral analysis. JAMA. *285:* 67-72, 2001.

10. Baumgartner, A. M., Jones, P. F., Baumgartner, W. A., and Black, C. T. Radioimmunoassay of hair for determining opiate-abuse histories. J Nucl Med. *20:* 748-752, 1979.

11. Baumgartner, A. M., Jones, P. F., and Black, C. T. Detection of phencyclidine in hair. J Forensic Sci. *26:* 576-581, 1981.

12. Baumgartner, W. A., Black, C. T., Jones, P. F., and Blahd, W. H. Radioimmunoassay of cocaine in hair: concise communication. J Nucl Med. *23:* 790-792, 1982.

13. Smith, F. P. and Pomposini, D. A. Detection of phenobarbital in bloodstains, semen, seminal stains, saliva, saliva stains, perspiration stains, and hair. J Forensic Sci. *26:* 582-586, 1981.

14. Valente, D., Cassini, M., Pigliapochi, M., and Vansetti, G. Hair as the sample in assessing morphine and cocaine addiction. Clin Chem. *27:* 1952-1953., 1981.

15. Klug, E. Zur morphinbestimmung in kopfhaaren. Zeitschrift Rechtsmedizin. *84:* 189-193, 1980.

16. Suzuki, O. Detection of trace amounts of methamphetamine in biological materials by mass fragmentometry. Koenshu-Iyo Masu Kenkyukai. *6:* 123-132, 1981.

17. Ishiyama, I., Nagai, T., and Toshida, S. Detection of basic drugs (methamphetamine, antidepressants, and nicotine) from human hair. J Forensic Sci. *28:* 380-385, 1983.

18. Viala, A., Deturmeny, E., Aubert, C., Estadieu, M., Durand, A., Cano, J. P., and Delmont, J. Determination of chloroquine and monodesethylchloroquine in hair. J Forensic Sci. *28:* 922-928, 1983.

19. Suzuki, O., Hattori, H., and Asano, M. Detection of methamphetamine and amphetamine in a single human hair by gas chromatography/chemical ionization mass spectrometry. J Forensic Sci. *29:* 611-617, 1984.

20. Holbrook, K. A. and Minami, S. I. Hair follicle embryogenesis in the human: Characterization of events *in vivo* and *in vitro*. Ann N Y Acad Sci. *642:* 167-196, 1991.

21. Chase, H. B. Growth of the hair. Physiol Revs. *34:* 113-126, 1954.

22. Millar, S. E., Willert, K., Salinas, P. C., Roelink, H., Nusse, R., Sussman, D. J., and Barsh, G. S. WNT signaling in the control of hair growth and structure. Dev Biol. *207:* 133-149, 1999.

23. Epstein, W. L. and Maibach, H. I. Cell proliferation and movement in human hair bulbs. *In:* W. Montagna and R. L. Dobson (eds.), Advances in Biology of Skin, Vol. IX, pp. 83-97. Oxford: Pergamon Press, 1967.

24. Parakkal, P. F. The fine structure of anagen hair follicle of the mouse. *In:* W. Montagna and R. L. Dobson (eds.), Advances in Biology of Skin, Vol. IX, pp. 441-469. Oxford: Pergamon Press, 1967.

25. Robbins, C. R. Chemical and physical behavior of human hair, 3rd edition. New York: Springer-Verlag, 1994.

26. Harkey, M. R. Anatomy and physiology of hair. Forensic Sci Int. *63:* 9-18., 1993.

27. Rusting, R. L. Hair: Why it grows, why it stops. Scientific American. *284:* 70-79, 2001.

28. Paus, R. and Cotsarelis, G. The biology of hair follicles. N Engl J Med. *341:* 491-497, 1999.

29. Henderson, G. L. Mechanisms of drug incorporation into hair. Forensic Sci Int. *63:* 19-29, 1993.

30. Cone, E. J. Mechanisms of drug incorporation into hair. Ther Drug Monit. *18:* 438-443, 1996.

31. Baumgartner, W. A., Hill, V. A., and Blahd, W. H. Hair analysis for drugs of abuse. J Forensic Sci. *34:* 1433-1453, 1989.

32. Huestis, M. A., Henningfield, J. E., and Cone, E. J. Blood cannabinoids. I. Absorption of THC and formation of 11-OH-THC and THCCOOH during and after smoking marijuana. J Anal Toxicol. *16:* 276-282., 1992.

33. Cirimele, V., Kintz, P., and Mangin, P. Testing human hair for cannabis. Forensic Sci Int. *70:* 175-182, 1995.

34. Jurado, C., Gimenez, M. P., Menendez, M., and Repetto, M. Simultaneous quantification of opiates, cocaine and cannabinoids in hair. Forensic Sci Int. *70:* 165-174, 1995.

35. Wilkins, D., Haughey, H., Cone, E., Huestis, M., Foltz, R., and Rollins, D. Quantitative analysis of THC, 11-OH-THC, and THCCOOH in human hair by negative ion chemical ionization mass spectrometry. J. Anal. Toxicol. *19:* 483-491, 1995.

36. Nakahara, Y., Ochiai, T., and Kikura, R. Hair analysis for drugs of abuse. V. The facility in incorporation of cocaine into hair over its major metabolites, benzoylecgonine and ecgonine methyl ester. Arch Toxicol. *66:* 446-449, 1992.

37. Harkey, M. R., Henderson, G. L., and Zhou, C. Simultaneous quantitation of cocaine and its major metabolites in human hair by gas chromatography/chemical ionization mass spectrometry. J Anal Toxicol. *15:* 260-265, 1991.

38. Cone, E. J., Yousefnejad, D., Darwin, W. D., and Maguire, T. Testing human hair for drugs of abuse. II. Identification of unique cocaine metabolites in hair of drug

abusers and evaluation of decontamination procedures. J Anal Toxicol. *15:* 250-255, 1991.

39. Moller, M. R., Fey, P., and Rimbach, S. Identification and quantitation of cocaine and its metabolites, benzoylecgonine and ecgonine methyl ester, in hair of Bolivian coca chewers by gas chromatography/mass spectrometry. J Anal Toxicol. *16:* 291-296, 1992.

40. Gerstenberg, B., Schepers, G., Voncken, P., and Volkel, H. Nicotine and cotinine accumulation in pigmented and unpigmented rat hair. Drug Metab Dispos. *23:* 143-148, 1995.

41. Nakahara, Y. and Kikura, R. Hair analysis for drugs of abuse. XIII. Effect of structural factors on incorporation of drugs into hair: the incorporation rates of amphetamine analogs. Arch Toxicol. *70:* 841-849, 1996.

42. Borges, C. R., Wilkins, D. G., and Rollins, D. E. Amphetamine and N-acetylamphetamine incorporation into hair: An investigation of the potential role of drug basicity in hair color bias. J Anal Toxicol. *25:* 221-227, 2001.

43. Nakahara, Y., Takahashi, K., and Kikura, R. Hair analysis for drugs of abuse. X. Effect of physicochemical properties of drugs on the incorporation rates into hair. Biol Pharm Bull. *18:* 1223-1227, 1995.

44. Kidwell, D. A. and Blank, D. L. Hair analysis: techniques and potential problems. *In:* I. Sunshine (ed.) Recent Developments in Therapeutic Drug Monitoring and Clinical Toxicology, pp. 555. New York: Marcel Dekker, 1992.

45. Cone, E. J. and Joseph, R. E. J. The potential for bias in hair testing for drugs of abuse. *In:* P. Kintz (ed.) Drug testing in hair, pp. 69-93. Boca Raton, Forida: CRC Press, 1996.

46. Joseph, R. E., Jr., Tsai, W. J., Tsao, L. I., Su, T. P., and Cone, E. J. *In vitro* characterization of cocaine binding sites in human hair. J Pharmacol Exp Ther. *282:* 1228-1241, 1997.

47. Bolt, A. G. Interactions between human melanoprotein and chlorpromazine derivatives. I. Isolation and purification of human melanoprotein from hair and melanoma tissue. Life Sci. *6:* 1277-1283., 1967.

48. Bolt, A. G. and Forrest, I. S. Interaction between human melanoprotein and chlorpromazine derivatives. II. Spectrophotometric studies. Life Sci. *6:* 1285-1292, 1967.

49. Stout, P. R. and Ruth, J. A. Comparison of *in vivo* and *in vitro* deposition of rhodamine and fluorescein in hair. Drug Metab Dispos. *26:* 943-948, 1998.

50. Larsson, B., Oskarsson, A., and Tjalve, H. Binding of paraquat and diquat on melanin. Exp Eye Res. *25:* 353-359, 1977.

51. Larsson, B. and Tjalve, H. Studies on the mechanism of drug-binding to melanin. Biochem Pharmacol. *28:* 1181-1187, 1979.

52. Larsson, B. S. Interaction between chemicals and melanin. Pigment Cell Res. *6:* 127-133, 1993.

53. Stepien, K. B. and Wilczok, T. Studies of the mechanism of chloroquine binding to synthetic DOPA- melanin. Biochem Pharmacol. *31:* 3359-3365, 1982.

54. Howells, L., Godfrey, M., and Sauer, M. J. Melanin as an adsorbent for drug residues. Analyst. *119:* 2691-2693, 1994.

55. Shimada, K., Baweja, R., Sokoloski, T., and Patil, P. N. Binding characteristics of drugs to synthetic levodopa melanin. J Pharm Sci. *65:* 1057-1060, 1976.

56. Baweja, R., Sokoloski, T. D., and Patil, P. N. Competitive binding between cocaine and various drugs to synthetic levodopa melanin. J Pharm Sci. *66:* 1544-1547, 1977.

57. Mars, U. and Larsson, B. S. Pheomelanin as a binding site for drugs and chemicals. Pigment Cell Res. *12:* 266-274, 1999.

58. Ings, R. M. J. The melanin binding of drugs and its implications. Drug Metab Rev. *15:* 1183-1212, 1984.

59. Debing, I., Ijzerman, A. P., and Vauquelin, G. Melanosome binding and oxidation-reduction properties of synthetic L- dopa-melanin as *in vitro* tests for drug toxicity. Mol Pharmacol. *33:* 470-476, 1988.

60. Carr, C. J., Forrest, I. S., Potts, A. M., Woert, M. H. V., VanderWende, C., and Forrest, F. M. Melanin affinity and psychopharmacologic effects of drugs. Psychopharmacology Bulletin. *10:* 38-47, 1974.

61. Lowrey, A. H., Famini, G. R., Loumbev, V., Wilson, L. Y., and Tosk, J. M. Modeling drug-melanin interaction with theoretical linear solvation energy relationships. Pigment Cell Res. *10:* 251-256, 1997.

62. Raghavan, P. R., Zane, P. A., and Tripp, S. L. Calculation of drug-melanin binding energy using molecular modeling. Experientia. *46:* 77-80, 1990.

63. Joseph, R. E., Jr., Su, T. P., and Cone, E. J. *In vitro* binding studies of drugs to hair: influence of melanin and lipids on cocaine binding to Caucasoid and Africoid hair. J Anal Toxicol. *20:* 338-344, 1996.

64. Potsch, L., Skopp, G., and Moeller, M. R. Influence of pigmentation on the codeine content of hair fibers in guinea pigs. J Forensic Sci. *42:* 1095-1098, 1997.

65. Gygi, S. P., Wilkins, D. G., and Rollins, D. E. A comparison of phenobarbital and codeine incorporation into pigmented and nonpigmented rat hair. J Pharm Sci. *86:* 209-214, 1997.

66. Hubbard, D. L., Wilkins, D. G., and Rollins, D. E. The incorporation of cocaine and metabolites into hair: effects of dose and hair pigmentation. Drug Metab Dispos. *28:* 1464-1469, 2000.

67. Nakahara, Y., Kikura, R., and Takahashi, K. Hair analysis for drugs of abuse XX. Incorporation and behaviors of seven methamphetamine homologs in the rat hair root. Life Sci. *63:* 883-893, 1998.

68. Hold, K., Wilkins, D., Crouch, D., Rollins, D., and Maes, R. Detection of stanozolol in hair by negative ion chemical ionization mass spectrometry. J Anal Toxicol. *20:* 345-349, 1996.

69. Slawson, M. H., Wilkins, D. G., and Rollins, D. E. The incorporation of drugs into hair: relationship of hair color and melanin concentration to phencyclidine incorporation. J Anal Toxicol. *22:* 406-413, 1998.

70. Uematsu, T., Sato, R., Fujimori, O., and Nakashima, M. Human scalp hair as evidence of individual dosage history of haloperidol: a possible linkage of haloperidol excretion into hair with hair pigment. Arch Dermatol Res. *282:* 120-125, 1990.

71. Uematsu, T., Miyazawa, N., Okazaki, O., and Nakashima, M. Possible effect of pigment on the pharmacokinetics of ofloxacin and its excretion in hair. J Pharm Sci. *81:* 45-48, 1992.

72. Mieczkowski, T. and Newel, R. Statistical examination of hair color as a potential biasing factor in hair analysis. Forensic Sci Int. *107:* 13-38, 2000.

73. Kelly, C. K., Mieczkowski, T., Sweeney, S. A., and Bourland, J. A. Hair analysis for drugs of abuse. Hair color and race differentials or systematic differences in drug preferences? Forensic Sci Int. *107:* 63-86, 2000.

74. Mieczkowski, T. Is a "color effect" demonstrated for hair analysis of carbamazepine? Life Sci. *67:* 39-43, 2000.

75. Nakahara, Y. The effects of physiochemical factors on incorporation of drugs into hair and behavior of drugs in hair root. *In:* T. Mieczkowski (ed.) Drug Testing Technology, pp. 49-72. Boca Raton, FL: CRC Press LLC, 1999.

76. Borges, C. R., Roberts, J. C., Wilkins, D. G., and Rollins, D. E. Cocaine, benzoylecgonine, amphetamine, and N-acetylamphetamine binding to melanin subtypes., Submitted.

77. D'Amato, R. J., Lipman, Z. P., and Snyder, S. H. Selectivity of the parkinsonian neurotoxin MPTP: toxic metabolite MPP+ binds to neuromelanin. Science. *231:* 987-989, 1986.

78. D'Amato, R. J., Benham, D. F., and Snyder, S. H. Characterization of the binding of N-methyl-4-phenylpyridine, the toxic metabolite of the parkinsonian neurotoxin N-methyl-4-phenyl-1,2,3,6- tetrahydropyridine, to neuromelanin. J Neurochem. *48:* 653-658, 1987.

79. Lindquist, N. G. Accumulation of drugs on melanin. Acta Radiol [Diagn]. *325:* 1-92, 1973.

80. Ben-Shachar, D. and Youdim, M. B. Iron, melanin and dopamine interaction: relevance to Parkinson's disease. Prog Neuropsychopharmacol Biol Psychiatry. *17:* 139-150, 1993.

81. Bruenger, F. W., Stover, B. J., and Atherton, D. R. The incorporation of various metal ions into *in vivo-* and *in vitro-* produced melanin. Radiat Res. *32:* 1-12, 1967.

82. Potts, A. M. and Au, P. C. The affinity of melanin for inorganic ions. Exp Eye Res. *22:* 487-491, 1976.

83. Felix, C. C., Hyde, J. S., Sarna, T., and Sealy, R. C. Interactions of melanin with metal ions: Electron spin resonance evidence for chelate complexes of metal ions with free radicals. J Am Chem Soc. *100:* 3922-3926, 1978.

84. Mason, C. G. Ocular accumulation and toxicity of certain systemically administered drugs. J Toxicol Environ Health. *2:* 977-995, 1977.

85. Zemel, E., Loewenstein, A., Lei, B., Lazar, M., and Perlman, I. Ocular pigmentation protects the rabbit retina from gentamicin-induced toxicity. Invest Ophthalmol Vis Sci. *36:* 1875-1884, 1995.

86. Conlee, J. W., Bennett, M. L., and Creel, D. J. Differential effects of gentamicin on the distribution of cochlear function in albino and pigmented guinea pigs. Acta Otolaryngol. *115:* 367-374, 1995.

87. Barr-Hamilton, R. M., Matheson, L. M., and Keay, D. G. Ototoxicity of cis-platinum and its relationship to eye colour. J Laryngol Otol. *105:* 7-11, 1991.

88. D'Amato, R. J., Alexander, G. M., Schwartzman, R. J., Kitt, C. A., Price, D. L., and Snyder, S. H. Evidence for neuromelanin involvement in MPTP-induced neurotoxicity. Nature. *327:* 324-326, 1987.

89. D'Amato, R. J., Alexander, G. M., Schwartzman, R. J., Kitt, C. A., Price, D. L., and Snyder, S. H. Neuromelanin: a role in MPTP-induced neurotoxicity. Life Sci. *40:* 705-712, 1987.

90. Kaliszan, R., Kaliszan, A., and Wainer, I. W. Prediction of drug binding to melanin using a melanin-based high- performance liquid chromatographic stationary phase and chemometric analysis of the chromatographic data. J Chromatogr. *615:* 281-288, 1993.

91. Wilkerson, V. A. The chemistry of human epidermis. II. The isoelectric points of the stratum corneum, hair and nails as determined by electrophoresis. J Biol Chem. *112:* 329, 1935.

92. Dehn, D. L., Claffey, D. J., Duncan, M. W., and Ruth, J. A. Nicotine and cotinine adducts of a melanin intermediate demonstrated by matrix-assisted laser desorption/ionization time-of-flight mass spectrometry. Chem Res Toxicol. *14:* 275-279, 2001.

93. Scott, G. and Zhao, Q. Rab3a and SNARE proteins: potential regulators of melanosome movement. J Invest Dermatol. *116:* 296-304, 2001.

94. Prota, G. Melanins and Melanogenesis, p. 290. San Diego: Academic Press, 1992.

95. Novellino, L., Napolitano, A., and Prota, G. Isolation and characterization of mammalian eumelanins from hair and irides. Biochim Biophys Acta. *1475:* 295-306, 2000.

96. Prota, G. Melanin-producing cells. Melanins and Melanogenesis, pp. 14-33. San Diego: Academic Press, 1992.

97. Seiberg, M., Paine, C., Sharlow, E., Andrade-Gordon, P., Costanzo, M., Eisinger, M., and Shapiro, S. S. Inhibition of melanosome transfer results in skin lightening. J Invest Dermatol. *115:* 162-167, 2000.

98. McGuire, J. Three sites for hormonal control of the pigment cell. *In:* W. Montagna, E. J. Van Scott, and R. B. Stoughton (eds.), Advances in Biology of Skin--Pharmacology and the Skin, Vol. XII, pp. 421-445. New York: Meredith Corporation, 1972.

99. Mottaz, J. H. and Zelickson, A. S. Melanin transfer: a possible phagocytic process. J Invest Dermatol. *49:* 605-610, 1967.

100. Wolff, K., Jimbow, K., and Fitzpatrick, T. B. Experimental pigment donation *in vivo*. J Ultrastruct Res. *47:* 400-419, 1974.

101. Okazaki, K., Uzuka, M., Morikawa, F., Toda, K., and Seiji, M. Transfer mechanism of melanosomes in epidermal cell culture. J Invest Dermatol. *67:* 541-547, 1976.

102. Barnicott, N. A. and Birbeck, M. S. Electron microscope studies on pigment formation in human hair follicles. *In:* M. Gordon (ed.) Pigment Cell Biology, pp. 549-561. New York: Academic Press, 1959.

103. Prota, G. Genetic and hormonal regulation of melanogenesis. Melanins and Melanogenesis, pp. 185-207. San Diego: Academic Press, 1992.

104. Schallreuter, K., Slominski, A., Pawelek, J. M., Jimbow, K., and Gilchrest, B. A. What controls melanogenesis? Exp Dermatol. *7:* 143-150, 1998.

105. Park, H. Y., Perez, J. M., Laursen, R., Hara, M., and Gilchrest, B. A. Protein kinase C-beta activates tyrosinase by phosphorylating serine residues in its cytoplasmic domain. J Biol Chem. *274:* 16470-16478, 1999.

106. Park, H. Y., Russakovsky, V., Ohno, S., and Gilchrest, B. A. The beta isoform of protein kinase C stimulates human melanogenesis by activating tyrosinase in pigment cells. J Biol Chem. *268:* 11742-11749, 1993.

107. Prota, G. Photobiology and photochemistry of melanogenesis. Melanins and Melanogenesis, pp. 208-224. San Diego: Academic Press, 1992.

108. Wood, J. M., Schallreuter-Wood, K. U., Lindsey, N. J., Callaghan, S., and Gardner, M. L. A specific tetrahydrobiopterin binding domain on tyrosinase controls melanogenesis. Biochem Biophys Res Commun. *206:* 480-485, 1995.

109. Schallreuter, K. U., Wood, J. M., Korner, C., Harle, K. M., Schulz-Douglas, V., and Werner, E. R. 6-Tetrahydrobiopterin functions as a UVB-light switch for de novo melanogenesis. Biochim Biophys Acta. *1382:* 339-344, 1998.

110. Palumbo, A., d'Ischia, M., Misuraca, G., Carratu, L., and Prota, G. Activation of mammalian tyrosinase by ferrous ions. Biochim Biophys Acta. *1033:* 256-260, 1990.

111. Eller, M. S., Ostrom, K., and Gilchrest, B. A. DNA damage enhances melanogenesis. Proc Natl Acad Sci U S A. *93:* 1087-1092, 1996.

112. Psychemedics www.psychemedics.com. Psychemedics Web Site, 2001.

113. Tsatsakis, A. M., Psillakis, T., and Paritsis, N. Phenytoin concentration in head hair sections: a method to evaluate the history of drug use. J Clin Psychopharmacol. *20:* 560-573, 2000.

114. Nakahara, Y. Hair analysis for abused and therapeutic drugs. J Chromatogr B Biomed Sci Appl. *733:* 161-180, 1999.

115. Tsatsakis, A. M., Psillakis, T., Stefis, A., Assithianakis, P., Vlahonikolis, I. G., Michalodimitrakis, M. N., and Helidonis, E. Determination of phenytoin in sections of head hair: a preliminary study to evaluate the history of drug use. Boll Chim Farm. *137:* 459-466, 1998.

116. Psillakis, T., Tsatsakis, A. M., Christodoulou, P., Michalodimitrakis, M., Paritsis, N., and Helidonis, E. Carbamazepine levels in head hair of patients under long-term treatment: a method to evaluate the history of drug use. J Clin Pharmacol. *39:* 55-67, 1999.

117. Goldberger, B. A., Darraj, A. G., Caplan, Y. H., and Cone, E. J. Detection of methadone, methadone metabolites, and other illicit drugs of abuse in hair of methadone-treatment subjects. J Anal Toxicol. *22:* 526-530, 1998.

118. Goulle, J. P. and Kintz, P. [A new tool for biological study: hair analysis. Value in medical practice]. Rev Med Interne. *17:* 826-835, 1996.

119. Miyazawa, N., Uematsu, T., Mizuno, A., Nagashima, S., and Nakashima, M. Ofloxacin in human hair determined by high performance liquid chromatography. Forensic Sci Int. *51:* 65-77, 1991.

120. Uematsu, T., Miyazawa, N., and Nakashima, M. The measurement of ofloxacin in hair as an index of exposure. Eur J Clin Pharmacol. *40:* 581-584, 1991.

121. Paulsen, R. B., Wilkins, D. G., Slawson, M. H., Shaw, K., and Rollins, D. E. Effect of four laboratory decontamination procedures on the quantitative determination of cocaine and metabolites in hair., Submitted.

122. Joseph, R. E., Jr., Hold, K. M., Wilkins, D. G., Rollins, D. E., and Cone, E. J. Drug testing with alternative matrices II. Mechanisms of cocaine and codeine deposition in hair. J Anal Toxicol. *23:* 396-408, 1999.

123. Joseph, R. E., Jr., Oyler, J. M., Wstadik, A. T., Ohuoha, C., and Cone, E. J. Drug testing with alternative matrices I. Pharmacological effects and disposition of cocaine and codeine in plasma, sebum, and stratum corneum. J Anal Toxicol. *22:* 6-17, 1998.

124. Kidwell, D. A., Lee, E. H., and DeLauder, S. F. Evidence for bias in hair testing and procedures to correct bias. Forensic Sci Int. *107:* 39-61, 2000.

125. DeLauder, S. F. and Kidwell, D. A. The incorporation of dyes into hair as a model for drug binding. Forensic Sci Int. *107:* 93-104, 2000.

126. Rollins, D. E., Wilkins, D. G., Mizuno, A., Slawson, M. H., and Borges, C. R. The role of pigmentation in the disposition of drugs of abuse in human hair. Clin Pharm Exp Ther. *67:* 113, 2000.

127. Gygi, S. P., Joseph, R. E., Jr., Cone, E. J., Wilkins, D. G., and Rollins, D. E. Incorporation of codeine and metabolites into hair. Role of pigmentation. Drug Metab Dispos. *24:* 495-501, 1996.

128. Slawson, M. H., Wilkins, D. G., Foltz, R. L., and Rollins, D. E. Quantitative determination of phencyclidine in pigmented and nonpigmented hair by ion-trap mass spectrometry. J Anal Toxicol. *20:* 350-354, 1996.

129. Ito, S. Reexamination of the structure of eumelanin. Biochim Biophys Acta. *883:* 155-161, 1986.

130. Ito, S. and Wakamatsu, K. Chemical degradation of melanins: application to identification of dopamine-melanin. Pigment Cell Res. *11:* 120-126, 1998.

131. Ozeki, H., Wakamatsu, K., Ito, S., and Ishiguro, I. Chemical characterization of eumelanins with special emphasis on 5,6-dihydroxyindole-2-carboxylic acid content and molecular size. Anal Biochem. *248:* 149-157, 1997.

132. Kolb, A. M., Lentjes, E. G., Smit, N. P., Schothorst, A., Vermeer, B. J., and Pavel, S. Determination of pheomelanin by measurement of aminohydroxyphenylalanine isomers with high-performance liquid chromatography. Anal Biochem. *252:* 293-298, 1997.

133. Sealy, R. C., Puzyna, W., Kalyanaraman, B., and Felix, C. C. Identification by electron spin resonance spectroscopy of free radicals produced during autoxidative melanogenesis. Biochim Biophys Acta. *800:* 269-276, 1984.

134. Kalyanaraman, B., Felix, C. C., and Sealy, R. C. Electron spin resonance-spin stabilization of semiquinones produced during oxidation of epinephrine and its analogues. J Biol Chem. *259:* 354-358, 1984.

135. al-Kazwini, A. T., O'Neill, P., Adams, G. E., Cundall, R. B., Maignan, J., and Junino, A. One-electron oxidation of C(2) and C(3) methyl substituted 5,6-dihydroxyindoles: model pathways of melanogenesis. Melanoma Res. *4:* 343-350, 1994.

136. Bertolino, N. L., Klein, L. M., and Freedberg, I. M. Biology of hair follicles. *In:* T. E. Fitzpatrick, A. Z. Eisen, K. Wolff, I. M. Freedberg, and F. K. Austen (eds.), Dermatology in General Medicine, pp. 289. New York: McGraw-Hill, 1994.

137. Gallagher, R. P., Hill, G. B., Bajdik, C. D., Coldman, A. J., Fincham, S., McLean, D. I., and Threlfall, W. J. Sunlight exposure, pigmentation factors, and risk of nonmelanocytic skin cancer. II. Squamous cell carcinoma. Arch Dermatol. *131:* 164-169, 1995.

138. Gallagher, R. P., Hill, G. B., Bajdik, C. D., Fincham, S., Coldman, A. J., McLean, D. I., and Threlfall, W. J. Sunlight exposure, pigmentary factors, and risk of nonmelanocytic skin cancer. I. Basal cell carcinoma. Arch Dermatol. *131:* 157-163, 1995.

139. Bliss, J. M., Ford, D., Swerdlow, A. J., Armstrong, B. K., Cristofolini, M., Elwood, J. M., Green, A., Holly, E. A., Mack, T., and MacKie, R. M. Risk of cutaneous melanoma associated with pigmentation characteristics and freckling: systematic overview of 10 case-control studies. The International Melanoma Analysis Group (IMAGE). Int J Cancer. *62:* 367-376, 1995.

140. Fenselau, C. Tandem mass spectrometry: the competitive edge for pharmacology. Annu Rev Pharmacol Toxicol. *32:* 555-578, 1992.

141. Ito, S. and Fujita, K. Microanalysis of eumelanin and pheomelanin in hair and melanomas by chemical degradation and liquid chromatography. Anal Biochem. *144:* 527-536, 1985.

142. Wakamatsu, K. and Ito, S. Preparation of eumelanin-related metabolites 5,6-dihydroxyindole, 5,6-dihyroxyindole-2-carboxylic acid, and their O-methyl derivatives. Anal Biochem. *170:* 335-340, 1988.

143. Ito, S., Inoue, S., Yamamoto, Y., and Fujite, K. Synthesis and antitumor activity of cysteinyl-3,4-dihydroxyphenylalanines and related compounds. J Med Chem. *24:* 673-677, 1981.

144. Ito, S., Wakamatsu, K., and Ozeki, H. Spectrophotometric assay of eumelanin in tissue samples. Anal Biochem. *215:* 273-277, 1993.

145. Anderson, R. L. Practical Statistics for Analytical Chemistry. Practical Statistics for Analytical Chemistry, pp. 89-121. New York: Van Nostrand-Reinhold, 1987.

146. Gygi, S. P., Colon, F., Raftogianis, R. B., Galinsky, R. E., Wilkins, D. G., and Rollins, D. E. Dose-related distribution of codeine and its metabolites into rat hair. Drug Metab Dispos. *24:* 282-287, 1996.

147. Napolitano, A., Pezzella, A., Vincensi, M. R., and Prota, G. Oxidative degradation of melanins to pyrrole acids: a model study. Tetrahedron. *51:* 5913-5920, 1995.

148. Napolitano, A., Pezzella, A., d'Ischia, M., and Prota, G. New pyrrole acids by oxidative degradation of eumelanins with hydrogen peroxide. Further hints to the mechanism of pigment breakdown. Tetrahedron. *52:* 8775-8780, 1996.

149. Ito, S., Imai, Y., Jimbow, K., and Fujita, K. Incorporation of sulfhydryl compounds into melanins *in vitro*. Biochim Biophys Acta. *964:* 1-7, 1988.

150. d'Ischia, M., Napolitano, A., and Prota, G. Sulphydryl compounds in melanogenesis. Part II. Reactions of cysteine and glutathione with dopachrome. Tetrahedron. *43:* 5357-5362, 1987.

151. Reid, R. W., O'Connor, F. L., Deakin, A. G., Ivery, D. M., and Crayton, J. W. Cocaine and metabolites in human graying hair: pigmentary relationship. J Toxicol Clin Toxicol. *34:* 685-690, 1996.

152. Kronstrand, R., Forstberg-Peterson, S., Kagedal, B., Ahlner, J., and Larson, G. Codeine concentration in hair after oral administration is dependent on melanin content. Clin Chem. *45:* 1485-1494, 1999.

153. Rollins, D., Wilkins, D., Gygi, S., Slawson, M., and Nagasawa, P. Testing for drugs of abuse in hair-experimental observations and indications for future research. Forensic Sci. Rev. *9:* 23-36, 1996.

154. Jurado, C., Menendez, M., Repetto, M., Kintz, P., Cirimele, V., and Mangin, P. Hair testing for cannabis in Spain and France: is there a difference in consumption? J Anal Toxicol. *20:* 111-115, 1996.

155. Choi, M. H. and Chung, B. C. GC-MS determination of steroids related to androgen biosynthesis in human hair with pentafluorophenyldimethylsilyl-trimethylsilyl derivatisation. Analyst. *124:* 1297-1300, 1999.

156. Kintz, P., Cirimele, V., Jeanneau, T., and Ludes, B. Identification of testosterone and testosterone esters in human hair. J Anal Toxicol. *23:* 352-356, 1999.

157. Hold, K. M., Borges, C. R., Wilkins, D. G., Rollins, D. E., and Joseph, R. E., Jr. Detection of nandrolone, testosterone, and their esters in rat and human hair samples. J Anal Toxicol. *23:* 416-423, 1999.

158. Kintz, P., Cirimele, V., and Ludes, B. Physiological concentrations of DHEA in human hair. J Anal Toxicol. *23:* 424-428, 1999.

159. Kintz, P., Cirimel, V., Devaux, M., and Ludes, B. Dehydroepiandrosterone (DHEA) and testosterone concentrations in human hair after chronic DHEA supplementation. Clin Chem. *46:* 414-415, 2000.

160. Choi, M. H., Kim, K. R., and Chung, B. C. Determination of estrone and 17 beta-estradiol in human hair by gas chromatography-mass spectrometry. Analyst. *125:* 711-714, 2000.

161. Deng, X. S., Kurosu, A., and Pounder, D. J. Detection of anabolic steroids in head hair. J Forensic Sci. *44:* 343-346, 1999.

162. Kintz, P., Cirimele, V., Sachs, H., Jeanneau, T., and Ludes, B. Testing for anabolic steroids in hair from two bodybuilders. Forensic Sci Int. *101:* 209-216, 1999.

163. Segura, J., Pichini, S., Peng, S. H., and de la Torre, X. Hair analysis and detectability of single dose administration of androgenic steroid esters. Forensic Sci Int. *107:* 347-359, 2000.

164. Halmekoski, J. and Saarinen, P. Synthesis of acetyl derivatives of some sympathomimetic amines. Farmaseuttinen Aikakauslehti. *75:* 335-353, 1966.

165. Borges, C. R., Roberts, J. C., Wilkins, D. G., and Rollins, D. E. Relationship of melanin degradation products to actual melanin content: Application to human hair. Anal Biochem. *290:* 116-125, 2001.

166. Mieczkowski, T. and Kruger, M. Assessing the effect of hair color on cocaine positive outcomes in a large sample: A logistic regression on 56,445 cases using hair analysis. TIAFT Bulletin. *31:* 9-11, 2001.

167. Limat, A., Salomon, D., Carraux, P., Saurat, J. H., and Hunziker, T. Human melanocytes grown in epidermal equivalents transfer their melanin to follicular outer root sheath keratinocytes. Arch Dermatol Res. *291:* 325-332, 1999.

168. Lindquist, N. G. and Ullberg, S. The melanin affinity of chloroquine and chlorpromazine studied by whole body autoradiography. Acta Pharmacol Toxicol (Copenh). *2:* 1-32, 1972.

169. Fukuda, M. and Sasaki, K. Changes in the antibacterial activity of melanin-bound drugs. Ophthalmic Res. *22:* 123-127, 1990.

170. Wu, E. Y., Chiba, K., Trevor, A. J., and Castagnoli, N., Jr. Interactions of the 1-methyl-4-phenyl-2,3-dihydropyridinium species with synthetic dopamine-melanin. Life Sci. *39:* 1695-1700, 1986.

171. d'Ischia, M. and Prota, G. Biosynthesis, structure, and function of neuromelanin and its relation to Parkinson's disease: a critical update. Pigment Cell Res. *10:* 370-376, 1997.

172. Prota, G. and d'Ischia, M. Neuromelanin: a key to Parkinson's disease. Pigment Cell Res. *6:* 333-335, 1993.

173. Ibrahim, H. and Aubry, A. F. Development of a melanin-based high-performance liquid chromatography stationary phase and its use in the study of drug-melanin binding interactions. Anal Biochem. *229:* 272-277, 1995.

174. Martin, A. N., Swarbrick, J., and Camarata, A. Physical Pharmacy, p. 434. Philadelpha, PA: Lea & Febiger, 1969.

175. Ebbing, D. D. General Chemistry, 4th edition. Boston, MA: Houghton Mifflin Company, 1993.

176. Mieczkowski Drug Testing Technology. Boca Raton, FL: CRC Press LLC, 1999.

177. Krueger, G. G., Jorgensen, C. M., Matsunami, N., Morgan, J. R., Liimatta, A., Meloni-Ehrig, A., Shepard, R., and Petersen, M. J. Persistent transgene expression and normal differentiation of immortalized human keratinocytes *in vivo*. J Invest Dermatol. *112:* 233-239, 1999.

178. Bennett, D. C., Cooper, P. J., and Hart, I. R. A line of non-tumorigenic mouse melanocytes, syngeneic with the B16 melanoma and requiring a tumour promoter for growth. Int J Cancer. *39:* 414-418, 1987.

179. Parker, R. B., Williams, C. L., Laizure, S. C., and Lima, J. J. Factors affecting serum protein binding of cocaine in humans. J Pharmacol Exp Ther. *275:* 605-610, 1995.

180. Franksson, G. and Anggard, E. The plasma protein binding of amphetamine, catecholamines and related compounds. Acta Pharmacol Toxicol. *28:* 209-214, 1970.

181. Wilkins, D. G., Valdez, A. S., Nagasawa, P. R., Gygi, S. P., and Rollins, D. E. Incorporation of drugs for the treatment of substance abuse into pigmented and nonpigmented hair. J Pharm Sci. *87:* 435-440, 1998.

182. Wilkins, D. G., Mizuno, A., Borges, C. R., Slawson, M. H., Rollins, D. E., and Mizuno, A. Ofloxacin as a reference marker for hair analysis., Submitted.